6-1-2015

Development of New Synthetic Methods, Mechanistic Elucidation of Novel Organic Reactions Using Quantum Calculations, and Harnessing the Power of Continuous Flow Technologies

Trevor A. Hamlin
University of Connecticut - Storrs, domofloge@gmail.com

Development of New Synthetic Methods, Mechanistic Elucidation of Novel Organic Reactions Using Quantum Calculations, and Harnessing the Power of Continuous Flow Technologies

Trevor A. Hamlin, Ph.D.

University of Connecticut, 2015

The development of synthetic methodologies can be aided and improved upon by a critical understanding of the mechanistic pathways at play during a chemical reaction. Computational modeling has proven very valuable in this endeavor. My graduate research has focused on three areas in particular: (1) development of synthetic methodologies, (2) quantum chemical modeling, and (3) utilization of emerging technologies. These topics are highly relevant in the literature today and serve as a foundation to aid researchers in generations to come.

Development of New Synthetic Methods, Mechanistic Elucidation of Novel Organic Reactions Using Quantum Calculations, and Harnessing the Power of Continuous Flow Technologies

Trevor A. Hamlin

B. S. Albright College, **2010**

A Dissertation

Submitted in Partial Fulfillment of the

Requirements for the Degree of

Doctor of Philosophy

at the

University of Connecticut

2015

APPROVAL PAGE

Doctor of Philosophy Dissertation

Development of New Synthetic Methods, Mechanistic Elucidation of Novel Organic Reactions Using Quantum Calculations, and Harnessing the Power of Continuous Flow Technologies

Presented by
Trevor A. Hamlin B. S.

Major Advisor _____

Nicholas E. Leadbeater, Ph.D.

Associate Advisor _____

Robert R. Birge, Ph.D.

Associate Advisor _____

José A. Gascón, Ph.D.

Associate Advisor _____

Jing Zhao, Ph.D.

Associate Advisor _____

Ronald J. Wikholm, Ph.D.

University of Connecticut

2015

Acknowledgements

Chemistry has been an intimate part of my life for many years now. Studying chemistry in Graduate School has been a challenging, yet extremely rewarding endeavor. At times, the process seemed too much to handle, but I was constantly reminded about the invaluable opportunity before me. My parents never had such an opportunity. They worked multiple jobs just so my sister and I could have a better life. My father is the hardest working person I know and serves as my inspiration for never giving up. I thank him for understanding my decision to move to Connecticut and then to The Netherlands and for always encouraging me to follow my own path. My mother passed away at the end of my fourth year of graduate school, a stressful time already, but managing it all allowed me to obtain a more mature worldview. She meant the world to me and it hurts to know that she will not be here to see me achieve all my goals. She serves as my source to always strive for nothing but the best.

My wife has been my rock, serving to keep me grounded and always be a source of love and support. Mary Kate Hamlin and I were married at the beginning of my fourth year of graduate school and I am convinced it was her presence in my life that kept me going strong. I am grateful for her understanding nature while working around my graduate studies. She has supported me and all of my endeavors and I am confident we will happily grow old together.

I would like to acknowledge my advisor Nicholas E. Leadbeater for always supporting my willingness to create. Dr. Leadbeater provided me the opportunity to build the theoretical chemistry component of the New Synthetic Methodology group from the ground up. He was one of the few who supported my desire for my Ph.D. to be comprised of both theoretical and experimental chemistry. I must also acknowledge my undergraduate advisor and mentor, Dr. Christian Hamann; for it was he who challenged me to go to pursue a Ph.D. in the first place. He pushed me to not only perform cutting edge computational research, but then also present the work across the United States at various local and national meetings.

I value my friends and am confident that they allowed the process of obtaining a Ph.D. as enjoyable as possible. I would like to acknowledge Christopher Kelly, who has been a great motivator and source of chemistry knowledge. Christopher, along with Michael Mercadante, gave me the skills to allow me a proficient synthetic chemist. I thank them for their support and friendship. I would also like to acknowledge Jordan Greco, who is the kindest person I've ever met. He has been an amazing friend and has always extended himself for the service of others.

Finally, I would like to thank my committee members for generously supporting me along the way towards my Ph.D. I would also like to acknowledge my former advisor Dr. Birge for giving me invaluable advice on my research and for also just being a good hearted person. Our time spent with each other, whether in the laboratory or out of the building, is always filled with great stories and endless laughter. Lastly I would like to thank Dr. Gascon for all the fruitful conversation we have had about calculations over that past few years. Your insight was extremely valuable and I thank you very much.

Table of Contents

List of Abbreviations

Ar	aryl
atm	atmosphere
Bn	benzyl
BPR	back-pressure regulator
$CDCl_3$	deuterated chloroform
DBN	1,5-diazabicyclo(4.3.0)non-5-ene
DBU	1,8-diazabicycloundec-7-ene
DCM	dichloromethane
EDG	electron-donating group
Et_2O	diethyl ether
EtOAc	ethyl acetate
Eq.	molar equivalent
EWG	electron-withdrawing group
GC	gas chromatography
HFIP	hexafluoroisopropanol
HRMS	high resolution mass spectrometry
LC	liquid chromatography
MeCN	acetonitrile
MS	mass spectrometry
NMR	nuclear magnetic resonance
OTf	trifluoromethylsulfonate
Ph	phenyl
ppm	parts per million
r.t.	room temperature
Temp	temperature
TBAF	tetrabutylammonium fluoride
^tBu	tert-butyl
THF	tetrahydrofuran
TLC	thin layer chromatography
TMS, Me_3Si	trimethylsilyl
TMS-CF_3	trimethyl(trifluoromethyl)silane
TFMK	trifluoromethyl ketone

List of Publications

[10] Insight Theoretical and Experimental Studies of the Mechanism of Oxoammonium Salt Oxidations in Various Reaction Scaffolds using a Hydride Transfer Model. **Hamlin, T. A.**; Kelly, C. B.; Ovian, J. M.; Wiles, R. J.;Tilley, L. J.; Leadbeater, N. E. *manuscript in preparation.*

[9] Real-time Monitoring of Reactions Performed Using Continuous-flow Processing: The Preparation of 3-Acetylcoumarin as an Example. **Hamlin, T. A.**; Leadbeater, N. E. *In press.*

[8] Delocalization of Charge and Electron Density in the Humulyl Cation-Implications for Terpene Biosynthesis. **Hamlin, T. A**., Hamann, C. S., Tantillo, D. J. *J. Org. Chem.* **2015**, *80*, 4046.

[7] A Continuous-Flow Approach to 3,3,3-Trifluoromethylpropenes: Bringing Together Grignard Addition, Peterson Elimination, Inline Extraction, and Solvent Switching. **Hamlin, T. A**.; Lazarus, G. M. L.; Kelly, C. B. Leadbeater, N. E. *Org. Process. Res. Dev.*, **2014**, *18*, 1253.

[6] 1,3-γ-Silyl-Elimination in Electron-Deficient Cationic Systems. Mercadante, M. A.; Kelly, C. B. **Hamlin, T. A**.; Delle Chiaie, K. R.; Fager, D. C.; Glod, B. L. C.; Hansen, K. E.; Hill, C. R.; Leising, R. M.; Lynes, C. L.; MacInnis, A. E.; McGohey, M. R.; Murray, S. A.; Piquette, M. C.; Roy, S. L.; Smith, R. M. Sullivan, K. R.; Truong, B. H.; Vailonis, K. M.; Gorbatyuk, V.; Leadbeater, N. E.; Tilley, L. J. *Chem. Sci.*, **2014**, *5*, 3983.

[5] Methylenation of Perfluoroalkyl Ketones Using a Peterson Olefination Approach. **Hamlin, T. A.**; Kelly, C. B.; Cywar, R. M.; Leadbeater, N. E. *J. Org. Chem.*, **2014**, *79*, 1145.

[4] Oxoammonium Salt Oxidations of Alcohols in the Presence of Pyridine Bases. Bobbitt, J. M.; Bartelson, A. L.; Bailey, W. F.; **Hamlin, T. A.**; Kelly, C. B. *J. Org. Chem.*, **2014**, *79*, 1055.

[3] Raman Spectroscopy as a Tool for Monitoring Mesoscale Continuous-Flow Organic Synthesis: Equipment Interface and Assessment in Four Medicinally-Relevant Reactions. **Hamlin, T. A.**; Leadbeater, N. E. *Beilstein J. Org. Chem.*, **2013**, *9*, 1843.

[2] Dehydrogenation of Perfluoroalkyl Ketones by Using a Recyclable Oxoammonium Salt. **Hamlin, T. A.**; Kelly, C. B.; Leadbeater, N. E. *Eur. J. Org. Chem.*, **2013**, 3658.

[1] Oxidation of α-Trifluoromethyl Alcohols Using a Recyclable Oxoammonium Salt. Kelly, C. B.; Mercadante, M. A.; **Hamlin, T. A.**; Fletcher, M. H.; Leadbeater, N. E. *J. Org. Chem*., **2012**, *77*, 8131.

List of Contributions for Collaborative Projects

Oxidation of α-Trifluoromethyl Alcohols Using a Recyclable Oxoammonium Salt. Kelly, C. B.; Mercadante, M. A.; **Hamlin, T. A.**; Fletcher, M. H.; Leadbeater, N. E. *J. Org. Chem*., **2012**, *77*, 8131.

Contributions to this project:
TAH: Performed kinetics studies, assisted with manuscript revisions, assisted with supporting information
CBK: Prepared α-CF_3 alcohols, substrate screen, prepared manuscript, assisted with supporting information
MAM: Prepared α-CF_3 alcohols, substrate screen, kinetics, assisted with manuscript preparation, prepared supporting information
MHF: Reaction optimization

Dehydrogenation of Perfluoroalkyl Ketones Using an Oxoammonium Salt. **Hamlin, T. A.;** Kelly, C. B.; Leadbeater, N. E. *Eur. J. Org. Chem.* **2013**, 3658.

Contributions to this project:
TAH: Performed reaction optimization, performed substrate screens and TFMK substrates, performed mechanistic studies, assisted with manuscript preparation, prepared supporting information
CBK: Reaction discovery and development, prepared TFMK substrates, prepared manuscript, assisted with supporting information preparation

Methylenation of Perfluoroalkyl Ketones using a Peterson Olefination Approach. **Hamlin, T. A.**; Kelly, C. B.; Cywar, R. M.; Leadbeater, N. E. *J. Org Chem.*, **2014**, *79*, 1145.

Contributions to this project:
TAH: Prepared TFMK substrates, performed reaction optimization, prepared β-silyl alcohols, performed substrate screens, performed application reactions, assisted with manuscript preparation, prepared supporting information
CBK: Prepared TFMK substrates, performed applications reactions, prepared manuscript, assisted with supporting information preparation
RMC: Assisted in performing application reactions, assisted with supporting information preparation

1,3-γ-Silyl-Elimination in Electron-Deficient Cationic Systems. Mercadante, M. A.; Kelly, C. B.; **Hamlin, T. A.**; Delle Chiaie, K. R.; Drago, M. D.; Duffy, K. K.; Dumas, M .T.; Fager, D. C.; Glod, B. L. C.; Hansen, K. E.; Hill, C. R.; Leising, R. M.; Lynes, C. L.; MacInnis, A. E.; McGohey, M. R.; Murray, S. A.; Piquette, M. C.; Roy, S. L.; Smith, R. M.; Sullivan, K. R.; Truong, B. H.; Vailonis, K. M; Gorbatyuk, V.; Leadbeater, N. E.; Tilley L. J. *Chem. Sci.* **2014**, *5*, 3983.

Contributions to this project:

TAH: Performed quantum chemical calculations on solvolysis reactions, performed HOMA/isodesmic/and KIE studies, assisted in manuscript preparation, prepared computational supporting information

CBK: Prepared CF_3 alcohols for aryl systems, solvolysis of sulfonate esters and acetates, assisted in manuscript preparation, assisted in experimental supporting information preparation, 2D NMR analysis for diastereomers

MAM: Prepared CF_3 alcohols and tosylates for α-aryl systems, prepared substrates for kinetic studies, prepared sulfonate esters and acetates, kinetic studies using conductometric methods, assisted in manuscript preparation, assisted in experimental supporting information preparation

VG: Assisted in 2D NMR analysis for diastereomers

Stonehill College: Preparation of kinetic substrates and non α-aryl systems, solvolysis of non α-aryl systems, deuterium kinetic isotope effect studies, assisted in manuscript preparation, assisted in supporting information

Oxoammonium Salt Oxidations of Alcohols in the Presence of Pyridine Bases Bobbitt, J. M.; Bartelson, A. L.; Bailey, W. F.; **Hamlin, T. A.**; Kelly, C. B. *J. Org. Chem.*, **2014**, *79*, 1055.

Contributions to this project:

TAH: Performed computational studies on mechanistic models for oxidation, NMR studies on hydrogen bonding, assisted in GC studies on esterification, assisted in manuscript preparation, prepared supporting information

CBK: Conceptual project design for hydrogen bonding model for mechanistic studies, NMR studies on hydrogen bonding, assisted in manuscript preparation, assisted in supporting information preparation

JMB: Performed substrate screens, conceptual design for oxidation mechanism, GC studies on esterification, prepared manuscript

ALB: Screening of oxidative esterification reaction, isolation of "Adam's salt", studies of effect of basicity/base structure on ester formation

WFB: Assisted in manuscript preparation

Theoretical and Experimental Studies of the Mechanism of Oxoammonium Salt Oxidations in Various Reaction Scaffolds using a Hydride Transfer Model. **Hamlin, T. A.**; Kelly, C. B.; Ovian, J. M.; Wiles, R. J.; Tilley, L. J.; Leadbeater, N. E. *manuscript in preparation.*

Contributions to this project:
TAH: Performed computational studies on mechanistic models for oxidation, assisted in manuscript preparation, prepared supporting information for computational section
CBK: Performed computational studies on mechanistic models for oxidation, assisted in manuscript preparation, prepared supporting information for experimental section
JMO: Performed competitive rate studies, assisted in preparation of experimental supporting information
RJW: Performed tropylium experimental studies under the guidance of LJT

Raman Spectroscopy as a Tool for Monitoring Mesoscale Continuous-Flow Organic Synthesis: Equipment Interface and Assessment in Four Medicinally-Relevant Reactions. **Hamlin, T. A.**; Leadbeater, N. E. *Beilstein J. Org. Chem.*, **2013**, *9*, 1843.

Contributions to this project:
TAH: Performed continuous flow runs, engineered flow apparatus, performed quantum chemical calculations, worked up spectra, manuscript preparation, preparation of supporting information

A Continuous-Flow Approach to 3,3,3-Trifluoromethylpropenes: Bringing Together Grignard Addition, Peterson Elimination, Inline Extraction, and Solvent Switching. **Hamlin, T. A.**; Lazarus, G. M. L.; Kelly, C. B.; Leadbeater, N. E. *Org. Process Res. Dev.* **2014**, *18*, 1253.

Contributions to this project:
TAH: Conceptual design of optimized flow system and transition to flow, synthesis of substrates, performing flow runs, optimization studies in flow, assisted in preparation of manuscript, prepared supporting information
CBK: Assisted in troubleshooting quench of the Grignard reaction in flow, assisted in manuscript preparation
GML: Optimization of Grignard and elimination reactions in flow

List of Figures

List of Tables

Chapter 1: Development of New Synthetic Methods

1.1 INTRODUCTION

Interest in the development of methods for the incorporation of fluorine in organic molecules has increased in recent years.[1] The pharmaceutical and agrochemical industries, along with academic laboratories have focused their efforts towards this goal. Nearly 30% of the leading 30 blockbuster drugs contain at least one fluorine atom and a number contain the trifluoromethyl group.[1b] The incorporation of a fluorine atom can be achieved through a variety of methods. Examples include (1) electrophilic fluorination using reagents such as Selectfluor®, (2) nucleophilic fluorination using Ruppert-Prakash reagent, TMS-CF_3; Togni's reagent; or Umemoto's reagent, and radical coupling reactions.[2] A major reason why incorporation of a fluorine atom has become so popular is because of its profound effect on the physical and chemical properties of the resultant molecule. Specifically for the agrochemical and pharmaceutical industries, one of the most important properties is lipophilicity. Fluorine has a dramatic effect on the lipophilicity of polar molecules and acts to facilitate passage through the

[1] (a) Hiyama, T. *Organofluorine Compounds. Chemistry and Applications*; Springer: New York, **2000;** (b) O'Hagan, D. *J. Fluorine Chem*, **2010**, *131*, 1071; (c) Müller, K.; Faeh, C.; Diederich, F. *Science* **2007**, *317*, 1881.

[2] ***For a review and specific examples of electrophilic fluorination, see:*** (a) Mikami, K.; Itoh, Y.; Yamanaka, M. *Chem. Rev.* **2004**, *104*, 1; (b) Beeson, T. D.; MacMillan, D. W. C. *J. Am. Chem. Soc.* **2005**, *127*, 8826; (c) Parsons, A. T.; Buchwald, S. L. *Angew. Chem., Int. Ed.* **2011**, *50*, 9120; (d) Xu, J.; Fu, Y.; Luo, D.-F.; Jiang, Y.-Y.; Xiao, B.; Liu, Z.-J.; Gong, T.-J.; Liu, L. *J. Am. Chem. Soc.* **2011**, *133*, 15300; (e) Wang, X.; Ye, Y.; Zhang, S.; Feng, J.; Xu, Y.; Zhang, Y.; Wang, J. *J. Am. Chem. Soc.* **2011**, *133*, 16410. ***For a review and specific example of nucleophilic fluorination, see:*** (f) Chu, L.; Qing, F.-L. *Org. Lett.* **2012**, *14*, 2106; (g) Gao, Z.; Lim, Y. H.; Tredwell, M.; Li, L.; Verhoog, S.; Hopkinson, M.; Kaluza, W.; Collier, T. L.; Passchier, J.; Huiban, M.; Gouverneur, V. *Angew. Chem., Int. Ed.* **2012**, *51*, 6733; (h) Lee, E.; Kamlet, A. S.; Powers, D. C.; Neumann, C. N.; Boursalian, G. B.; Furuya, T.; Choi, D. C.; Hooker, J. M.; Ritter, T. *Science* **2011**, *334*, 639. ***For specific examples of radical fluorination, see:*** (i) Tius, M. A. *Tetrahedron* **1995**, *51*, 6605; (j) Rueda-Becerril, M.; Sazepin, C. C.; Leung, J. C. T.; Okbinoglu, T.; Kennepohl, P.; Paquin, J.-F.; Sammis, G. M. *J. Am. Chem. Soc.*, **2012**, *134*, 4026.

blood brain barrier.[3] Many drugs and advanced drug candidates treating a wide range of illnesses feature fluorine for this reason (Figure 1).[1b,4]

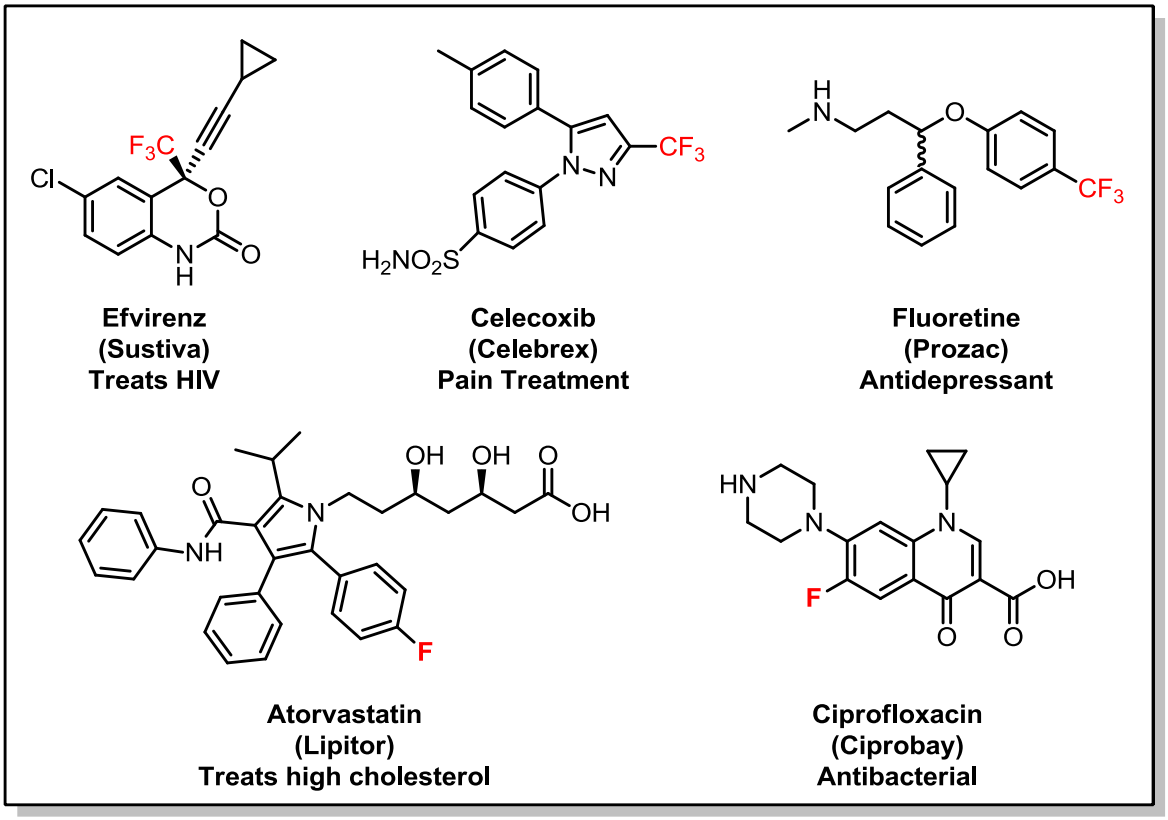

Figure 1: A brief overview of "blockbuster" fluorinated drugs

Another desirable quality of fluorine is its effect on metabolic stability.[1] Fluorinated natural products are very rare; as a result, living organisms lack the necessary enzymatic framework for degradation, thus resulting in a longer lifetime in the body.[1] Fluorine is the most electronegative element and forms very strong bonds with carbon.[5] The strong bonding character of the C–F bond manifests itself as the highest bond dissociation energy (BDE) in organic frameworks (C–F

[3] Hagmann, W. K. *J. Med. Chem.* **2008**, *51*, 4359.
[4] Ismail, F. M. D. *J. Fluorine Chem.* **2002**, *118*, 27.
[5] (a) O'Hagan, D. *Chem. Soc. Rev.*, **2008**, *37*, 308; (b) Lemal, D. M. *J. Org. Chem.* **2004**, *69*, 1; (c) Blanksby, S. J.; Ellison, B. *Acc. Chem. Res.* **2003**, *36*, 255.

bond average is around 105.4 kcal mol^{-1}). The high BDE can be attributed to highly polarized electrostatic-like character of the C–F bond.[5a]

For these reasons and more, we chose to establish a research program dedicated to exploring novel routes to access trifluoromethyl-containing moieties. Specifically, we focused on methodologies to construct trifluoromethyl ketones (TFMKs), α, β-unsaturated trifluoromethyl ketones, and trifluoromethyl alkenes (TFMAs). The following sections of this chapter will outline these efforts.

1.2 SYNTHESIS OF TRIFLUOROMETHYL CONTAINING MOLECULES

1.2.1 Background of TFMKs[6]

Unlike monofluoromethyl- or difluoromethyl-groups, the trifluoromethyl group has received the most attention from a synthetic standpoint. This is likely due to the fact that the trifluoromethyl group has the ability to serve as a bioisostere to methyl esters. This quality allows the group to alter the steric and electronic properties of molecules and also acts to prevent metabolic degradation.[6] The first class of trifluoromethyl containing compounds we focused on is the α-trifluoromethyl ketone (TFMK). The TFMK is a privileged motif benefitting from significant focus due to their role as critical intermediates in the synthesis of a heterocycles, pharmaceutical drugs, and fluorinated natural product analogues (Figure 2).[7] A relevant example of the use of a TFMK in the pharmaceutical industry was realized for the synthesis of the leading antiretroviral drug for the treatment of HIV, Efavirenz (Sustiva^{TM}).[8]

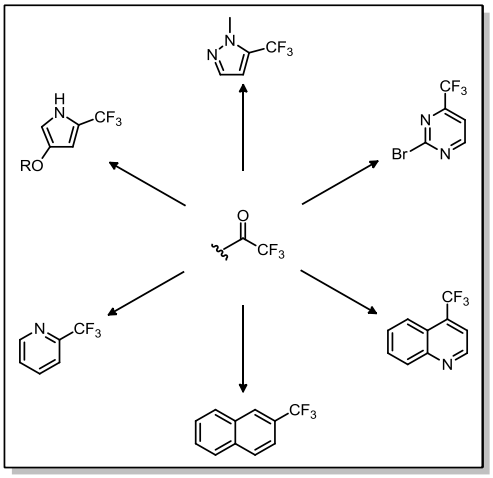

Figure 2: Various trifluoromethyl-containing molecules accessible from TFMKs

[6] Kelly, C. B.; Mercadante, M. A.; Leadbeater, N. E. *Chem. Commun.* **2013**, *49*, 11133.
[7] (a) Rodeschini, V.; Van de Weghe, P.; Salomon, E.; Tarnus, C.; Eustache, J. *J. Org. Chem.* **2005**, *70*, 2409; (b) Abid, M.; Török, B. *Adv. Synth. Catal.* **2005**, *347*, 1797.
[8] (a) Pierce, M. E.; Parsons Jr., R. L.; Radesca, L. A.; Lo, Y. S.; Silverman, S.; Moore, J. R.; Islam, Q.; Choudhury, A.; Fortunak, J. M. D.; Nguyen, D.; Luo, C.; Morgan, S. J.; Davis, W. P.; Confalone, P. N. *J. Org. Chem.*, **1998**, *63*, 8536; (b) Nicolaou, K. C.; Krasovskiy, A.; Majumder, U.; Trépanier, V. E.; Chen, D. Y.-K. *J. Am. Chem. Soc.*, **2009**, *131*, 3690.

The van der Waals volumes of an ethyl group and a TFMK are very similar; therefore these two groups can be interchanged without significantly altering the molecules size.[1c] The trifluoromethyl group has a significant effect on the nature of the carbonyl group of the TFMK. The electron withdrawing nature of the CF_3 group causes the carbonyl carbon to have an increased δ^+ character. This causes the carbonyl to be more prone to nucleophilic attack. As a result many TFMKs hydrate and form an equilibrium between the keto and hydrate forms (Figure 3).

When electron withdrawing groups are adjacent to the TFMK group, the hydrate form predominates.[9] The hydrate form has significant solubility in water; therefore methodologies for the preparation of these compounds need to be tailored to avoid aqueous work-up, as they diminish the yield. Molecular sieves can be employed to remove water and shift the equilibrium towards the keto form.

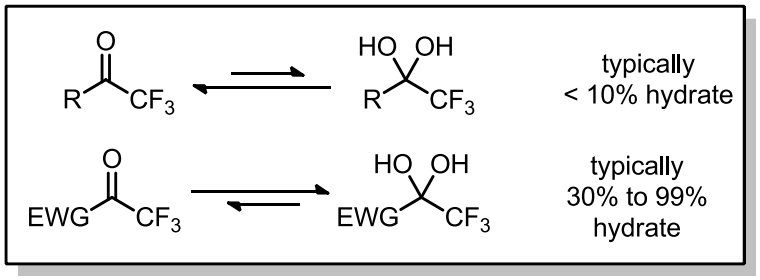

Figure 3: Electronic effect on the equilibrium between TFMKs and their corresponding hydrates

TFMKs can have a significant impact on biological systems and have proven to be reversible competitive inhibiters of a number of enzymes. This is in part due to their ability to form covalent bonds with key residues as well as their predisposition to nucleophilic attack. These qualities render TFMKs as attractive competitive inhibitors, thus potential pharmacons. TFMKs

[9] Salvador, R. L.; Saucier, M. *Tetrahedron* **1971**, *27*, 1221.

have been found to inhibit enzymes that primarily serve to degrade biomolecules, such as proteases, esterases, lipases, and deacetylases.[10]

1.2.2 Background on the Oxoammonium Salt

Oxidation is an extremely important class of reaction in an organic chemist's toolbox; therefore the development of selective and efficient methods to achieve the transformation is particularly attractive.[11] Oxidations allow for functional group inter-conversion (e.g. alcohol to carbonyl derivative), activation (e.g. amine to an iminium species), and even removal (e.g. oxidative cleavage).[11] Among the various functional groups that can be oxidized, arguably the most common target for oxidation is the alcohol. Notable named reactions, such as the Jones,[12] Collins[13]/PCC,[14] Oppenauer,[15] Swern[16] (and other DMSO-based oxidants[17]), Ley,[18] IBX,[19] and

[10] (a) Andreini, C.; Bertini, I.; Cavallaro, G.; Holliday, G. L.; Thornton, J. M. *J. Biol. Inorg. Chem.* **2008**, *13*, 1205; (b) Ilies, M.; Dowling, D. P.; Lombardi, P. M.; Christianson, D. W. *Bioorg. Med. Chem. Lett.* **2011**, *21*, 5854; (c) Walter, M .W.; Felici, A.; Galleni, M.; Soto, R. P.; Adlington, R. M.; Baldwin, J. E.; Frère, J.-M.; Gololobov, M.;. Schofield, C. J. *Bioorg. Med. Chem. Lett.* **1996**, *6*, 2455; (d) Frey, R. R.; Wada, C. K.; Garland, R. B.; Curtin, M. L.; Michaelides, M. R.; Li, J.; Pease, L. J.; Glaser, K. B.; Marcotte, P. A.; Bouska, J. J.; Murphy, S. S.; Davidsen, S. K. *Bioorg. Med. Chem. Lett.* **2002**, *12*, 3443.

[11] (a) Smith, M. B.; March, J., *March's Advanced Organic Chemistry*. 5th ed.; J. W. Wiley: New York, New York, **2001**; (b) Bäckvall, J.-E. *Modern Oxidation Methods* WILEY-VCH: Weinheim, **2004**; (c) Trost, B. M.; Fleming I. *Comprehensive Organic Synthesis: Selectivity, Strategy, and Efficiency in Modern Organic Chemistry* Oxford: Pergamon Press, **1991**; (d) Caron, S. *Practical Synthetic Organic Chemistry: Reactions, Principles, and Techniques* Wiley-VCH: Weinheim, **2011**.

[12] (a) Bowden, K.; Heilbron, I. M.; Jones, E. R. H.; Weedon, B. C. L. *J. Chem. Soc.* **1946**, 39; (b) Heilbron, I. M.; Jones, E. R. H.; Sondheimer, F. *J. Chem. Soc.* **1949**, 604.

[13] Collins, J. C.; Hess, W. W.; Frank, F. J. *Tetrahedron Lett.* **1968**, *9*, 3363.

[14] (a) Corey, E. J.; Suggs, J. W.; *Tetrahedron Lett.* **1975**, *16*, 2647; (b) Corey, E. J.; Schmidt, G. *Tetrahedron Lett.* **1979,** *20*, 399.

[15] (a) Oppenauer, R.V. *Recl. Trav. Chim. Pays-Bas* **1937**, *56*, 137; (b) Wettstein, A. *Helv. Chim. Acta*, **1940**, *23*, 388; (c) Mandell, L. *J. Am. Chem. Soc.* **1956**, *78*, 3199.

[16] (a) Omura, K.; Swern, D. *Tetrahedron*, **1978**, *34*, 1651-1660; (b) Mancuso, A. J.; Huang, S.-L.; Swern, D. *J. Org. Chem.* **1978**, *43*, 2480.

[17] (a) Corey, E. J.; Kim, C. U. *J. Am. Chem. Soc.* **1972**, *94*, 7586; (b) Pfitzner, K. E.; Moffatt, J.G. *J. Am. Chem. Soc.* **1963**, *85*, 3027; (c) Parikh, J. R.; Doering, W. v. E. *J. Am. Chem. Soc.* **1967**, *89*, 5505.

[18] Griffith, W. P.; Ley, S. V.; Whitcombe, G. P.; White, A. D. *J. Chem. Soc., Chem. Commun.* **1987**, 1625.

[19] (a) Frigerio, M.; Santagostino, M.; Sputore, S. *J. Org. Chem.* **1999**, *64*, 4537; (b) Frigerio, M.; Santagostino, M. *Tetrahedron Lett.* **1994**, *35*, 8019; (c) Duschek, A.; Kirsch, S. F. *Angew. Chem. Int. Ed.* **2011**, *50*, 1524.

Dess-Martin periodinane[20] oxidations, provide a plethora of options for generating the desired carbonyl from a starting alcohol. In the interest of mitigating various drawbacks of these oxidations,[21] alternative oxidants have been sought in recent years. To this end, oxoammonium salts have been found to be highly attractive species because they are environmentally benign, recyclable oxidants that are very user-friendly and accomplish oxidation under extremely mild conditions.[22] As such, they have gained popularity as alternatives to more traditional oxidizing reagents.[23] A nice feature of oxoammonium salt oxidations is that they are typically colorimetric processes, with the progress of the reaction being related to the color of the solution (Figure 4).

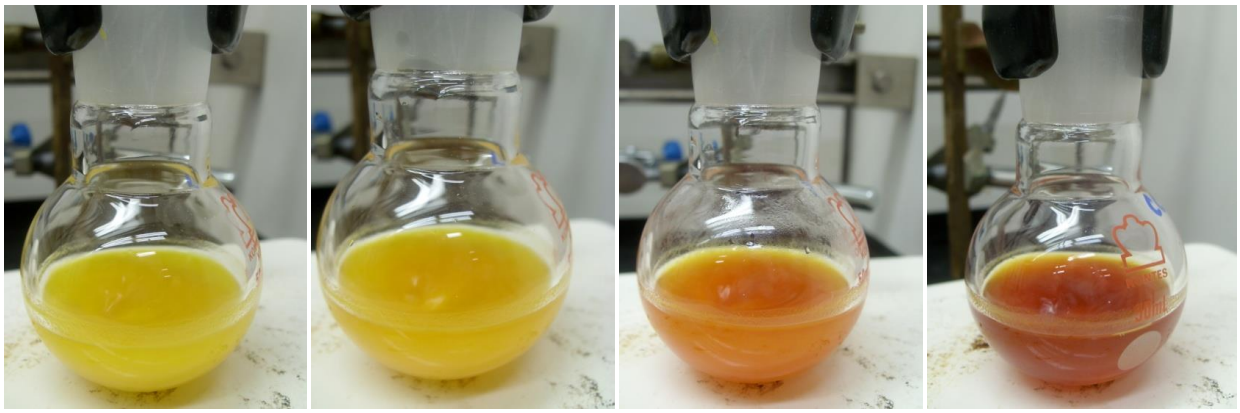

Figure 4: Colorimetric reaction of the oxoammonium salt oxidations. Time lapse from the start to end of the reaction (total of 60 min).

Numerous oxoammonium salts have been shown to be useful in various oxidation reactions. The salt that became of interest to our laboratory is 4-acetamido-2,2,6,6-tetramethylpiperidine-1-oxoammonium tetrafluoroborate (**1.1a**, "Bobbitt's Salt", AcNH-TEMP=O^+ BF_4^-) (Figure 5).

---

[20] (a) Dess, D. B.; Martin, J. C. *J. Org. Chem.* **1983**, *48*, 4155; (b) Dess, D. B. Martin, J. C. *J. Am. Chem. Soc.* **1991**, *113*, 7277.
[21] (a) Cohen, M. D.; Kargacin, B.; Klein, C. B.; Costa, M. *Crit. Rev. Toxicol.***1993**, *23*, 255; (b) Tidwell, T.T. *Org. React.* **1990**, *39*, 297.
[22] ***For reviews see:*** (a) Mercadante, M. A.; Kelly, C. B.; Bobbitt, J. M.; Tilley, L. J.; Leadbeater, N. E. *Nat. Protoc.* **2013**, *8*, 666. (b) Kelly, C. B. *Synlett*, **2013**, *24*, 527. (c) Bobbitt, J. M.; Bruckner C.; Merbouh, N. *Org. React.*, **2009**, *74*, 103. (d) Bobbitt, J. M.; Merbouh, N. *Org. Synth.*, **2005**, *82*, 80.
[23] (a) Qui, J.; Pradhan, P. P.; Blanck, N. B.; Bobbitt, J. M.; Bailey, W. F. *Org. Lett.* **2012**, *14*, 350; (b) N. Merbouh, J. M. Bobbitt, C. Bruckner, *J. Org. Chem.* **2004**, *69*, 5116.

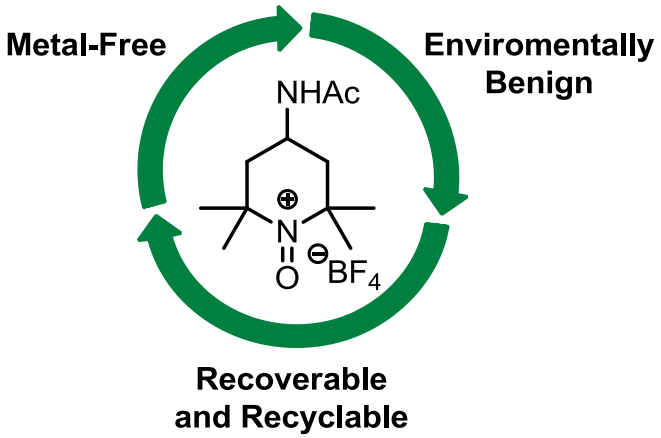

Figure 5: Key aspects of Bobbitt's Salt (**1.1a**)

This salt is a very versatile oxidant that is air stable and can be prepared on very large scales for a minimal cost (< $1 per gram) (Figure 6).[22a] We prepare the salt in house, however it may also be purchased from Sigma Aldrich for approximately $7 per gram. Moreover, 4-acetamido-(2,2,6,6-tetramethyl-piperidin-1-yl)oxyl (**1.1b**, AcNH-TEMPO, a TEMPO analog) is prepared as an intermediate in the salt preparation. The oxidant is built off a TEMPO scaffold, of which the oxyl analog **(**similar to **1.1b**, without the NHAc functionality) has been utilized as a stoichiometric terminal oxidant (often in conjunction with commercial bleach containing NaOCl.[24] There are many instances of **1.1b** being used in oxidation reactions where the oxoammonium cation is subsequently formed *in situ*.[25]

[24] a) Tojo, G.; Fernandez, M. I. *Oxidation of Primary Alcohols to Carboxylic Acids: A Guide to Current Common Practice*, 1st ed. Springer, **2007**; (b) Sheldon, R. A., Arends, I. W. C. E., Brink, G.-J.; Dijksman, A. *Acc. Chem. Res.* **2002**, *35*, 774; (c) Ciriminna, R.; Pagliaro, M. *Org. Process Res. Dev.* **2010**, *14*, 245; (d) Anelli, P. L.; Montanari, F.; Quici, S. *Org. Synth.1990*, **69**, 212; (e) Anelli, P. L.; Biffi, C.; Montanari, F.; Quici, S. *J. Org. Chem.***1987**, *52*, 2559; (f) Anelli, P. L.; Banfi S.; Montanari, F.; Quici, S. *J. Org. Chem.* **1989**, *54*, 2970.
[25] (a) Ma, Z.; Bobbitt, J.M. *J. Org.Chem* **1991,** *56*, 6110; (b) Banwell, M. G.; Bridges, V. S.; Dupuche, J. R.; Richards, S. L.; Walter, J. M. *J. Org. Chem.***1994**, *59*, 6338.

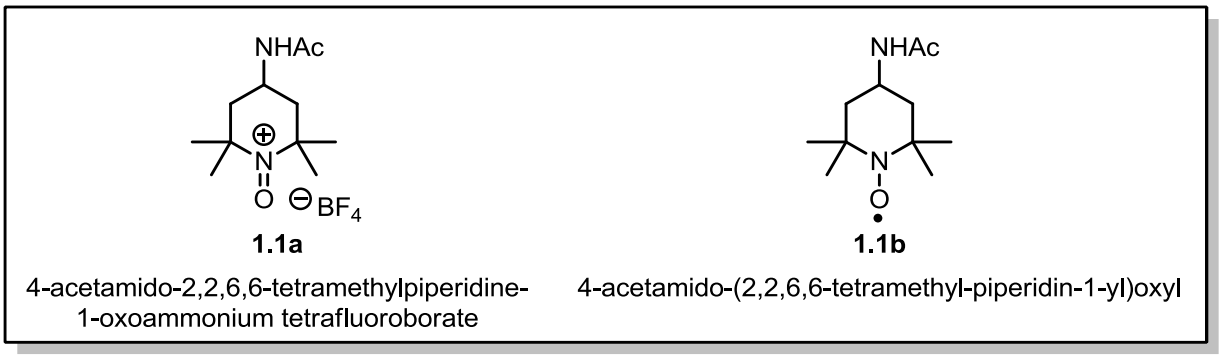

Figure 6: Structures of 4-acetamido-2,2,6,6-tetramethylpiperidine-based oxidants

Much of the literature involving oxoammonium salts centers around the conversion of alcohols into the corresponding carbonyl species. A range of functional groups can be accessed by using this strategy including aldehydes,[26] carboxylic acids,[23a] ketones,[26] and even esters.[23b] Under neutral conditions, after oxidizing an alcohol, the oxoammonium salt is reduced to the protonated hydroxylamine (**1.1c**). The reaction mechanism is very different when the reaction is conducted in the presence of pyridyl bases. Under basic conditions, after oxidizing an alcohol, the oxoammonium salt is reduced to hydroxylamine (**1.1d**). This then undergoes comproportionation with **1.1a** to generate the radical, **1.1b**. The process is shown in detail in Figure 7 and the mechanism of these reactions will be investigated further in Chapters 2.2-2.3.

[26] Bobbitt, J. M. *J. Org. Chem.* **1998**, *63*, 9367.

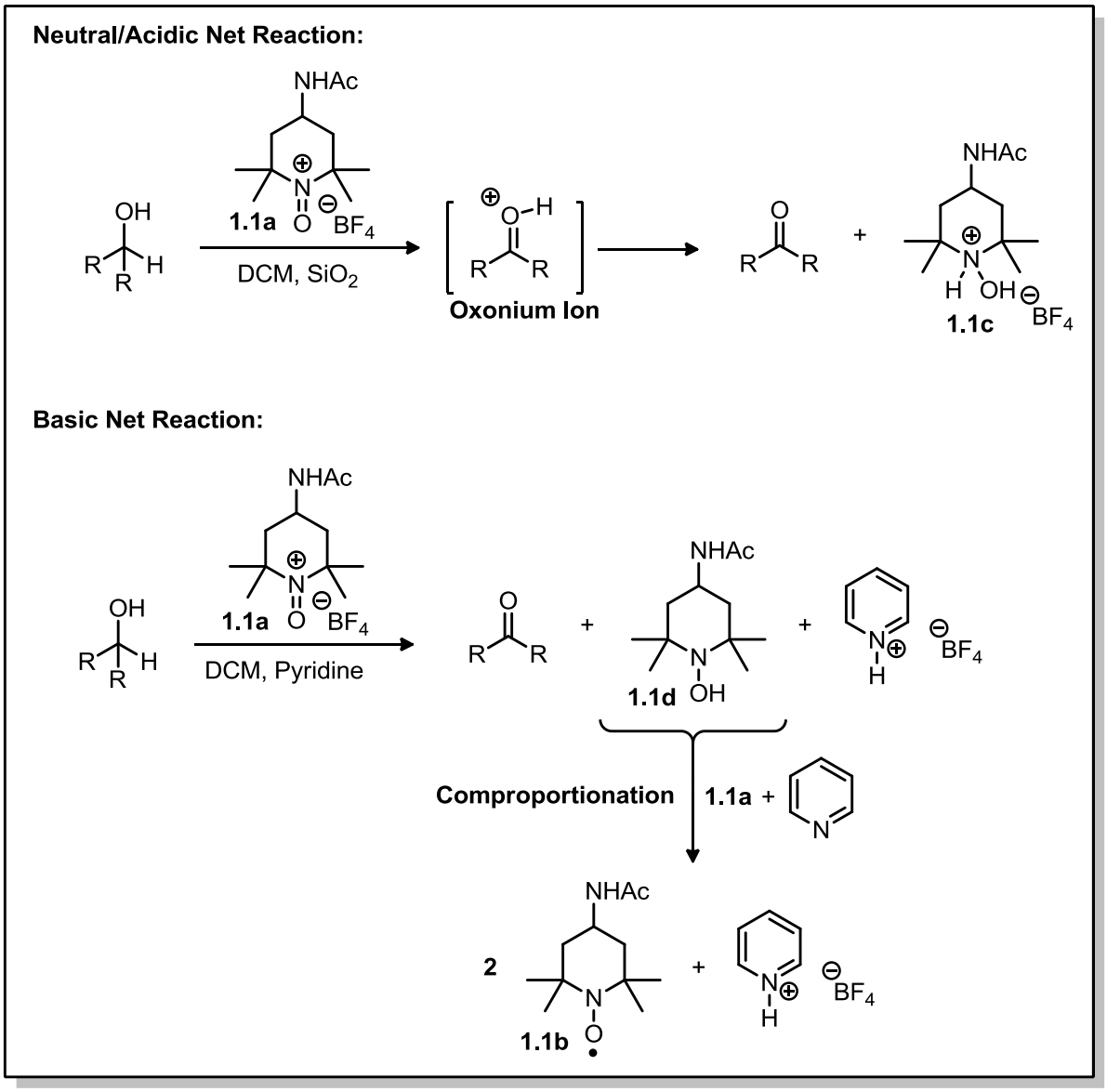

Figure 7: Modes of alcohol oxidation by oxoammonium salt **1.1a** controlled by reaction media

1.2.3 Synthesis of α-Trifluoromethyl Ketones Using an Oxoammonium Salt[27]

Historically, perfluoroalcohols have been notoriously difficult to oxidize likely due to their electron-deficient nature.[28] Oxidations have typically been carried out using the powerful, but

[27] Kelly, C. B.; Mercadante, M. A.; Hamlin, T. A.; Fletcher, M. H.; Leadbeater, N. E. *J. Org. Chem.*, **2012**, *77*, 8131.
[28] Linderman, R. J.; Graves, D. M. *Tetrahedron Lett.* **1987**, *28*, 4259.

expensive reagent Dess-Marin periodinane (DMP).[29] Seeking a more practical and cost effective method, we chose to use 4-acetylamino-2,2,6,6-tetramethylpiperidine-1-oxoammonium tetrafluoroborate ("Bobbitt's Salt"), **1.1a**.[22] Initial studies in mildly acidic media (SiO_2) failed, likely due to the highly destabilized carbocation intermediate (Figure 8).

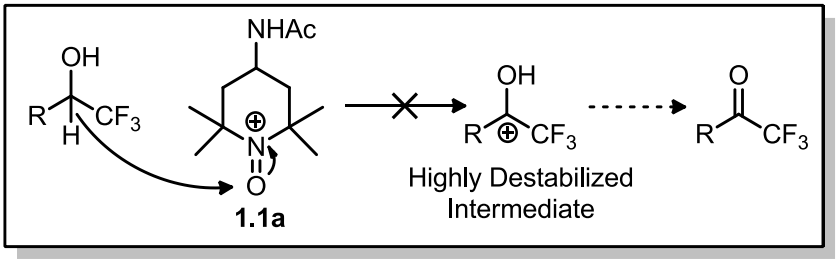

Figure 8: Rationale for failure of oxidations under non-basic conditions

From a thermodynamic standpoint, our attempts to oxidize these α-CF_3 alcohols failed due to the high activation barrier of this process, which will be discussed in depth in Chapter 2.3.2.[30,23a] It is known that β-oxygen compounds, which share electronics similar to those of α-CF_3 alcohols, fail to oxidize readily when treated with **1.1a** under standard conditions, likely for the same reason.[22] We found that addition of a pyridine base facilitated the oxidation reaction, and that as basicity increases, so does the rate of reaction (e.g. pyridine < 2,6-lutidine < 2,4,6-collidine).

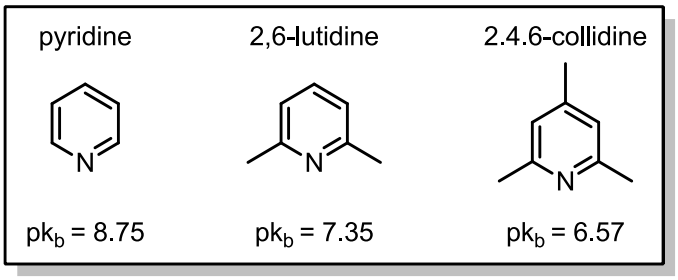

Figure 9: Trend in basicity of various pyridyl bases

[29] Linderman, R. J.; Graves, D. M. *J. Org. Chem.* **1989**, *54*, 661.
[30] Bailey, W. F.; Bobbitt, J. M.; Wiberg, K. B. *J. Org. Chem*. **2007**, *72*, 4504

2,6-Lutidine was chosen as the ideal base for this reaction because it allowed reactions to be complete in a few hours and also allowed for an easy work-up. The optimized reaction conditions are shown in Figure 10.

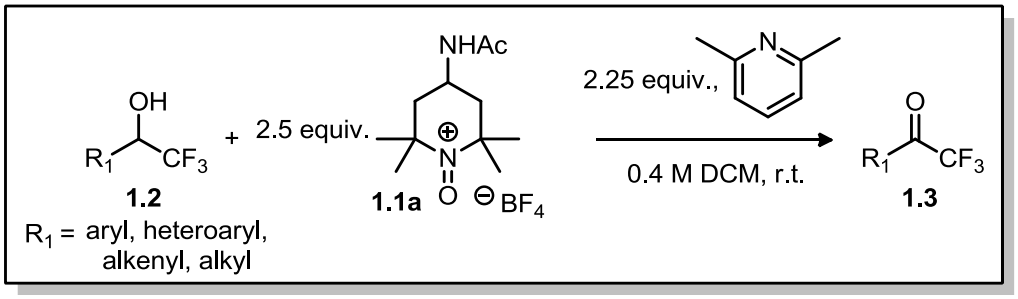

Figure 10: Optimized reaction conditions for the oxidation of α-CF_3 alcohols

A wide range of α-CF_3 alcohols bearing an aryl group could be easily oxidized by **1.1a**, facilitating good to excellent yields of the respective TFMKs (68-99%, Table 1).

Table 1: Oxidation of aryl-functionalized substrates[a]

Entry	α-CF_3 Alcohol[b]	TFMK	Yield (%)[c]
1	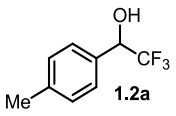	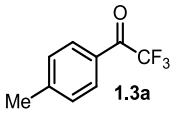	71%
2	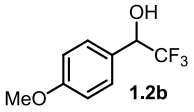	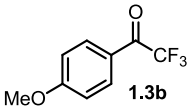	90%
3	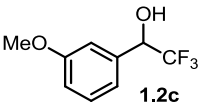	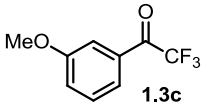	89%
4	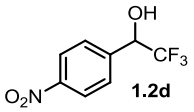	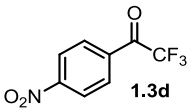	99%
5	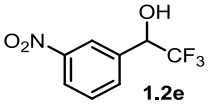	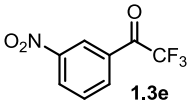	96%

Entry	α-CF_3 Alcohol[b]	TFMK	Yield (%)[c]
6	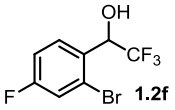 **1.2f**	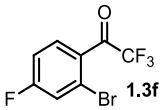 **1.3f**	78%
7	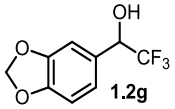 **1.2g**	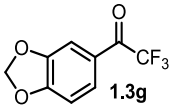 **1.3g**	97%
8	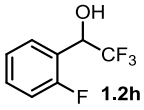 **1.2h**	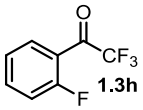 **1.3h**	73%
9	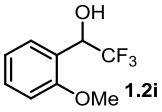 **1.2i**	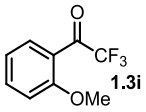 **1.3i**	96%
10	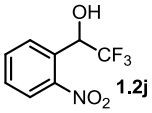 **1.2j**	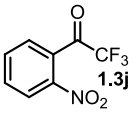 **1.3j**	89%
11	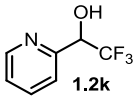 **1.2k**	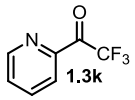 **1.3k**	96%[d]

[a]Conditions unless otherwise noted: α-CF_3 alcohol (1 equiv), oxoammonium salt (1.1a) (2.5 equiv), 2,6-lutidine (2.25 equiv), DCM (0.4 M in starting alcohol) [b]α-CF_3 alcohols were prepared *via* trifluoromethylation of the corresponding aldehydes using TMS-CF_3 [c]Isolated yield after purification [d]Yield of stable hydrate

Interestingly, alkyl α-CF_3 alcohols failed to oxidize under standard conditions. As a result, a stronger base, 1,5-diazabicyclo[4.3.0]non-5-ene (DBN), was employed which allowed for rapid oxidation of these systems. An issue with using this base is that the purification procedure was more complex due to a side reaction between DBN and **1.1a** and as a result, yields were diminished (Table 2).

Table 2: Oxidation of alkyl- and allyl-functionalized substrates[a]

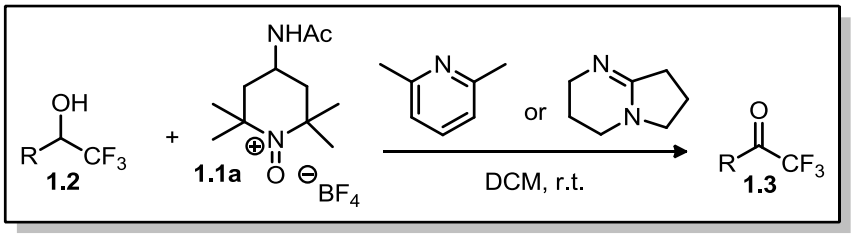

Entry	α-CF_3 Alcohol	CF_3 Ketone	Yield[b]
1[c]	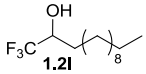	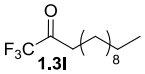	50%
2[c]	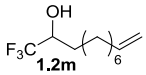	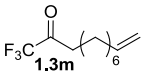	60%
3[c]	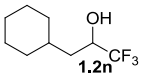	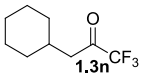	49%
4[d]	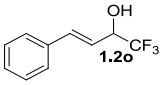	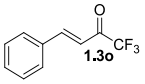	72%
5[d]	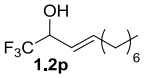	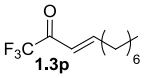	93%
6[d]	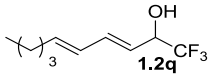	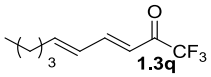	99%
7[d]	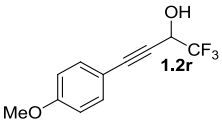	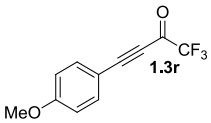	85%
8[d]	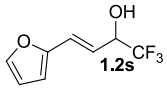	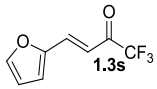	68%

[a]α-CF_3 alcohols were prepared via trifluoromethylation of the corresponding aldehydes using TMS-CF_3 [b]Isolated yield after purification [c]Conditions: α-CF_3 alcohol (1 equiv), 1 (3.0 equiv), DBN (2.5 equiv), DCM (0.1 M in starting alcohol) [d]Conditions: α-CF_3 alcohol (1 equiv), 1 (2.5 equiv), 2,6-lutidine (2.25 equiv), DCM (0.4 M in starting alcohol)

The power of this oxidation methodology over current methods was exemplified by the chemoselective oxidation of **1.2t**. A substrate (**1.2t**) containing both an α-CF_3 alcohol (Figure 11, in blue) and benzyl alcohol (Figure 11, in red). Selective oxidation using most other oxidants is rare and a protecting group strategy would need to be employed. Here, by simply adjusting the reaction conditions chemoselective oxidation was possible. Oxidation of the benzyl alcohol proceeded smoothly in non-basic conditions, while the α-CF_3 alcohol group remained intact. The

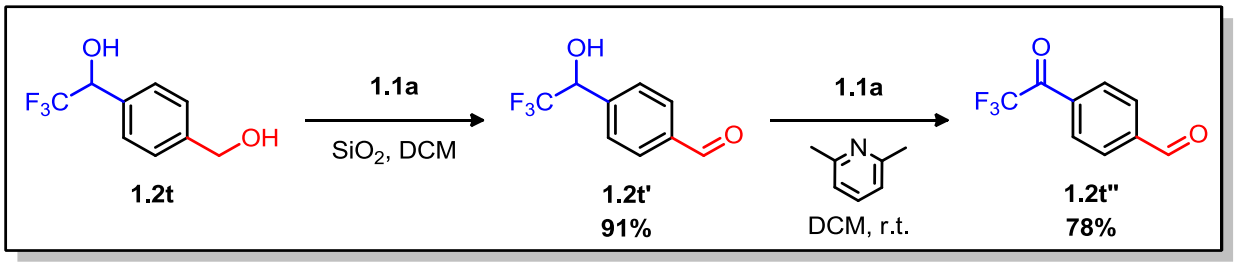

Figure 11: Chemoselective oxidation based on reaction media

α-CF_3 alcohol **1.2t′** could then be oxidized using the standard basic conditions to afford **1.2t"** in good yield.

To gain further insight into the reaction, we obtained rate data for our oxidation using the method of Mullet and Nodding.[31] Unlike the competitive rate studies typically used,[26a] we believed that this alternative method would be more effective for our systems in obtaining this information because of complications that arose when analyzing ^{1}H and ^{19}F NMR spectra. We determined the relative rates of oxidation of five representative substrates (Table 3). Aryl-substituted substrates all oxidized at about the same rate: therefore, we utilized **1.2a** as our model substrate for comparison. From the data in Table 3, we theorize that there is a large steric component to the reaction. We suggest that the combined electronic repulsion by the highly electron-rich CF_3 group and the steric repulsion by any β-substituent contribute significantly to oxidant/alcohol complexation and hence successful oxidation. This likely explains the drastic increase in rate with increasing conjugation as well as the large rate acceleration observed for **1.2r** over **1.2a** and is in agreement with the current model for oxidation by oxoammonium cations under basic conditions.[30a]

[31] Mullet, G. M.; Nodding, C. R. *Science* **1962**, *138*, 1346.

Table 3: Relative rates of oxidation of α-CF_3 alcohols to their corresponding TFMKs by oxoammonium salt oxidation

Entry	α-CF_3 Alcohol	Relative Oxidation Rate[a]
1	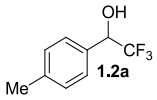 **1.2a**	1.00
2	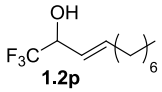 **1.2p**	0.24
3	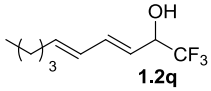 **1.2q**	0.50
4	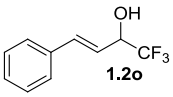 **1.2o**	0.61
5	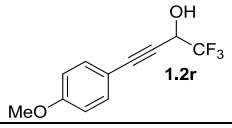 **1.2r**	120

[a]Determined by GC-MS analysis.

Finally, to determine if the spent oxidant could be recycled, crude **1.1b** from several reactions was dissolved in water and salted-out with sodium chloride to afford an 87% recovery of **1.1b**. This recovered nitroxide was converted into **1.1a**, in the standard manner, in comparable yield (70%). The recovered **1.1b** was used in later oxidations with no detrimental effect on oxidant reactivity and with a TFMK yield no more than 5% different than when using freshly made **1.1a**.

In summary, we have reported here an effective, mild method for the oxidation of α-CF_3 alcohols to their corresponding TFMKs. The reaction is compatible with a wide array of substrates; proceeds rapidly, can be used to affect chemoselective oxidations, and affords TFMKs in excellent yield. Moreover, the spent oxidant can be easily recovered and recycled.

1.2.4 Dehydrogenation of Perfluoroalkyl Ketones Using an Oxoammonium Salt[32]

Following the study outline above, we investigated an unusual side product we encountered when attempting to oxidize aliphatic α-CF_3 alcohols, namely the over-oxidized α,β-unsaturated TFMKs (Figure 12). With essentially no precedence for this type of direct dehydrogenation transformation by an oxoammonium species,[33] we sought to exploit this serendipitous finding.

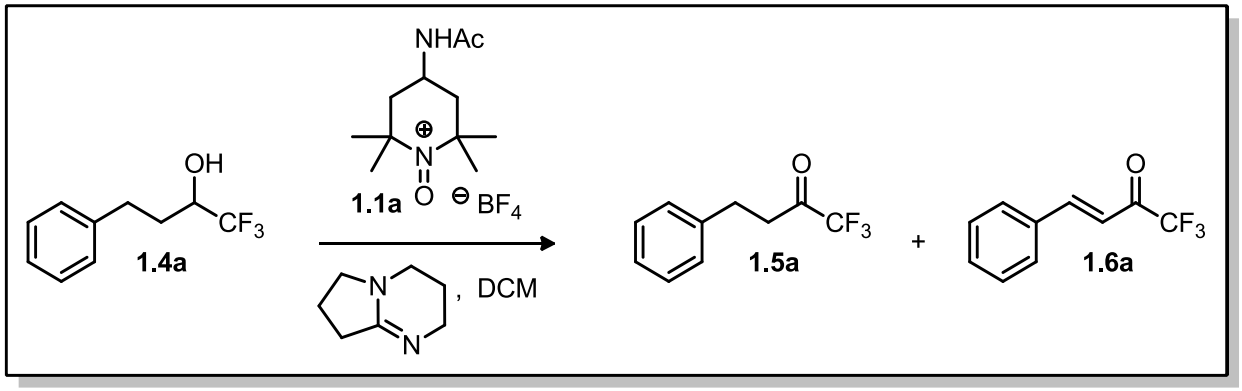

Figure 12: Previously observed result when attempting oxidation of 1,1,1-trifluoro-4-phenylbutan-2-ol

Initially, we sought to convert a model aliphatic α-CF_3 alcohol, 1,1,1-trifluoro-4-phenylbutan-2-ol (**1.4a**) directly into its corresponding α,β-unsaturated TFMK (1.6a). However, several complications arose when attempting this endeavor. First, a large excess amount of salt was required to ensure complete conversion into the desired material. In addition, the stronger oxidant, DBN, was required for initial oxidation of the alcohol and, as a result of competitive decomposition of this base (this deleterious side reaction was eluded to in the previous chapter); an extensive purification procedure was required to isolate the product. Given these complications, we chose instead to start from aliphatic TFMK (**1.5a**), which could readily be

[32] Hamlin, T. A.; Kelly, C. B.; Leadbeater, N. E. *Eur. J. Org. Chem.* **2013**, 3658.
[33] H. Richter, O. Mancheño García, *Eur. J. Org. Chem.* **2010**, 4460–4467.

prepared by an alternative method we developed.[34] Treatment with DBN and the oxoammonium salt did facilitate rapid dehydrogenation of this TFMK, which indicates that the dehydrogenation event is independent of alcohol oxidation. However, an excess amount of salt was still required, and we again encountered significant difficulty when purifying the product at the end of the reaction. Seeking to circumvent these roadblocks, we wondered if a pyridyl base could be used in place of DBN. We found that this was indeed the case. Upon treatment of **1.5a** with the oxoammonium salt (2.6 equiv.) and pyridine (2.2 equiv.) in dichloromethane as the solvent, we observed slow but steady formation of dehydrogenated product **1.6a** at r.t. Seeking to accelerate the rate of dehydrogenation, we opted for the more basic 2,6-lutidine. Although a marked increase in the reaction rate was noted, the requisite reaction time was still quite long (48 h). We therefore performed the reaction at reflux, which allowed us to shorten the reaction time to 24-48 h. Using these conditions (Figure 13), we were not only able to obtain the pure dehydrogenation product in good yield, but we were also able to recover spent oxidant **1.1b**.

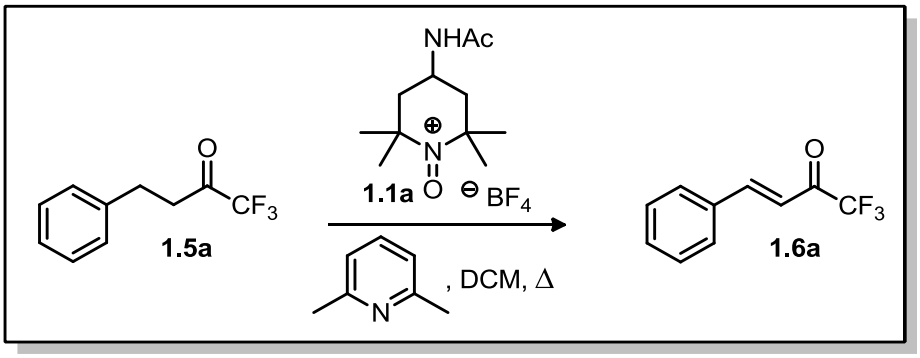

Figure 13: Dehydrogenation of **1.5a** under the optimized conditions

Seeking to explore the scope of this transformation, we prepared a number of aliphatic TFMKs and subjected them to our optimized dehydrogenation conditions. The results are shown

[34] Rudzinski, D. M.; Kelly, C. B.; Leadbeater, N. E. *Chem. Commun.* **2012**, *48*, 9610.

in Table 4. Initially we chose to screen a variety of hydrocinnamyl derivatives. We found that both electron-rich (Table 4, Entries 2–4) and electron-poor (Table 4, Entries 5–7) substrates readily underwent dehydrogenation to give similar yields of the product, albeit at different rates. A significant rate enhancement in the systems bearing electron-deficient arenes was observed, and these reactions reached completion typically in 12–16 h.

Table 4: Scope of the dehydrogenation of various trifluoromethyl ketones[a]

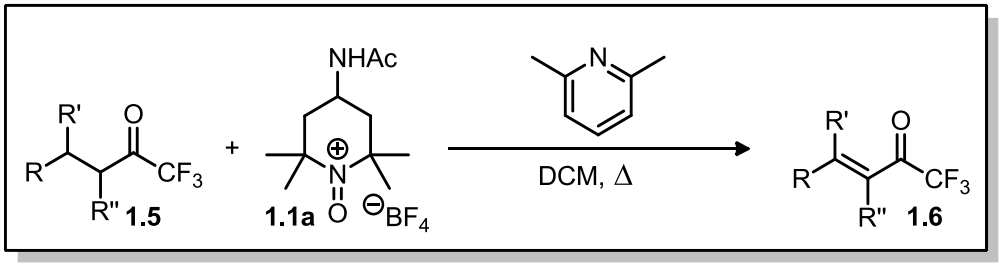

Entry	TFMK	α,β-Unsaturated TFMK	Time (h)	Yield (%)[b]
1	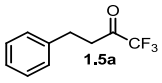 1.5a	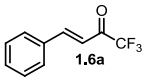 1.6a	24	65
2	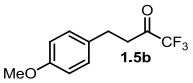 1.5b	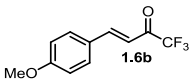 1.6b	32	69
3	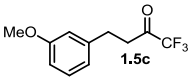 1.5c	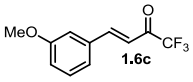 1.6c	24	74
4	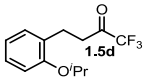 1.5d	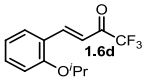 1.6d	48	64
5	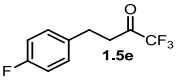 1.5e	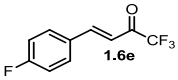 1.6e	12	56
6	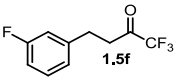 1.5f	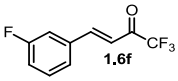 1.6f	16	62
7	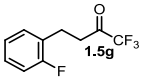 1.5g	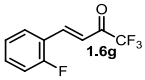 1.6g	12	69
8	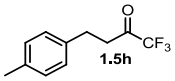 1.5h	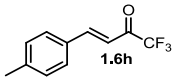 1.6h	24	83
9	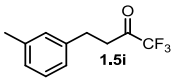 1.5i	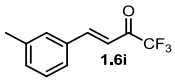 1.6i	24	69
10	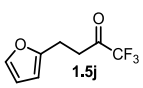 1.5j	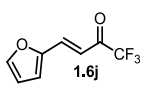 1.6j	16	64

Entry	TFMK	α,β-Unsaturated TFMK	Time (h)	Yield (%)[b]
11	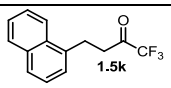 1.5k	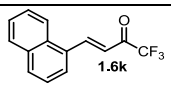 1.6k	24	98
12	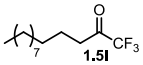 1.5l	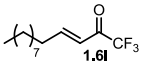 1.6l	72	-[c,d]
13	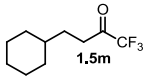 1.5m	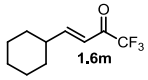 1.6m	48	53
14	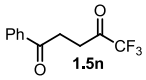 1.5n	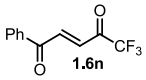 1.6n	4	80
15	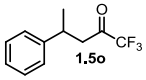 1.5o	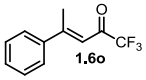 1.6o	24	-[c]
16	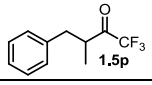 1.5p	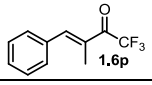 1.6p	-	-

[a]Conditions: TFMK (1 equiv.), **1.1a** (2.6 equiv.), 2,6-lutidine (2.2 equiv.), DCM (0.1 M in starting TFMK) [b]Isolated yield after purification [c]Substrate was completely consumed by GC-MS analysis [d]Contained inseparable impurities following workup

The sterically-encumbering *o*-isopropyl ether (Table 4, Entry 4) did undergo dehydrogenation, but required a slightly longer reaction time to ensure complete conversion. A representative heterocyclic system (Table 4, Entry 10) and a polycyclic system (Table 4, Entry 11) were next screened, and they afforded their corresponding dehydrogenation products in good yield. Suspecting the driving force for dehydrogenation to be extended conjugation (and an activated benzyl methylene moiety), we shifted our attention to non-aryl substituted substrates. As expected, we obtained substantially diminished yields and far longer reaction times were required (Table 4, Entries 12 and 13). In the case of **1.5l** (Table 4, Entry 12), although full conversion was achieved, desired product **1.6l** could not be obtained in acceptable purity or yield. To probe further the importance of an activated β-methylene, we prepared a diketo substrate (Table 4, Entry 14). Such a system would possess far more acidic β-hydrogen atoms. Dehydrogenation of this substrate proceeded extraordinarily fast and gave the unsaturated product in excellent yield, which corroborated the necessity for an activated β-methylene moiety.

It should be stressed that the spent oxidant could easily be recovered and reclaimed, which make the dehydrogenation process inherently recyclable.

To gain further mechanistic insight, we prepared α- and β-methyl hydrocinnamyl substrates (Table 4, Entries 15 and 16). Interestingly, both failed to undergo dehydrogenation, but in the case of the β-methyl system, the starting material was completely consumed by GC analysis. Intrigued by this finding, we conducted a ^{19}F NMR spectroscopy study using model system **1.5a**. We found that three unique fluorinated species were present within 30 min of starting the reaction. Whereas two of these signals corresponded to starting material and product respectively, the third signal was initially puzzling, as it appeared at a rather unique chemical shift (-86.2 ppm). We postulated that rather than proceeding in a concerted pathway, the reaction likely was a two-step process. The first step likely involved a precedented α-alkylation of the intermediate enolate (or enol), whose formation was likely facilitated by 2,6-lutidine.[35] Once the TFMK is alkylated, the carbonyl undergoes rapid hydration by any trace amount of water in the system (i.e., from the salt or solvent).[36] On the basis of the ^{19}F chemical shift of similar α-alkoxy trifluoromethyl hydrates,[37] we believe this explains the third peak observed in the NMR spectroscopy studies. This deters the known α-oxidation pathway, by decreasing the acidity of the α-proton, opening up an E2-like elimination pathway. Elimination of the alkoxyamine solely affords the E-isomer. It is likely that this results from steric clash between the β-substituent and the bulky tetramethylpiperidine moiety, which restricts the conformational freedom of the

[35] (a) Eddy, N. A.; Kelly, C. B.; Mercadante, M. A.; Leadbeater, N. E.; Fenteany, G. *Org. Lett.* **2012**, *14*, 498; (b) Golubev , V. A.; Miklyush, R. V. *Zh. Org. Khim.* **1972**, *8*, 1376; (c) Liu, Y.; Ren, T.; Guo, Q. *Chin. J. Chem*. **1996**, *14*, 252.

[36] During our studies we noted that the addition of water to the reaction mixture (0.2 mL) greatly accelerated the rate of the reaction, but complicated the isolation. Additionally, rigorously dried crystalline oxoammonium salt caused the reaction to proceed at a much slower rate, which indicated that the low levels of water found in the powdered form did assist in the reaction.

[37] Iskra, J.; Bonnet-Delpon, D.; Bégué, J.-P. *J. Fluorine Chem.* **2005**, *126*, 549.

molecule. The resultant gem-diol then undergoes rapid dehydration, as the equilibrium substantially favors the keto form of α, β-unsaturated TFMKs over the gem-diol.[37] The proposed mechanism for the reaction is shown in Figure 14.

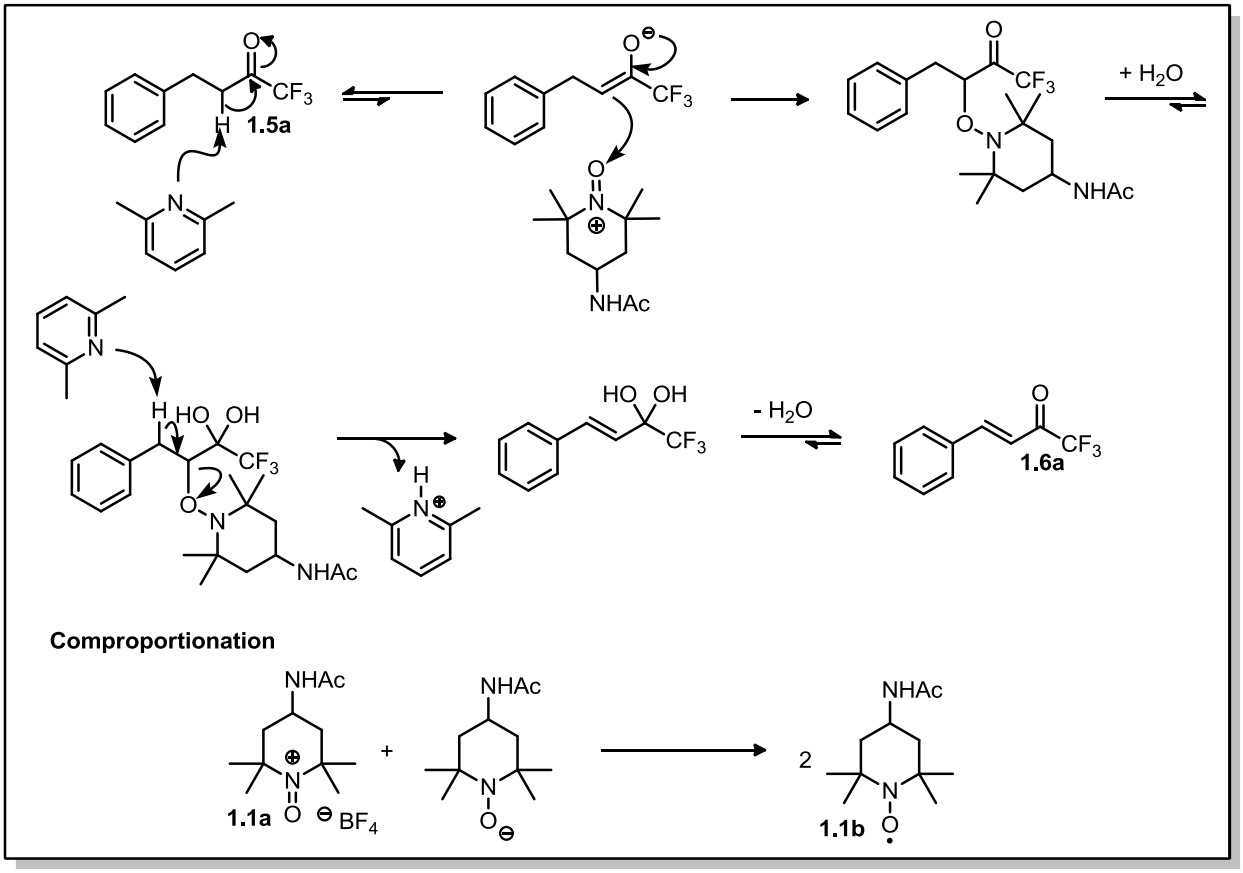

Figure 14: Plausible mechanistic pathway of the dehydrogenation reaction

With this plausible mechanism in hand, we sought to test whether other perfluoroalkyl substrates and even non-fluorinated systems would undergo dehydrogenation under our optimized conditions (Table 5). As expected, a substrate bearing a pentafluoroethyl group readily dehydrogenated to yield the desired alkene in superior yield to its trifluoromethyl analogue (Table 5, Entry 1). Interestingly, the less-destabilizing pentafluorophenyl-substituted system (Table 5, Entry 2) gave a very low yield of the chalcone-like product. Based on our posited

mechanism, we believe that the intermediate of the α-alkylation was much less prone to hydration, and hence, either competitive α-oxidation or lack of further reactivity contributed to the marked low yield. Aliphatic ketones (Table 5, Entries 3 and 4) failed to undergo dehydrogenation, which is in line with the proposed mechanism.

Table 5: Scope of dehydrogenation of various perfluoroalkyl and aliphatic ketones[a]

Entry	Substrate	Product	Yield (%)[b]
1	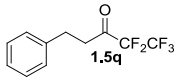 1.5q	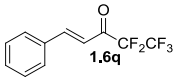 1.6q	77
2	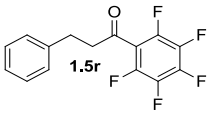 1.5r	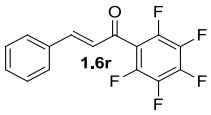 1.6r	26
3	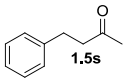 1.5s	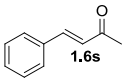 1.6s	-
4	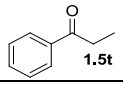 1.5t	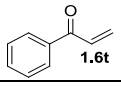 1.6t	-

[a]Conditions: **1.5** (1 equiv.), **1.1a** (2.6 equiv.), 2,6-lutidine (2.2 equiv.), DCM (0.1 M in starting TFMK) [b]Isolated yield after purification

In summary, we developed the first direct dehydrogenation of simple ketones using an oxoammonium salt. The reaction can be conducted under mild conditions and gives good yields of the corresponding α,β-unsaturated products. While specific to perfluoroalkyl ketones, an array of β-substituents is tolerated. The proposed mechanism involves a two-step process invoking α-alkylation followed by an E2-like elimination. Although this study was focused on perfluoroalkyl ketones, extension of this reaction to other substrates bearing electron-withdrawing groups may be possible.

1.3 SYNTHESIS OF PERFLUOROALKYL-SUBSTITUTED ALKENES

1.3.1. Methylenation of Perfluoroalkyl Ketones using a Peterson Olefination Approach[38]

Another class of compounds that greatly benefits from CF_3 substitution is alkenes. Of particular interest is the 3,3,3-trifluoropropenyl ($CF_3CR=CR$-) moiety, which is attractive to medicinal chemistry as an isostere to certain amino acid groups,[39] and to agrochemistry[40] as a key intermediate in the synthesis of potent insecticides (or, in some cases, insecticides[40a] themselves). Macrocycles containing this moiety, such as 26-trifluoro-(*E*)-9,10-dehydroepothilone,[41] are promising anti-cancer compounds, while conjugating the 3,3,3-trifluoropropenyl group into higher order π-systems yields potential organic light-emitting diodes (OLEDs).[42]

The synthetic approach taken to prepare trifluoromethyl-functionalized alkenes is highly dependent on the location of the CF_3 group on the alkene. In the case of β-CF_3 alkenes, such as β-trifluoromethylstyrene derivatives, several strategies have been reported.[43] Of note are two recent reports by Buchwald[43a]and Prakash[43b] that contrast two distinct approaches to CF_3 alkene

[38] Hamlin, T. H.; Kelly, C. B.; Cywar, R. M.; Leadbeater, N. E. *J. Org Chem.*, **2014**, *79*, 1145.
[39] (a) Wipf, P.; Henninger, T. C.; Geib, S. J. *J. Org. Chem.* **1998**, *63*, 6088; (b) Xiao, J.; Weisblum, B.; Wipf, P. *J. Am. Chem. Soc.* **2005,** *127*, 5742; (c) Maes, V. ; Tourwé, D. *Aspects of Peptidomimetics, in Peptide and Protein Design for Biopharmaceutical Applications*; John Wiley & Sons, Ltd, Chichester, UK, **2009**; (d) Inokuchi, E.; Narumi, T.; Niida, A.; Kobayashi, K.; Tomita, K. Oishi, S.; Ohno, H.; Fujii N. *J. Org. Chem.* **2008**, *73*, 3942; (e) Kobayashi, K.; Narumi, T.; Oishi, S.; Ohno, H.; Fujii, N. *J. Org. Chem.* **2009**, *74*, 4626; (f) Fustero, S.; Chiva, G.; Piera, J.; Sanz-Cervera, J. F.; Volonterio, A.; Zanda, M.; Ramirez de Arellano, C. *J. Org. Chem.* **2009**, *74*, 3122.
[40] (a) Kobayashi, T.; Eda, T.; Tamura, O.; Ishibashi H. *J. Org. Chem.* **2002**, *67*, 3156; (b) Cassayre, J. Y.; Renold, P.; El Qacemi, M.; Pitterna, T.; Toueg, J. C. (Syngenta Crop Protection LLC) US Patent 20120238517 A1 **2012**; (c) Ikeda, E.; Komoda, M.; Maeda, K.; Mita, T.; Toyama, K.-I.; Yamada, Y. (Nissan Chemical Industries, Ltd.) European Patent EP 2199287 A1, **2010**.
[41] (a) Rivkin, A.; Yoshimura,F.; Gabarda, A. E.; Cho, Y. S.; Chou, T.-C.; Dong, H.; Danishefsky, S. J. *J. Am. Chem. Soc.* **2004**, *126*, 10913; (b) Wu, K.-D.; Cho Y. S.; Katz, J.; Ponomarev, V.; Chen-Kiang, S.; Danishefsky, S. J.; Moore, M. A. S. *Proc. Nat. Acad. Sci.* **2005**, *102*, 10640; (c) Rivkin, A.; Chou, T.-C.; Danishefsky, S. J. *Angew. Chem. Int. Ed.*, **2005**, *44*, 2838.
[42] Shimizu, M.; Takeda, Y.; Higashi, M.; Hiyama, T. *Angew. Chem. Int. Ed.* **2009**, *48*, 3653.
[43] (a) Parsons, A. T.; Senecal, T. D.; Buchwald, S. L. *Angew. Chem. Int. Ed.* **2012**, *51*, 2947; (b) Prakash, G. K. S.; Krishnan, H. S.; Jog, P. V.; Iyer, A. P.; Olah, G. A. *Org. Lett.* **2012**, *14*, 1146; (c) Iqbal, N.; Choi, S.; Kim, E.; Cho E. J. *J. Org. Chem.* **2012**, *77*, 11383; (d) Yasu, Y.; Koike, T.; Akita. M. *Chem. Commun.* **2013**, *49*, 2037; (e) Hanamoto,T.; Morita, N.; Shindo, K. *Eur. J. Org. Chem.* **2003**, 4279.

construction: *via* direct trifluoromethylation of activated alkenes, or by transition metal-mediated cross coupling using simple CF_3 alkenyl building blocks, respectively.

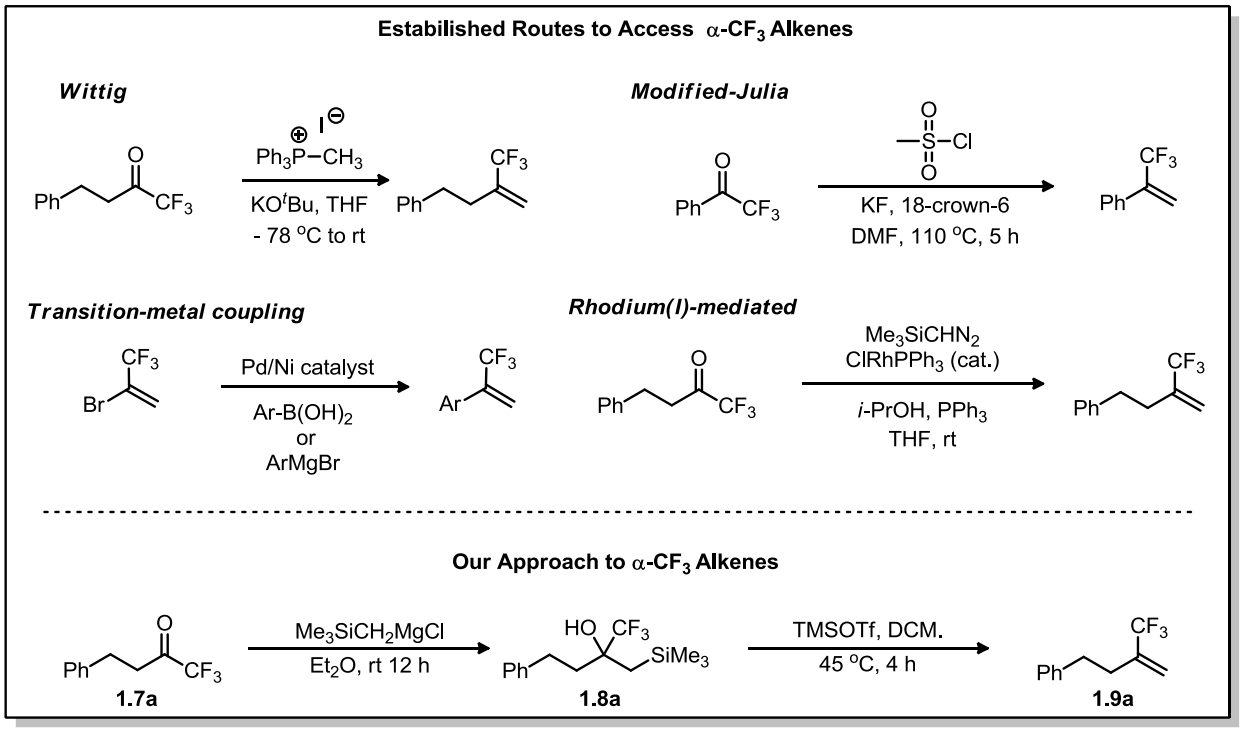

Figure 15: Strategies to access α-CF_3 alkenes from TFMKs

α-CF_3 Alkenes can be accessed by the methylenation of trifluoromethyl ketones (TFMKs) or by transition metal coupling. In the case of the former, classical approaches employing Wittig[44] chemistry or a modified Julia approach[45] have been utilized. A protocol using Wilkinson's catalyst, $ClRh(PPh_3)_3$, has also been developed.[46] However, excess PPh_3 and trimethylsilyldiazomethane are required, limiting scalability and requiring the use of a potentially explosive reagent. Alternatively, arenes can be coupled with 2-bromo-3,3,3-trifluoroprop-1-ene

[44] Representative example of this strategy: Ichikawa, J.; Yokota, M.; Kudo, T.; Umezaki, S. *Angew. Chem. Int. Ed.* **2008** , *47*, 4870.
[45] Nader, B. S.; Cordova, J. A.; Reese, K. E.; Powell, C. L. *J. Org. Chem.* **1994**, *59*, 2898.
[46] Lebel, H.; Paquet, V. *Org. Lett.* **2002**, *4*, 1671.

using Suzuki,[47] Negishi,[48] or Kumada[49] coupling reactions. While useful, these methods are limited to preparing α-CF_3 styryl derivatives.

Building on our successes in developing methods to access various TFMKs,[6] we envisioned that constructing α-perfluoroalkyl alkenes by dehydrative desilylation in a Peterson manner[50] might offer an attractive alternative to the established protocols. To our knowledge, no such approach had been reported previously. Such a methodology has several advantages over current approaches: (1) it would be metal- and phosphine-free, (2) it would avoid the use of highly toxic trimethylsilyldiazomethane, (3) the process would be scalable, (4) the reaction conditions would be mild, (5) the reaction is operationally simple, and (6) reagents are low cost.

We began our investigation by first constructing a representative α-trifluoromethyl-β-hydroxysilyl alcohol, **1.8a**. With this alcohol in hand, we explored a variety of acid catalysts to promote dehydrative desilylation to yield the desired alkene **1.9a** (Table 6). Initially, we hoped to use the crude ethereal mixture of **1.8a** obtained after workup and treat it with hydrochloric acid to facilitate elimination (Table 6, Entry 1). However, we did not observe any elimination in this case. We then transitioned to other solvents and screened a variety of protic and aprotic Lewis acids to evaluate the propensity for dehydrative desilylation. Surprisingly, **1.8a** proved remarkably resilient to this transformation with nearly all traditional Lewis acids giving little to no **1.9a** (Table 6, Entries 2-9). This is in stark contrast to traditional Peterson olefination reactions, which proceeds easily using HCl or other standard Lewis acids.[50] The combined effect of diminished oxygen nucleophilicity and high activation barrier for E2-like elimination makes

[47] Pan, R.-q.; Liu, X.-x.; Deng, M.-z. *J. Fluorine Chem.* **1999**, *95*, 167.
[48] Jiang, B.; Xu, Y. *J. Org. Chem.* **1991**, *56*, 7336.
[49] Kobayashi, O.; Uraguchi, D.; Yamakawa, T. *J. Fluorine Chem.* **2009**, *130*, 591.
[50] ***Seminal work:*** Peterson, D. J. *J. Org. Chem.*, **1968**, *33*, 780. ***Recent review:*** van Staden, L. F.; Gravestock, D.; Ager, D. J. *Chem. Soc. Rev.* **2002**, *31*, 195.

the olefination process too energetically unfavorable (Figure 16).[50] To circumvent this, we turned to a more powerful catalyst, TMSOTf, and encountered success, albeit with low conversion.

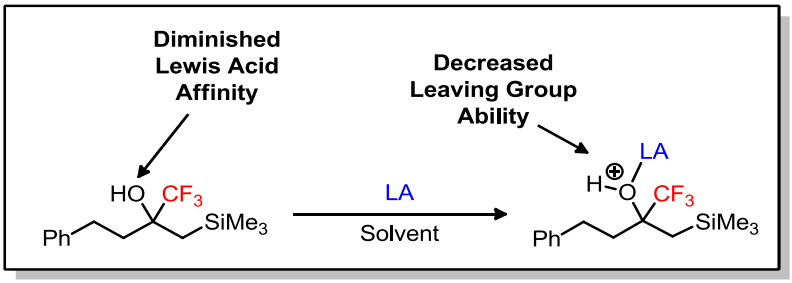

Figure 16: Possible explanation for resistance to dehydrative desilylation

Solvent had a significant role, with dichloromethane being superior to the more Lewis basic diethyl ether and acetonitrile. To expedite elimination, we chose to heat the reaction to reflux and slightly increase the loading of TMSOTf from 0.10 to 0.15 equiv, allowing complete conversion to the desired alkene in 4 h.

Table 6: Catalyst screen for dehydrative desilylation[a]

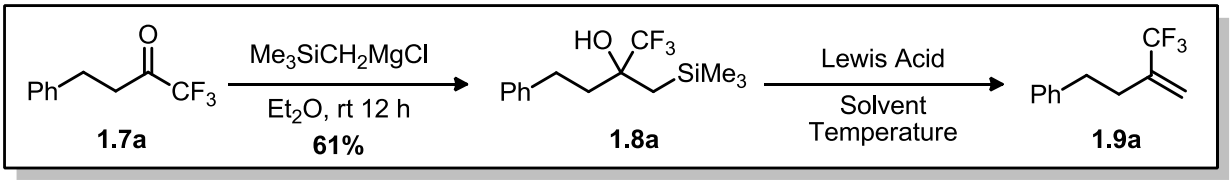

Entry	Solvent	Lewis Acid Catalyst	Temp. (°C)	Time (h)	Conversion (%)[b]
1[c]	Et_2O	2M HCl	25	1.0	0
2	DCM	$Sc(OTf)_3$	25	0.5	0
3	DCM	$Gd(OTf)_3$	25	0.5	0
4	DCM	$Mg(OTf)_2$	25	0.5	0
5	DCM	TFA	25	0.5	0
6	DCM	p-TSA	25	0.5	0
7	DCM	$SnCl_4$	25	0.5	0
8	DCM	$BF_3 \cdot OEt_2$	25	0.5	0
9	DCM	TfOH	25	0.5	Trace
10	Et_2O	TMSOTf	25	1.0	0
11	MeCN	TMSOTf	25	0.5	0
12	DCE	TMSOTf	25	0.5	9
13	DCM	TMSOTf	25	0.5	16

Entry	Solvent	Lewis Acid Catalyst	Temp. (°C)	Time (h)	Conversion (%)[b]
14	DCM	TMSOTf	45	0.5	30
15[d]	DCM	TMSOTf	45	1.0	55
16[d]	DCM	TMSOTf	45	4.0	100 (74)[e]

[a]Reaction conditions unless otherwise noted: **1.7a** (0.3 mmol, 1 equiv.), catalyst (0.03 mmol, 0.1 equiv.), solvent (1.5 mL) [b]Conversion determined by ^{1}H NMR [c]0.5 equiv catalyst used [d]0.15 equiv. catalyst used [e]Value in parentheses indicates isolated yield of **1.9a**.

With the optimized reaction conditions in hand, we next explored the scope of this process. We were pleased to find that our protocol could be extended to a range of functionalities. Electron-rich (Table 7, Entries 1-3, 5) and electron-poor arenes (Table 7, Entry 4) were both tolerated under our reaction conditions, though with a significant disparity in reactivity. Electron-rich and electron-neutral arenes underwent elimination in as little as 15 min at room temperature, while electron- poor arenes required our original optimized conditions. An exception to this trend is **1.8d** (Table 7, Entry 3). This substrate behaved much like an electron-poor arene, requiring a significantly higher reaction temperature and catalyst loading to reach completion. This reversal of reactivity can likely be attributed to protonation of the dimethylamino group during the course of the reaction, thereby preventing electron donation into the ring system. Heteroarenes (Table 7, Entries 7 and 8) showed a similar, more pronounced disparity in reactivity based on the electronics of the ring system. We attribute the failure of the pyridyl system (Table 7, Entry 7) to a similar rationale to the dimethylaniline case. The protonation (or silylation) of the nitrogen combined with the inherent deactivation of the pyridyl ring prohibited dehydrative desilylation.

We next explored aliphatic carbinols and found that unbranched and branched examples were amenable to dehydrative desilylation (Table 7, Entries 9-11). A representative furyl system (Table 7, Entry 12) was also screened in these trials. However, extensive polymerization occurred when attempting dehydrative desilylation of this substrate, even at lower temperatures

and catalyst loadings. We next turned our attention to different perfluoroalkyl groups (Table 7, Entries 13-15). As one might expect, the more destabilizing α-CF_2CF_3 group required higher temperatures to facilitate elimination; hence, dichloroethane (DCE) was employed as the solvent. Likewise, the less destabilized α-CF_2H and α-CFH_2 carbinols underwent dehydrative desilylation more rapidly than their trifluoromethyl congeners.

Table 7: Scope of the dehydrative desilylation of α-perfluoroalkyl-β-hydroxysilyl carbinols[a]

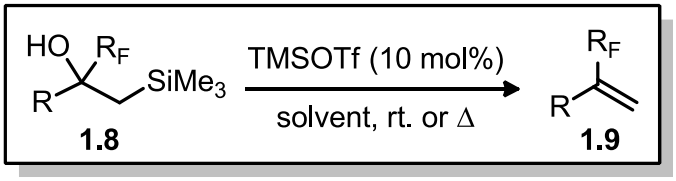

Entry	β-Hydroxysilyl Alcohol	Alkene	Temp. (°C)	Time (min)	Yield (%)[b]
1	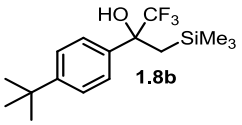	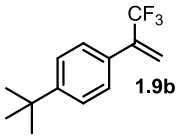	25	15	86
2	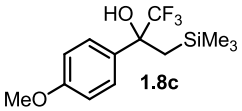	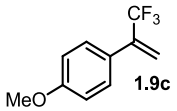	25	15	80 (88)[c]
3[d,e]	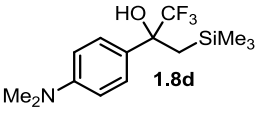	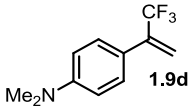	90	270	95
4	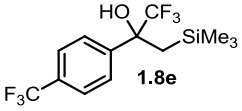	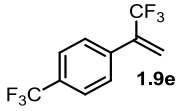	45	240	63
5	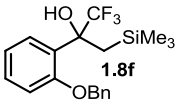	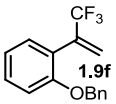	25	15	85
6	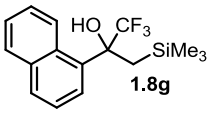	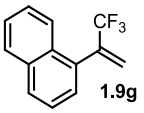	25	15	91

Entry	β-Hydroxysilyl Alcohol	Alkene	Temp. (°C)	Time (min)	Yield (%)[b]

7[d]	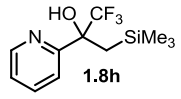 **1.8h**	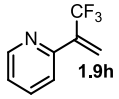 **1.9h**	90	270	-[f]
8	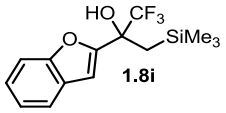 **1.8i**	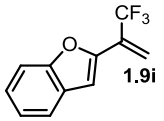 **1.9i**	25	15	86
9	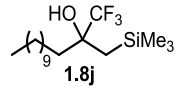 **1.8j**	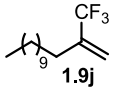 **1.9j**	45	240	88
10	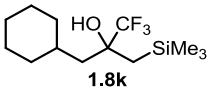 **1.8k**	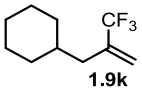 **1.9k**	45	240	65
11	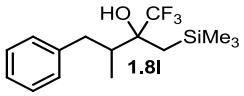 **1.8l**	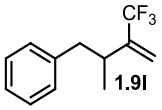 **1.9l**	45	240	84
12	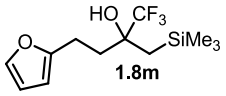 **1.8m**	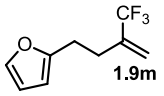 **1.9m**	-78	60	-[g]
13	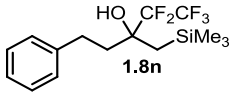 **1.8n**	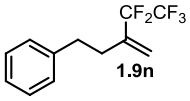 **1.9n**	90	240	84
14[d]	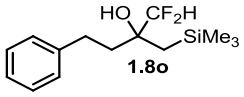 **1.8o**	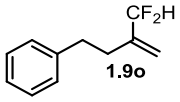 **1.9o**	25	15	92
15	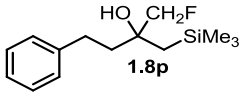 **1.8p**	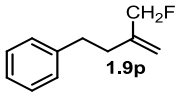 **1.9p**	25	15	72
16	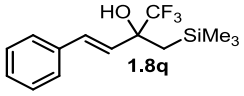 **1.8q**	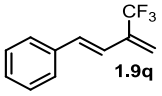 **1.9q**	25	15	80
17	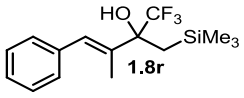 **1.8r**	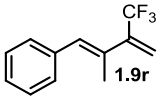 **1.9r**	25	15	86
18	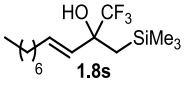 **1.8s**	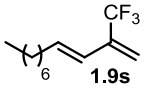 **1.9s**	25	60	85
19	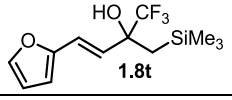 **1.8t**	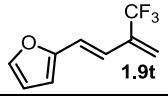 **1.9t**	25	30	-[g]

[a]Reaction conditions unless otherwise noted: Alcohol **1.8** (1 equiv), TMSOTf (0.15 equiv), DCM (0.2 M in alcohol) [b]Isolated yields [c]Values in parentheses indicates isolated yield of alkene on 57 mmol scale [d]Performed in DCE [e]0.3 equiv of TMSOTf was used [f]No reaction even at 2 equiv TMSOTf loading [g]Extensive polymerization

We also investigated whether conjugated dienes could be accessed *via* this methodology and we met mixed success. While cinnamyl-derived and straight chain dienes (Table 7, Entries 16-

18) could be prepared in good yield, the furyl-substituted alkene (Table 7, Entry 19) gave the same result as its saturated counterpart (Table 7, Entry 12); namely polymerization. Finally, it should be noted that in nearly all cases, the intermidate carbinol can be carried directly to the dehydrative desilylation reaction without need for further purification. Additionally, this process can be scaled up substantially (Table 7, Entry 2, 57 mmol scale) without compromising yield.

To probe the utility of the alkene products prepared in this study, we conducted several derivatization reactions using **1.9c** as a representative alkene (Figure 17). We selected reactions that would either provide potentially valuable synthons for further elaboration or that demonstrate key functionalizations that capitalize on the unique electronic nature of the 3,3,3-trifluoropropenyl system. We first explored difluoromethylcyclopropanation using the conditions recently disclosed by Hu and Prakash.[51] We were pleased to find we could obtain the highly-fluorinated cyclopropane **1.9c'** in excellent yield. Next, we sought to convert our representative alkene into a potential partner for cross-coupling processes. We successfully prepared the vinyl bromide **1.9c″** in similarly good yield using a modified literature protocol.[52] Next, based on reports by Bégué and Bonnet-Delpon,[53] we sought to access functionalized *gem*-difluoroalkenes by treatment of **1.9c** with the appropriate organolithium species. While we were unable to react phenyllithium successfully with **1.9c**, treatment with lithiated piperidine led to the successful amination and the generation of difluoroalkene **1.9c‴** in good yield. Finally, we subjected **1.9c**

[51] Wang, F.; Luo, T.; Hu, J.; Wang, Y.; Krishnan, H. S.; Jog, P. V.; Ganesh, S. K.; Prakash, G. K. S.; Olah, G. A. *Angew. Chem. Int. Ed.*, **2011**, *50*, 7153.
[52] Alem, K. v.; Belder, G.; Lodder, G.; Zuilhof, H. *J. Org. Chem.* **2005**, *70*, 179.
[53] (a) Begue, J.-P.; Bonnet-Delpon, D.; Rock, M. H. *Tetrahedron Lett.*, **1995**, *36*, 5003; (b) Begue, J.-P.; Bonnet-Delpon, D.; Rock, M. H. *J. Chem. Soc., Perkin Trans. 1* **1996**, 1409.

to dihydroxylation using traditional Upjohn conditions.[54] This too was successful, giving the diol **1.9c′′′′** in 85% yield.

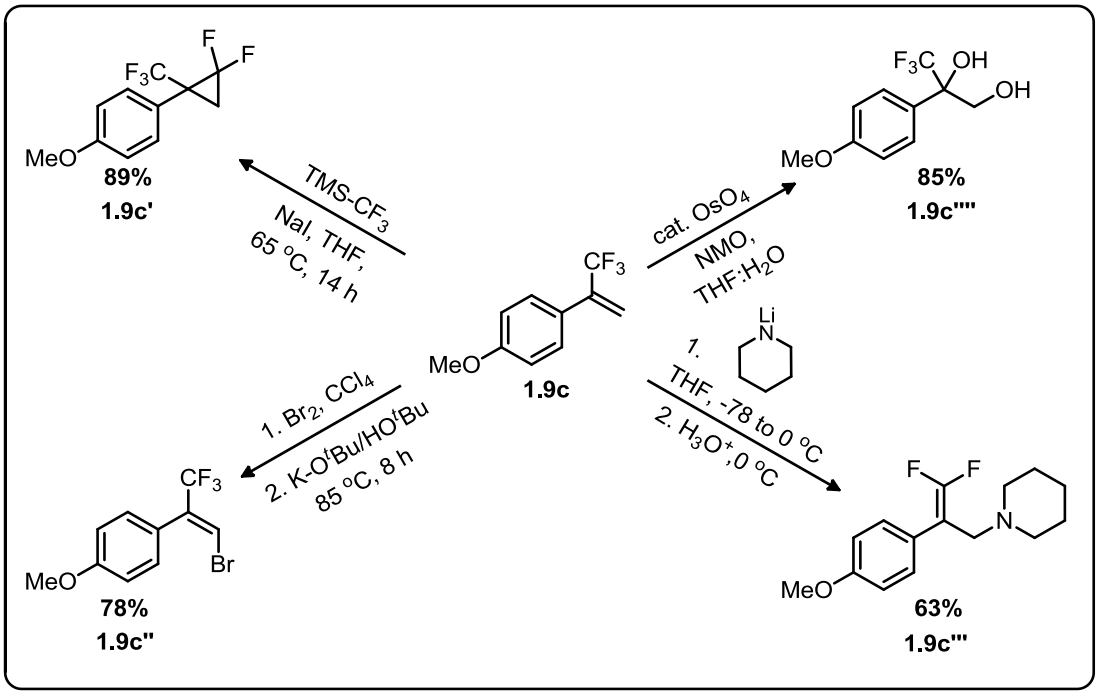

Figure 17: Applications of α-CF_3-substituted alkenes

In summary, we have developed an effective, user-friendly methodology for the preparation of α-perfluoroalkyl-functionalized alkenes by the dehydrative desilylation of α-trifluoromethyl-β-hydroxysilyl carbinol using TMSOTf. The reaction is compatible with a range of functionalities and the alkene products can be obtained in good to excellent yields. The reaction is scalable and minimal product purification is required. Finally, these alkenes can be used to access a number of valuable fluorinated products.

[54] (a) Schneider, W. P.; McIntosh, A. V. (Upjohn) US Patent 2769824; (b) VanRheennen, V.; Kelly, R. C.; Cha, D. Y. *Tetrahedron Lett.* **1976**, *17*, 1973.

Chapter 2: Mechanistic Elucidation of Novel Organic Reactions Using Quantum Calculations

2.1 INTRODUCTION

The utility of employing quantum chemical calculations as a tool to gain insight into complex chemistry is an ever popular endeavor.[55] In the 1960's, Hoffman reported the utility of extended Hückel theory to solve fundamental problems, such as the rotational barriers in various hydrocarbons.[56] There are earlier examples of work in the field, but this was one of the first examples of calculations successfully describing non-aromatic systems. The field has blossomed significantly since then, due in part to Pople's work in the development of the Gaussian program.[57] Much of the computational work summarized herein, has been calculated using Gaussian 09.[58] Calculations have extended beyond the gas-phase and can now be performed in numerous solvents using solvation parameters[59], albeit some caution should be exercised[60]. With the development of accurate density functionals and ever-increasing computational power, quantum chemical studies have become essential to a well-rounded study.[61] Key thermodynamic quantities can be calculated, allowing for the population of potential energy surfaces. By modeling the reactants, transition-states, and products, one can compare the energies for a number of potential pathways. This critical analysis makes use of transition-state theory, which

[55] Young, D. *Computational Chemistry: A Practical Guide for Applying Techniques to Real World Problems*; Wiley: New York, **2001**.
[56] Hoffmann, R. *J. Chem. Phys.* **1963**, *39*, 1397
[57] Hehre, W. J.; Radom, L.; Schleyer, P. v. R.; Pople, J. A. *Ab Initio Molecular Orbital Theory*; Wiley: New York, **1986**.
[58] Frisch, M. J. et al. Gaussian 09, revision A.02; Gaussian, Inc.:Wallingford, CT, **2009**
[59] Miertuš, S.; Scrocco, E., Tomasi, J. *Chem. Phys.*, **1981**, *55*, 117.
[60] Plata, R. E.; Singleton, D. A. *J. Am. Chem. Soc.* **2015**, *137*, 3811.
[61] ***For a recent perspective, see:*** Cheng, G.-J.; Zhang, X.; Chung, L. W.; Xu, L.; Wu, Y.-D. *J. Am. Chem. Soc.* **2015**, *137*, 1706−1725.

has been met with considerable success to a wide variety of processes.[62] There are a number of other techniques that are useful for probing chemical reactivity *in silico*, such as: molecular dynamics[63] and Monte Carlo[64], however, these will not be focused on in this thesis. We have made use of transition-state theory for the study of various chemistries, described below.

[62] Laldler, K. J.; King, M. C. *J. Phys. Chem.* **1983**, *87*, 2657.
[63] (a) McCammon, J. A.; Harvey, S. C. *Dynamics of Proteins and Nucleic Acids*; Cambridge University: Cambridge, **1987**; (b) McCammon, J. A.; Karplus, M. *Acc. Chem. Res.* **1983**, *16*, 187.
[64] ***For a review,* see**: Jorgensen, W. L. *J. Phys. Chem*. **1983**, *87*,5304.

2.2 QUANTUM CHEMICAL CALCULTIONS OF CF_3 CYCLOPROPANES[65]

2.2.1 Background on Accessing Trifluoromethylcyclopropanes via 1,3-γ-Silyl Elimination

The construction of highly-strained ring systems and the creation of quaternary centers are arduous processes coveted by synthetic chemists. One unique unexplored route to simultaneously perform these tasks exploits 1,3-γ-silyl elimination. In 1946, Sommer and Whitmore reported on the ability of a γ-silyl substituent to donate electron density to the α-carbon, thereby enhancing the reactivity of this centre.[66] Subsequently, this type of interaction has been observed in a wide variety of γ-silyl scaffolds, particularly in carbocationic systems.[67,68] Shiner and others reported on homohyperconjugative stabilization of the developing p-orbital of a cationic center by back-lobe ("percaudal") participation of the C-Si bond of the γ-silyl substituent.[67,68] Unfortunately, this transient percaudal interaction has not been effectively harnessed for ring closure to access substituted cyclopropanes. Shiner and others have shown that the major product-forming pathways in the solvolysis studies of γ-silyl substituted sulfonate esters were solvent substitution with retention of stereochemistry (Figure 18, Product **2.2c**) and rearrangement to give β-silyl elimination (Figure 18, Product **2.2b**), with 1,3-γ-silyl elimination to give cyclopropanation

[65] Mercadante, M. A.; Kelly, C. B. Hamlin, T. A.; Delle Chiaie, K. R.; Fager, D. C.; Glod, B. L. C.; Hansen, K. E.; Hill, C. R.; Leising, R. M.; Lynes, C. L.; MacInnis, A. E.; McGohey, M. R.; Murray, S. A.; Piquette, M. C.; Roy, S. L.; Smith, R. M. Sullivan, K. R.; Truong, B. H.; Vailonis, K. M.; Gorbatyuk, V.; Leadbeater, N. E.; Tilley, L. J. *Chem. Sci.*, **2014**, *5*, 3983 – Reproduced by permission of The Royal Society of Chemistry (RSC).

[66] Sommer, L. H.; Dorfman, E.; Goldberg, G. M.; Whitmore, F. C. *J. Am. Chem. Soc.* **1946**, 68, 488.

[67] (a) Sommer, L. H.; Van Strien, R. E.; Whitmore, F. C. *J. Am. Chem. Soc.* **1949**, *71*, 3056; (b) Sommer, L. H.; Marans, N. S. *J. Am. Chem. Soc.* **1950**, *72*, 1935; (c) Fleming, I.; Goldhill, J. *J. Chem. Soc., Perkin Trans. 1*, **1980**, 1493; (d) Lambert, J. B.; Finzel, R. B. *J. Am. Chem. Soc.* **1982**, *104*, 2020; (e) Shiner Jr., V. J.; Davidson, E. R. *J. Am. Chem. Soc.* **1986**, *108*, 3135; (f) Coope, J.; Shiner Jr., V. J.; Ensinger, M. W. *J. Am. Chem. Soc.* **1990**, *112*, 2834; (g) Shiner Jr., V. J.; Ensinger, M. W.; Rutkowske, R. D. *J. Am. Chem. Soc.* **1987**, *109*, 804; (h) Creary X.; Kochly, E. D. *J. Org. Chem.* **2009**, *74*, 9044; (i) Fleming, I.; Patel, S. K.; Urch, C. *J. Chem. Soc., Perkin Trans. 1*, **1989**, 115; (j) Fujio, M.; Nakashima, T.; Fujiyama, R.; Kim, H.-J.; Tsuno, Y. *J. Phys. Org. Chem.* **2000**, *13*, 612; (k) Tilley, L. J.; Shiner Jr., V. J. *J. Phys. Org. Chem.* **1999**, *12*, 564; (l) Coope, J.; Shiner Jr., V. J. *J. Org. Chem.*, **1989**, *54*, 4270.

[68] (a) Shiner Jr., V. J.; Kriz, G. S.; Halley K. A.; Ensinger, M. W. *J. Org. Chem.*, **1990**, *55*, 653; (b) Bentley, W. T.; Kirmse, W.; Llewellyn G.; Sollenbohmer, F. *J. Org. Chem.* **1990**, *55*, 1536; (c) Kirmse, W.; Sollenbohmer, F. *J. Am. Chem. Soc.*, **1989**, *111*, 4127.

(Figure 18, Product **2.2a**) being a minor path.[67g] Even cyclic systems, wherein the leaving group and the γ-silyl substituent are in the ideal cis "W" conformation for maximum percaudal interaction, gave only slightly higher percentages of cyclopropanation (Product **2.2a**).[68a]

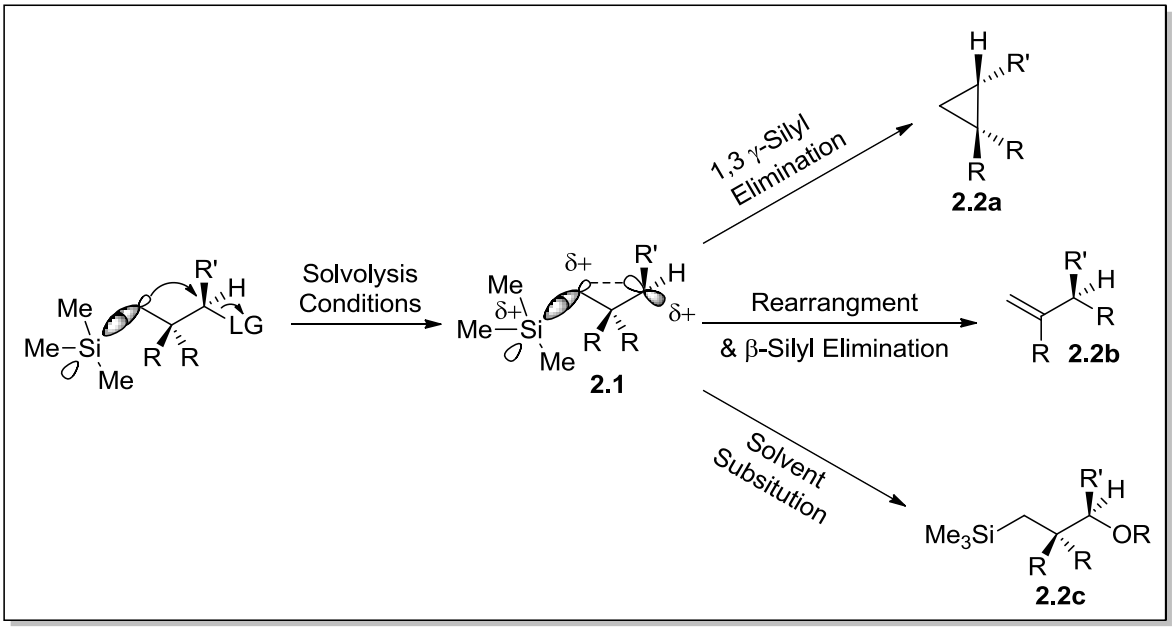

Figure 18: Possible pathways of γ-silyl stabilized carbocations

One logical solution to enhance cyclopropanation would be to increase the electron-donating character of the γ-substituent. Indeed, Kuivila reported that the solvolysis of 1-aryl-3-trimethylstannyl 3,5-dinitrobenzoates led exclusively to cyclopropanation *via* 1,3-γ-stannyl elimination.[69] Elimination products in Yoshida's competitive study of a dual γ-stannyl and γ-silyl system arose solely from the γ-stannyl substituent.[70] However, potentially toxic organostannanes limit the synthetic utility of this solvolytic reaction. As a potential surrogate for a γ-stannyl group, we hypothesized that an umpolung strategy would be to augment the γ-silyl percaudal

[69] (a)McWilliam, D. C.; Balasubramanian, T. R.; Kuivila, H. G. *J. Am. Chem. Soc.* **1978**, *100*, 6407; (b) Verdone, J. A.; Mangravite, J. A.; Scarpa, N. M.; Kuivila, H. G. *J. Am. Chem. Soc.* **1975**, *97*, 843; (c) Kuivila, H. G.; Scarpa, N. M. *J. Am. Chem. Soc.* **1970**, *92*, 6990.
[70] Yoshida, J.; Sugawara, M. *J. Org. Chem.* **2000**, *65*, 3135.

interaction by installing a CF_3 group at the α-carbon. Work by Gassman and others supports this hypothesis by suggesting that "the placement of a strongly electron-withdrawing group at the incipient cationic center can magnify the influence of a related series of neighboring groups" by generating an "electron-deficient" carbocation.[71] This strategy is supported by the known delocalization of electron density from adjacent π- and σ-orbitals into the C-F σ*-orbital.[72]

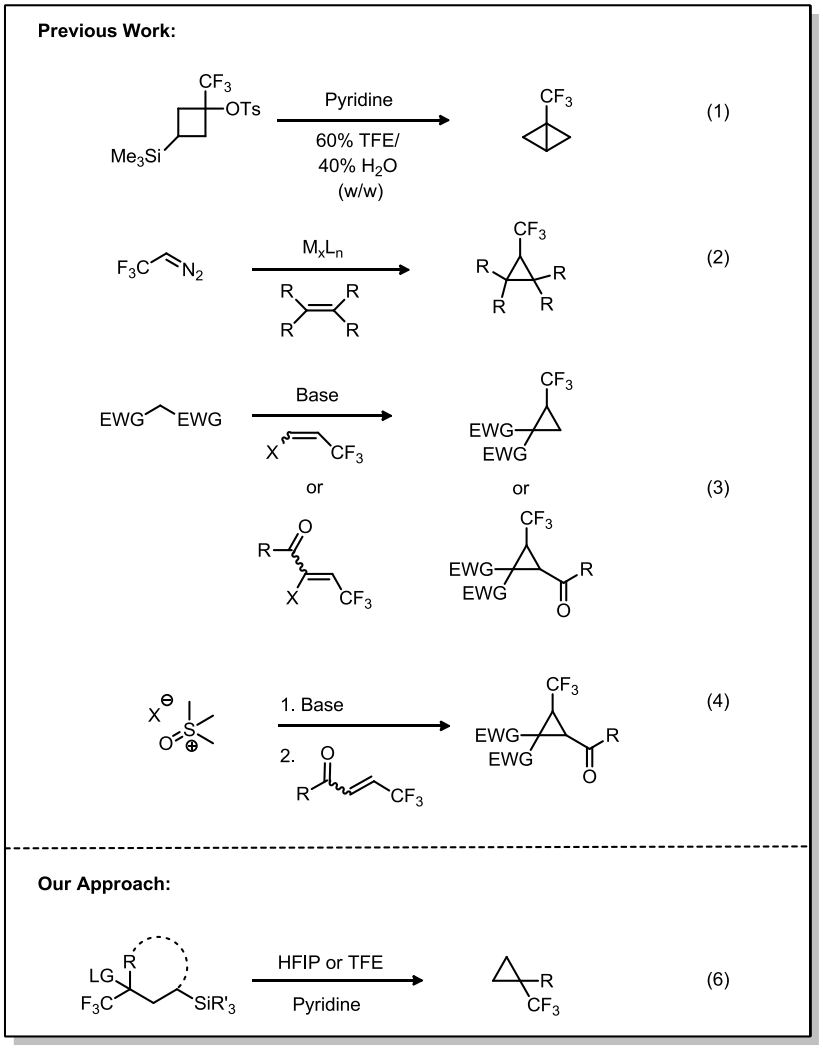

Figure 19: Overview of current methods for effecting trifluoromethylcyclopropanation and our approach

[71] (a) Gassman, P. G.; Hall, J. B. *J. Am. Chem. Soc.* **1984**, *106*, 4267; (b) Gassman, P. G.; Doherty, M. M. *J. Am. Chem. Soc.* **1982**, *104*, 3742; (c) Nelson, D. W.; O'Reilly, N. J.; Speier, J.; Gassman, P. G. *J. Org. Chem.*, **1994**, *59*, 8157. (d) Gassman P. G.; Tidwell, T. T. *Acc. Chem. Res.* **1983**, *16*, 279.

[72] (a) Borden, W. T. *Chem. Commun.*, **1998**, 1919; (b) Greenberg, A.; Liebman, J.; Dolbier Jr., W. R.; Medinger, K. S.; Skancke, A. *Tetrahedron*, **1983**, *39*, 1533.

Trifluoromethylcyclopropanes (CF_3 cyclopropanes) are highly attractive synthetic targets for medicinal chemists due to their compact, rigid structure and their lipophilic properties.[1a,73,74] This small-ring motif can be found in a variety of recent candidates for the treatment of cancer, hepatitis, HIV, obesity, diabetes, and inflammatory diseases as well as in potential pharmacons for management of cholesterol levels and pain.[73b] Likewise, CF_3 cyclopropane-containing substances have found use as pesticides and paratiscides.[73b] Recently, the CF_3 cyclopropyl group has been found to be a suitable replacement for the *tert*-butyl group, but with enhanced metabolic stability.[75]

A member of our group had previously validated this strategy by synthesizing the highly strained 1-(trifluoromethyl)bicyclo[1.1.0]butane via exclusive 1,3-γ-silyl elimination (Figure 19, Eq. 1).[76] This result was in stark contrast to studies by Creary and co-workers on analogous γ-trimethylsilyl alkyl cyclobutyl systems in which no 1,3-γ-silyl elimination was observed.[67h] After showing the generality of our method in the context of a potential synthetic route to CF_3 cyclopropanes containing a quaternary center, we sought to explore the 1,3-γ-silyl interactions using quantum calculations.

[73] (a) Duncton, M. A. J.; Singh, R. *Org. Lett.* **2013**, *15*, 4284; (b) Grygorenko, O. O.; Artamonov, O. S.; Komarov, I. V.; Mykhailiuk, P. K. *Tetrahedron* **2011**, *67*, 803.
[74] ***Information on cyclopropanes in medicinal chemistry*:** (a) Donaldson, W. A. *Tetrahedron* **2001**, *57*, 8589; (b) Faust, R. *Angew. Chem. Int. Ed.* **2001**, *40*, 2251; (c) Salaün, J. *Top. Curr. Chem.* **2000**, *207*, 1.
[75] Barnes-Seeman, D.; Jain, M.; Bell, L.; Ferreira, S.; Cohen, S. Chen, X.-H.; Amin, J.; Snodgrass, B.; Hatsis. P. *ACS Med. Chem. Lett.* **2013**, *4*, 514.
[76] Kelly, C. B.; Colthart, A. M.; Constant, B. D.; Corning, S. R.; Dubois, L. N. E.; Genovese, J. T.; Radziewicz, J. L.; Sletten, E. M.; Whitaker, K. R.; Tilley, L. J. *Org. Lett.*, **2011**, *13*,1646

2.2.2 Quantum Calculations on CF_3 Cyclopropanes Formation via 1,3-γ-Silyl Elimination

Quantum chemical calculations were performed using Gaussian 09.[58] All optimized geometries were calculated using B3LYP[77], a hybrid density functional, with the 6-31+G(d) basis set[78]. For γ-stannyl systems, geometry optimizations were carried out using B3LYP and a mixed basis set of LANL2DZ[79] for Sn and 6-31+G(d) for all other atoms. This modified calculation was employed to more accurately describe the electronic nature of the γ-stannyl group. The addition of diffuse functions to the double split-valence basis set ensured an adequate description of the charged systems and the effect of the $-CF_3$ group. Stationary points were characterized by frequency calculations at 298 K, with structures at energy minima showing no negative frequencies and transition-states showing one negative frequency. Intrinsic reaction coordinate (IRC) calculations[80] followed by optimization and frequency calculation were performed on transition state structures to connect the two respective ground states. Thermal energies, enthalpies and Gibbs free energies were corrected using the appropriate thermodynamic correction factor. Solvation energies were evaluated using a self-consistent field (SCRF) using the polarization continuum model (PCM)[81] model. All energetic values shown are in kcal mol^{-1}; bond lengths are reported in Ångstroms (Å), bond and pyramidalization angles in degrees (˚). Molecular structures were generated using CYLView.[82]

[77] (a) Becke, A. D. *J. Chem. Phys*. **1993**, *98*, 5648; (b) Lee, C.; Yang, W.; Parr, R. G. *Phys. Rev. B* **1988**, *37*, 785; (c) Vosko, S. H.; Wilk, L.; Nusair, M. *Can. J. Phys.* **1980**, *58*, 1200; (d) Stephens, P. J.; Devlin, F. J.; Chabalowski, C. F.; Frisch, M. J. *J. Phys. Chem.* **1994**, *98*, 11623.
[78] (a) Ditchfield, R.; Hehre, W. J.; Pople, J. A. *J. Chem. Phys.*, **1971**, *54*, 724; (b) Hehre, W. J.; Ditchfield, R.; Pople, J. A. *J. Chem. Phys.*, **1972**, *56*, 2257; (c) Hariharan, P. C.; Pople, J. A. *Theor. Chim. Acta*, **1973**, *28*, 213.
[79] Hay, P. J.; Wadt, W. R. *J. Chem. Phys*. **1985**, *82*, 270.
[80] (a) Fukui, K. *Acc. Chem. Res*. **1981**, *14*, 363; (b) Hratchian, H. P.; Schlegel, H. B. *Theory and Applications of Computational Chemistry: The First 40 Years*, Dykstra, C. E.; Frenking, G.; Kim, K. S.; Scuseria, G. Elsevier, Amsterdam, **2005**, 195.
[81] (a) Miertuš, S.; Scrocco, E.; Tomasi, J. *Chem. Phys.* **1981**, *55*, 117; (b) Cammi, R.; Tomasi, J. *J. Chem. Phys.* **1994**, *100*, 7495.
[82] Legault, C. Y. CYLview, 1.0b. Université de Sherbrooke; **2009**. http://www.cylview.org.

First we investigated the cyclization for α-phenyl systems. The cyclization of aryl substrates likely proceeds via a carbocation intermediate because solvent substitution was observed and secondary KIEs supported reduced participation of the γ-group. The calculated secondary KIEs for **3a** and **3b** were found to be in excellent accord with experiment (computed KIE for 3a = 0.98; 3b = 0.96).

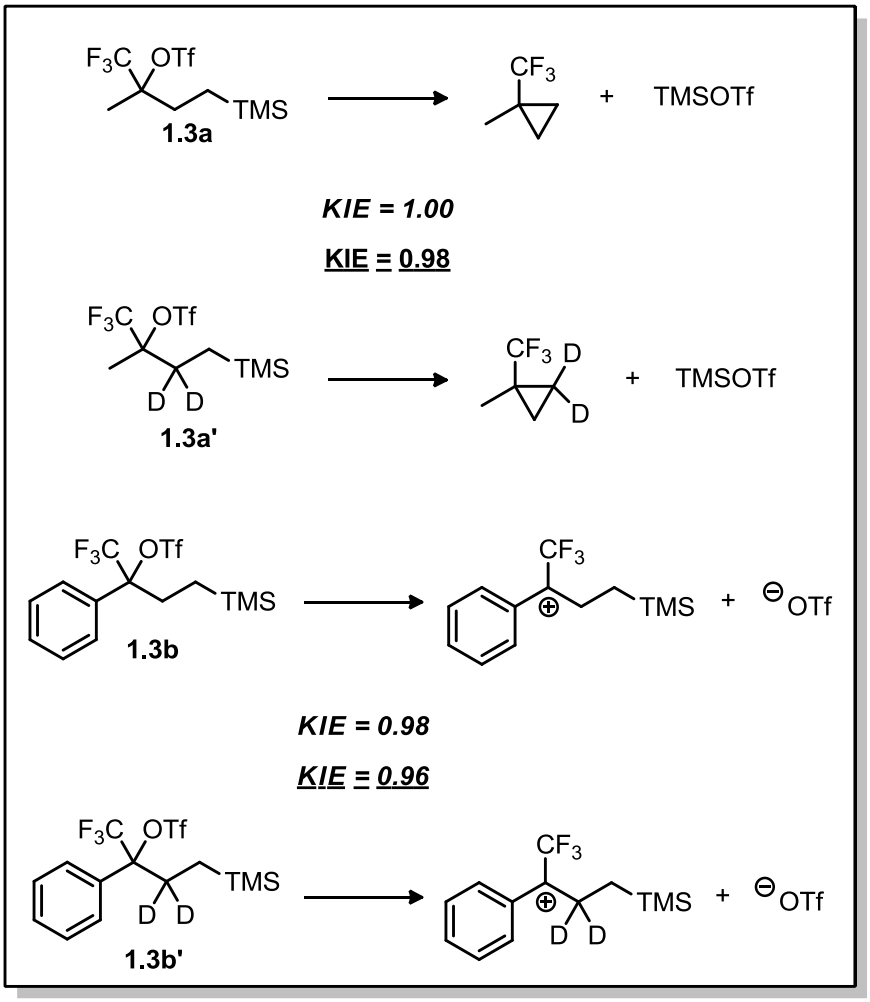

Figure 20: Systems for which the secondary KIE was determined. KIE in *italics* is experimental value. KIE underlined is the calculated value. See Appendix III for details.

Although the computed KIE results on the aliphatic and carbocyclic systems indicate extensive neighboring group participation, the lack of substitution does not provide sufficient

evidence to unambiguously conclude a mechanistic pathway. Exclusive 1,3-γ-silyl elimination could result from either poor solvent nucleophilicity preventing substitution on a bridged ion intermediate, or because of a concerted pathway. To further glean mechanistic insight, the electronic and conformational effects on γ-silyl participation (and subsequent 1,3-elimination) in α-CF_3 cationic systems were investigated by additional computational modeling.

An isodesmic study[83] of a-aryl systems (Figure 21) was conducted to elucidate the balance between phenyl resonance- and γ-silyl-mediated carbocation stabilization. Isodesmic studies are useful when comparing the energies of two systems with differing atomic composition. Notice that there are the same total number of atoms on the left and right of the arrow. In all cases γ-silyl cations were slightly more stable than their carbon analogs (Table 8). A clear inverse correlation can be observed between the degree of γ-silyl stabilization and the available electron density of the aryl ring (Table 8).

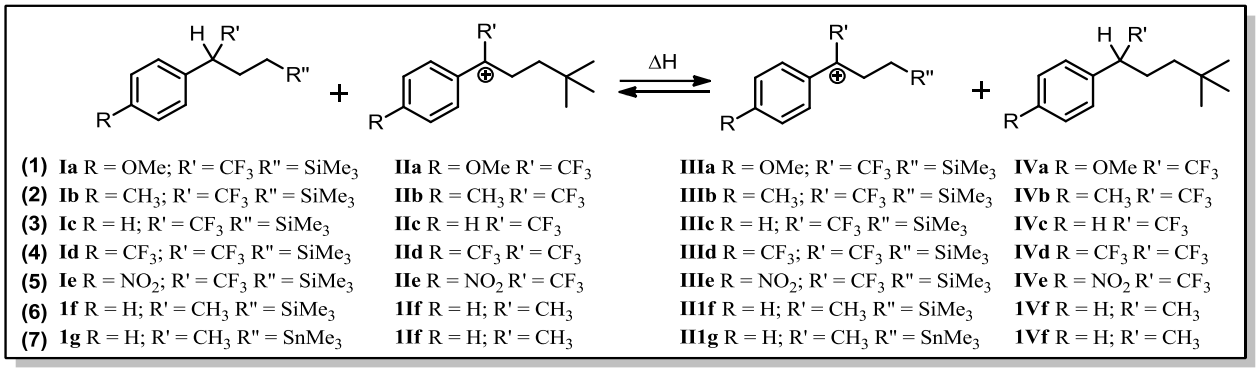

(1)	**Ia** R = OMe; R' = CF_3 R" = $SiMe_3$	**IIa** R = OMe R' = CF_3	**IIIa** R = OMe; R' = CF_3 R" = $SiMe_3$	**IVa** R = OMe R' = CF_3
(2)	**Ib** R = CH_3; R' = CF_3 R" = $SiMe_3$	**IIb** R = CH_3 R' = CF_3	**IIIb** R = CH_3; R' = CF_3 R" = $SiMe_3$	**IVb** R = CH_3 R' = CF_3
(3)	**Ic** R = H; R' = CF_3 R" = $SiMe_3$	**IIc** R = H R' = CF_3	**IIIc** R = H; R' = CF_3 R" = $SiMe_3$	**IVc** R = H R' = CF_3
(4)	**Id** R = CF_3; R' = CF_3 R" = $SiMe_3$	**IId** R = CF_3 R' = CF_3	**IIId** R = CF_3; R' = CF_3 R" = $SiMe_3$	**IVd** R = CF_3 R' = CF_3
(5)	**Ie** R = NO_2; R' = CF_3 R" = $SiMe_3$	**IIe** R = NO_2 R' = CF_3	**IIIe** R = NO_2; R' = CF_3 R" = $SiMe_3$	**IVe** R = NO_2 R' = CF_3
(6)	**1f** R = H; R' = CH_3 R" = $SiMe_3$	**1If** R = H; R' = CH_3	**III1f** R = H; R' = CH_3 R" = $SiMe_3$	**1Vf** R = H; R' = CH_3
(7)	**1g** R = H; R' = CH_3 R" = $SnMe_3$	**1If** R = H; R' = CH_3	**III1g** R = H; R' = CH_3 R" = $SnMe_3$	**1Vf** R = H; R' = CH_3

Figure 21: Isodesmic Calculations Evaluating γ-Silyl Stabilization of Cations **IIIa-g**

IIIa and **IIIb** are only slightly more energetically stable than **IIa** and **IIb**, respectively, due to more available ring electron density and, in the case of **IIIa**, an additional resonance contributor. This stabilization thereby mitigates the need for γ-silyl cation

[83] Hehre, W. J.; Ditchfield, R.; Radom, L. Pople, J. A. *J. Am. Chem. Soc.*, **1970**, *92*, 4796.

stabilization. However, **IIId** and **IIIe** are ~2 kcal mol^{-1} more stable than **IId** and **IIe**, respectively, due to diminished available ring electron density thereby necessitating enhanced γ-silyl participation. Comparison to the corresponding α-CH_3 substituted γ-silyl and γ-stannyl systems **IIIf** and **IIIg** leads further credence to the electronic intermediacy of our α-CF_3 γ-silyl system in terms of the γ-substituents ability to participate in cation stabilization. Little difference between **IIIf** and **IIf** confirms minimal participation[2k] of the γ-silyl group in 3^o system while the γ-stannyl system is ~2 kcal mol^{-1} more stabilizing and is consistent[67h,69] with its ability to contribute significantly *via* bridging in the aromatic systems even without the added demand of the α-CF_3 group. Energetically, the contribution of the γ-stannyl substituent appears to be equivalent to that of a γ-silyl system with both an α-CF_3 and a 4-CF_3-substituted-α-aryl substituent.

Table 8: Relative stabilization energies[a] and *HOMA* values for γ-metalloidal carbenium ions and the corresponding carbon analogues

Entry	Eq. in Scheme in Figure 21	ΔH^b kcal mol^{-1}	*HOMA*[c] IIa-g	*HOMA*[c] IIIa-g	Δ*HOMA*[d] (III - II)
a	(1)	-0.37	0.487	0.511	0.0242
b	(2)	-0.68	0.633	0.663	0.0296
c	(3)	-1.00	0.714	0.747	0.0335
d	(4)	-1.67	0.781	0.825	0.0448
e	(5)	-2.18	0.812	0.872	0.0609
f	(6)	-0.53	0.834	0.846	0.0111
g	(7)	-1.60	0.834	0.860	0.0257

[a]In kcal mol^{-1} at 298 K [b]A negative value indicates that the γ-silyl carbenium ion **IIa-e** is more stabilized that the corresponding carbon analog carbenium ion **IIIa-e** [c]HOMA values range from 0-1. HOMA = 0 for completely nonaromatic system and HOMA = 1 for fully aromatic system (all C-C bonds R_{opt} = 1.388 Å) [d] Difference between HOMA **IIa-e** and HOMA **IIIa-e**. Positive values indicate a higher degree of aromaticity.

To further probe these electronic effects, the relative degree of aromaticity of the α-aryl ring as a function of cation structure was assessed using the *Harmonic Oscillator Model of Aromaticity* (HOMA; Eq. 1) for **IIa**, **IIIa**, **IIb IIIb**, etc.[84]

$$(1)\ HOMA = 1 - \frac{a}{n}\sum_{i=1}^{n}(R_{opt} - R_i)^2$$

In Equation (1), α is a normalization constant (α = 257.7 for C-C bonds), *n* is the number of C-C bonds included in the summation, R_{opt} = 1.388 Å, and R_i = length of successive C-C bonds. Using HOMA, the degree of aromatic character of a system relative to benzene can be assessed numerically. A *HOMA* value of 0 corresponds to a completely nonaromatic system, while a *HOMA* of 1 is equal in aromatic character to benzene.

Analysis of the Δ*HOMA* values confirmed that in all cases the aryl ring had more aromatic character in γ-silyl systems than in their carbon analogues. This implies that the extent of aryl stabilization is diminished in these systems because of compensatory γ-silyl participation. As dispersal of charge into the aryl ring becomes less favorable, γ-silyl stabilization is enhanced and allows the ring system to retain a higher degree of aromaticity. With the removal of the CF_3 decreasing electronic demand, **IIIf** and **IIIg** both show little difference from the carbon analogue **IIf**; with the slightly higher degree of aromaticity **IIIg** consistent with participation from the tin.

For the 4-CF_3, 4-CH_3, and 4-H systems, thermodynamically favorable isodesmic values correlated with empirical cyclopropanation as did the γ-stannyl[69] system **IIIg**. However, experimental solvolysis of the 4-OMe system resulted in predominant solvent substitution, suggesting some thermodynamic threshold had been crossed. To better understand the relative energetics of the cyclization and solvolytic pathways, we

[84] (a) Kruszewski, J.; Krygowski, T. M. *Tetrahedron Lett.*, **1972**, *13*, 3839; (b) Kostenko, A.; Muller, B.; Kaufmann, F.-P.; Apeloig, Y.; Siehl, H.-U. *Eur. J. Org. Chem.*, **2012**, 1730.

populated the potential energy surface (Figure 22). Initial attempts to locate transition state structures involved chemical intuition. If these attempts proved fruitless, QST3 calculations were employed where the reactant, product and initial estimation of the transition state were inputted.[85]

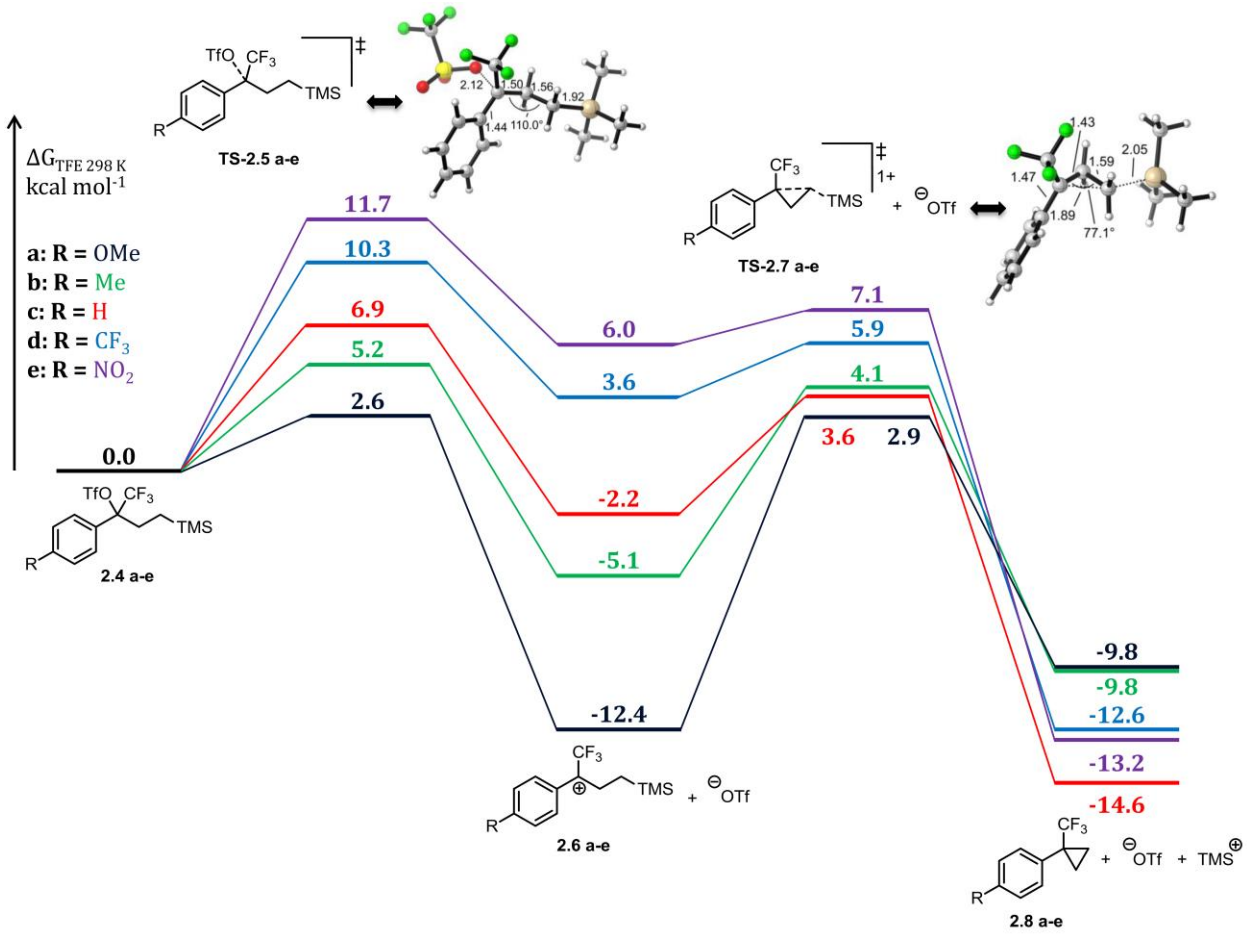

Figure 22: Reaction coordinate for the cyclopropanation of α-phenyl systems (**2.4a-e**). Relative Gibbs free energy values calculated at PCM-TFE-B3LYP/6-31+G(d). Numeric values indicate energies in kcal mol^{-1}.

The ionization step of **2.4a-c** is an exergonic process (summing cation and leaving-group anion energies), but is energetically unfavorable for **2.4d** and **2.4e**. The higher

[85] (a) Peng, C. Schlegel, H. B. *Israel J. of Chem.* **1993**, *33*, 449; (b) Peng, C.; Ayala, P. Y.; Schlegel, H. B.; Frisch, M. J. *J. Comp. Chem.* **1996**, *17*, 49.

activation barrier for **2.4d** explains the requisite heating in the experimental solvolysis study (**2.4e** was not studied experimentally). In the case of **2.4a**, however, the highly electron rich nature of the 4-OMe substituent indicates a potentially competing rate-determining second step, which can explain the preferential solvent substitution in this system.

In all observed cases, the energetics of the second step controls product formation. In this "product-determining" step of the solvolysis, the cyclization is exergonic for **2.6b-e**. Cyclization of cationic intermediates **2.6c-e** proceeds *via* **TS-2.7c-e**, the energy barrier for which decreases systematically as the aryl substituent becomes more deactivating. Once the 4-Me system is reached, the activation energy increases slightly compared to **2.6c**. This is likely due to the increased stability of the intermediate **2.6b** starting to disfavor the cyclization pathway. Indeed, in the case of **2.6a**, the predicted cyclization step becomes rate determining. This change in energetics suggests either a longer-lived cation for this pathway (allowing for competing substitution) or simply other potentially lower energy "product-determining" pathways. These alternative reaction pathways are consistent with our experimental observation that solvent substitution predominates. Efforts to locate a transition state for a substitution pathway were unsuccessful.

Attempts to perform analogous isodesmic studies of the straight-chain aliphatic and carbocyclic systems did not provide the expected results based on the assumption of a stable bridged ion-intermediate. Optimization of the ground-state structures of the γ-silyl cations of these systems resulted in spontaneous cyclization. No stable carbocationic intermediate could be located. Consistent with these results was location of an uncyclized intermediate cation for the α-CH_3 γ-silyl system analogous to **2.4c**, but only a cyclized

ground state for the α-CH_3 γ-stannyl analogue. Since the optimized ground state-structures of the silyl systems had different bond arrangements than their carbon analogs (which were located as the expected uncyclized carbocations), isodesmic studies could not be performed. The inability to locate a bridged ion, pointed toward a concerted mechanism or at least an ionization step with a very early transition state. Furthermore, in our attempts to locate a transition state corresponding to an ionization step, we discovered a transition state corresponding to both ionization and cyclization.

We therefore explored the potential energy surfaces of the straight-chain and carbocyclic systems with the premise that there is a single transition state involving both ionization and cyclization (Figure 23). In all cases the ring-closing reaction was exergonic and a marked difference in the activation barrier was observed between cyclic and acyclic systems (compare **TS-2.12a** to **TS-2.12c-e**). This disparity in energy likely stems from conformational restriction and is consistent with experimental requirements for less reactive leaving groups in the cyclic systems.

In a select case we also explored the competing concerted β-hydride elimination reaction pathway and compared it to the γ-silyl elimination path, as this was a system where some elimination was observed experimentally. Comparing the two pathways from straight chain systems leading to **TS-2.10a** and **TS-2.12a**, it is clear that the controlling factor for elimination in γ-silyl α-CF_3 cationic systems is almost certainly kinetic. While the cyclopropane **2.13a** is ultimately higher in energy, its activation barrier is significantly lower than the barrier leading to **2.11a** ($\Delta\Delta G^{\ddagger}$ = 3.0 kcal mol^{-1}), allowing this pathway to predominate.

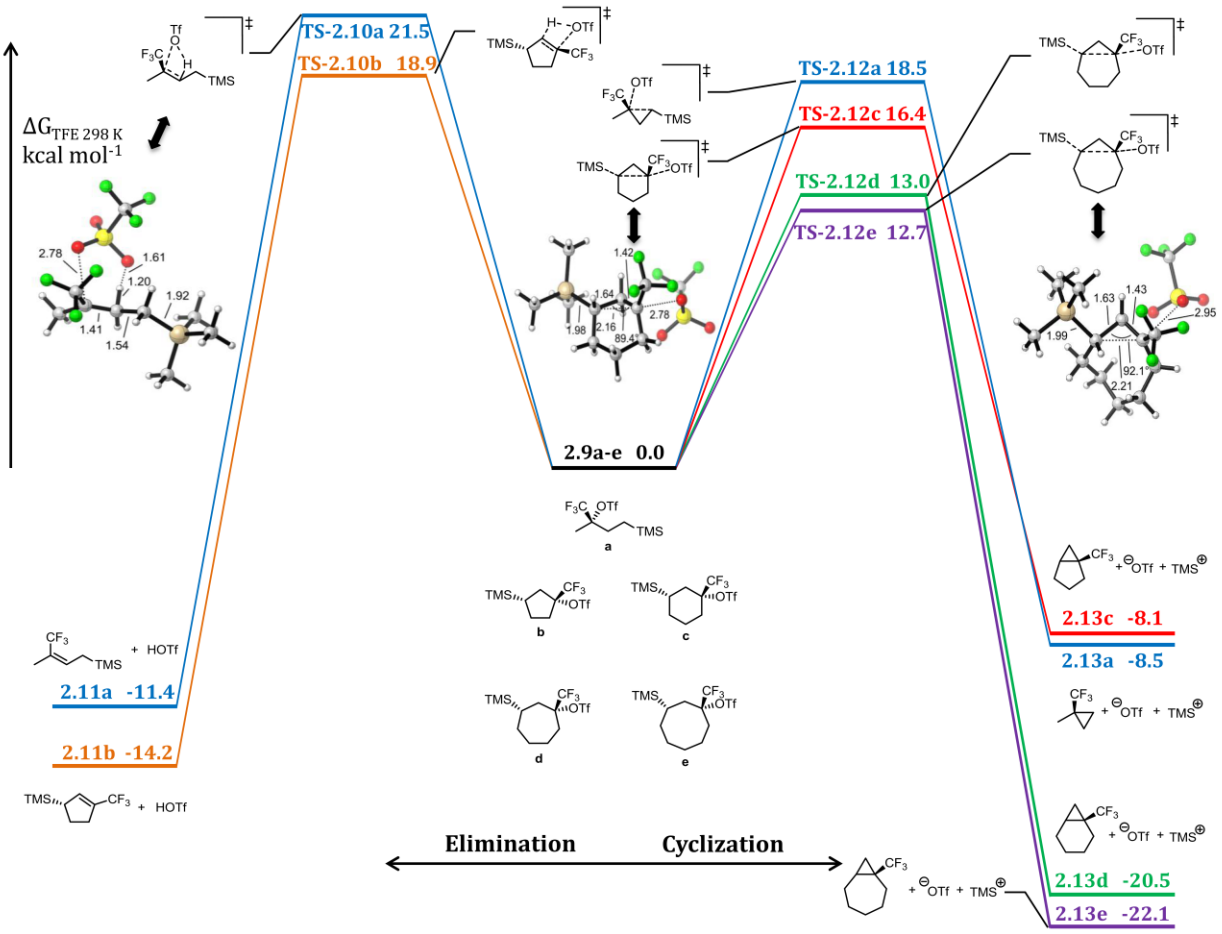

Figure 23: Reaction coordinate for the cyclopropanation of both cyclic and straight chain systems (**2.9a-e**). Relative Gibbs free energy values calculated at PCM-TFE-B3LYP/6-31+G(d). Numeric values indicate energies in kcal mol^{-1}.

Additionally, the so-called "perfluoroalkyl effect" initially described by Lemal, may provide some kinetic stability to this strained system by preventing electrophilic degradation and raising activation energies of isomerization.[86] In the case of the cyclopentyl system we could not locate a transition-state for cyclopropanation. The structure of the system cannot adopt the geometry required for γ-silyl stabilization; as a result the preferred stabilizing interaction was hyperconjugation of the β C-H bond,

[86] (a) Lemal, D. M.; Dunlap Jr., L. H. *J. Am. Chem. Soc*., **1972**, *94*, 6562; (b) Grayston, M. W.; Lemal, D. M. *J. Am. Chem. Soc*., **1976**, *98*, 1278; (c) Wirth, D.; Lemal, D. M. *J. Am. Chem. Soc*., **1982**, *104*, 847; (d) Lemal, D. M.; Staros, J. V.; Austel, V. *J. Am. Chem. Soc*., **1969**, *91*, 3373; (e) Greenberg, A.; Liebman, J. F.; Vechten, D. V. *Tetrahedron*, **1980**, *36*, 1161.

leading to concerted elimination (**2.11b**), which was observed from experimental solvolysis studies.

While treatment of most cyclic systems with assumption that both steps were concerted was appropriate, the cyclobutyl system proved to be an exception (Figure 24, **2.16**). Indeed, even unsubstituted cyclobutyl systems are known to receive anchimeric assistance from the C-C σ-bonds in the ring.[87] Such assistance would diminish the dependency on direct γ-silyl-promoted elimination and lead to a longer-lived ion. However, analysis of the ground state structure **2.16** still showed the hallmarks of γ-silyl stabilization (e.g. ring contraction, elongation of the C-Si bond).

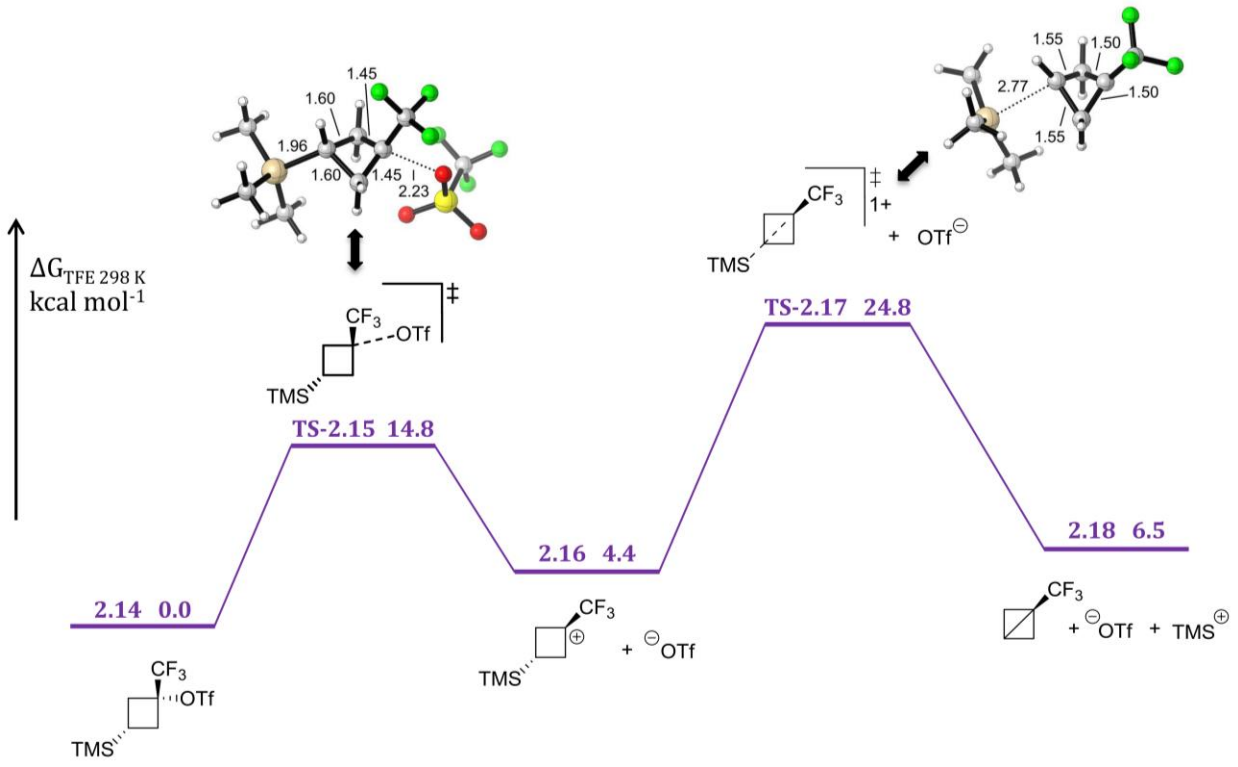

Figure 24: Reaction coordinate for the cyclopropanation of the cyclobutyl system (**2.14**). Relative Gibbs free energy values calculated at PCM-TFE-B3LYP/6-31+G(d). Numeric values indicate energies in kcal mol^{-1}.

[87] Roberts, D. J. *J. Org. Chem*. **1971**, *36*, 1913.

To quantify the degree of γ-silyl stabilization in this system, we conducted an isodesmic study in a manner similar to our previous study of the α-phenyl system (Figure 25, Table 8). This study revealed that not only was γ-silyl stabilization present, but it was quite substantial as compared to the straight-chain α-phenyl systems (-15.4 kcal mol^{-1} vs. -0.37 to -2.18 kcal mol^{-1}) and significantly more than the corresponding α-CH_3 system. To give a comparison of disparate stabilizing effects (resonance vs. anchimeric assistance), an isodesmic study was conducted using a α-vinyl substituent. This study produced stabilization energy more in line with the α-phenyl systems (-2.25 kcal mol^{-1}). Additionally, we were able to quantify the degree of energetic stabilization afford by the α-CF_3 group in this system by comparing it to its α-CH_3 congener (5.58 kcal mol^{-1}). Therefore, while stabilizing, the anchimeric assistance of C-C σ-bonds is not nearly as competitive to γ-silyl homohyperconjugative stabilization as resonance stabilization.

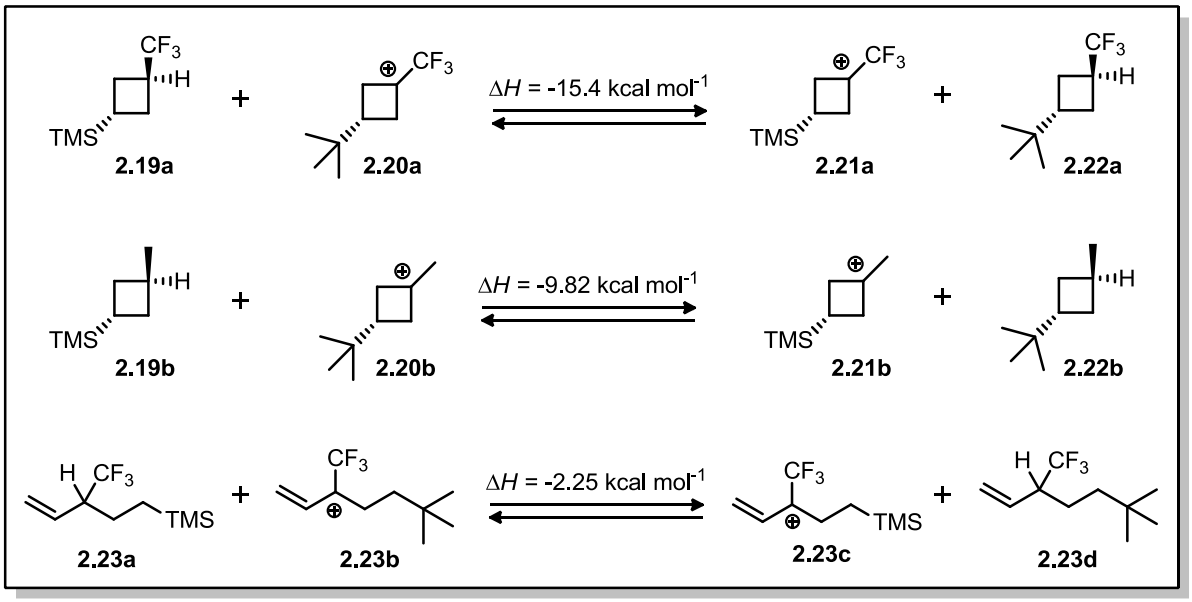

Figure 25: Isodesmic calculations evaluating γ-silyl stabilization of cations **2.21a/b** & **2.23c**. Relative enthalpy energy values calculated at PCM-TFE-B3LYP/6-31+G(d).

Finally, to address the discrepancy between the endothermic nature of the potential energy surface (Figure 24) for the cyclobutyl system and the highly successful bridging under experimental conditions, we offer the following rationales: (1) The high Baeyer strain of **2.18** in the resulting bicyclobutyl system dramatically increases the energy of this system, (2) the γ-silyl homohyperconjugative stabilization is very significant in this system leading to a highly electropositive silicon, (3) the formation of the bond between the electropositive silicon and the solvent, which was not accounted for in these computations, may offset the energetic cost of forming this system and would allow this reaction to be permissible from a thermodynamic standpoint, (4) the "perfluoroalkyl effect," may provide some kinetic stability to this resulting strained system thereby trapping it in a potential energy well.[86]

2.3 MECHANISTIC STUDIES OF OXOAMMONIUM SALT OXIDATION OF ALCOHOLS[88]

2.3.1 Background on Developing Mechanistic Proposal for Oxoammonium Salt Oxidation of Alcohols

After using the oxoammonium salt (**1.1a**) for several useful transformations, we turned our attention to gaining a better understanding of the operative mechanism. Recently, Wiberg and Bailey probed the oxidation of alcohols under un-assisted and base-assisted mechanisms using computational modelling.[30] In their report, they invoked a hydride transfer under neutral conditions while, under basic conditions, they argued for a complex similar to the one proposed by Semmelhack.[89] A few assumptions were made during their study of the oxidation reaction that we felt we could improve upon, so we took the opportunity to design a more thorough computational study. We sought to modify the proposed mechanism based on the inclusion of experimental observations.

Our main premise for oxoammonium salt oxidations is that under non-basic conditions, the concerted asynchronous process first involves a formal hydride transfer from the α-carbon of the alcohol to the electropositive oxygen atom of the oxoammonium salt.[22] Once the hydride is transferred, the α-carbon has a substantial buildup of positive charge and the now basic nitrogen of the hydroxylamine deprotonates the alcohol. Substituents that stabilize this buildup of positive charge on the α-carbon lead to lower activation energy for H^- transfer and hence faster oxidations (e.g. benzyl alcohols react faster than aliphatic primary alcohols). However, the mechanism changes significantly when a base is added to the reaction media.[22] Under basic oxidation conditions (notably the addition of a pyridyl base), oxidation occurs much more

[88] Bobbitt, J. M.; Bartelson, A. L.; Bailey, W. F.; Hamlin, T. A.; Kelly, C. B. *J. Org. Chem.*, **2014**, *79*, 1055.
[89] Semmelhack, M. F.; Schmid, C. R.; Cortés, D. A. *Tetrahedron Lett.* **1986**, *27*, 1119.

rapidly and is less sensitive to electronic modulation at the α-carbon in the transition-state structure. Oxidation is controlled primarily by steric interactions.[22,90] Alcohols with less steric bulk undergo oxidation at a significantly faster rate than hindered ones (e.g. primary alcohols react faster than secondary). As a consequence of the presence of a base, the weakly acidic proton of the resulting hydroxylamine is deprotonated; this anion comproportionates with the oxoammonium species to give two equivalents of **1.1b**.[22] Hence, under basic conditions, super stoichiometric quantities (≈2.2-2.5 equiv.) of the oxoammonium salt and of the base are required for complete oxidation.[22] Both mechanistic proposals were explored in depth as part of this dissertation and will be discussed in detail later in this chapter.

A more concrete rationale for the appreciable differences between the unassisted and base-assisted oxidations needed to be addressed. As a means to gain preliminary mechanistic information, Dr. Bobbitt and our group measured the relative reactivities of some alcohols towards oxidations under basic oxidative conditions. Primary alcohols, interestingly, have negligible differences in reactivities and are all set to a reactivity of benzyl alcohol (**2.24b)** (Table 9, Entries 2-4). This is in sharp contrast to the reactivities noted by Bobbitt under non-basic conditions where benzyl alcohols and secondary alcohols were ten and two times more reactive, respectively as compared to primary alcohols.[22] However, there are noticeable differences in benzyl alcohols with varying ring electron densities (Table 9, Entries 1, 2, 5). Interestingly, secondary alcohols are quite slow to oxidize (Table 9, Entries 6, 7). Moreover, the sterically hindered neopentyl alcohol (Table 9, Entry 8) was ten times less prone to oxidation, despite being a primary alcohol.

[90] Israeli, A.; Patt, M.; Oron, M.; Samuni, A.; Kohen, R.; Goldstein, S. *Free Radical Bio. Med.* **2005**, *38*, 317.

Table 9: Initial relative reactivities of various alcohols under basic oxidative conditions[a]

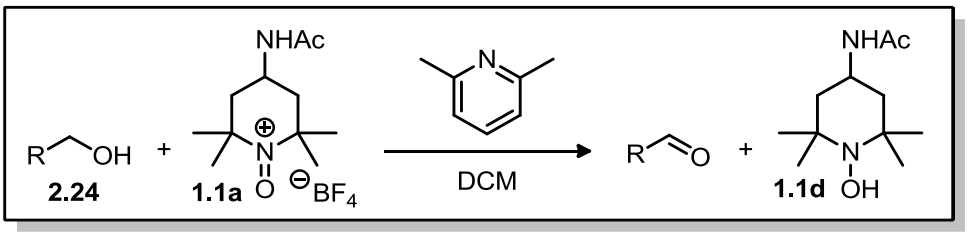

Entry	Alcohol	Relative Reactivity[b]
1	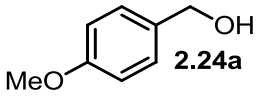	1.2
2	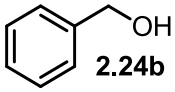	1.0
3	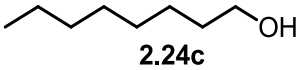	1.0
4	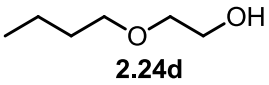	1.0
5	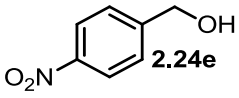	0.5
6	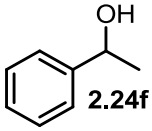	0.2
7	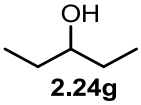	0.1
8	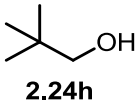	0.1

[a]Alcohol **2.24** (1 equiv, 0.04 M in DCM), benzyl alcohol (1 equiv), 2,6-lutidine (2 equiv), **1.1a** (2 equiv) [b]Determined by ratio of aldehyde peaks in ^{1}H NMR spectrum

Based on these rate data and prior observations in this thesis, Dr. Bobbitt and our group suggested the operative mechanism in both SiO_2 conditions and basic conditions is one that involves a hydride transfer from the alcohol to the oxoammonium cation. The question then arises as to whether the hydride is transferred to the nitrogen or to the oxygen of the oxoammonium cation. In the 2,2,6,6-tetramethylpiperidyl scaffold as in our oxoammonium cation, the nitrogen is surrounded by two quaternary carbon groups. Thus, for steric reasons, it is very likely that the hydride is transferred to the oxygen in the positively charged nitrogen-oxygen bond ($N=O^+$). This situation can be more clearly rationalized using a space-filling model of oxoammonium cation shown above in (Figure 26).

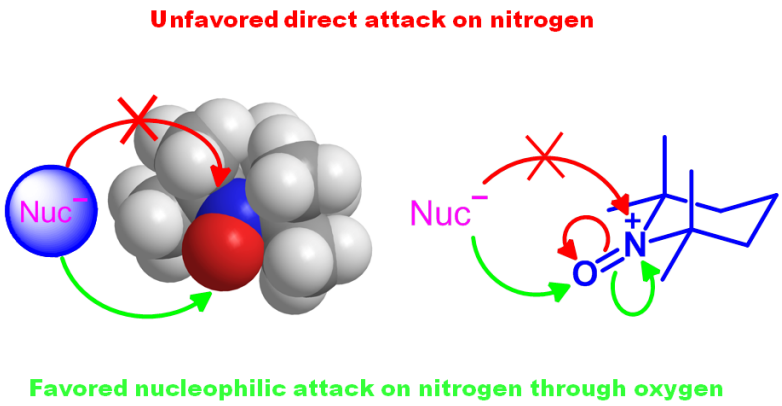

Figure 26: Reaction of the oxoammonium cation with nucleophiles

Essentially, the oxoammonium cation can behave as though the positive charge is on the oxygen, giving rise to an *electrophilic oxygen* which is rarely encountered in organic chemistry. This has an important additional mechanistic implication. In most alcohol oxidation mechanisms, the electrons used to form the carbonyl double bond come from the α-C-H bond of the carbinol.[11] In oxoammonium oxidations, the electrons used to form the carbonyl double bond

come from the O-H bond of the hydroxyl group following the hydride transfer.[91] Other oxidations involving hydride transfers (i.e. when electrons used to form the carbonyl double bond come from the hydroxyl group of the carbinol*)* are known. Three oxidation systems involving a hydride transfer similar to the oxoammonium system exist: the Oppenauer oxidation,[92] the Cannizzaro reaction, and in the action of alcohol dehydrogenase on ethanol with NAD^+ as a cofactor[93].

If a hydride transfer of the α-H is indeed at play, it implies that a buildup of positive charge is formed at the α-carbon during the course of an oxidation. The steric congestion of the transition-state leading to the hydride transfer event and the stability of the resulting α-carbon would therefore directly influence the activation energy and in turn the relative reactivity (Figure 27). This is in line with experimental observations. In simple alcohol oxidations without base assistance, the hydride transfer is facilitated by an electron-rich hydroxyl group. In alcohols containing an electron-withdrawing group close to the carbinol carbon such as β-oxygen systems, α-CF_3 systems, acyloxy alcohols,[48,94] and the *p*-nitrobenzyl group, this electron density is reduced, as is the reactivity. The reactivity is also reduced in sterically hindered systems. If this hydride transfer model is the operative mechanism in both the unassisted and base-assisted mechanism, the question then becomes what role the base plays.

[91] Golubev, V. A.; Borislavskii, V. N.; Aleksandrov, A. L. *Russ. Chem. Bull.* **1977**, *9*, 1874 (English translation)
[92] Kurti, L.; Czakó, B. *Strategic Applications of Named Reactions in Organic Synthesis*; Elsevier Academic Press: Boston, **2005**.
[93] Agarwal, P. K.; Webb, S. P.; Hammes-Schiffer, S. *J. Am. Chem. Soc.* **2000**, *122*, 4803.
[94] Kreutter, K. D.; Lu, T.; Lee, L.; Giardino, E. C.; Patel, S.; Huang, H.; Xu, G.; Fitzgerald, M.; Haertlein, B. J.; Mohan, V.; Cryaler, C.; Eisennagel, S.; Dasgupta, M.; McMillan, M.; Spurlino, J. C.; Huebert, N. D.; Maryanoff, B. E.; Tomczuk, B. E.; Damiano, B. P.; Player, M. R. *Bioorg. Med. Chem. Lett.* **2008**, *18*, 2865.

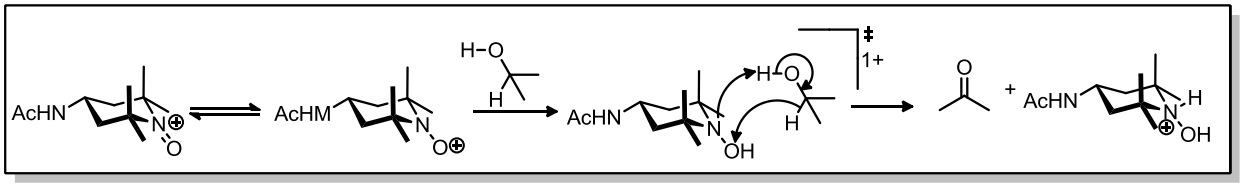

Figure 27: Mechanism of oxidation under non-basic conditions

The mechanisms of pyridine base-mediated oxidations make more sense if viewed in light of the neutral oxidations. The oxidation of an alcohol by an oxoammonium cation under non-basic conditions results in the transfer of a hydride and a proton to the salt from the alcohol. Hydrogen bonding likely occurs as part of this mechanism and is appealing since it offers a six-membered transition state. Early mechanistic studies by Semmelhack suggested that the mechanism of base assisted oxoammonium salt oxidation of alcohols involved nucleophilic attack of alkoxides on the positive nitrogen of the oxoammonium cation followed by an intramolecular, E2-like elimination (Figure 28).[89]

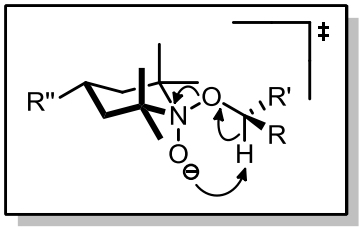

Figure 28: Key transition-state structure proposed by Semmelhack

This is by far the prevailing mechanism in the literature, but seems counter-intuitive given the severe steric constraints of the nitrogen in this scaffold.[22c,95] Indeed, even in his seminal report, Semmelhack notes that carbon nucleophiles attack solely at the oxygen, so one would expect

[95] (a) Vogler, T.; Studer, A. *Synthesis*, **2008**, 1979; (b) Montanari, F.; Quici, S.; Henry-Riyad, H.; Tidwell, T. T.; Studer, A.; Vogler, T. *2,2,6,6-Tetramethylpiperidin-1-oxyl* in *Encyclopedia of Reagents for Organic Synthesis*; John Wiley & Sons: New York, 2007; (c) Garcia Mancheño, O.; Stopka, T. *Synthesis*, **2013**, *45*, 1602; (d) Cao, Q.; Dornan, L. M.; Rogan, L.; Hughes, N. L.; Muldoon, M. J. *Chem. Commun.*, **2014**, *50*, 4524.

other nucleophiles to behave in a similar manner. The electrostatic attraction between the anionic alkoxide, which resulted from formal deprotonation by the pyridyl base, and the oxoammonium cation was also supported by Golvev.[91] In this chapter, we will argue that the primary mode of operation of these cations is through an electrophilic oxygen (Figure 26).[88] From this standpoint, one of the mechanisms ruled out by Semmelhack becomes far more viable, namely hydride transfer from an activated C-H bond to the electrophilic oxygen of the oxoammonium cation.

A major issue arises, as pyridyl bases are not known to formally deprotonate alcohols. They are known, however, to form hydrogen bonds with alcohols in polar and non-polar organic solvents.[96] Using the alcohol as the solvent and the coordinating species, Solomonov found that addition of pyridine leads to an exothermic specific interaction enthalpies ($\Delta H_{int(sp)}$) in all cases (MeOH, ^{t}BuOH, 1-octanol, TFE).[96c] This indicates that the hydrogen-bonded complex is highly favorable. Additionally, using an alcohol and pyridine in CCl_4, monomeric hydrogen bonding (**V**) and linear dimeric hydrogen bonding (**VI**) complexes are known to form (Figure 29).[96c,d] These complexes are highly favorable, exhibiting largely exothermic $\Delta H_{int(sp)}$.[96c,d] Additionally, base strength appears to play a role in that 4-picoline forms a enthalpically more favorably complex with *n*-BuOH than pyridine.[96]

[96] (a) Arnett, E. M. ; Joris, L.; Mitchell, E.; Murty, T. S. S. R.; Gorrie, T. M.; Schleyer P. v. R. *J. Am. Chem. Soc.* **1970**, *92*, 2365; (b) Stephenson, W. K. Fuchs, R. *Can. J. Chem.* **1985**, *63*, 2540; (c) Solomonov, B. N.; Novikov, V. B.; Varfolomeev, M. A.; Klimovitskii, A. E. *J. Phys. Org. Chem.* **2005**, *18*, 1132; (d) Solomonov, B. N.; Varfolomeev, M. A.; Novikov, V. B. *J. Phys. Org. Chem.* **2006**, *19*, 263.

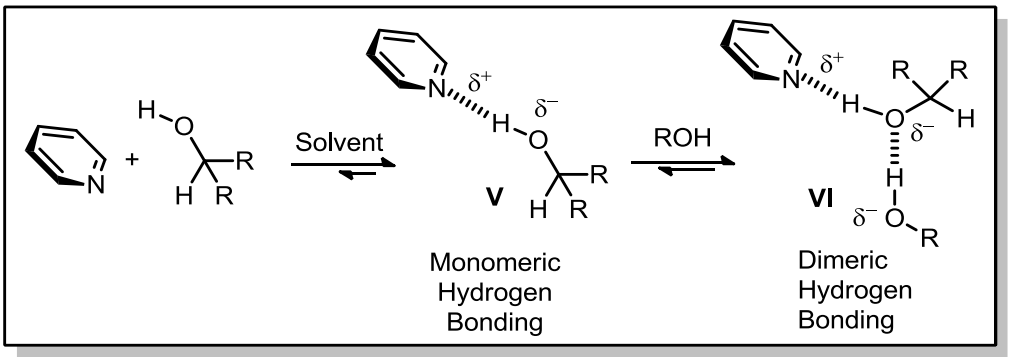

Figure 29: Hydrogen bonding complexes between pyridine and an alcohol

While no specific evidence exists for hydrogen bonding complexation in DCM (enthalpic values or otherwise), the existence of such an interaction can likely be inferred from observational and NMR data. If one mixes an alcohol and pyridine, heat is given off, indicating a favorable intermolecular interaction of some type is occurring. Further evidence of such an interaction is observed by ^{1}H NMR (Figure 30). The hydroxyl proton in acryloxyethanol in deuterated DCM appears at 2.0 ppm and is well-defined peak. If one adds varying equivalents of pyridine, the hydroxyl protons shift consistently downfield and become far less defined, implying a mixed mode of hydrogen bonding.[97]

[97] (a) Demarco, P. V.; Farkas, E.; Doddrell, D.; Mylari, B. L.; Wenkert, E. *J. Am. Chem. Soc.* **1968**, *90*, 5480; (b) Pimentel, G. C.; McClellan, A. L. *The Hydrogen Bond*; W. H. Freeman: New York, **1960**.

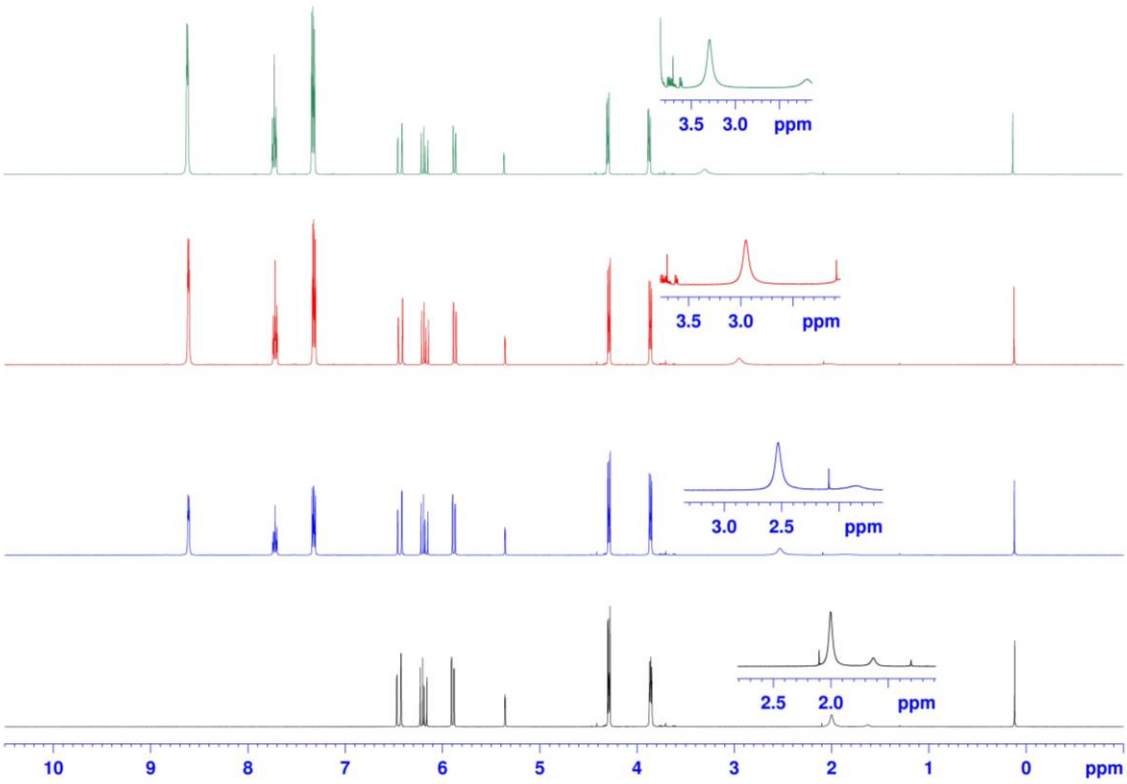

Figure 30: NMR experiment showing the shift of the OH peak of acryloxyethanol in the presence of pyridine. *Conditions:* Black: 0.1 M acryloxyethanol in CD_2Cl_2; Blue: 0.1 M 2-hydroxyethyl acrylate in CD_2Cl_2 , 1 equiv pyridine; Red: 0.1 M acryloxyethanol in CD_2Cl_2 , 2 equiv pyridine; Green: 0.1 acryloxyethanol in CD_2Cl_2 , 3 equiv pyridine.

For simplicity, a monomeric hydrogen bonding complex will be utilized (**VII**) (Figure 31). One can imagine that this hydrogen bonded complex will form a new ternary complex (**VIII**) upon encountering the oxoamonium cation in the same way that any alcohol does when encountering this species. The H-bonded complexation process allows the process to be considered bimolecular (H-bonded complex + **1.1a**), which is more viable than a trimolecular (alcohol + pyridine + **1.1a**) process in a dilute solution.

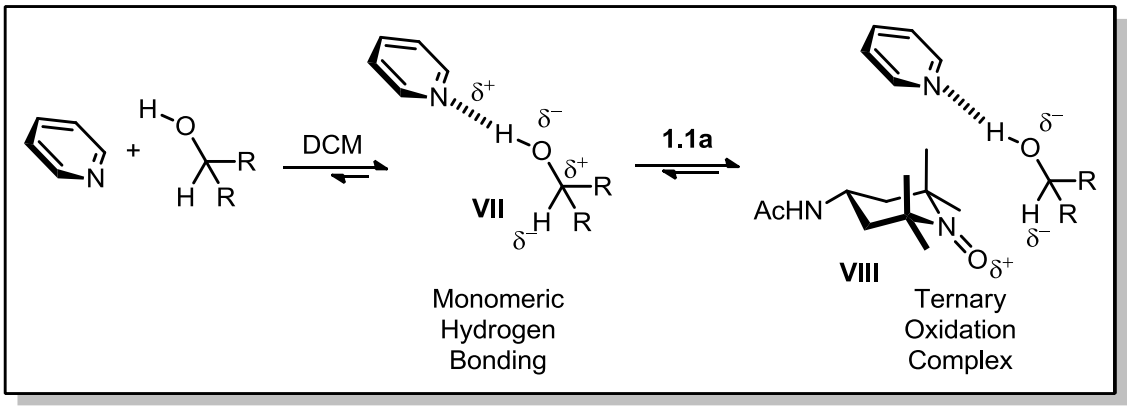

Figure 31: Proposed hydrogen-bonded complex and its reaction with **1.1a**

Hydrogen bonding leads to bond polarization such that the α-hydrogen atom carries a substaintially larger partial negative charge thus enhancing the hydridic character of the α-hydrogen and likely lower the activation barrier. Moreover, increasing base strength leads both to a stronger hydrogen bonding interaction[96a] and further augments the hydridic character of this hydrogen. The observed rate data is consistent with this postulate in that all alcohols of similar steric size have similar reactivities (e.g. an aliphatic 1˚ alcohol and a benzyl 1˚ substituted alcohol both have rates of near 1.0). Electronics do appear to have an effect in extreme cases, such as alcohols with neighboring a-EWGs. For example, while most α-CF_3 alcohols do oxidize under basic conditions, the hydridic nature of the a-hydrogen is diminished by inductive effects, and thus the relative reactivities of such alcohols are effective zero when compared to benzyl alcohols. For α-CF_3 alcohols, a neighboring π-system is needed to counter balance the induction of the CF_3 group to lower the activation energy of the hydride transfer. A more polarizing base (e.g. DBU or DBN) is required for systems lacking a stabilizing moiety. Sterics play a more substantial role than electronics in this type of oxidation. Increasing the substitution pattern on alcohols leads to a smaller equilibrium constant for hydrogen bonding complexation with

pyridine bases.[98] Additionally, the steric clash with the methyl groups of the oxidant likely impact the formation of this ternary complex and have a significant effect on oxidation rates (e.g. 2˚ alcohols oxidize far slower than 1˚ alcohols).

Given the concepts discussed above, a mechanism can be proposed for the base-mediated oxidation (Figure 32). The first step involves a reversible hydrogen-bonding complex between the pyridyl base and an alcohol (the model system is comprised of pyridine and methanol). The activation energy for the hydride transfer from this polarized complex is likely lower, thereby allowing for facile oxidation. Ultimately this results in the protonation of pyridine and the formation of the hydroxylamine, which comproportionates in the same manner as described above.

Faced with a number of issues and questions about the actual mechanism of the unassisted and base assisted oxidations, we turned to the power of computational modeling. Using the mechanisms shown in Figures 27 & 32 as a starting point, we opted to test the oxidation of a simplified system by the oxoammonium cation. We specifically wished to calculate the energetics of H-bond formation as well as explore the energetics of the key hydride transfer step.

[98] Demeter, A.; Mile, V.; Bérces, T. *J. Phys. Chem. A* **2007**, *111*, 8942

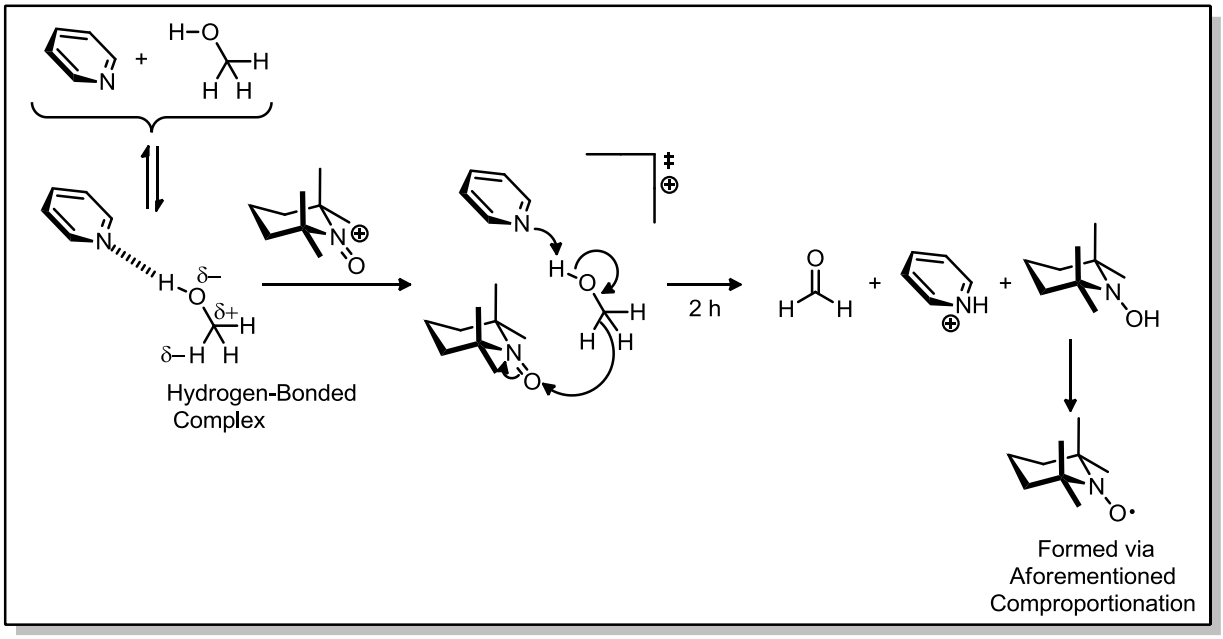

Figure 32: Proposed mechanism of oxidation under basic conditions

2.3.2 Theoretical Studies of Oxidation of Methanol by an Oxoammonium Salt

To gain further mechanistic insight, we modeled both the unassisted and base-assisted mechanisms using quantum mechanical calculations with methanol as the substrate and DCM as solvent. The calculations on the base-assisted mechanisms were made assuming hydrogen bonding, represented by dashed lines (Figure 32). It should also be noted that the TEMPO cation was used to simplify the calculations. The thermodynamics of these pathways were probed by means of DFT calculations using Gaussian 09.[58] The computational procedure involved geometry optimizations at the B3LYP/6-31+G(d) level of theory,[77,78] followed by single-point energy calculations at the B3LYP/6-311++G(d,p) level. The thermodynamic correction factors were obtained from the frequency calculations and were used to correct the more accurate stationary point energy. Both the geometry optimization and the single-point calculations employed the PCM solvation model.[81]

The energy of complexation is enthalpically favorable for both mechanisms with DCM as the implicit solvent (Table 10) in accordance with the previously mentioned enthalpic data. There is a steric component to this H-bond complexation, as pyridine has the lowest barrier and as you add methyl groups in the 2 and 6 position the barrier increases to >5 kcal mol^{-1}.

Table 10: Thermodynamics of H-bond complexation[a]

Structures	**6-311++G(d,p)**	
	ΔH_{rxn}	ΔG_{rxn}
pyridine + methanol → H bond complex	-4.5	3.2
lutidine + methanol → H bond complex	-4.2	5.1
2,4,6-collidine + methanol → H bond complex	-4.4	5.2

[a]Values reported in kcal mol^{-1}

As previously mentioned, a key component of our proposed hydrogen bonding-mediated mechanism is that it enables polarization of the bonds, possibly resulting in greater partial negative character of the α-hydrogen on the alcohol substrate. This can effectively enhance the hydridic character of the α-hydrogen and possibly lowers the activation energy of the hydride transfer step in the oxidations. As basicity increases, the transition-state structure more resembles the products (Table 11). The existent of deprotonation and hydride transfer is greater for stronger pyridyl bases.

It is immediately evident that oxidation in the absence of a pyridyl base has a much higher activation energy than those utilizing a pyridyl base (37.8 kcal mol^{-1} vs 25.4-27.5 kcal mol^{-1}, Figure 33). This deviation in activation energy has been experimentally observed via the difference in reaction rate. Reaction times of neutral oxidations (red) are much longer (12-48 h) than analogous base reactions (1-4 h).[22]

Table 11: Key geometric parameters for base mediated transition-state structures (all distances in Å)

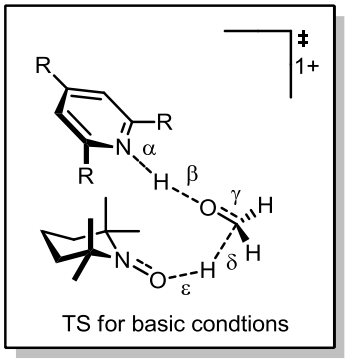

Base	α	β	γ	δ	ε
pyridine (2.25b)	1.055	1.651	1.297	1.309	1.272
2,6-lutidine(2.25c)	1.045	1.730	1.297	1.301	1.283
2,4,6-lutidine (2.25d)	1.043	1.744	1.297	1.299	1.285

By altering the basicity of pyridyl base, we were able to observe how polarization affects the activation energy. As basicity increases (thereby further polarizing the hydrogen-bonded complex), the activation energy to reach the transition states decreases (Figure 33). Thus, the reactions should be faster for the more basic pyridines, which we have observed experimentally previously.[27]

At this point we had concluded our initial mechanistic investigation and made some assumptions to make the calculations shorter and more feasible, such as: only investigating the oxidation of methanol and using TEMPO cation instead of **1.1a**. We had answered many of the mechanistic questions and understood the nuances of oxoammonium salt oxidations of alcohols in the absence and presence of pyridyl bases.

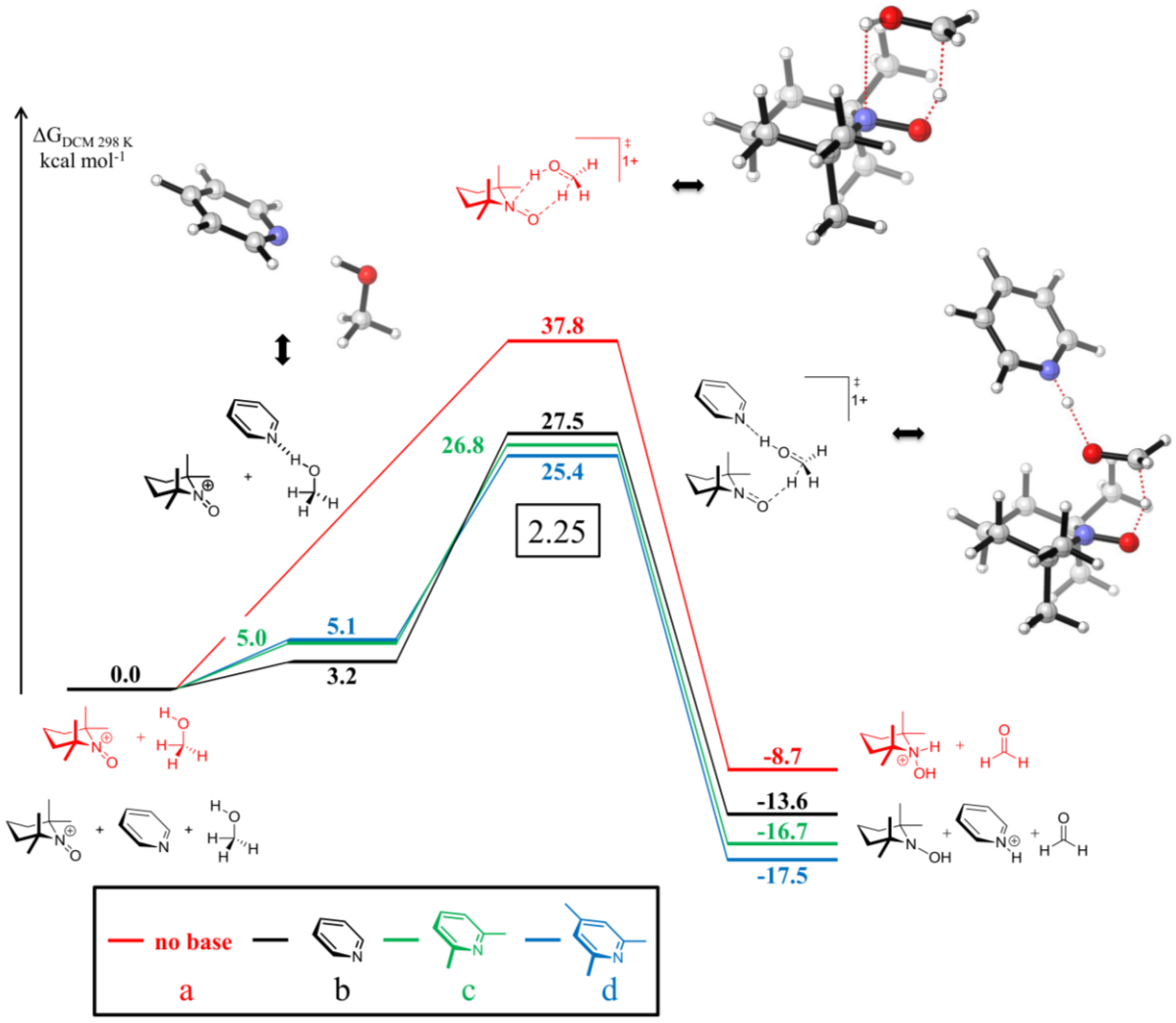

Figure 33: Reaction coordinate for the oxidation of methanol with and without pyridyl bases. Relative Gibbs free energy values calculated at PCM-DCM-B3LYP/6-31+G(d)//PCM-DCM-B3LYP/6-311++G(d,p). Numeric values indicate energies in kcal mol^{-1}.

Mechanistic studies suggest that a hydride transfer model is appropriate for this oxidation manifold. The major difference between unassisted and base-assisted oxidative conditions stems from the polarization of the alcohol via hydrogen bonding. Many other types of oxidation reactions and a numerous substrates will be investigated in the following section.

2.4 MECHANISTIC STUDIES OF OXOAMMONIUM SALT OXIDATION OF VARIOUS SCAFFOLDS[99]

2.4.1 Background on Oxidation of Various Scaffolds by an Oxoammonium Salt

The analysis is broken down into three subject areas based on the substitution pattern of the substrate C-H bond being oxidized: oxidations occurring α to a C-O bond, α to a C-N bond, and those lacking any neighboring heteroatom substitution. Experimental evidence and computationally-derived models are reported in these sections. Quantum chemical calculations were performed using Gaussian 09.[58] The method used for the calculations of non-metal containing systems reported in our paper follows: (i) geometry optimization and vibrational frequency calculations in implicit DCM or MeCN using CPCM[100] at the B3LYP/6-31+G(d) level of theory,[77,78] (ii) single-point solvation free energy calculation in DCM or MeCN using CPCM with B3LYP/6-311++G(d,p). The method used for the calculations of iron containing systems reported in our paper follows: (i) geometry optimization and vibrational frequency calculations in implicit DCM or MeCN using CPCM at the B3LYP/LANL2DZ[79] level of theory for iron and B3LYP/6-31+G(d) level of theory for all other atoms in the system, (ii) single-point solvation free energy calculation in DCM or MeCN using CPCM with B3LYP/SDD[101] for iron and B3LYP/6-311++G(d,p) for all other atoms in the system. Gibbs free energies in solution are obtained by adding the thermal correction to the Gibbs free energy from (i) to the solvation electronic energy calculated in (ii). Stationary points were characterized by frequency calculations at 298 K, with structures at energy minima showing no negative frequencies and transition-states showing one negative frequency. Intrinsic reaction coordinate (IRC) calculations[80] followed by optimization and frequency calculations were performed to

[99] Hamlin, T. A.; Kelly, C. B.; Ovian, J. M.; Wiles, R. J.; Tilley, L. J.; Leadbeater, N. E. *manuscript in preparation.*
[100] (a) Baron, V.; Cossi, M. *J. Phys, Chem. A.* **1998**, *102*, 1995; (b) Barone, V.; Cossi, M.; Tomasi, J. *J. Comp. Chem.* **1998**, 19, 404.
[101] Cao, X. Y.; Dolg, M. *J. Mol. Struct. (Theochem),* **2002**, *581*, 139.

unambiguously connect transition-state structures with associated reactants and products along the reaction coordinate. All energetic values shown are in kcal mol^{-1}; bond lengths are reported in Ångstroms (Å), bond angles in degrees (˚). Molecular figures were generated using CYLView.[82]

2.4.2 Oxidation α to a C-O Bond - Alcohol Oxidation

Given that oxoammonium salts are primarily used for the routine oxidation of alcohols to aldehydes, we focused much of our initial efforts on exploring the details of this transformation. Moreover, preliminary studies on this type of oxidation were described in detail in Chapter 2.3.2 of this thesis.[88] We hypothesized that a deep understanding of this type of oxidation would be instrumental in elucidating the key features governing other oxidations α to C-O bonds. Ultimately, we sought to evaluate: (1) the disparity between base-assisted and non-base assisted oxidation, (2) the role of electronics in this oxidation manifold, (3) the overall nature of the oxidation (concerted or stepwise).

We began by using benzyl alcohol as the representative system to probe the differences between the unassisted and base-assisted oxidation. While we had evaluated this in our past report in the preceding section, there are two key differences in this contribution: (1) we invoked the formation of a dipole-stabilized pre-oxidation complex between the oxidant and the alcohol, (2) we used **1.1a** itself rather than the TEMPO cation. The formation of a dipole-stabilized pre-oxidation complex was performed based on recent computational studies by Wiberg on the oxidation of amines to nitriles[102] and IRC studies, while the change in oxidant was done to improve the overall accuracy of our

[102] Lambert, K. M.; Bobbitt, J. M.; Eldirany, S. A.; Wiberg, K. B.; Bailey, W. F. *Org. Lett.* **2014**, *16*, 6484.

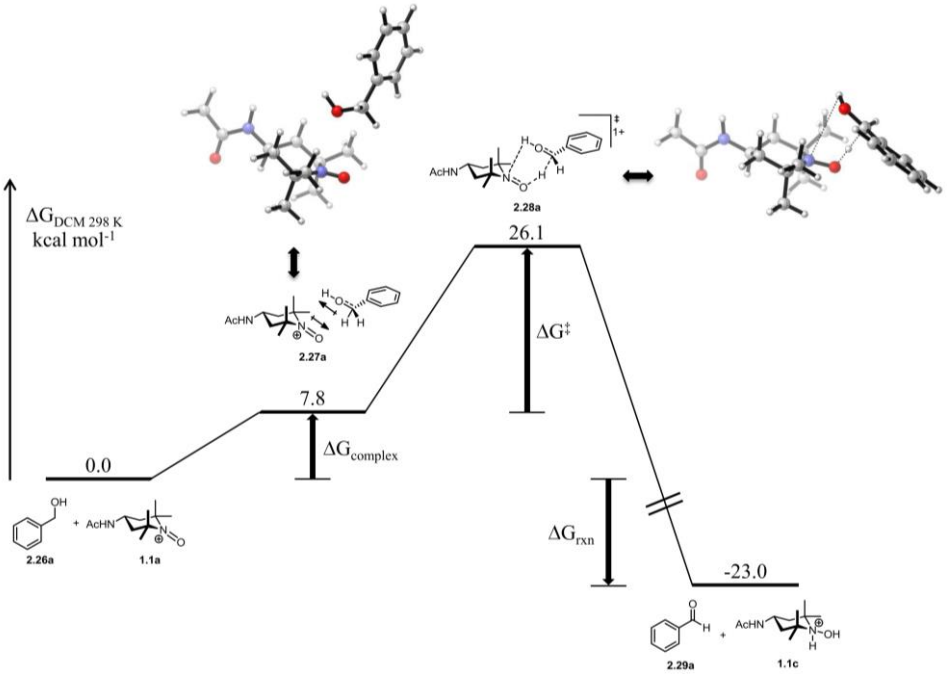

Figure 34: Reaction coordinate for the oxidation of benzyl alcohol under non-basic conditions. Relative Gibbs free energy values calculated at CPCM-DCM-B3LYP/6-31+G(d)//CPCM-DCM-B3LYP/6-311++G(d,p). Numeric values indicate energies in kcal mol-1.

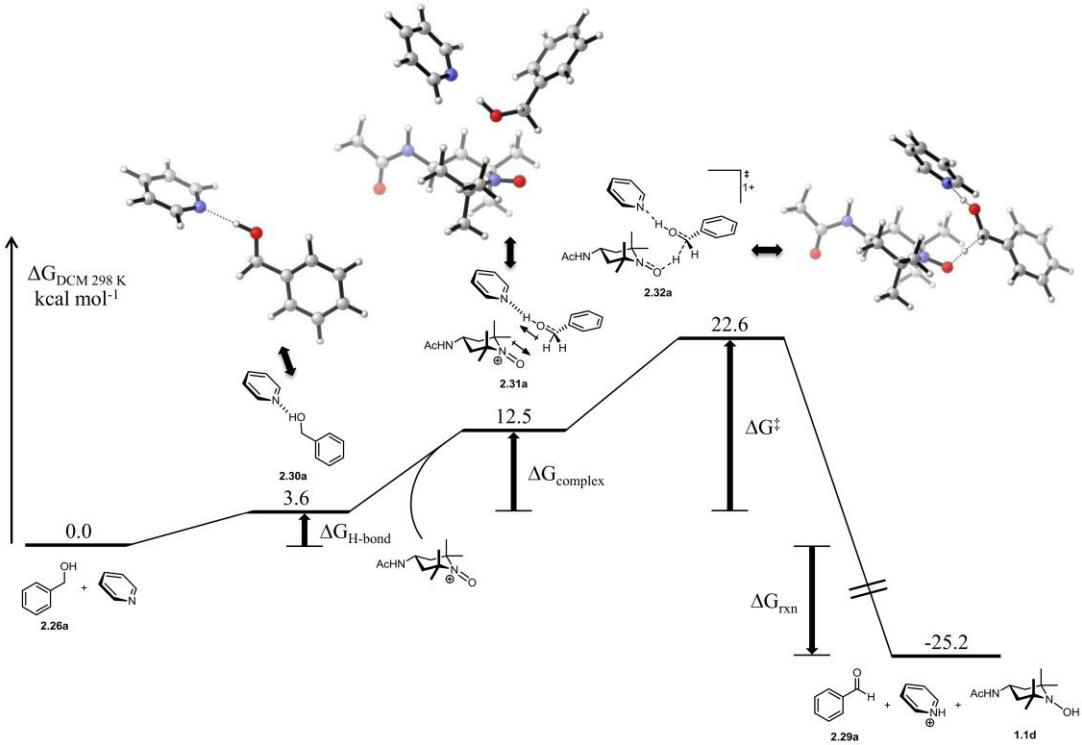

Figure 35: Reaction coordinate for the oxidation of benzyl alcohol under base-assisted conditions (base in this case is pyridine). Relative Gibbs free energy values calculated at CPCM-DCM-B3LYP/6-31+G(d)//CPCM-DCM-B3LYP/6-311++G(d,p). Numeric values indicate energies in kcal mol^{-1}.

modeling by using the complete oxidant. Using the results of this study we were able to construct the potential energy surface for both reaction types (Figures 34 & 35).

In the case of the non-base assisted mechanism, we observed a concerted asynchronous oxidation event where the primary molecular motion in the transition-state structure is that of the hydride transfer from the alcohol to the electrophilic oxygen of **1.1a** followed by a proton transfer to the now basic nitrogen of the hydroxylamine. These two distinct events can be observed when analyzing the IRC calculations (note the curvature on the red line) shown in Figure 36. It should be pointed out that the energy minima corresponding to the reactant, is in fact the dipole-stabilized pre-oxidation complex (**2.27a**).

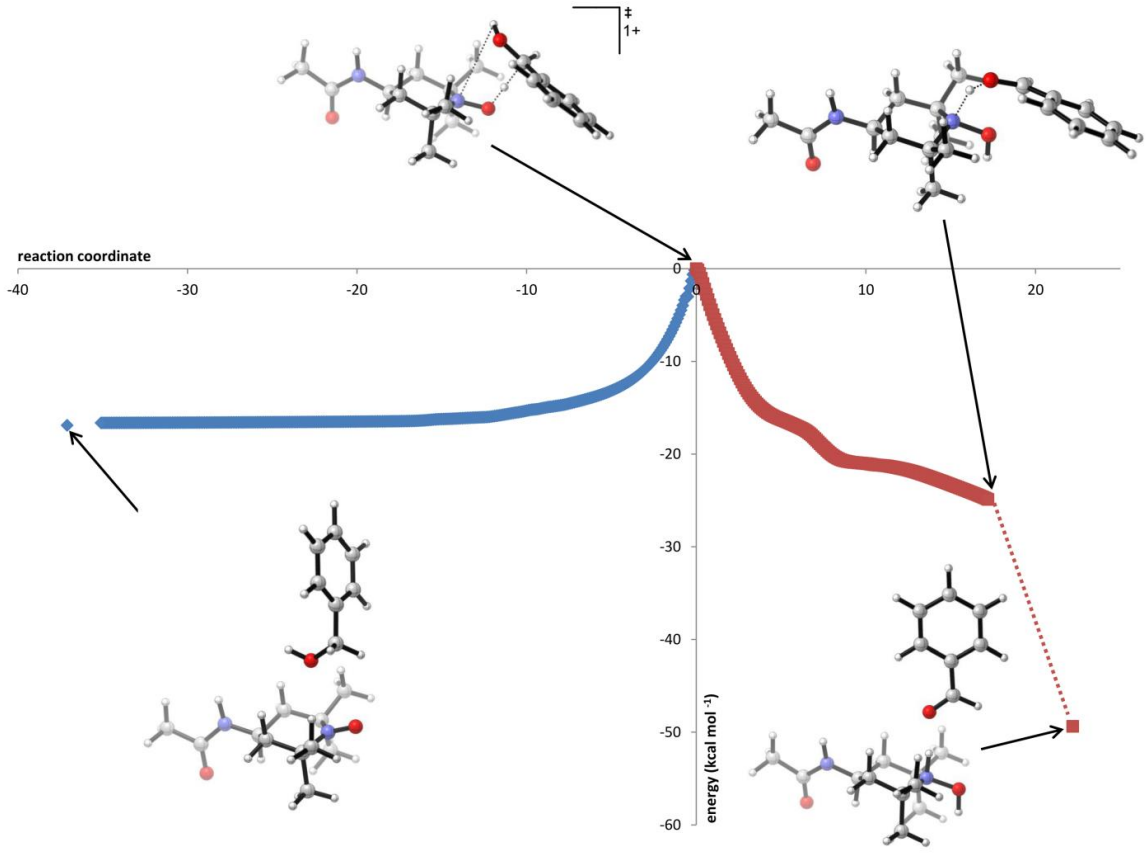

Figure 36: IRC for non-basic oxidation of benzyl alcohol (**2.26a**) by the oxoammonium salt (**1.1a**)

The $\Delta G^{\ddagger}$ from the pre-oxidation complex is reasonable (18.3 kcal mol^{-1}) and the overall reaction is thermodynamically favorable. The required energy to reach the pre-oxidation complex is a consequence of a more organized complex and the pathway has a $\Delta S_{complex}$ = -0.028 kcal mol^{-1} (See Appendix III for analysis of entropy of complexation).

In the base-assisted mechanism, we presupposed the formation of a hydrogen-bonded complex (energetically defined as $\Delta G_{H\text{-}bond}$) between benzyl alcohol and pyridine based on evidence from our previous report.[88] From there, we assumed the likely reversible formation of a dipole-stabilized pre-oxidation complex. Not surprisingly the overall change in energy to reach this even more entropically demanding state ($\Delta S_{complex}$ = -0.037 kcal mol^{-1}) was higher as compared to the non-base assisted mechanism ($\Delta G_{complex}$ = 7.8 kcal mol^{-1} in the non-base assisted mechanism vs ($\Delta G_{complex}$ = 8.9 kcal mol^{-1} from the hydrogen-bonded complex). While this mechanism is similarly highly exergonic compared to the non-base assisted mechanism, from the pre-oxidation complex is substantially lower ($\Delta G^{\ddagger}$ = 10.1 kcal mol^{-1}). This explains the significant rate acceleration observed for of the base-assisted mechanism. The IRC for this process is shown in (Figure 37) and again was useful in confirming the existence of the dipole stabilized pre-oxidation complex.

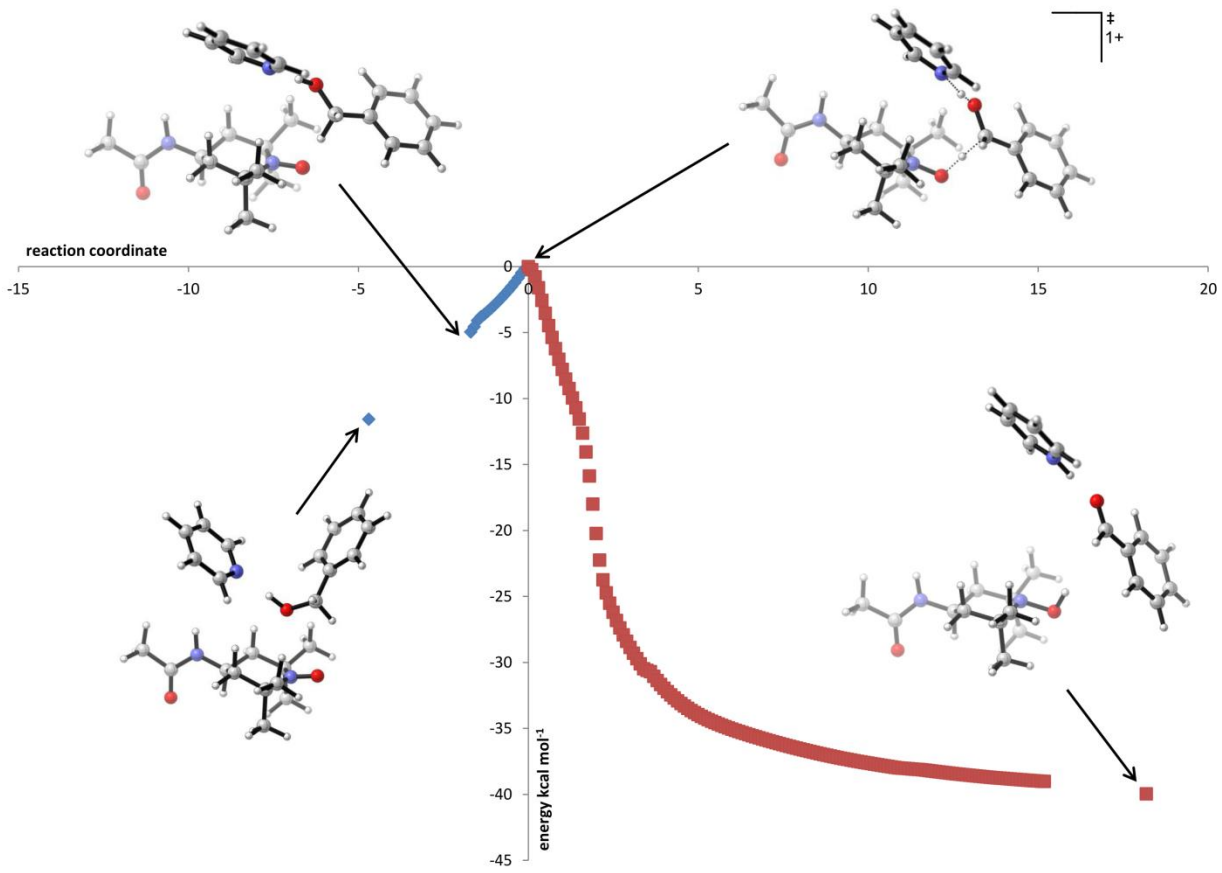

Figure 37: IRC for base-assisted mediated oxidation of benzyl alcohol (**2.26a**) by the oxoammonium salt (**1.1a**)

To further investigate factors governing oxidation in both mechanistic pathways, we modelled the theoretical oxidation of alcohols with varying steric and electronic environments. The results of these studies are in Tables 12 & 13. Also included in these studies are the relative reactivities of alcohols in oxoammonium salt oxidations obtained by experimental studies performed by us. Using these data, we were not only able to elucidate some interesting trends, but also to provide some commentary on the limitations of relative rate studies in this type of reaction.

Steric and electronic interactions appear to have a noticeable effect on the ability to form the requisite dipole-stabilized complex. However, the effect is somewhat complex.

Distant electron-withdrawing groups (EWGs) or sterically-demanding environments deter complexation (Table 1, Entries 4-6, 9 and 10) while nearby EWGs appear to favour complexation (Table 1, Entries 11-13). We quickly ascertained that while the experimentally-derived relative reactivities are mostly a function of the $\Delta G^{\ddagger}$ of oxidation, the $\Delta G_{complex}$ also plays a role. Alcohols with near-identical activation barriers but with disparate energies of complexation have differing reactivity values. This difference may be an artefact of how the reactivity studies are conducted experimentally. Relative rates were determined by competition studies (conducted in DCM), and there is a very limited amount of **1a** in solution at any one time (solubility: 0.1 g per 100 mL of CH_2Cl_2) to the point where it could be deemed rate-limiting. Since formation of the two pre-oxidation complexes (one with each alcohol in the competition experiment) is likely under thermodynamic control, the lower energy complex will be preferred regardless of the activation energy for oxidation, and thus limit the availability of **1a**/**1a′** to oxidize the other competing alcohol. This explains instances such as Entries 2 & 7 or Entries 1 & 8, in Table 1, where the $\Delta G^{\ddagger}$ is almost identical but the $\Delta G_{complex}$ varies significantly thus causing a disparity in the observed relative reactivities.

Table 12: Energetics of alcohol oxidation in the non-basic mechanism for various systems

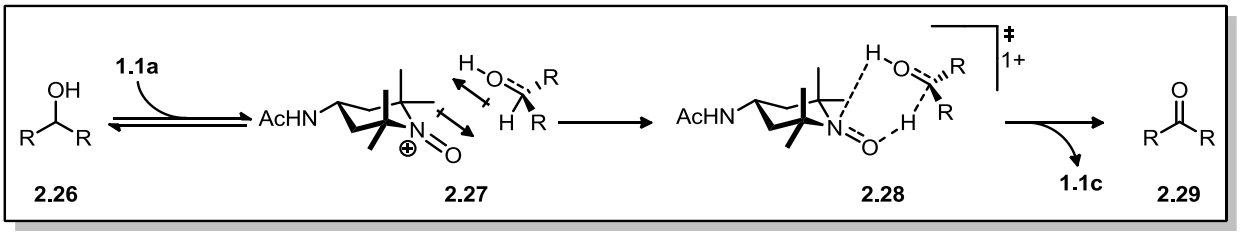

Entry	Alcohol	$\Delta G_{complex}$ 2.26 to 2.27	$\Delta G^{‡}$ 2.27 to 2.28	Rel. React.
1	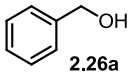 2.26a	7.8	18.3	1
2	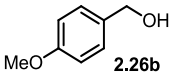 2.26b	7.8	13.1	4.81
3	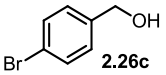 2.26c	7.8	20.0	0.61
4	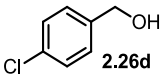 2.26d	8.4	17.5	0.64
5	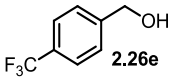 2.26e	9.1	19.3	0.20
6	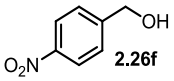 2.26f	8.5	21.9	0.10
7	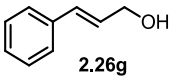 2.26g	7.5	13.2	5.29
8	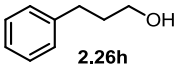 2.26h	9.4	20.0	0.03
9	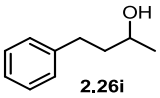 2.26i	9.9	18.2	0.06
10	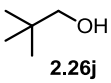 2.26j	8.8	23.4	0.01
11	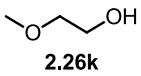 2.26k	5.5	29.6	0

Entry	Alcohol	$\Delta G_{complex}$ 2.26 to 2.27	$\Delta G^{‡}$ 2.27 to 2.28	Rel. React.
12	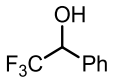 **2.26l**	7.6	32.1	0
13	 **2.26m**	6.7	39.5	0

In the non-basic mechanism, $\Delta G^{‡}$ is most certainly a function of the stability of the forming oxonium-like ion as there is build-up of charge in the TS. This trend is apparent when comparing the effects EWGs and EDGs have on alcohols of near-identical steric environments (Entries 1-6). Alcohols with great substitution and those that are more apt to participate in resonance stabilization have lower overall activation barriers. Inductively destabilizing groups can negate the benefits of substitution and dramatically raise $\Delta G^{‡}$. Severely sterically encumbered alcohols also have higher activation barriers likely due to steric repulsion (Entries 9-13, Table 12).

Using these same alcohols, we probed the energetic differences and trends in the base-assisted mechanism. The results of this study are shown in (Table 13). Two trends become immediately apparent: (1) The magnitude of $\Delta G^{‡}$ (from the dipole stabilized complex) is about half that of the non-basic $\Delta G^{‡}$ (from the dipole stabilized complex), (2) the energy required to form the pre-oxidation complex is very close to the energy needed for the hydride transfer event (though the magnitude of each value is independent of one another). Taken together, this implies that oxidation should proceed rapidly and the oxidation should be less sensitive to electronic perturbations. Indeed, oxidations under base-assisted conditions proceed much faster at room temperature (≈ 1-2 h on average) as

compared to analogous non-basic oxidations (≈ 6-48 h). Additionally, the relative reactivates reflect a relative insensitivity to alcohol structure.

Table 13: Energetics of alcohol oxidation in the base assisted mechanism for various systems

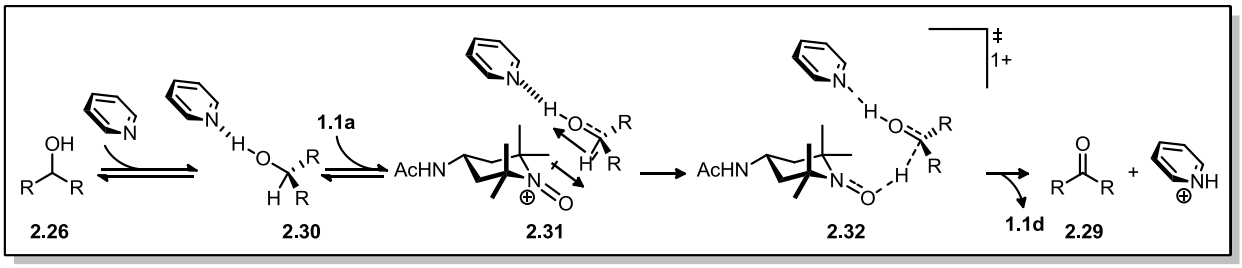

Entry	Alcohol	$\Delta G_{\text{H-bond}}$ 2.26-2.30	$\Delta G_{\text{complex}}$ 2.30 to 2.31	$\Delta G^{\ddagger}$ 2.31 to 2.32	Rel. React.
1	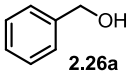 2.26a	3.6	9.0	9.9	1
2	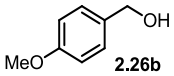 2.26b	4.5	8.4	7.5	1.3
3	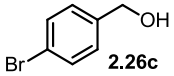 2.26c	4.1	8.7	12.6	0.83
4	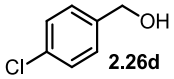 2.26d	3.9	8.2	12.4	0.85
5	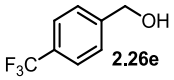 2.26e	3.6	9.3	12.6	0.78
6	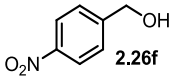 2.26f	2.9	10.5	12.2	0.77
7	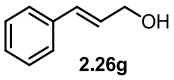 2.26g	4.0	7.4	8.4	2.1
8	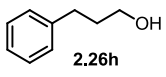 2.26h	5.2	7.1	13.4	0.62
9	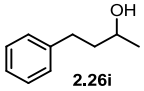 2.26i	6.8	8.5	14.1	0.12

Entry	Alcohol	$\Delta G_{\text{H-bond}}$ 2.26-2.30	$\Delta G_{\text{complex}}$ 2.30 to 2.31	$\Delta G^{\ddagger}$ 2.31 to 2.32	Rel. React.
10	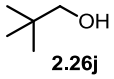 **2.26j**	4.4	10.2	13.3	0
11	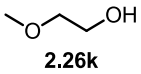 **2.26k**	3.6	8.5	13.8	-
12	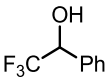 **2.26l**	2.2	11.4	14.9	0
13	 **2.26m**	2.5	8.7	18.4	0

Subtle trends are also apparent. The value of $\Delta G_{\text{H-bond}}$ appears to be a function of alcohol acidity. Thus this explains the less uniform $\Delta G_{\text{complex}}$ values for benzyl alcohols (which have identical steric environments) with varying electronic environments. The value of $\Delta G_{\text{H-bond}}$ is also a function of the pyridyl base, as noted in our previous report that was detailed in the previous section.[88] As in the non-basic mechanism, formation of the pre-oxidation complex is mostly a function of steric interactions. Thus, since this mechanism has a more sterically (and entropically) demanding complex, the values for complexation are on a whole, larger than in the non-basic mechanism. While the relative reactivities are influenced by the respective values of $\Delta G_{\text{H-bond}}$ and $\Delta G_{\text{complex}}$, the overriding factor in reaction success is $\Delta G^{\ddagger}$ from the dipole stabilized complex.

We were also able to use the results from both studies to assess what effect electronic changes have on both reaction mechanisms. By analyzing the bond angles and distances of the computed structures, we were able to comment on the overall nature of the mechanism as a function of electronic perturbations. More O'Ferral-Jencks (MOJ)-style

diagram is a useful tool in visualizing the asynchronicity of transition-states.[103] The More O'Ferral-Jencks-style diagrams in Figures 38 & 39 describe the non-assisted and base assisted reactions (bottom left to top right). MOJ diagrams are a useful tool in visualizing the synchronicity of certain events for related reactions. The diagrams are concerned with the synchronicity of a hydride (expressed as the b-c bond order) and proton transfer (expressed as the a-d bond order). The green and blue lines on the periphery represent the extreme step-wise pathways (the intermediates for these pathways are at the vertices). The diagonal red line and represents a transition structure that is concerted synchronous (in terms of the hydride and proton transfer events). The light blue, black and orange lines correspond to the calculated pathways for various electronic substitutions that are concerted but asynchronous. However, the degree of concertedness appears to be influenced by the electronics of the alcohol being oxidized. In the non-basic mechanism, oxonium-like species with enhanced stability result in a more stepwise-like mechanism. In the base assisted mechanism, a loss in concerted character results from an alcohol being more electron-deficient.

[103] (a) More O'Ferrall, R. A. *J. Chem. Soc. (B)*, **1970**, 274; (b) Jencks, W. P. *Chem. Rev*. **1972**, *72*, 705; (c) Horsley, J. A.; Jean, Y.; Moser, C.; Salem, L.; Stevens, R. M.; Wright, J. S. *J. Am. Chem. Soc.* **1972**, *94*, 279; (d) Salem, L. *Acc. Chem. Res.***1971**, *4*, 322.

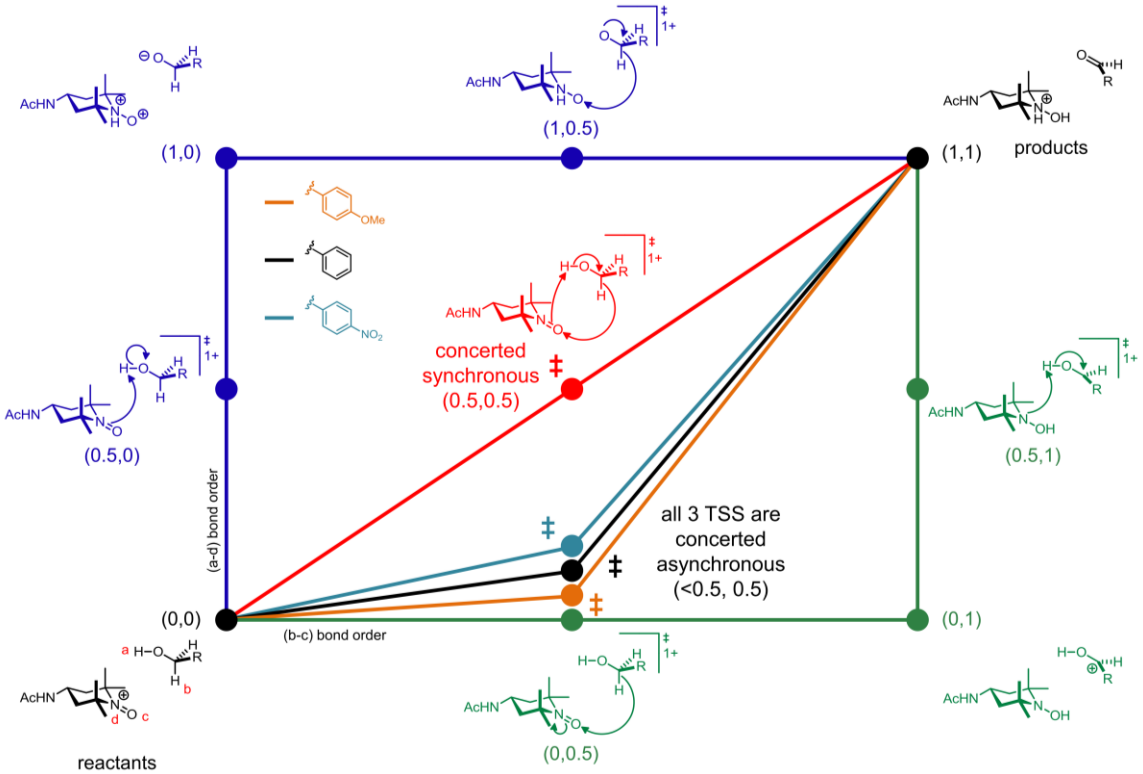

Figure 38: More O'Ferral-Jencks-style diagram for the non-base assisted alcohol oxidation

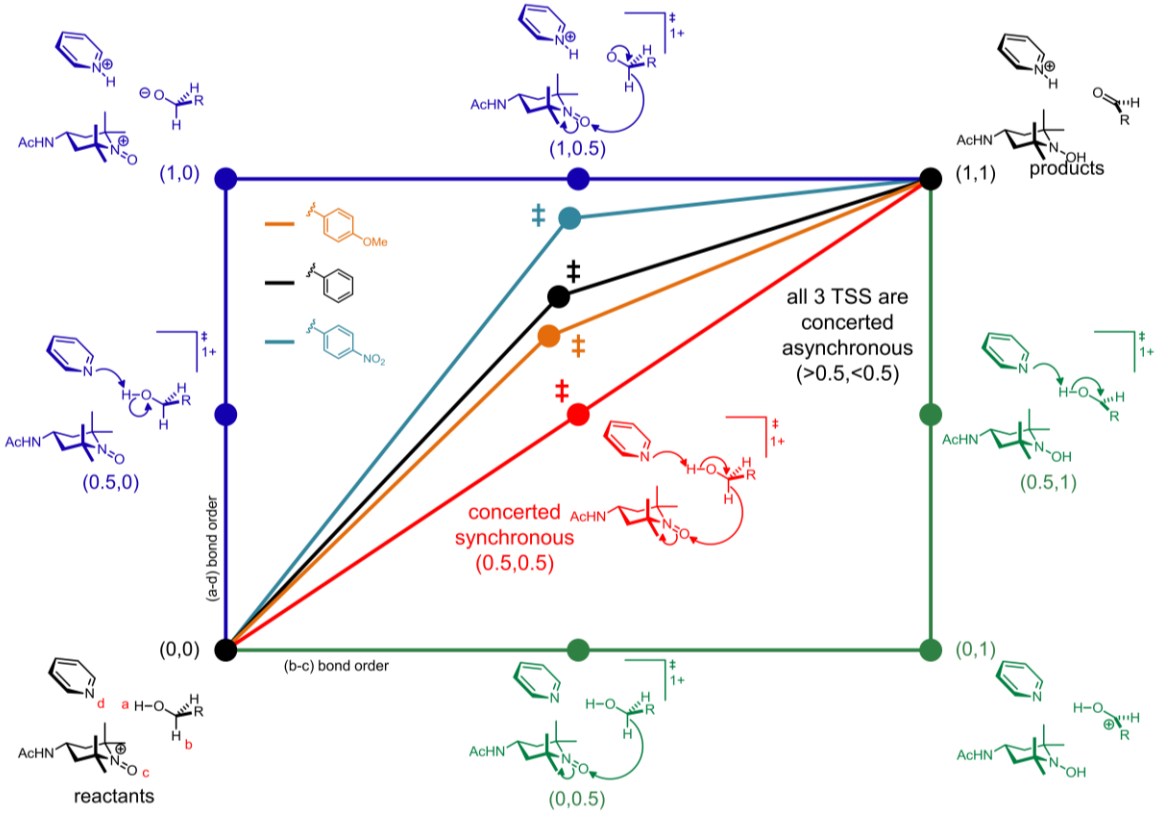

Figure 39: More O'Ferral-Jencks-style diagram for the base assisted alcohol oxidation

As a means to use the data collected in a predictive manner, we computed the energies of oxidation of two classes of carbinols that have not been subjected to oxoammonium salt oxidations: α-fluoromethyl and α-difluoromethyl alcohols. Specifically, we examine an aliphatic fluoromethyl alcohol (**2.33**) and a benzyl difluoromethyl alcohol (**2.34**). Based on their computed values for $\Delta G^{\ddagger}$ and $\Delta G_{complex}$ in the non-base assisted mechanism, one would expect both alcohols to fail to oxidize. Experimental results confirmed this prediction. Also, a tentative cut off value for $\Delta G^{\ddagger}$ between successful and unsuccessful oxidation without base was determined via this analysis. This barrier must lie between 23.4-29.6 kcal mol^{-1} (most likely closer to the lower end of the range given the lower relative reactivity of **2.26j (**Entry 10, Table 12).

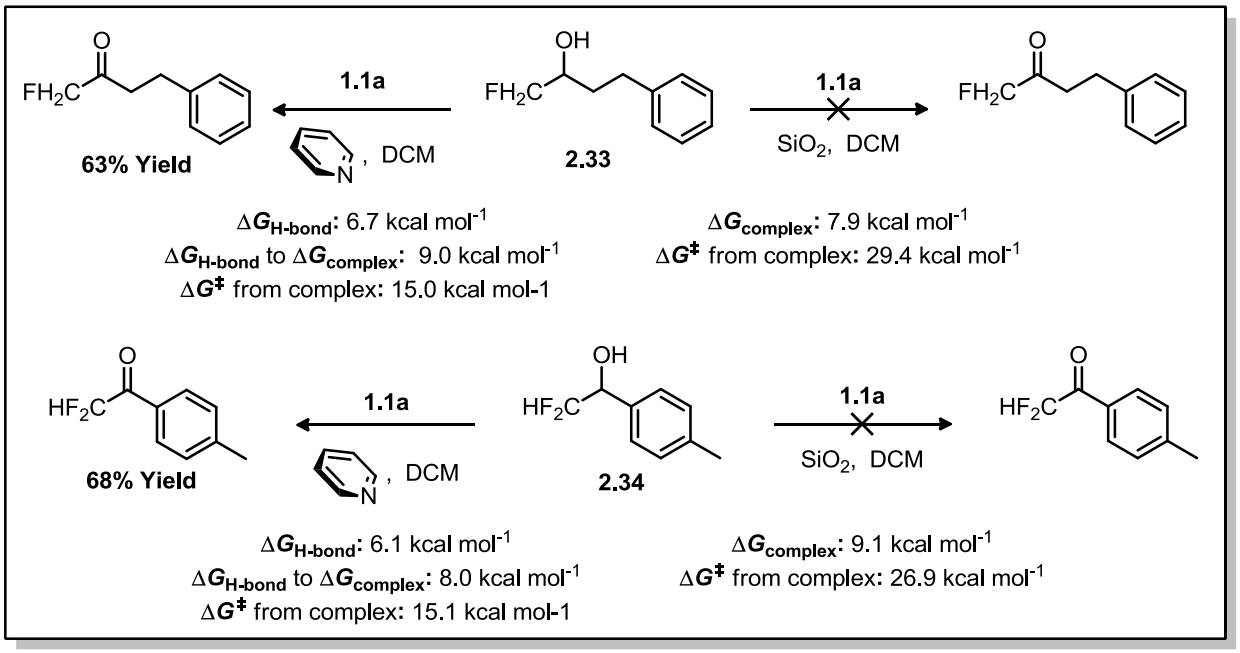

Figure 40: Comparison of the theoretical and experimental oxidation of α-CH_2F and α-CF_2H alcohols in the base and non-base assisted mechanisms

We performed a similar calculation using the base-assisted mechanism. The computed values suggested that both would be readily oxidized and this was indeed the case experimentally. The

cut-off for oxidation in the base-assisted mechanism is likely around 15.0-18.4 kcal mol^{-1} based these results and those for 55 12 and 13 of Table 13.

2.4.3 Oxidation α to a C-O Bond – Oxidative Functionalization of Isochromane

In 2010, Garcia-Mancheño and co-workers disclosed that C(sp^3)-H bonds adjacent to a heteroatom could be functionalized under mild conditions in presence of stoichiometric amounts of the TEMPO derived salt.[104] This dehydrogenative functionalization reaction employs a metal catalyst, $Fe(OTf)_2$, and an enolizable species to accomplish alkylation of the intermediate oxonium ion.

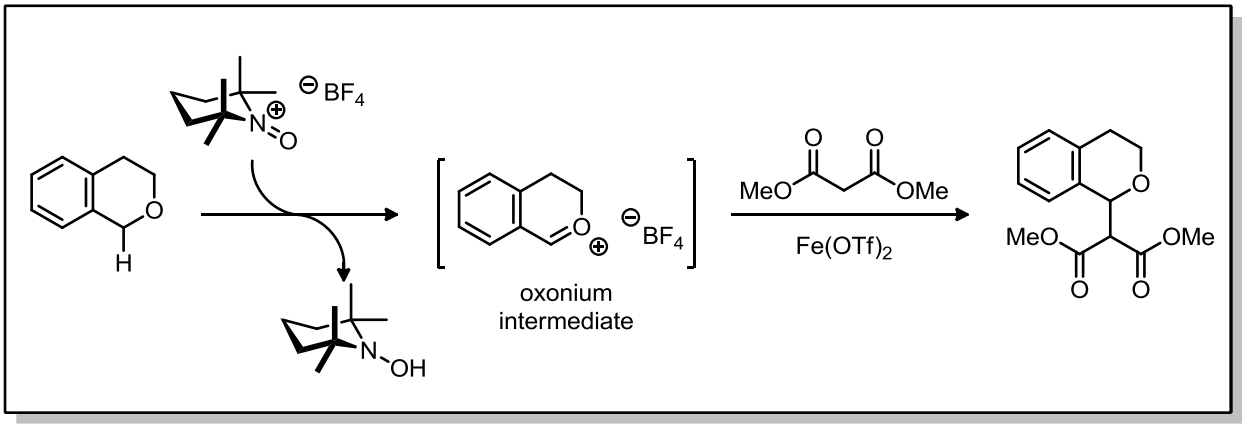

Figure 41: Functionalization of isochromane

The key step in the reaction sequence is the formation of the oxonium intermediate. The authors proposed the possibility of two punitive pathways to this species, one radical and one ionic. Their brief mechanistic studies were inconclusive and therefore the operative mechanism remains in question. To continue our study of oxidations at alkyl groups α to a C-O bond, we explored the theoretical oxidative functionalization of

[104] (a) Rohlmann, R.; Stopka, T.; Richter, H.; Mancheño, O. G. *J. Org. Chem.* **2013**, *78*, 6050; (b) Richter, H.; Mancheño, O. G. *Eur. J. Org. Chem.* **2010**, *4460.*

isochromane with a diester. The energetics of both the radical and ionic pathway were calculated and the respective potential energy surfaces are shown in Figure 42. In the radical pathway (red pathway), a high energy single electron transfer (SET) precedes a low barrier hydrogen atom transfer while the ionic pathway (green pathway) involves a hydride transfer in the transition-state. The hydride transfer TS of the ionic pathway was found to be favoured compared to the radical pathway by 8.5 kcal mol^{-1}. Thus the likely pathway is indeed ionic.

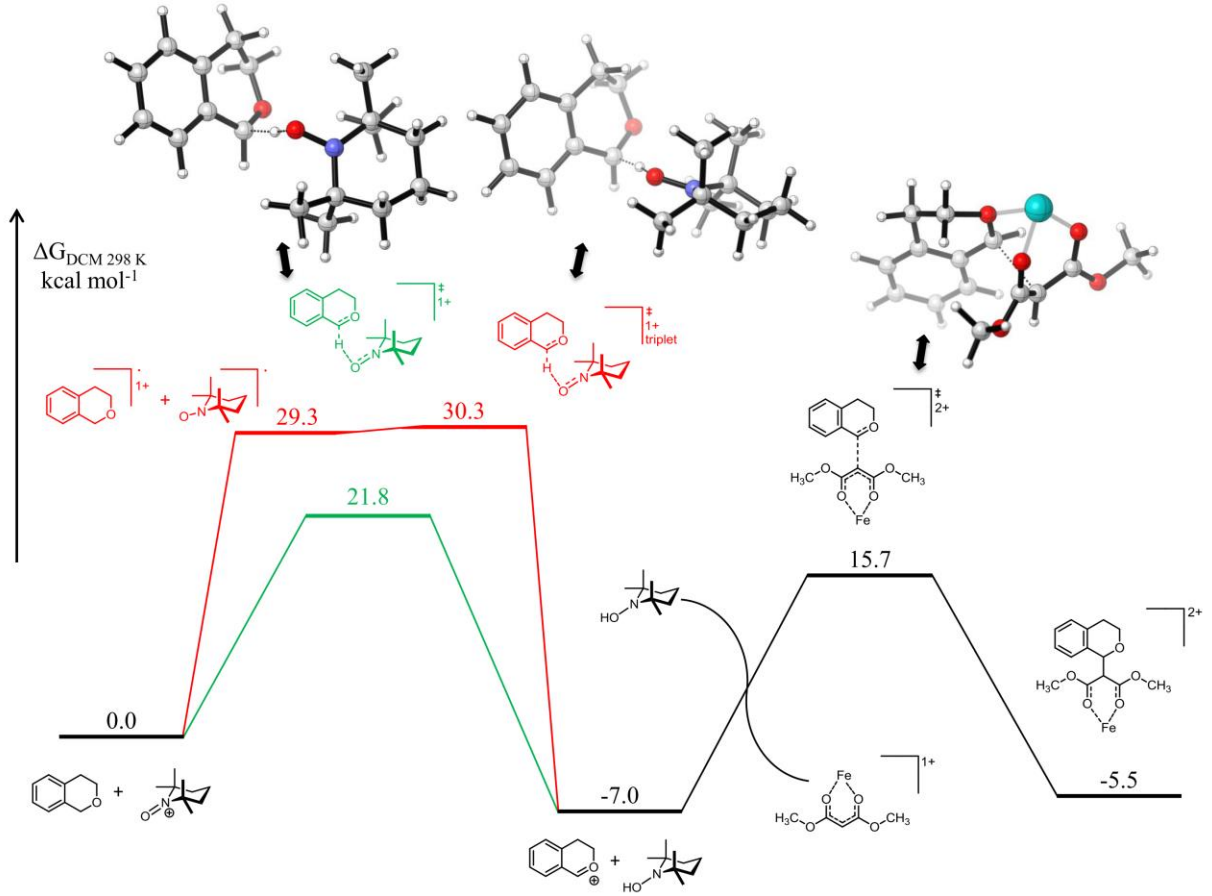

Figure 42: Reaction coordinate for the oxidative functionalization of isochromane. Relative Gibbs free energy values calculated at CPCM-DCM-B3LYP/6-31+G(d)//CPCM-DCM-B3LYP/6-311++G(d,p). Numeric values indicate energies in kcal mol^{-1}.

The formation of the cyclic ether cationic intermediate is exergonic by -7.0 kcal mol^{-1}. This oxonium intermediate then reacts with an iron–enolate complex and has a modest activation barrier of 20.8 kcal mol^{-1} from the ion and an overall favourable ΔG_{rxn}. The alkylation transition state structure (TSS) was simplified by assuming complete dissociation of the triflate ligands from $Fe(OTf)_2$. Multiple conformations of the TSS were computed, with the most energetically favourable structure being that shown above. The overall reaction scheme is exergonic and the theoretical results are in agreement with the reaction reaching completion in several hours at r.t. Furthermore, it is likely that upon decomplexation of the iron atom from the system, the reaction will be even more exergonic than that shown above.

2.4.4 Oxidation α to a C-N Bond - Oxidation of Imines

Wiberg and Bailey recently reported on the oxidation of amines to nitriles.[105] They posited the reaction proceed through an imine which formed following a hydride transfer and a deprotonation. Subsequently this imine was rapidly oxidized to a nitrile by a second hydride transfer event with a concerted deprotonation. This sequence is shown in Figure 43.

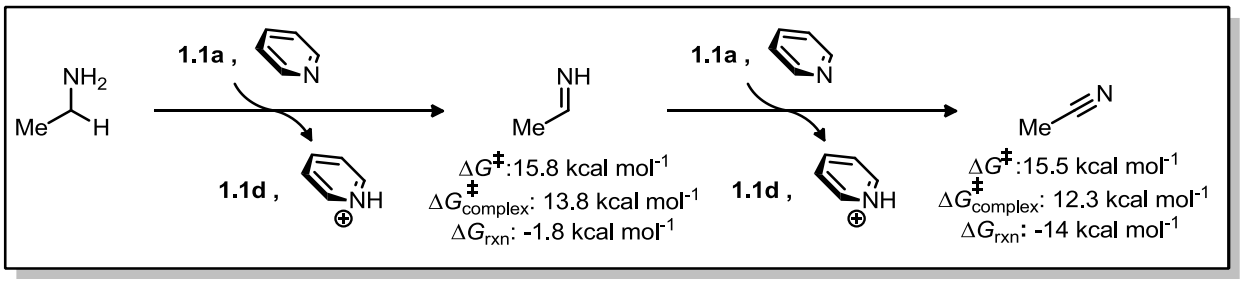

Figure 43: Proposed mechanism and computed energetics of the pathway

[105] Lambert, K. M.; Bobbitt, J. M.; Eldirany, S.A.; Wiberg, K. B.; Bailey, W. F. *Org. Lett.*, **2014**, *16*, 6484.

Using ethyl amine as a model amine, they explored the energetics of oxidation computationally in the context of a hydride transfer model and their results supported their putative mechanism. The activation barriers for each hydride transfer event were reasonable (≈ 16 kcal mol^{-1}). Not surprisingly, the activation barrier for a hydride transfer in aliphatic α-nitrogen systems is markedly lower than analogous α-oxygen systems, thus supporting the concept that the hydride transfer process is a function of the stability of the forming cationic species. The oxidation to the imine differed in its ΔG_{rxn} as compared to similar oxidations of alcohols to aldehydes ($\Delta G_{rxn(imine)}$: -1.8 kcal mol^{-1} vs $\Delta G_{rxn(aldehyde)}$: ≈ -20 kcal mol^{-1}), but this is to be expected give the disparity in bond strength between C=N and C=O bonds.

Our group has reported on a method to convert aldehydes and alcohols to nitriles using hexamethyldisilazane (HMDS) and **1.1a**.[106] Experimental mechanistic studies confirmed the intermediacy of an *N*-silyl imine. Interestingly, this reaction was highly exothermic (giving off a significant amount of heat), but required at least room temperature conditions to initiate. The reaction proceeded rapidly once initiated and resulted in the formation of Me_3Si-F as a by-product of oxidation. While confident that this oxidation similarly proceeded by a hydride transfer mechanism, we wanted to contrast the energetics of this oxidation with the report by Wiberg and Bailey (Figure 44). In comparison to the analogous oxidation from an imine to a nitrilium ion, the activation barrier for our more However, the overall ΔG_{rxn} of the process (including desilylation of the intermediate nitrilium ion with the fluoride anion) is 2.43 times more exergonic (-14.0

[106] Kelly, C. B.; Lamber, K. M.; Mercadante, M. A.; Ovian, J. M.; Bailey, W. F.; Leadbeater, N. E. *Angew. Chem. Int. Ed.* **2015**, *54*, 4241.

kcal mol^{-1} reported by Wiberg vs -39.9 kcal mol^{-1} reported here). The observed energetic disparities between the two reactions account for the experimental observations.

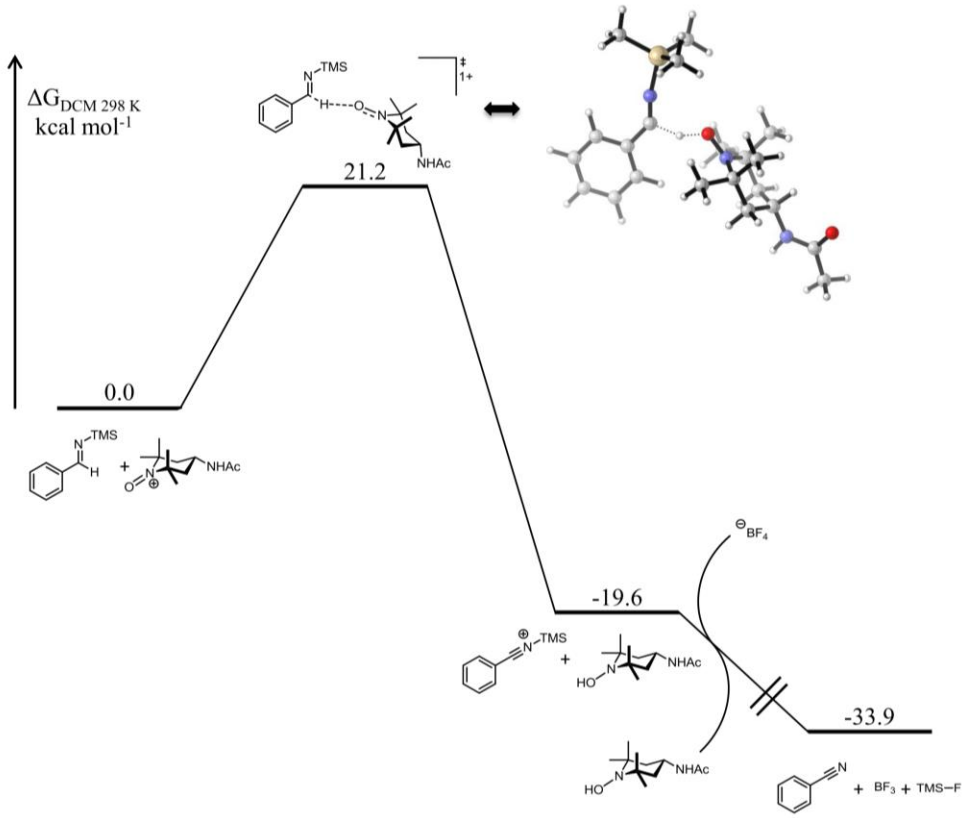

Figure 44: Reaction coordinate for the conversion of a silylated imine to a nitrile. Relative Gibbs free energy values calculated at CPCM-DCM-B3LYP/6-31+G(d)//CPCM-DCM-B3LYP/6-311++G(d,p). Numeric values indicate energies in kcal mol^{-1}.

2.4.5 Oxidation of Activated C-H Bonds - Allylic Oxidation

Based on previous unpublished experimental and computational work on the oxidation of cycloheptatriene by **1.1a**, we wondered whether the reported facile reaction of an oxoammonium species with a trisubstituted alkene reported by Bailey and coworkers[107] also proceeded by a hydride transfer pathway. The reaction leads to the formation of allylic alkoxyamines (Figure 45).

[107] Pradhan, P. P.; Bobbitt, J. M.; Bailey, W. F. *Org. Lett.* **2006**, *8*, 5485.

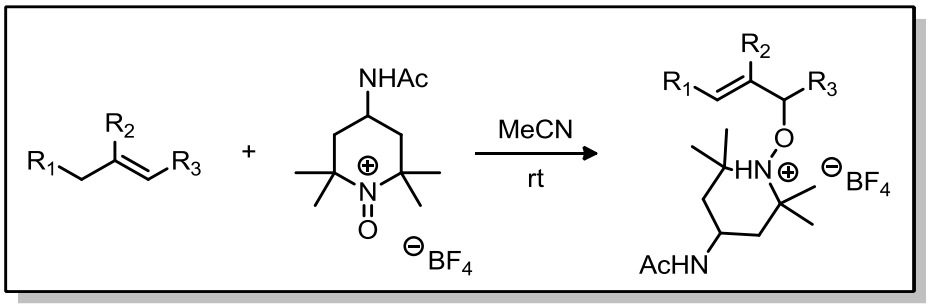

Figure 45: Ene-like addition of **1.1a** to alkenes

Bailey suggested that this reaction proceed through a concerted ene-like mechanism. The nucleophilic addition was said to proceed in a simultaneous manner with removal of the allylic proton and C-O bond formation (Figure 46).

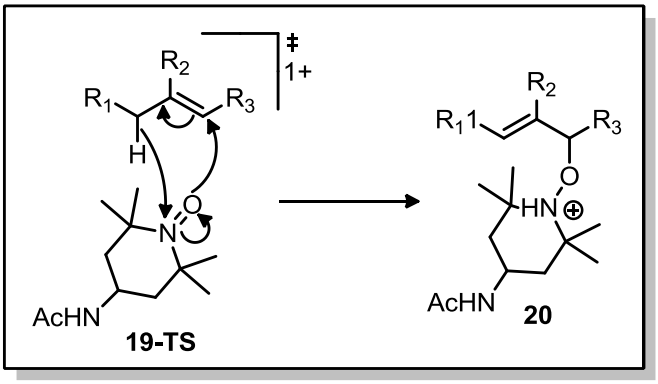

Figure 46: Ene-like mechanism proposed by Bailey leading to allylic alkoxyamines

To determine the operative pathway, we explored the energetics of both literature proposed route as well as the putative hydride transfer mechanism. When modelling the previously proposed ene-like pathway (Figure 45), we found the process to be concerted (Figure 47) as expected. The activation barrier for the concerted process was found to be 28.4 kcal mol^{-1} for 2-methyl-2-butene. Comparatively, the rate determining hydride transfer step in the theoretical stepwise pathway has an activation barrier of 29.7 kcal mol^{-1}.

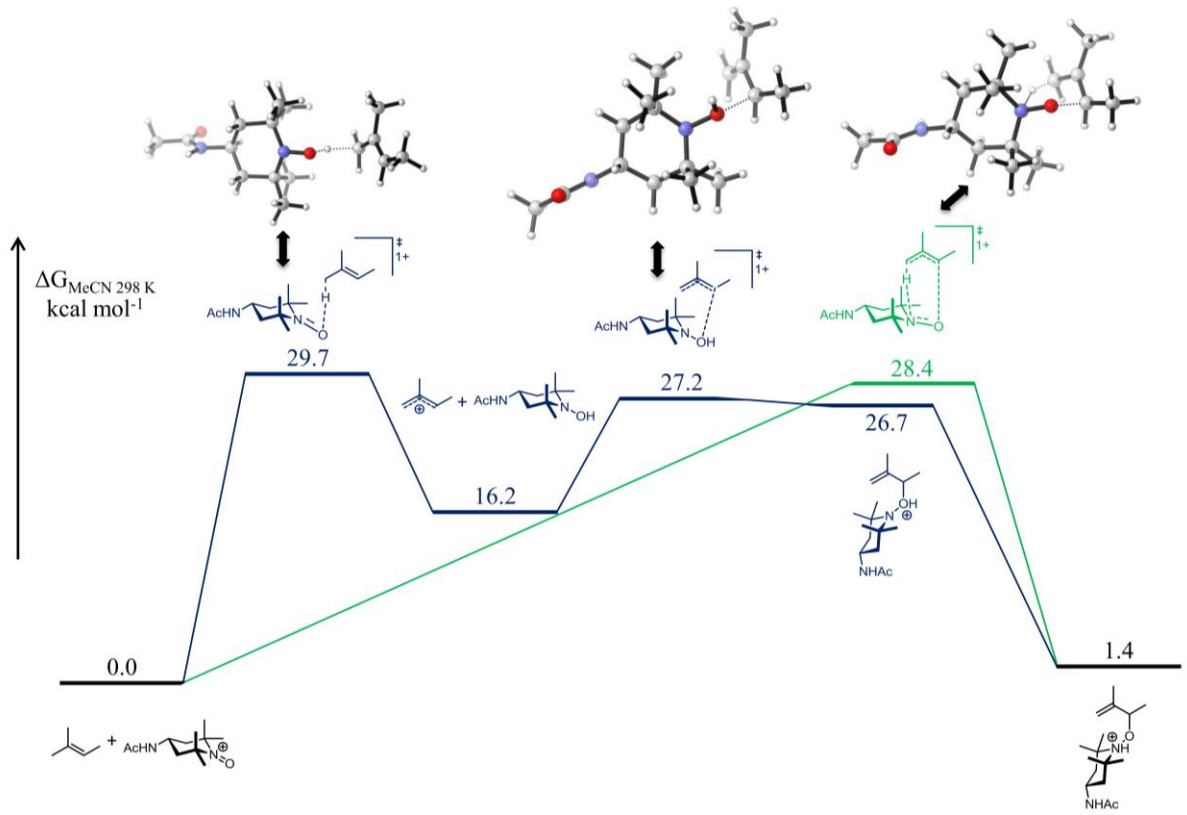

Figure 47: Reaction coordinate for the ene-like addition of **1.1a** and a simple alkene. Relative Gibbs free energy values calculated at CPCM-DCM-B3LYP/6-31+G(d)//CPCM-DCM-B3LYP/6-311++G(d,p). Numeric values indicate energies in kcal mol^{-1}.

The $\Delta\Delta G^{\ddagger}$ between the hydride transfer and the ene-like pathway is modest (1.3 kcal mol^{-1}). The ΔG_{rxn} to the carbocation is highly endergonic. In this case, the resulting cation is a stronger oxidant (i.e. a better hydride acceptor) than the oxoammonium cation. The thermodynamically unfavourable hydride transfer results in the inability to proceed forward in the reaction. Thus, while kinetically these two plausible mechanisms are almost equal, the unfavourable ΔG_{rxn} precludes a hydride transfer mechanism in this reaction manifold. Therefore we conclude that this is an exception to the hydride transfer mechanism with the six-membered transition-state structure being preferred.

2.4.6 Conclusions of Computational Studies

In closing, we have utilized experiment to confirm the existence of a possible H-bonded intermediate and have employed IRC experiments to confirm the existence of a dipole stabilized pre-oxidation complex. The concerted nature of the unassisted and base-assisted oxidation transition-state structures were probed using MOJ-style diagrams. They showed that in both the base and non-base mechanisms, the process was concerted asynchronous in nature. We next explored the effect of steric and electronics on the multiple steps of the oxidation process by modelling several diverse alcohols. Next we shifted our focus to oxidations α to a C-O bond and found the hydride transfer mechanism to be favourable compared to the proposed biradical pathway. Oxidations α to a C-N bond were also shown to likely proceed through a hydride transfer process, as confirmed by experimental and computational results. Such a hydride transfer mechanism provides an alternative to the commonly cited mechanism for oxoammonium cation-mediated oxidations originally proposed by Semmelhack.

Chapter 3: Harnessing the Power of Continuous Flow Technologies

3.1 BACKGROUND ON REACTION MONITORING IN MICROWAVE AND CONTINUOUS FLOW

Continuous-flow processing is used in the chemical industry on production scales. In a research and development setting, there has been increasing interest in using flow chemistry on smaller scales. To this end, a wide range of companies now produce equipment for both micro- and mesofluidic flow chemistry.[108] Some of the advantages of these devices are increased experimental safety, easy scale-up and thorough mixing of reagents.[109] It is not surprising, therefore, that a wide range of synthetic chemistry transformations have been reported using this equipment.[110] When it comes to evaluating the outcome of reactions performed using flow chemistry and optimizing reaction conditions, one option is to use inline product analysis. This opens the avenue for fast, reliable assay in comparison with the traditional approach in which performance is evaluated based on offline product analysis. When interfaced with microreactors, inline analysis has taken significant strides in recent years.[93e,111] Spectroscopic tools such as infrared[112], UV–visible[113], NMR[114], Raman[115], and mass spectrometry[116] have all been interfaced

[108] (a) Wiles, C.; Watts, P. Micro Reaction Technology in Organic Synthesis; CRC Press: Boca Raton, FL, USA, **2011**; (b) Luis, S. V.; Garcia-Verdugo, E., Eds. Chemical Reactions and Processes under Flow Conditions; Royal Society of Chemistry: Cambridge, U.K, **2010**.
[109] (a) Wiles, C.; Watts, P. *Chem. Commun.* **2011**, *47*, 6512; (b) Wegner, J.; Ceylan, S.; Kirschning, A. *Chem. Commun*. **2011**, *47*, 4583; (c) Razzaq, T.; Kappe, C. O. *Chem.–Asian J.* **2010**, *5*, 1274; (d) Mark, D.; Haeberle, S.; Roth, G.; von Stetten, F.; Zengerle, R. *Chem. Soc. Rev.* **2010**, *39*, 1153; (e) van den Broek, S. A. M. W.; Leliveld, J. R.; Delville, M. M. E.; Nieuwland, P. J.; Koch, K.; Rutjes, F. L. J. T. *Org. Process Res. Dev*. **2012**, *16*, 934.
[110] (a) Baxendale, I. R. *J. Chem. Technol. Biotechnol.* **2013**, *88*, 519; (b) Malet-Sanz, L.; Susanne, F. *J. Med. Chem.* **2012**, *55*, 4062.
[111] McMullen, J. P.; Jensen, K. F. *Annu. Rev. Anal. Chem.* **2010**, *3*, 19.
[112] (a) Moore, J. S.; Jensen, K. F. *Org. Process Res. Dev.* **2012**, *16*, 1409; (b) Greener, J.; Abbasi, B.; Kumacheva, E. *Lab Chip* **2010**, *10*, 1561.
[113] (a) Benito-Lopez, F.; Verboom, W.; Kakuta, M.; Gardeniers, J. G. E.; Egberink, R. J. M.; Oosterbroek, E. R.; van den Berg, A.; Reinhoudt, D. N. *Chem. Commun.* **2005**, 2857; (b) Lu, H.; Schmidt, M. A.; Jensen, K. F. *Lab Chip* **2001**, *1*, 22.

with success. There have been fewer reports when it comes to mesoflow systems. Perhaps most developed is the area of infrared monitoring. The now ubiquitous ReactIR equipment has been interfaced with commercially available flow equipment to allow for real-time analysis of reactions and on-the-fly optimization of conditions.[117]

3.1.1 Raman spectroscopy as a tool for monitoring mesoscale continuous-flow organic synthesis[118]

In our laboratory we have had success interfacing a Raman spectrometer with a scientific microwave unit.[119] This has allowed us to monitor reactions from both a qualitative[120] and quantitative[121] perspective. A recent report of the use of Raman spectroscopy for monitoring a continuous-flow palladium-catalyzed cross-coupling reaction[122] sparked our interest in interfacing our Raman spectrometer with one of our continuous-flow units and employing it for inline reaction monitoring of a number of key medicinally-relevant organic transformations.

In interfacing our Raman spectrometer with a continuous-flow reactor, our objective was to use a similar approach to that which proved successful when using microwave heating. Borosilicate glass is essentially "Raman transparent". Therefore reactions could be monitored by placing a Raman probe near the reaction vessel, without requirement to place any parts of the

---

[114] (a) Gökay, O.; Albert, K. *Anal. Bioanal. Chem*. **2012**, *402*, 647; (b) Jones, C. J.; Larive, C. K. *Anal. Bioanal. Chem.* **2012**, *402*, 61.
[115] (a) Mozharov, S.; Nordon, A.; Littlejohn, D.; Wiles, C.; Watts, P.; Dallin, P.; Girkin, J. M. *J. Am. Chem. Soc.* **2011**, *133*, 3601; (b) Lee, M.; Lee, J.-P.; Rhee, H.; Choo, J.; Chai, Y. G.; Lee, E. K. *J. Raman Spectrosc*. **2003**, *34*, 737.
[116] (a) Browne, D. L.; Wright, S.; Deadman, B. J.; Dunnage, S.; Baxendale, I. R.; Turner, R. M.; Ley, S. V. *Rapid Comm. Mass. Spectrosc.* **2012**, *26*, 1999; (b) Koster, S.; Verpoorte, E. *Lab Chip* **2007**, *7*, 1394.
[117] (a) Carter, C. F.; Lange, H.; Ley, S. V.; Baxendale, I. R.; Wittkamp, B.; Goode, J. G.; Gaunt, N. L. *Org. Process Res. Dev.* **2010**, *14*, 393–404; (b) Brodmann, T.; Koos, P.; Metzger, A.; Knochel, P.; Ley, S. V. *Org. Process Res. Dev.* **2012**, *16*, 1102.
[118] Hamlin, T. A.; Leadbeater, N. E. *Beilstein J. Org. Chem.*, **2013**, *9*, 1843.
[119] Leadbeater, N. E.; Schmink, J. R.; Hamlin, T. A. In Microwaves in Organic Synthesis, 3rd ed.; de la Hoz, A.; Loupy, A., Eds.; Wiley-VCH: Weinheim, Germany, **2012**.
[120] Leadbeater, N. E.; Schmink, J. R. Nat. Protoc. **2008**, *3*, 1.
[121] Schmink, J. R.; Holcomb, J. L.; Leadbeater, N. E. *Chem. Eur. J*. **2008**, *14*, 9943.
[122] Chaplain, G.; Haswell, S. J.; Fletcher, P. D. I.; Kelly, S. M.; Mansfield, A. *Aust. J. Chem.* **2013**, *66*, 208.

spectrometer inside the reaction vessel. The exposure of metallic components to the microwave field was avoided using a quartz light-pipe extending both the excitation laser and the acquisition fiber optic components of the spectrometer almost without any loss of light. The optimum distance of the light-pipe to the outside wall of the reaction vessel was found to be approximately 0.5 mm. Moving to our continuous-flow reactor, we decided to place the spectroscopic interface just after the back-pressure regulator assembly. This meant that we did not need to engineer a flow cell capable of holding significant pressure. Instead we used an off-the-shelf flow cell traditionally used in conjunction with other spectroscopic monitoring tools. The cell had screw-threaded inlet and outlet tubes of the same diameter as the tubing of the flow unit (i.d. 1 mm). The sample chamber had a width of 6.5 mm, height of 20 mm and a path length of 5 mm giving the cell a nominal internal volume of 0.210 mL (Figure 48, left). We built an assembly to allow us to hold the cell in a fixed location and vary the distance of the quartz light-pipe so as to optimize the Raman signal intensity. The apparatus is shown in Figure 48, right.

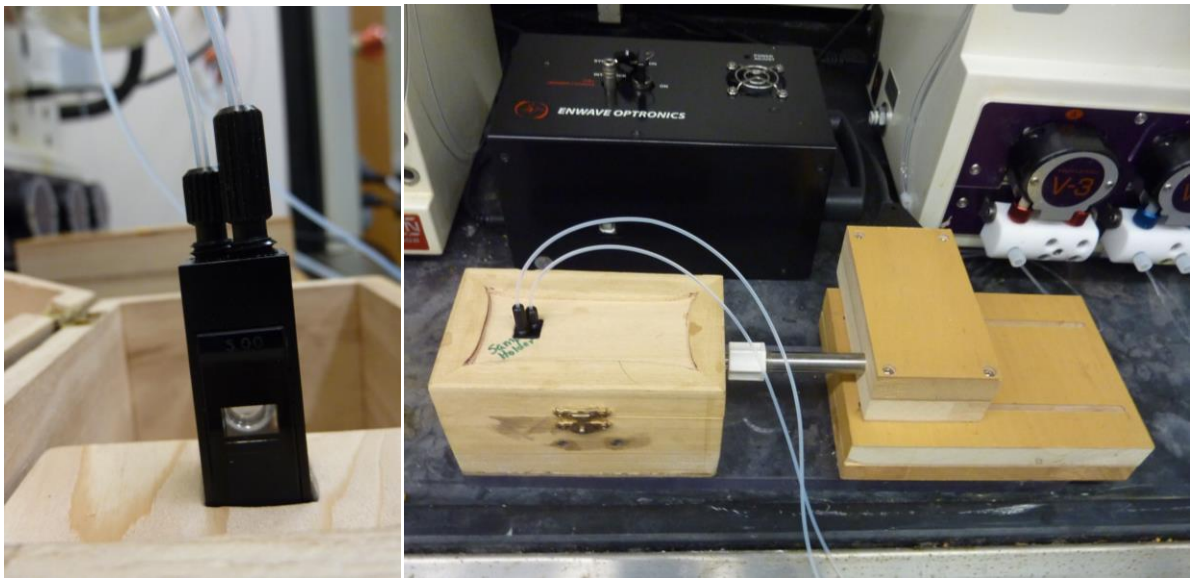

Figure 48: Flow cell (left), Raman interface used in the present study (right)

The first reaction we investigated was the piperidine-catalyzed synthesis of 3-acetylcoumarin (**3.1a**) from salicylaldehyde with ethyl acetoacetate (Figure 49). We had extensive experience of monitoring this reaction both qualitatively[120] and quantitatively[121] when using microwave heating so believed it would be a good starting point for our present study. The reaction works well when using ethyl acetate as the solvent. However, **3.1a** is not completely soluble at room temperature. To overcome potential clogging of the back-pressure regulator as well as mitigating the risk of having solid particles in the flow cell (which would perturb signal acquisition), we leveraged a technique our group had previously developed for this and other reactions.[123] Once the reaction stream has exited the heated zone, it is intercepted with a flow of a suitable organic solvent. This solubilizes the product and allows it to pass through the back-pressure regulator unimpeded. In the case of **3.1a**, we intercept the product stream with a flow of acetone.

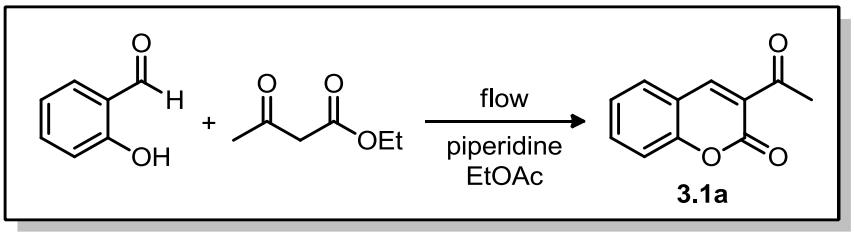

Figure 49: The reaction between salicylaldehyde and ethyl acetoacetate in the formation of 3-acetyl coumarin

Our first objective was to determine whether we could observe spectroscopically a slug of the coumarin passing through the flow cell. The Raman spectrum of 1 (Figure 50) exhibits strong Raman-active stretching modes at 1608 cm^{-1} and 1563 cm^{-1} while the salicylaldehyde and ethyl acetoacetate starting materials exhibit minimal Raman activity in this area. As a result, we chose to monitor the 1608 cm^{-1} signal.

[123] Kelly, C. B.; Lee, C.; Leadbeater, N. E. *Tetrahedron Lett.* **2011**, *52*, 263.

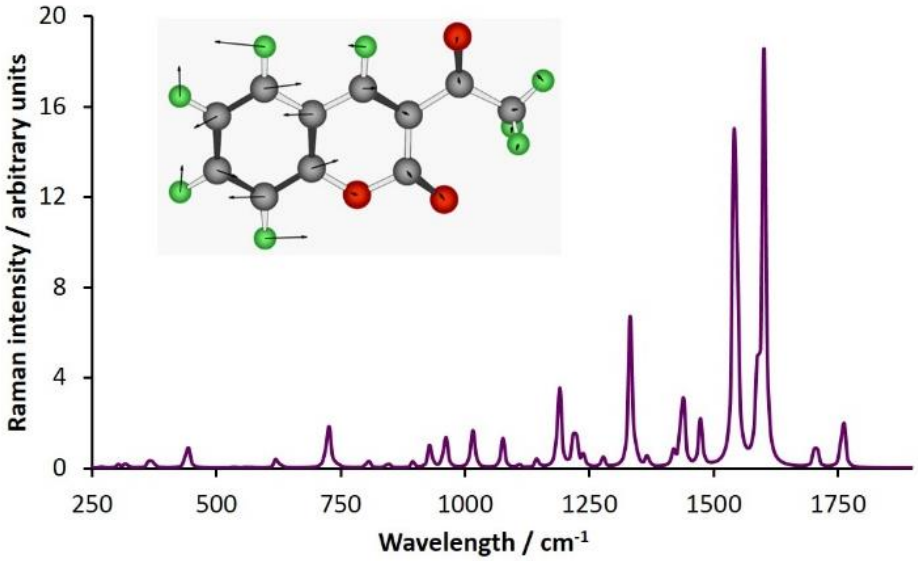

Figure 50: The Raman spectrum of 3-acetylcoumarin (**3.1a**) generated using Gaussian 09 at the B3LYP/6-31G(d) level of theory. The inset molecule illustrates the stretching mode responsible for the signal calculated at 1602 cm^{-1} (experimental: 1608 cm^{-1}). The Raman mode was visualized using Anamol 5.5.7, which is freely available from mathscriptor.org.

To mimic a product mixture, we pumped a solution of **3.1a** in acetone through our flow reactor, intercepted it with an equal volume of ethyl acetate and passed this mixture through the flow cell. We recorded a Raman spectrum every 15 s in an automated fashion as the coumarin passed through the cell by using the "continuous-scan" function on our spectrometer. By subtracting the spectrum of the solvent mixture (1:1 ethyl acetate : acetone) from the spectra recorded, we were able to clearly see the growth of the signal due to **3.1a** followed by a plateau as it passed through the cell and then a drop back to the baseline as the final aliquot exited (Figure 51).

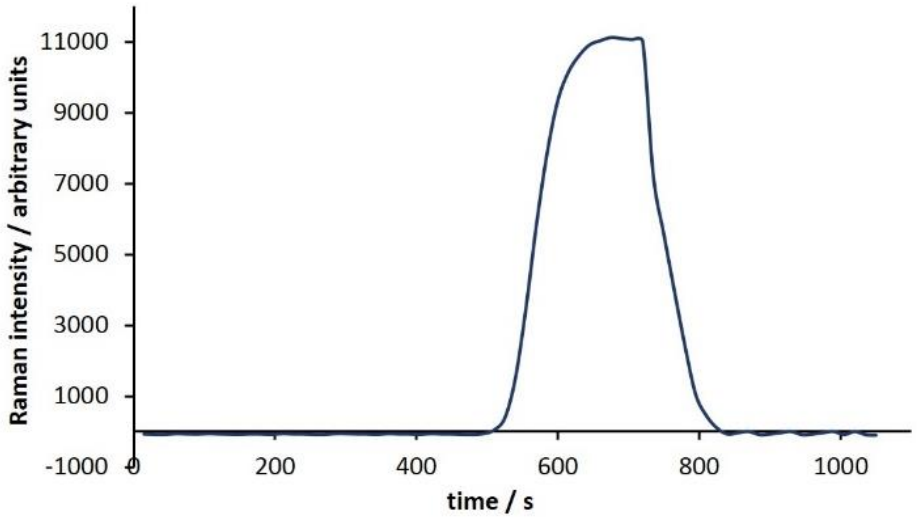

Figure 51: Monitoring an aliquot of 3-acetyl coumarin (**3.1a**) as it passes through the flow cell (scan time = 15 s, integration = 10 s)

Knowing we could observe the product as it passed through the flow cell, we next performed the complete reaction. As a starting point, we chose as conditions a flow rate of 1 mL min^{-1} through a 10 mL perfluoroalkoxy alkane (PFA) coil at room temperature. We were indeed able to monitor the reaction as shown in Figure 52. In an effort to optimize the reaction conditions, we varied both the temperature of the reactor coil and also the flow rate, monitoring each run and then compiling the data (Figure 52). While increasing the reaction temperature to 130 °C led to a marked increase in product conversion, reducing the flow rate from 1 mL min^{-1} to 0.5 mL min^{-1} at this temperature did not have a significant impact on the outcome of the reaction.

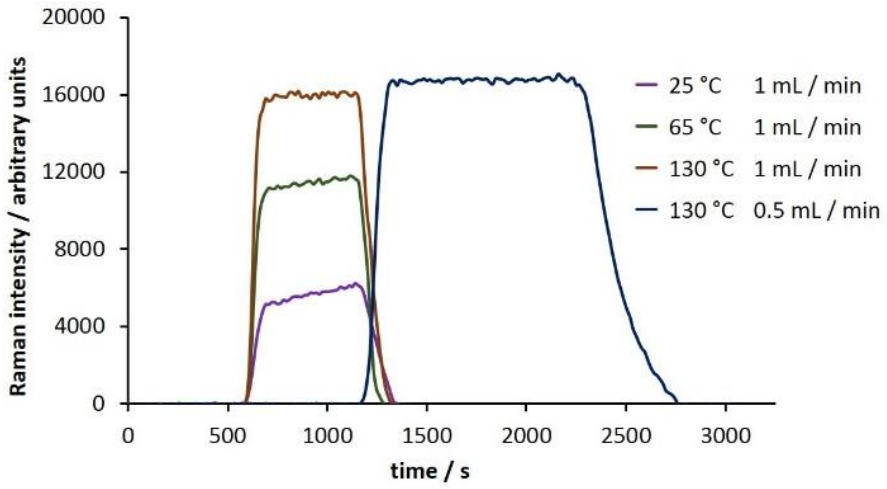

Figure 52: Monitoring the conversion of salicylaldehyde and ethyl acetoacetate to 3-acetylcoumarin (**3.1a**) across a range of reaction conditions (scan time = 15 s, integration = 10 s)

In an attempt to quantify product conversion, we needed next to obtain a calibration curve to allow us to convert units of Raman intensity to units of concentration in standard terms. To achieve this, we passed solutions of various concentrations of **3.1a** in ethyl acetate/acetone through the flow cell and collected the Raman spectrum. When the signal intensity at 1608 cm^{-1} is plotted against concentration, after subtraction of signals due to the solvent, the result is a straight line (Figure 53).

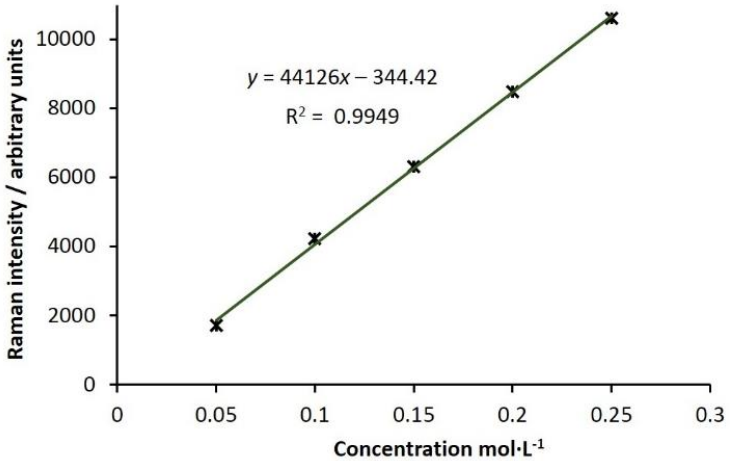

Figure 53: Plot of Raman intensity of the peak arising at 1608 cm^{-1} vs concentration of 3-acetyl coumarin (**3.1a**), yielding a straight line, y = mx + b; m = Raman intensity·M^{-1} of **3.1a**

The Stokes shift (which is being monitored) is inversely proportional to the temperature. Since the flow cell is situated after the product mixture exits the heated zone and because of the very efficient heat transfer observed using narrow-gauge tubing, the product mixture was at room temperature by the time it passed through the flow cell. As a result, it was not deemed necessary to involve a scaling factor to account for temperature effects. With the appropriate calibration curve in hand, we were able to obtain product conversion values for each set of reaction conditions screened, taking into account the fact that the product concentration is halved by the interception with acetone. To determine their accuracy, we also determined product conversion using NMR spectroscopy. Comparison of the values shows a good correlation (Table 14).

Table 14: Comparison of product conversion values obtained from Raman spectra with those obtained using NMR spectroscopy for the conversion of salicylaldehyde and ethyl acetoacetate to 3-acetylcoumarin (**3.1a**)

Conditions	**Raman monitoring**			**NMR**
	Concentration of **3.1a** when diluted with acetone (mol L^{-1})	Concentration of **3.1a** after normalizing for dilution by acetone (mol L^{-1})	Conv. (%)	Conv. (%)
25 °C, 1 mL min^{-1}	0.13	0.25	25	22
65 °C, 1 mL min^{-1}	0.27	0.55	55	58
130 °C, 1 mL min^{-1}	0.37	0.74	74	79
130 °C, 0.5 mL min^{-1}	0.39	0.78	78	80

We turned our attention next to the Knoevenagel condensation of ethyl acetoacetate with a range of aromatic aldehydes (Figure 54). Our objective was to optimize conditions using one aldehyde substrate spectroscopically from a qualitative standpoint and then screen other examples. We chose benzaldehyde as our initial substrate, ethyl acetate as the solvent and piperidine as a base catalyst. In order to determine the optimal spectral frequency at which to monitor we wanted to find a quick way to derive the Raman spectrum of the product **3.1b**. As was the case with **3.1a**, this could be achieved computationally using Gaussian 09 at the B3LYP/6-31G(d) level of theory, and a signal at 1598 cm^{-1} selected for monitoring.

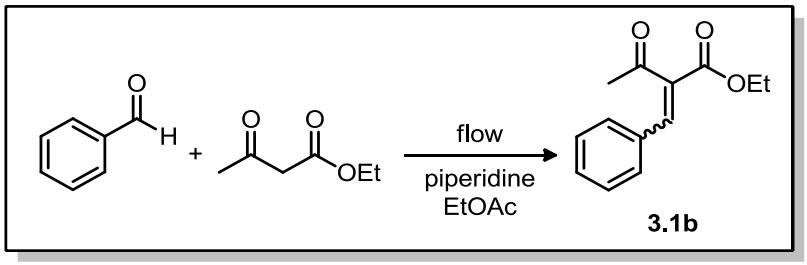

Figure 54: The Knoevenagel condensation of benzaldehyde and ethyl acetoacetate to yield (Z)-ethyl 2-benzylidene-3-oxobutanoate (**3.1b**)

Performing the reaction across a range of conditions, flowing the reaction mixture at 1 mL min^{-1} through the 10 mL coil heated to 130 °C proved to be optimal (Figure 55). A 67% conversion to 2a was obtained, as determined by GC analysis. Purification of the product mixture gave a 60% isolated yield of the E-isomer of **3.1b**.

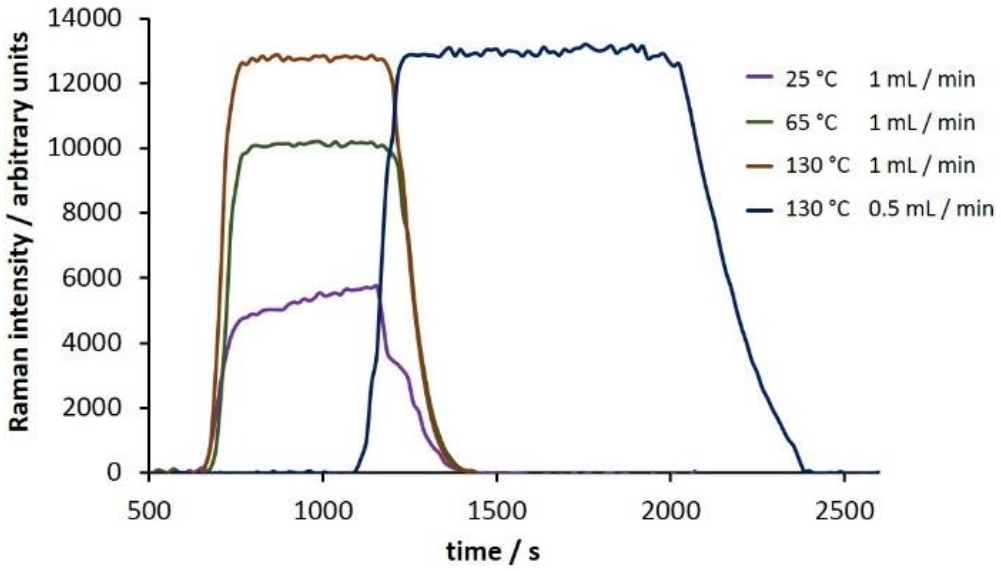

Conditions	Conversion to 3.1b (%)
25 °C, 1 mL min^{-1}	40
65 °C, 1 mL min^{-1}	63
130 °C, 1 mL min^{-1}	67
130 °C, 0.5 mL min^{-1}	68

Figure 55: Monitoring the conversion of benzaldehyde and ethyl acetoacetate to (Z)-ethyl 2-benzylidene-3-oxobutanoate (**3.1b**) across a range of reaction conditions (scan time = 15 s, integration = 10 s)

Using these optimized reaction conditions, we screened three para-substituted aldehyde substrates (Table 15). As expected, placing an electron-donating methoxy group on the aromatic ring led to lower product conversion as compared to benzaldehyde (Table 15, entry 2). A methyl- or fluoro-substituent has little effect on the outcome of the reaction (Table 15, Entries 3 and 4).

Table 15: Product conversion obtained for four aldehyde substrates in the Knoevenagel reaction with ethyl acetoacetate

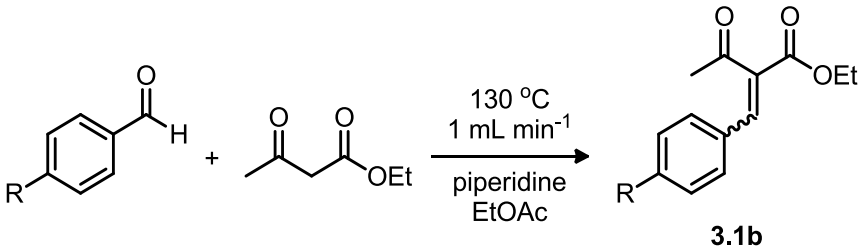

3.1b

Entry	R	Product	Conv. (%)[a]
1	H	3.1b	67 (60)[b]
2	OMe	3.1c	53
3	Me	3.1d	66
4	F	3.1e	63

[a]Conversion determined by GC analysis [b]Isolated yield after purification

We moved next to study the Claisen–Schmidt condensation of benzaldehyde with acetophenone to yield chalcone **3.1f** (Figure 56). Chalcones display interesting biological properties such as antioxidant, cytotoxic, anticancer, antimicrobial, antiprotozoal, antiulcer, antihistaminic, and anti-inflammatory activity.[124] They are also intermediates on the way to highly fluorescent cyanopyridine and deazalumazine dyes.[125] The calculated Raman spectrum of the product **3.1f** shows a very strong signal at 1604 cm^{-1}, which was selected for monitoring.

[124] Batovska, D. I.; Todorova, I. T. *Curr. Clin. Pharmacol*. **2010**, *5*, 1.
[125] .Bowman, M. D.; Jacobson, M. M.; Blackwell, H. E. *Org. Lett.* **2006**, *8*, 1645.

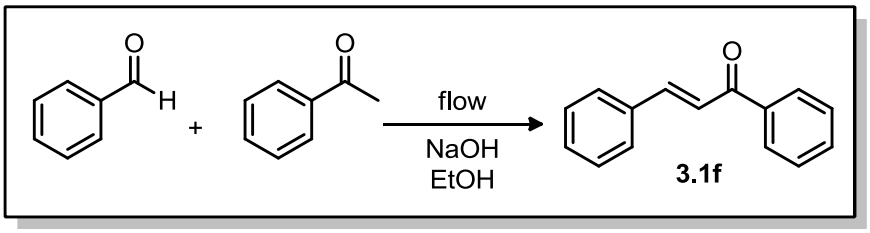

Figure 56: Claisen-Schmidt condensation of benzaldehyde with acetophenone to yield chalcone, **3.1f**

Using sodium hydroxide as the catalyst, the reaction was monitored under a range of reaction conditions (Figure 57). We fast discovered that at temperatures in excess of 65 °C we observed decomposition or else formation of a highly fluorescent byproduct, as evidenced by collapse of the Raman spectrum. We also observed a significant "tail" on the plot of signal intensity at 1604 cm^{-1} vs time. We attribute this to the fact that the chalcone product is very highly Raman active and even a trace in the flow cell can be readily detected. It does however highlight the fact that there may be both significant dispersion along the length of the reactor and the product is slow in clearing the flow cell. Dispersion is the consequence of laminar flow and some of the material takes longer to travel through the reactor than the rest. Thus, when a flow reactor is used to process a finite volume of reagents, the leading and trailing ends of the product emerging from the end of the reactor will have mixed to some extent with the solvent that preceded or followed it. This means that there are zones at the leading and trailing ends of the product stream in which the concentration of product is variable.

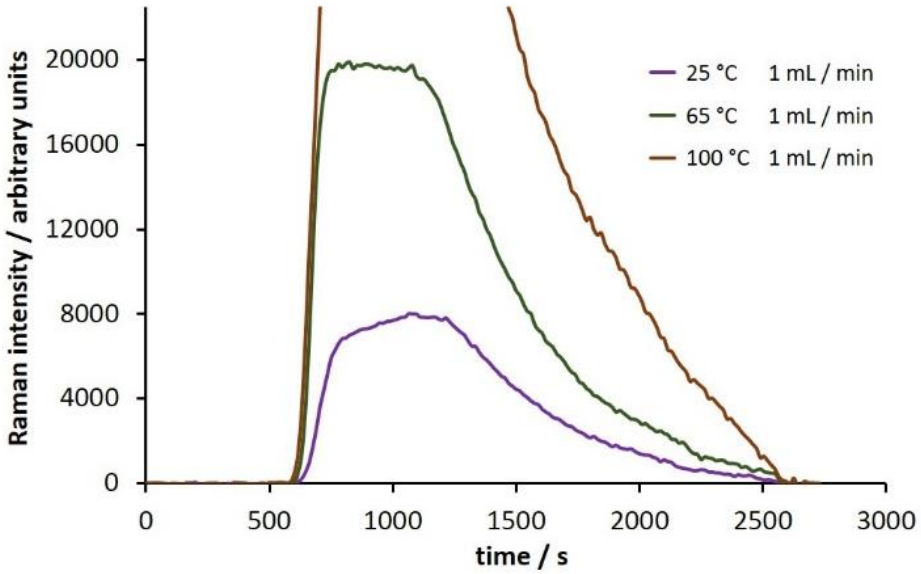

Conditions	Conversion to 3.1f (%)
25 °C, 1 mL min^{-1}	34
65 °C, 1 mL min^{-1}	90
100 °C, 1 mL min^{-1}	cannot monitor
65 °C, 0.5 mL min^{-1}	cannot monitor

Figure 57: Monitoring the conversion of benzaldehyde with acetophenone to chalcone, **3.1f**, across a range of reaction conditions (scan time = 15 s, integration = 10 s)

Our optimal conditions for the reaction were heating at 65 °C with a flow rate of 1 mL min^{-1}, this corresponding to a product conversion of 90%, as determined by GC analysis. Performing the reaction under these conditions using three substituted benzaldehydes as substrates, we obtained product conversions of 66-98% depending on the electronic nature of the aromatic ring of the aldehyde (Table 16).

Table 16: Product conversion obtained for four aldehyde substrates in the Claisen-Schmidt reaction with acetophenone

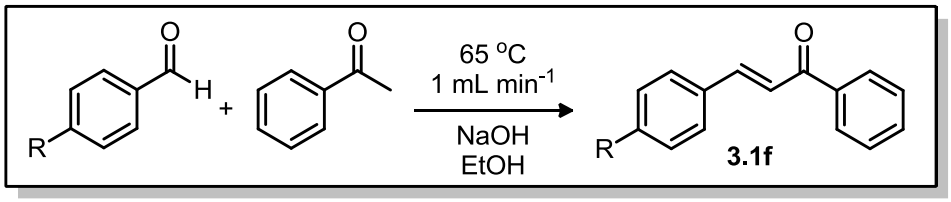

Entry	R	Product	Conv. (%)[a]
1	H	3.1f	90
2	OMe	3.1g	66
3	Me	3.1h	84
4	F	3.1i	98 (90)[b]

[a]Conversion determined by GC analysis [b]Isolated yield after purification

As our final reaction for study, we turned to the Biginelli reaction (Figure 58).[126] This acid-catalyzed cyclocondensation of urea, β-ketoesters and aromatic aldehydes to yield dihydropyrimidines has received significant attention, these products having pharmacological activity including calcium channel modulation, mitotic kinesin Eg5 inhibition, and antiviral and antibacterial activity.[127] The Biginelli reaction has been performed in flow previously as a route to densely functionalized heterocycles using HBr generated in a prior step as the catalyst for the reaction.[128] Copper catalysis has also been used in flow mode for preparing PEG-immobilized dihydropyrimidines.[129] We decided to screen a set of conditions for the reaction of benzaldehyde, ethyl acetoacetate and urea catalyzed by sulfuric acid (Figure 59).

[126] (a) Singh, K.; Singh, K. Adv. *Heterocycl. Chem.* **2012**, *105*, 223; (b) Panda, S. S.; Khanna, P.; Khanna, L. *Curr. Org. Chem.* **2012**, *16*, 507; (c) Kappe, C. O. *QSAR Comb. Sci.* **2003**, *22*, 630; (d) Mukhopadhyay, C.; Datta, A.; Banik, B. K. *J. Heterocycl. Chem*. **2011**, *44*, 979; (e) Fang, Z.; Lam, Y. *Tetrahedron* **2011**, *67*, 1294; (f) Dallinger, D.; Kappe, C. O. *Nat. Protoc*. **2007**, *2*, 317.
[127] (a) Singh, K.; Arora, D.; Singh, K.; Singh, S. *Mini-Rev. Med. Chem*. **2009**, *9*, 95; (b) .Kappe, C. O. *Eur. J. Med. Chem.* **2000**, *35*, 1043.
[128] Pagano, N.; Herath, A.; Cosford, N. D. P. *J. Flow Chem*. **2011**, *1*, 28.
[129] Prosa, N.; Turgis, R.; Piccardi, R.; Scherrmann, M.-C. *Eur. J. Org. Chem*. **2012**, 2188.

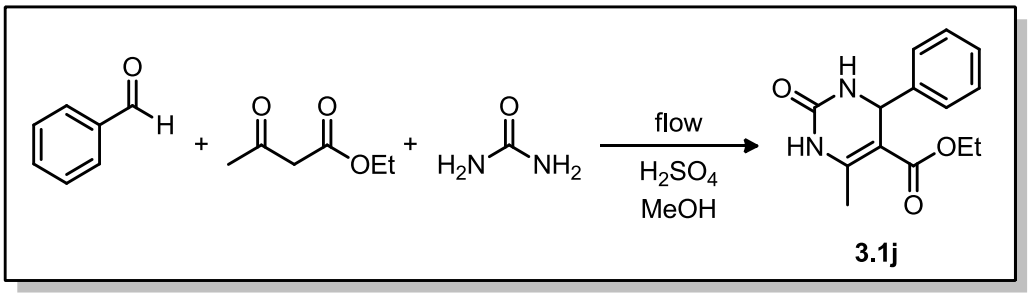

Figure 58: The Biginelli cyclocondensation of benzaldehyde, ethyl acetoacetate, and urea to yield 5-ethoxycarbonyl-6-methyl-4-phenyl- 3,4-dihydropyrimidin-2(1H)-one (**3.1j**)

The calculated Raman spectrum of the product, **3.1j**, shows a strong signal at 1598 cm^{-1} which was selected for monitoring. Using a catalyst loading of 10 mol% and a flow rate of 1 mL min^{-1}, we monitored the reaction over a temperature range from 25-120 °C. Seeing that the reaction did not reach completion within the 10 min in the heated zone, we then repeated the process at lower flow rates; first to 0.5 mL min^{-1} and then 0.25 mL min^{-1}.

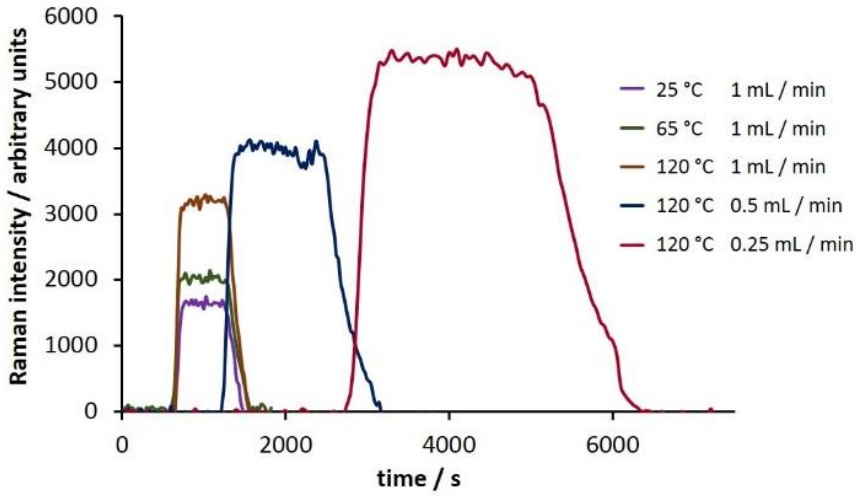

Conditions	Conversion to 3.1j (%)
25 °C, 1 mL min^{-1}	10
65 °C, 1 mL min^{-1}	20
120 °C, 1 mL min^{-1}	48
120 °C, 0.5 mL min^{-1}	62
120 °C, 0.25 mL min^{-1}	88

Figure 59: Monitoring the conversion of benzaldehyde, ethyl acetoacetate, and urea to 5-ethoxycarbonyl-6-methyl-4-phenyl-3,4-dihydropyrimidin-2(1H)-one (**3.1j**) across a range of reaction conditions (scan time = 15 s, integration = 10 s)

Our optimal conditions as determined by Raman monitoring were heating at 130 °C with a flow rate of 0.25 mL min^{-1}, this corresponding to a product conversion of 89% as determined by GC analysis and a product yield of 78% after purification. Performing the reaction using three other aldehyde substrates resulted in similar product conversions (Table 17).

Table 17: Product conversion obtained for four aldehyde substrates in the Biginelli reaction with ethyl acetoacetate and urea

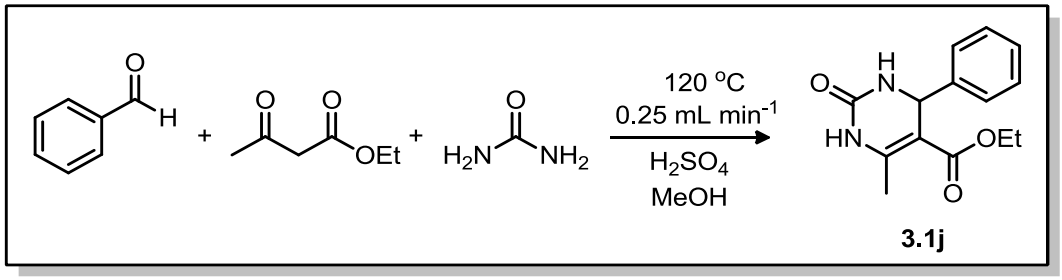

Entry	R	Product	Conv. (%)[a]
1	H	3.1j	88 (78)[b]
2	OMe	3.1k	85
3	Me	3.1l	87
4	F	3.1m	91

[a]Conversion determined by GC analysis [b]Isolated yield after purification

In conclusion, we have disclosed a method for real-time Raman monitoring of reactions performed using continuous flow processing. We assess its capability by studying four reactions. We find that it is possible to monitor reactions and also, by means of a calibration curve, determine product conversion from Raman spectral data as corroborated by data obtained using NMR spectroscopy.

3.2 TRANSITION OF A MULTISTEP REACTION FROM BATCH TO FLOW

3.2.1 A Continuous-Flow Approach to 3,3,3-Trifluoromethylpropenes: Bringing Together Grignard Addition, Peterson Elimination, Inline Extraction, and Solvent Switching[130]

After developing a method that utilized TFMKs as starting materials for the synthesis of 3,3,3-trifluoromethylpropenes in batch[38], we became interested in transitioning the methodology to continuous flow. The batch method, while being compatible with a wide range of functionalities, did have some drawbacks that could be overcome using flow reactors. The two-step process required isolation of the intermediate alcohol, thus limiting the amount of material produced per unit time and increasing waste. In an attempt to overcome these limitations, we wanted to transition our batch process to a continuous-flow approach.

We elected to first develop a method for the synthesis of the intermediate α-trifluoromethyl-β-hydroxysilyl alcohol before performing the two processes in tandem. Given the ubiquitous nature of main group organometallic reagents in organic chemistry, it comes as no surprise that there is literature precedent for their use in flow.[131] In batch, we performed the reaction at room temperature overnight. This is clearly too long a time for transition to flow processing. However, during our initial batch study we did not optimize the reaction. We therefore investigated the effects of temperature on the reaction. Using **3.2a** as a test substrate, we performed the reaction in THF, employing an excess of an approximately 1.8 M solution of the Grignard reagent. At room temperature, we obtained an 80% conversion to **3.2a** after 30 min (Table 18, Entry 1).

[130]Hamlin, T. A.; Lazarus, G. M. L.; Kelly, C. B.; Leadbeater, N. E. *Org. Process Res. Dev.* **2014**, *18*, 1253.

[131]***For examples:*** (a) Zhi, Z.; Jamison, T. F. *Angew. Chem. Int. Ed.* **2014**, *53*, 3353; (b) Murray, P. R. D.; Browne, D. L.; Pastre, J. C.; Butters, C.; Guthrie, D.; Ley, S. V. *Org. Process Res. Dev.* **2013**, *17*, 1192; (c) Polyzos, A.; O'Brien, M.; Petersen, T. P.; Baxendale, I. R.; Ley, S. V. *Angew. Chem. Int. Ed.* **2011**, *50*, 1190; (d) Riva, E.; Gagliardi, S.; Martinelli, M.; Passarella, D.; Vigo, D.; Rencurosi, A. *Tetrahedron* **2010**, *66*, 3242; (e) Roberge, D. M.; Bieler, N.; Mathier, M.; Eyholzer, M.; Zimmermann, B.; Barthe, P.; Guermeur, C.; Lobet, O.; Moreno, M.; Woehl, P. *Chem. Eng. Technol.* **2008**, *31*, 1146.

Performing the reaction at 40 °C increased the conversion to 95%, and complete conversion was observed when operating at 50 °C (Table 18, Entries 2 and 3) within the same length of time.

Table 18: Optimization of the Grignard reaction in continuous flow reactor[a]

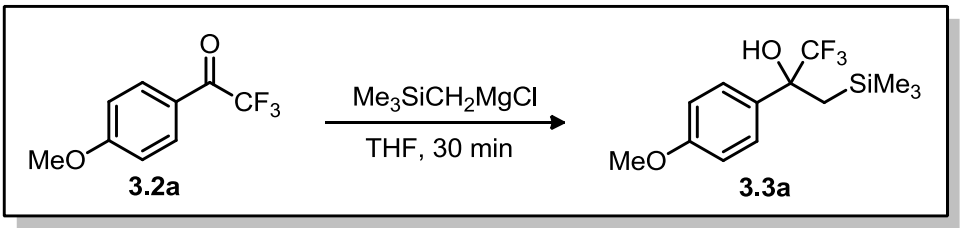

Entry	Temperature (^{o}C)	Conversion (%)[b]
1	25	80
2	40	95
3	50	100

[a]Reaction conditions unless otherwise noted: 2 mmol scale, **3.2a** (1 equiv, 1 M in anhydrous THF), Me_3SiCH_2MgCl (excess, ~1.8 M in anhydrous THF), 30 min [b]Determined by ^{1}H NMR spectroscopy

We next addressed the need for a solvent switch as the Lewis basic nature of THF would inhibit the Lewis acid catalyst. We proposed to undertake this at the same time as removing magnesium byproducts formed in the Grignard step. We believed that by performing an inline aqueous/organic extraction we would be able to remove the water-soluble magnesium salts as well as partitioning the THF into the aqueous phase with judicious choice of the new organic solvent. There have been many reports of inline extraction in flow.[132] One that particularly

[132] ***For examples:*** (a) Newby, J. A.; Huck, L.; Blaylock, D. W.; Witt, P. M.; Ley, S. V.; Browne, D. L. *Chem. Eur. J.* **2014**, *20*, 263; (b) Varas, A. C.; Noël, T.; Wang, Q.; Hessel, V. *ChemSusChem* **2012**, *5*, 1703; (c) Cervera-Padrell, A. E.; Morthensen, S. T.; Lewandowski, D. J.; Skovby, T.; Kiil, S.; Gernaey, K. V. *Org. Process Res. Dev.* **2012**, *16*, 888; (d) Hu, D. X.; O'Brien, M.; Ley, S. V. *Org. Lett.* **2012**, *14*, 4246; (e) O'Brien, M.; Koos, P.; Browne, D. L.; Ley, S. V. *Org. Biomol. Chem.* **2012**, *10*, 7031; (f) Sahoo, H. R.; Kralj, J. G.; Jensen, K. F. *Angew. Chem. Int. Ed.* **2007**, *46*, 5704.

attracted our attention involved a newly available membrane-based liquid−liquid separator (Figure 60).[133]

Figure 60: Membrane-based liquid−liquid separator employed in this study

The unit has excellent chemical compatibility, allows for operation under pressure (up to 300 psi), and can operate at flow rates up to 15 mL min^{-1}. In addition, it has a low separation pressure differential and therefore is suitable for the majority of aqueous/organic solvent pairs. Finally, it does not require any adjustments from the operator and so can be deployed as a "plug and play" unit. It exploits surface forces to achieve separation as shown schematically in Figure 61. When the two phases come in contact with the membrane, the wetting phase is prone to wet the membrane and travel through the membrane pores while the non-wetting phase is repelled. The membrane provides successful separation if the pressure differential across it is tightly controlled in order to let the wetting phase pass and not push the non-wetting phase through. To achieve this, the separator integrates a porous membrane (typically PTFE) with a high-precision pressure differential controller to ensure that optimal operating conditions are always maintained.

[133] (a) Adamo, A.; Heider, P. L.; Weeranoppanant, N.; Jensen, K. F. *Ind. Eng. Chem. Res*. **2013**, *52*, 10802; (b) Kralj, J. G.; Sahoo, H. R.; Jensen, K. F. *Lab Chip* **2007**, *7*, 256.

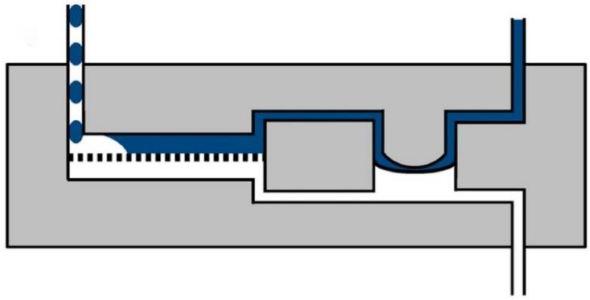

Figure 61: A schematic of the membrane-based separator employed in this study. The pressure differential controller (shown in the schematic with a deformed diaphragm (heavy curved line) provides a fixed pressure difference across the membrane (short vertical lines). The aqueous and organic phases are shown in blue and white, respectively.

Before using the separator, we returned to batch chemistry to find a suitable reaction medium for the TMSOTf-catalyzed dehydrative desilylation step. In our original approach we used DCM as the solvent. However, removal of THF from DCM would be difficult given its polar nature. We tried performing the desilylation in hexane, which would be a much more suitable solvent for removing THF by water washing, but the limited solubility of **3.3a** posed a problem. Moving to a 9:1 Hex/DCM mixture, we were able to perform the desilylation of **3.3a** in 10 min at room temperature with complete conversion to **3.4a** using TMSOTf (Figure 62).

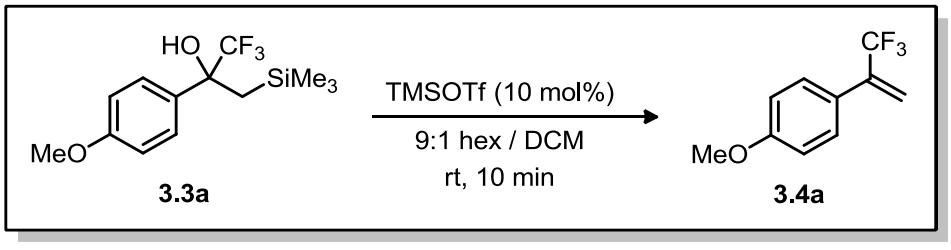

Figure 62: Dehydrative desilylation of **3.3a** to yield TFMA **3.4a**

Our strategy was to perform the Grignard reaction in THF in one flow coil, introduce a stream of dilute hydrochloric acid (to quench the Grignard reaction) followed by 9:1 Hex/DCM and then send this mixture into the aqueous/organic separator. Before attaching the separator, we wanted

to test the Grignard reaction in flow, followed by the solvent additions. We brought together THF solutions of **3.2a** (0.15 mL min^{-1}) and of Grignard reagent (0.22 mL min^{-1}), passing the mixture through a 10 mL PFA coil heated to 50 °C. We then introduced a stream of 10% HCl in water at a flow rate of 3 mL min^{-1} and 9:1 Hex/DCM at a flow rate of 0.75 mL min^{-1}. While the reaction was successful, we noted that the HCl quench led to the formation of a precipitate which, over time, clogged the tubing. To overcome this, we changed from HCl to HBF_4 as tetrafluoroborate salts typically have higher solubility than the corresponding halides. Using a 10% HBF_4 aqueous solution, we were able both to quench the Grignard reaction and ensure that the resulting magnesium by-products remained in solution. With these conditions in hand, we placed the separator inline. The separation was effective with alcohol **3.3a** remaining entirely in the organic phase. However there was also a significant amount of THF left in the organic phase. We hypothesized that the increased ionic strength of our aqueous stream decreased solubility of THF. To circumvent this issue, we decided to introduce a flow of deionized water into the organic stream leaving the first separator and then passed the resultant mixture through a second separator to remove more of the THF. We had to determine optimal flow rates for both aqueous streams in order to remove as much THF as possible. To achieve this, we started with a flow of THF (0.37 mL min^{-1}) introduced 10% aq. HBF_4, followed by 9:1 Hex/DCM (0.75 mL min^{-1}), passed this through the first separator, intercepted the organic output with a flow of water and then passed this through the second separator. Assaying the composition of the organic solvent mixture exiting this second separator by ^1H NMR spectroscopy as a function of flow rates of the two aqueous streams, we found that the optimal results were obtained when both operated at 3 mL min^{-1} (Table 19, Entry 3). We also probed the effect of separator membrane pore size. There was no observable difference between a 0.5 μm (Table 19, Entries 1-3) and 1.0 μm (Table 19,

Entries 4-6) pore size membrane. Under optimal working conditions, we were able to obtain an outlet stream with a relative molar composition of 9:3:1 of hexane, THF, and DCM, respectively.

Table 19: Effect of flow rate and membrane pore size on solvent composition[a]

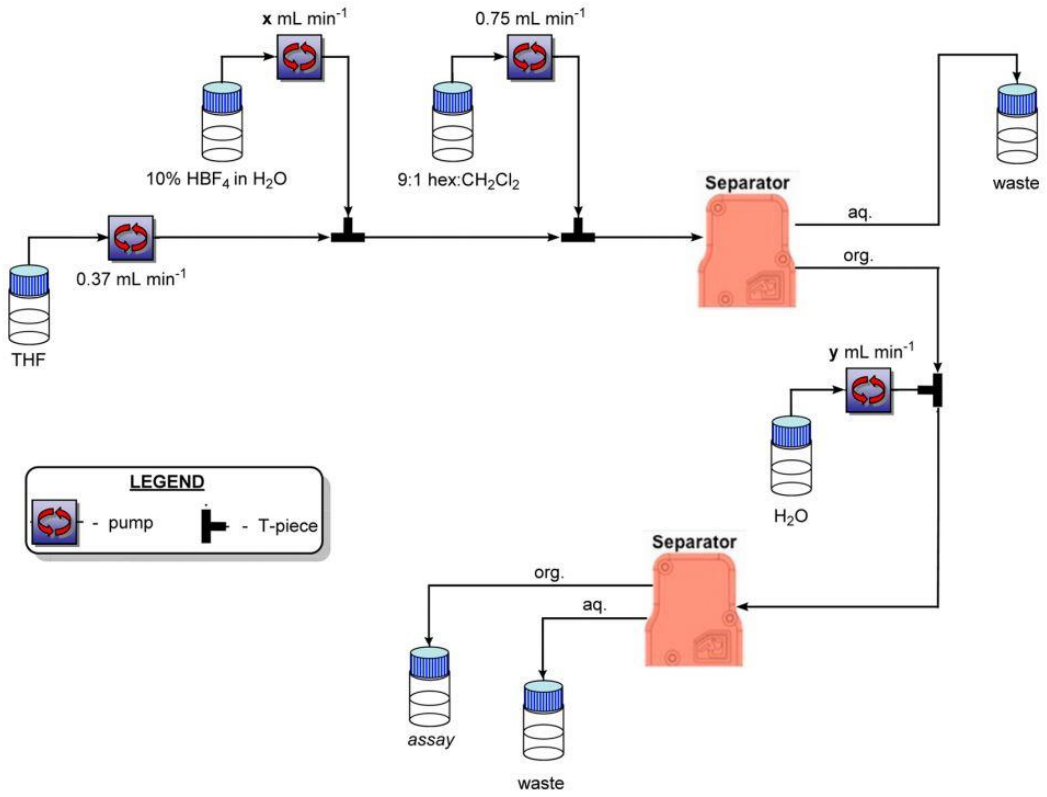

Entry	Pore Size (μm)	x (mL min^{-1})	y (mL min^{-1})	Hexane:THF:DCM
1	0.5	1	1	9:5:1
2	0.5	2	2	9:5:1
3	0.5	3	3	9:3:1
4	1.0	1	1	9:6:1
5	1.0	2	2	9:6:1
6	1.0	3	3	9:3:1

[a]Determined by 1 H NMR spectroscopy.

Knowing the composition of the solvent mixture exiting the second separator, we wanted to probe the sensitivity of the desilylation reaction to this quantity of THF in solution. We decided

to build margin into our experiments so instead of using a 9:3:1 molar ratio of hexane / THF / DCM, we opted to use a 9:3:1 volume ratio.

Table 20: Optimization of Lewis Acid loading and residence time[a]

Entry	TMSOTf (mol%)	Reaction Time (min)	Conversion (%)[b]
1	10	10	42
2	15	10	53
3	20	10	70
4	30	10	100
5	15	30	61

[a]Reaction conditions unless otherwise noted: silylated intermediate, **3.3a** (0.3 mmol scale, 1 equiv, 0.2 M in **3.3a**), TMSOTf, solvent (1.5 mL, 9:3:1 ~ Hexane:THF:DCM). [b]Determined by ^{1}H NMR spectroscopy.

This corresponds to a scenario where significantly more THF was in solution as compared to our ideal case.[134] To this end, we performed a series of small-scale batch tests in which we dosed different amounts of TMSOTf into a 9:3:1 (by volume) hexane/THF/DCM solution of **3.3a**. Operating at our previously published loading of 10 mol % TMSOTf we obtained a 42% conversion after a reaction time of 10 min (Table 20, entry 1). By increasing the catalyst loading to 30 mol %, we were able to obtain complete conversion (Table 20, entry 4). Using a catalyst loading of 15 mol % and extending the reaction time to 30 min did not offer an alternative strategy (Table 20, entry 5). We therefore opted to move forward with a TMSOTf loading of 30 mol % and a reaction time of 10 min for the desilylation in flow. With optimized conditions in hand for both steps of the reaction as well as for the separation/solvent swap, we concatenated our reactors, input streams, and separators to perform the synthesis of **3.4a** (Figure 63). Working on the 2 mmol scale, we obtained an 84% isolated yield of **3.4a**.

[134] A 9:3:1 molar ratio of Hex/THF/DCM corresponds to a 79:16:5 volume ratio.

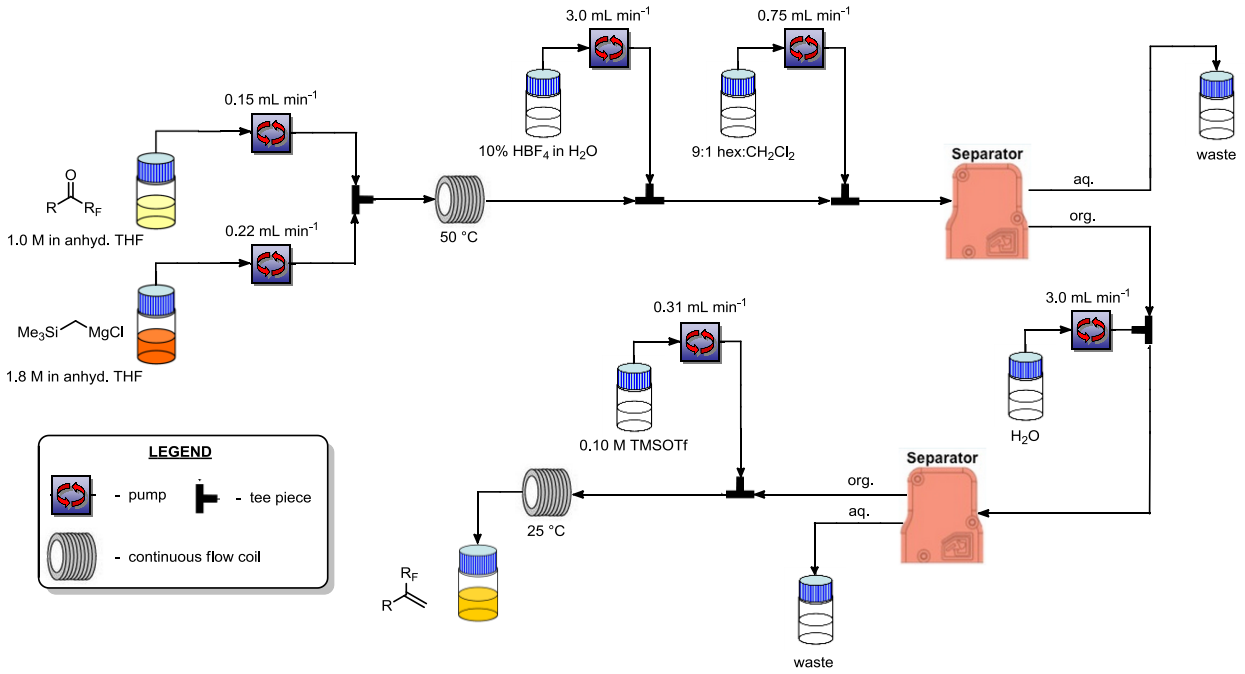

Figure 63: Flow configuration used for the methylenation of TFMKs

We next tested the substrate scope of the reaction, screening four additional TFMK starting materials. In each case, we obtained excellent isolated yields of the desired alkene products (Table 4, Entries 1−5).

Table 21: Methylenation of TFMKs in flow[a]

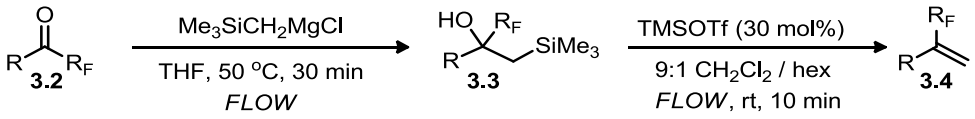

Entry	Ketone	Alkene	Yield in flow (%)[b]	Yield in batch (%)[c]
1	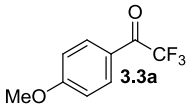 3.3a	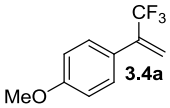 3.4a	84 (90)[d]	68
2	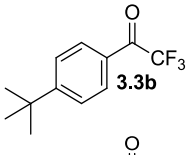 3.3b	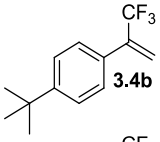 3.4b	90	65
3	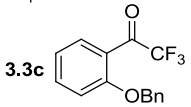 3.3c	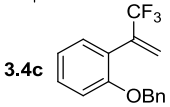 3.4c	89	67

Entry	Ketone	Alkene	Yield in flow (%)[b]	Yield in batch (%)[c]
4	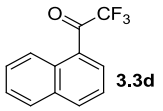 3.3d	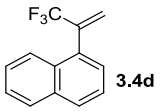 3.4d	92	72
5	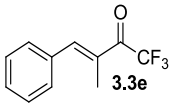 3.3e	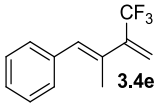 3.4e	92	75
6	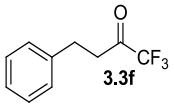 3.3f	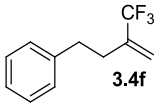 3.4f	94	85

[a]Reaction conditions unless otherwise noted: TFMK (2 mmol scale, 1 equiv, 1 M in anhyd. THF), Me_3SiCH_2MgCl (excess, ~1.8 M in anhyd. THF), TMSOTf (0.3 equiv, 0.33 M in hexane). [b]Isolated yield. [c]From ref 38. [d]Value in parentheses indicates isolated yield of alkene on 10 mmol scale.

The protocol works not only for TFMKs but also for a representative difluoromethyl analogue (entry 6). We also scaled up one example, processing 10 mmol of 1a and obtaining a 90% isolated yield of **3.3a** (entry 1). A comparison of yields obtained by the original batch and current flow methods is also shown in Table 4. Of note is that our flow approach is not only faster but also higher yielding than the corresponding batch methodology. This is because, in flow, there is no need for a workup step to isolate the alcohol intermediate. In addition, using the in-flow separator, we were able to obtain an improved separation during the extraction steps.

In summary, we have developed a continuous flow process for the synthesis of perfluoroalkyl alkenes. Transition from batch to continuous flow conditions allowed for higher yields, shorter reaction times, and facile scale out, allowing us to process ~14 g of TFMK per day. The process incorporates a solvent swap using a proprietary liquid−liquid extractor. This facilitates the twostep reaction sequence without isolation of the intermediate α- trifluoromethyl-β-hydroxysilyl alcohol. A range of substrates have been screened and, in each case, the reaction proceeded smoothly.

Closing Remarks

Chemistry is an interdisciplinary field and I am fortunate to have acquired substantial experience in both the physical and synthetic chemistry arenas. The future of the field will benefit greatly from the advantage computers provide chemists in the design and understanding of complex reactions. I have developed novel methodologies that are operationally easy and robust for the synthesis of fluorine containing molecules. I have studied two classes of reactions, oxidation reactions involving oxoammonium salts and 1,3-γ-silyl eliminations leading to strained CF_3 cyclopropanes, computationally and hope to have yielded insight into the features governing those reaction mechanisms. I have also utilized spectroscopic techniques, namely Raman spectroscopy, to quickly optimize reaction conditions in continuous flow. I have also recognized when a reaction would benefit from transition from batch to flow and successfully mitigate engineering issues, ultimately creating a multi-step flow sequence that has inline work-ups allowing for ~14 g of TFMK to be isolated per day. The time has now come to move on to new experiences in Europe at VU University Amsterdam!

Appendix I: *Preparation of Oxoammonium Salt **1.1a***

Synthesis of 4-acetamido-2,2,6,6-tetramethylpiperidine-1-oxoammonium tetrafluoroborate (1.1a, "Bobbitt's Salt", AcNH-TEMP=O$^+$ BF$_4^-$)[22a]

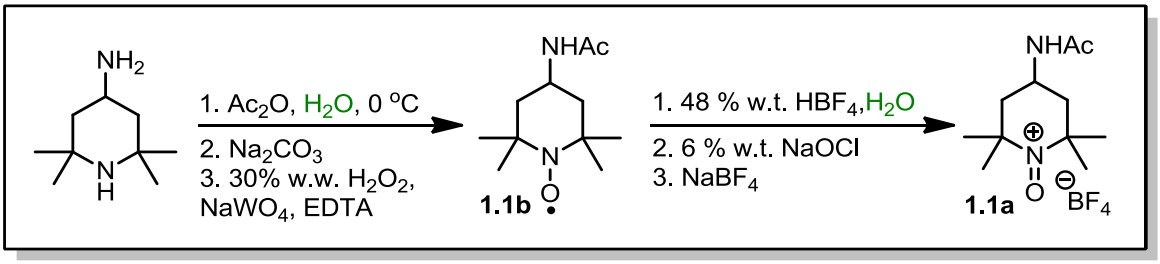

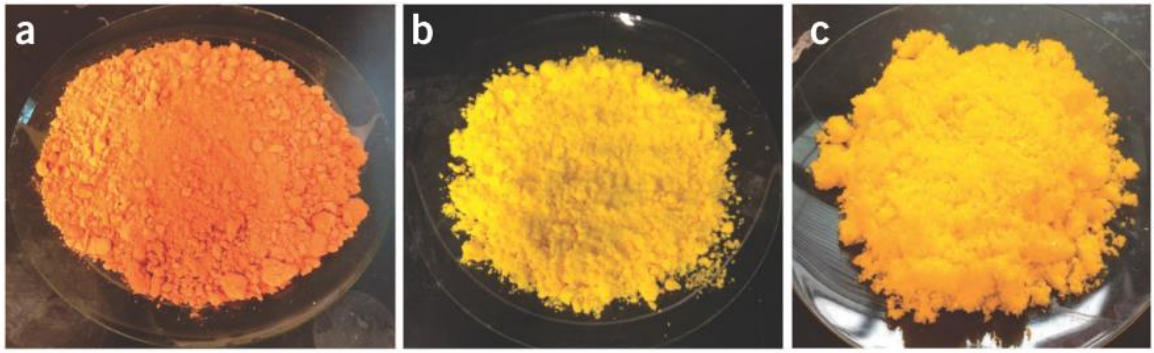

Figure X: Photographs of the compounds prepared using this procedure. (a) 4-Acetamido-(2,2,6,6-tetramethyl-piperidin-1-yl)oxyl (**1.1b**). (b) 4-Acetamido-(2,2,6,6-tetramethylpiperidine-1-oxoammonium tetrafluoroborate (**1.1a**). (c) Recrystallized 4-acetamido-2,2,6,6-tetramethylpiperidine-1-oxoammonium tetrafluoroborate (**1.1a'**).

Preparation of 4-acetamido-(2,2,6,6-tetramethyl-piperidin-1-yl)oxyl (1.1b)

In a 4-liter beaker, mix 4-amino-2,2,6,6-tetramethylpiperidine (**1.1e**) (156.27 g, 1.0 mol) and 200 ml of deionized water using a large stir bar. Place the beaker in a large ice bath and let the mixture stir for 15 min. Add 800 g of solid ice to the beaker and stir the mixture for 5 min. Add acetic anhydride (d = 1.082 g/mL) (122.4 g, 113.22 ml, 1.2 mol, 1.2 equiv.) to a 500 mL separatory funnel, and add this reagent to the beaker dropwise over 0.5 h. The temperature should be kept at 0 °C or lower during this addition. After the addition is complete, remove the reaction mixture from ice and allow it to stir for 1 h while warming to room temperature (r.t.; 20-27 °C).

At this time, slowly add solid sodium carbonate (148.4 g, 1.4 mol, 1.4 equiv.) in small portions (≈ 20 g each) to the aqueous mixture while stirring vigorously. ***Caution:*** *Some foaming will occur and CO_2 gas is evolved*. In addition, a precipitate is observed but will re-dissolve during the oxidation reaction. Next, slowly add sodium tungstate dihydrate (18.1 g, 0.055 mol 0.055 equiv.) while stirring vigorously. Slowly add EDTA (17.53 g, 0.060 mol, 0.06 equiv.) while stirring vigorously. Let the mixture stir for at least 10 minutes to ensure reagents are dissolved.

At this time, add fresh hydrogen peroxide (30 wt% in H_2O, d = 1.11 g/mL, 446.7 g, 402.4 ml, 3.94 mol, 3.94 equiv.) to the reaction mixture dropwise using a separatory funnel over 2 h while stirring vigorously.[135] ***Caution:*** *If the hydrogen peroxide is added too quickly, an exotherm is observed, resulting in overflow of the solution and in diminished yield*. To minimize this possibility, we recommended that the reaction mixture be placed in a large room temperature water bath to control the reaction rate. Stir the mixture for 24 h or until no more foaming is observed.[136]

The mixture will turn yellow, then orange, and finally a dense orange precipitate of nitroxide (**1.1b**) will form. Collect the resulting orange solid (**1.1b**) *via* vacuum filtration through a coarse fritted disk Büchner funnel. Transfer the solid to a large watch glass and let it air-dry to a constant weight.[137] A measure of 200 g of **1.1b** is obtained (94% yield, melting point 144-146 °C) as an orange solid. If desired, the nitroxide can be vacuum-dried at ≈ 50 °C. Although further purification is not needed, the nitroxide can be recrystallized from four times its weight of either deionized water or ethyl acetate, with a loss of about 15% in water and 10% in ethyl acetate. Compound **1.1b** can be stored in air indefinitely.

Preparation of 4-acetamido-(2,2,6,6-tetramethylpiperidine-1-oxoammonium tetrafluoroborate (1.1a, Bobbitt's salt)

In a 4-liter beaker, mix 4-acetamido-(2,2,6,6-tetramethyl-piperidin-1-yl)oxyl (**1.1b**) (200.0 g, 0.94 mol) with deionized water (376 ml, 2.5 M) using a large stir bar, yielding a thick orange slurry. Add tetrafluoroboric acid (48 wt% in water, d = 1.3 g/mL, 195.5 g, 1.07 mol, 1.14 equiv.) dropwise over 0.5 h using a separatory funnel while vigorously stirring the reaction mixture. Note that the slurry will turn from orange to yellow/brown (and occasionally black), and finally a yellow precipitate will form. Add commercial bleach (Clorox, 6% (wt/vol) NaOCl, 582 g, 0.47 mol, 0.5 equiv.) to the reaction mixture dropwise over 3 h using a separatory funnel while vigorously stirring the reaction mixture. ***Caution:*** *To avoid slight contamination from chlorinated material, an excess of bleach should not be used, and the Clorox solution should be added very slowly.*[138] Fresh Clorox should be used for optimal results. The solution will turn to a bright yellow color during this time.

At this time, add sodium tetrafluoroborate (102.9 g, 0.94 mol, 1 equiv.) and stir it for 10 min to 'salt out' the product. Place the beaker into a large ice bath and continue stirring for 2 h. Collect the resulting yellow solid (**1.1a**) *via* vacuum filtration using a coarse fritted disk Büchner funnel. Thoroughly wash the yellow solid with 200 ml of dichloromethane to remove any **1.1b** that might still be present. Transfer the solid to a large watch glass, and let it air-dry to constant weight. A measure of 256 g of 1 is obtained (91% yield, melting point 193–194 ^{o}C) as a bright yellow solid. If desired, the salt can be vacuum-dried at ≈ 50 ^{o}C. Although further purification is not needed, the salt can be recrystallized from deionized water (see next section). Alternatively, the salt can be vigorously stirred in dichloromethane (≈ 3 L) for 8 h to remove water and impurities. After filtration and being vacuum-dried, gives **1.1b** as a *very* fine bright yellow powder. Compound **1.1a** can be stored in air indefinitely.

[135] Another option is to add half of the hydrogen peroxide, let stir for 24 h then add the remaining hydrogen peroxide and let stir for at least 24 h.
[136] It is recommended that the reaction be left to stir for 3 days to obtain a higher the yield of #
[137] Drying in a vacuum oven gives
[138] Alternatively, the nitroxide can be a limiting reagent (0.98 equiv.) to avoid formation of chlorinated material.

Recrystallization of 4-acetamido-2,2,6,6-tetramethylpiperidine-1-oxoammonium tetrafluoroborate

The oxoammonium salt **1.1a** is pure enough for most oxidations. In rare cases, it must be recrystallized from deionized water. In a 250-ml beaker, boil 100 ml of deionized water while stirring with a medium-sized stir bar. Once the water is rapidly boiling, quickly add 40 g of **1.1a** while stirring. Note that the solution will turn black, but no apparent decomposition is observed. The origin of the intense black color is not known. After stirring for ≈ 1 min, filter the solution through a coarse filter in a pre-warmed funnel. Add sodium tetrafluoroborate (14.6 g, 0.13 mol, 1.0 equiv.) to the solution and stir the mixture for 1 min to dissolve the salt. Cool the solution quickly in an ice bath for 1 h. Collect the resulting yellow crystals of **1.1a** by vacuum filtration using a fritted disk Büchner funnel, washing with a minimum amount of cold deionized water. Transfer the yellow solid to a large watch glass and let it air-dry overnight. Expected recovery is 70–88%. Compound **1.1a** can be stored in air indefinitely.

Appendix II: *Experimental Procedure for Developed Synthetic Methods*

GENERAL EXPERIMENTAL DETAILS

All chemical transformations requiring inert atmospheric conditions or vacuum distillation utilized Schlenk line techniques with a 3,4, or 5-port dual-manifold or in a glove box. Nitrogen or argon was used to provide such an atmosphere. NMR Spectra (^{1}H, ^{13}C, ^{19}F) were collected at 298K on either a Brüker Avance Ultra Shield 300 MHz NMR, Brüker DRX-400 400 MHz NMR, or Brüker Avance 500 MHz NMR. ^{1}H NMR Spectra obtained in $CDCl_3$ were referenced to residual non-deuterated chloroform (7.26 ppm). ^{13}C NMR Spectra obtained in $CDCl_3$ were referenced to chloroform (77.3 ppm). ^{19}F NMR Spectra were referenced to or hexafluorobenzene (-164.9 ppm)[139]. Low resolution MS spectra were obtained on an Agilent Technologies 7820A Gas Chromatograph attached to a 5975 Mass Spectrometer. IR spectra were obtained using a Thermo Nicolet 3700. High-resolution mass spectra were obtained either using a JEOL AccuTOF-DART SVP 100 in positive direct analysis in real time (DART) ionization method, using PEG as the internal standard or an Agilent LC/MSD TOF (time-of-flight) mass spectrometer in an electrospray positive ionization mode via flow injection**.** TLC analysis was performed using hexanes/ethyl acetate as the eluent and visualized using permanganate stain, *p*-anisaldehyde stain, Seebach's Stain, and/or UV light. Flash chromatography was performed on either hand packed glass columns with Dynamic Adsorbants Inc. Flash Silica Gel (60 Å porosity, 32-63 µm). Automated Flash Chromotography was performed using either Biotage SNAP KP-SIL columns or Silicycle SiliaSep Flash Cartridges (60Å porosity, 40-63 µm).

[139] Ravikumar, I.; Saha, S.; Ghosh, P. *Chem. Commun*. **2011**, *47*, 4721.

EXPERIMENTAL DETAILS

Oxidation of α-Trifluoromethyl Alcohols Usng an Oxoammonium Salt

General Procedure for Oxidation of α-CF_3 Alcohols

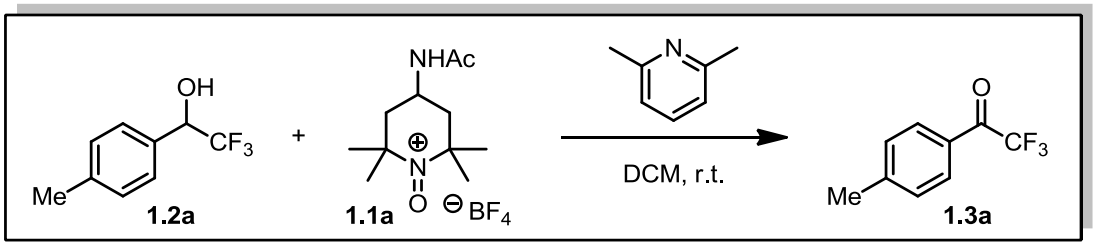

Preparation of 2,2,2-Trifluoro-1-(4-methylphenyl)ethanone (1.3a)

To a one-neck 50 mL round bottom flask equipped with stir bar was added oxoammonium salt, **1.1a** (3.01 g, 10 mmol, 2.5 equiv.), the α-CF_3 alcohol, **1.2a** (0.704 g, 4 mmol, 1 equiv.) in dichloromethane (10 mL, 0.4M in the alcohol) and 2,6-lutidine (0.964 g, 9 mmol, 2.25 equiv). The flask was sealed with a rubber septum and stirred overnight at room temperature. The solvent was removed *in vacuo* to afford a thick red residue. Anhydrous diethyl ether (≈ 30 mL) was added to the flask and allowed to stir for 10 min. This causes immediate precipitation of the nitroxide, **1.1b**. Note that it is imperative that the sides of the flask be scraped to ensure all the **1.1b** precipitates out releasing the product into solution. After stirring, the solution was filtered through a plug of silica (topped with a piece of filter paper to assist in recovery) and rinsed thoroughly (3-4 times) with anhydrous diethyl ether. The solvent was removed *in vacuo* by rotary evaporation in a room temperature water bath affording the pure TFMK **1.3a** (0.565 g, 75%) as a clear yellow oil.

^{1}H NMR ($CDCl_3$, 400 MHz) δ ppm 2.46 (s, 3 H) 7.35 (d, *J* = 8.07 Hz, 2 H) 7.98 (d, *J* = 7.83 Hz, 2 H) **^{13}C NMR** ($CDCl_3$, 101 MHz) δ ppm 22.0 (CH_3) 112.6 – 121.3 (q, $J_{\mathbf{C\text{-}F}}$ = 292.0 Hz, CF_3) 127.6 (C) 130.0 (CH_2) 130.4 (CH_2) 147.2 (C) 180.3 (q, $J_{\mathbf{C\text{-}C\text{-}F}}$ = 35.9 Hz, C) **^{19}F NMR** ($CDCl_3$, 377 MHz) δ ppm -71.38 **GC-MS** (EI) 188 ($[M]^+$, 15%, 119 (100%), 91 (67%), 89 (10%), 69 (5%), 65 (18%) **HRMS** (ESI+) calcd for $C_9H_7F_3O$ $[M + H]^+$ 189.0527, found: 189.0518.

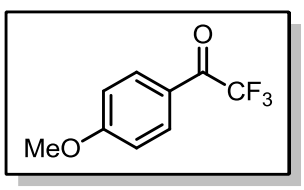

2,2,2-Trifluoro-1-(4-methoxyphenyl)ethanone (1.3b) (0.737 g, 90%) was prepared according to the representative procedure from 2,2,2-trifluoro-1-(4-methoxyphenyl)ethanol (**1.2b**) to give a clear yellow oil. **^{1}H NMR** ($CDCl_3$, 400 MHz) δ ppm 3.90 (s, 3 H) 6.99 (*apparent doublet*, *J* = 9.05 Hz, 2 H) 8.04 (*apparent doublet*, *J* = 8.07 Hz, 2 H) **^{13}C NMR** ($CDCl_3$, 101 MHz) δ ppm 55.9 (CH_3) 112.9 – 121.6 (q, $J_{\mathbf{C\text{-}F}}$ = 294.2 Hz, CF_3) 114.7 (CH) 123.1 (C) 133.0 (q, $J_{\mathbf{C\text{-}C\text{-}C\text{-}C\text{-}F}}$ =2.2 Hz, CH) 165.7 (C) 179.2 (q, $J_{\mathbf{C\text{-}C\text{-}F}}$ = 34.5 Hz, C) **^{19}F NMR** ($CDCl_3$, 377 MHz) δ ppm -71.06 **GC-MS** (EI) 204 (21%), 135 (100%), 107 (12%), 92 (24%), 77 (26%), 69 (4%), 64 (10%), 63 (10%) **HRMS** (ESI+), calcd for $C_9H_7F_3O_2$ $[M + H]^+$ 205.0476, found: 205.0475.

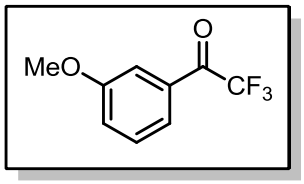

2,2,2-Trifluoro-1-(3-methoxyphenyl)ethanone (1.3c) (0.779 g, 89%) was prepared according to the representative procedure from 2,2,2-Trifluoro-1-(3-methoxyphenyl)ethanol (**1.2c**) to give a clear yellow oil. **^{1}H NMR** ($CDCl_3$, 400 MHz) δ ppm 3.87 (s, 3 H) 7.25 (ddd, *J* = 8.31, 2.69, 1.00 Hz, 1 H) 7.45 (t, *J* = 8.07 Hz, 1 H) 7.56 (s, 1 H) 7.65 (dq, *J* = 7.80, 1.00 Hz, 1 H) **^{13}C NMR** ($CDCl_3$, 101 MHz) δ ppm 55.7 (CH_3) 112.5-121.2 (q, $J_{\mathbf{C\text{-}F}}$ = 289.8 Hz, CF_3) 114.2 (q, $J_{\mathbf{C\text{-}C\text{-}C\text{-}C\text{-}F}}$ = 2.2 Hz, CH) 122.5 (CH) 123.0 (q, $J_{\mathbf{C\text{-}C\text{-}C\text{-}C\text{-}F}}$ = 2.9 Hz, CH) 130.3 (CH) 131.3 (C) 160.2 (C) 180.6 (q, $J_{\mathbf{C\text{-}C\text{-}F}}$ = 34.5 Hz, C) **^{19}F NMR** ($CDCl_3$, 377 MHz) δ ppm -71.26 **GC-MS** (EI) 204 ($[M]^+$, 37%), 135 (87%), 107 (36%), 92 (30%), 77 (35%), 69 (6%), 64 (14%), 63 (14%), 44 (11%), 40 (100%) **HRMS** (ESI+) calcd for $C_9H_7F_3O_2$ $[M + H]^+$ 205.0476, found: 205.0478.

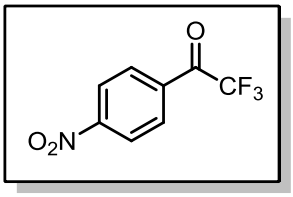

2,2,2-Trifluoro-1-(4-nitrophenyl)ethanone (1.3d) (0.870 g, 99%) was prepared according to the representative procedure from 2,2,2-trifluoro-1-(4-nitrophenyl)ethanol (**1.2d**) to give a powdery white solid (m.p. 42-44 °C, lit. 44-46 °C)[140]. **^{1}H NMR** (MeOD, 400 MHz) δ ppm 8.04 (*apparent doublet*, *J* = 9.05 Hz, 2 H) 8.45 (*apparent doublet*, *J* = 9.05 Hz, 2 H) **^{13}C NMR** (MeOD, 101 MHz) δ ppm 98.8 (q, $J_{\mathbf{C\text{-}C\text{-}C\text{-}F}}$ = 31.5 Hz, C) 121.2 – 129.7 (q, $J_{\mathbf{C\text{-}F}}$ = 287.6 Hz, CF_3) 125.6 (CH) 132.1 (d, $J_{\mathbf{C\text{-}C\text{-}C\text{-}C\text{-}F}}$ = 1.5 Hz, CH) 144.6 (C) 151.6 (C) **^{19}F NMR** (MeOD, 377 MHz) δ ppm -71.06 **GC-MS** (EI) 219 ($[M]^+$, 1%), 150 (100%), 104 (40%), 92 (18%), 76 (27%), 75 (13%), 69 (7%), 50 (14%) **HRMS** (ESI+) calcd for $C_8H_4F_3NO_3$ $[M + H + H_2O]^+$ 238.0327, found: 238.0346.

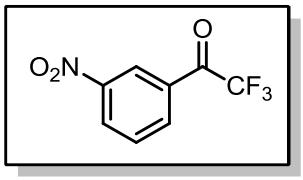

2,2,2-Trifluoro-1-(3-nitrophenyl)ethanone (1.3e) (0.830 g, 96%) was prepared according to the representative procedure from 2,2,2-trifluoro-1-(3-nitrophenyl)ethanol **(1.2e)** to give an off-yellow solid (m.p. 50-52 °C, lit. 54-56°C)[141]. **^{1}H NMR** (MeOD, 400 MHz) δ ppm 7.86 (t, *J* = 7.80 Hz, 1 H) 8.17 (dd, *J* = 7.83, 0.73 Hz, 1 H) 8.47 (ddd, *J* = 8.25, 2.26, 0.98 Hz, 1 H) 8.62 (d, *J* = 1.71 Hz, 1 H) **^{13}C NMR** ($CDCl_3$, 101 MHz) δ ppm 110.9-119.6 (q, $J_{\mathbf{C\text{-}F}}$ = 291.2 Hz, CF_3) 123.9 (q, $J_{\mathbf{C\text{-}C\text{-}C\text{-}C\text{-}F}}$ = 2.2 Hz, CH) 128.8 (CH) 129.9 (CH) 130.2 (C) 134.4 (q, $J_{\mathbf{C\text{-}C\text{-}C\text{-}C\text{-}F}}$ = 2.2 Hz, CH) 147.7 (C) 177.9 (q, $J_{\mathbf{C\text{-}C\text{-}F}}$ = 36.7 Hz, C) **^{19}F NMR** (MeOD, 377 MHz) δ ppm -71.90 **GC-MS** (EI) 219 ($[M]^+$, 1%), 204 (40%), 135 (95%), 107 (39%), 92 (33%), 77 (39%), 69 (7%), 64 (15%), 63 (15%), 22 (11%), 40 (100%) **HRMS** (ESI+) calcd for $C_8H_4F_3NO_3$ $[M + H + H_2O]^+$ 238.0327, found: 238.0344.

[140] Tyrra, W.; Kremlev, M. M.; Mushta, A. I.; Naumann, D.; Fischer, H. T. M.; Yagupolskii, Y. L. *J. Fluorine Chem.* **2007**, *128*, 1385.
[141] Srogl, J.; Liebeskind, L. S. *J. Am. Chem. Soc*, **2000**, *122*, 11260.

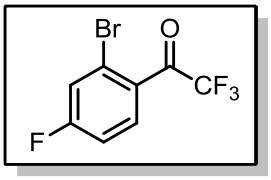

1-(2-Bromo-4-fluorophenyl)-2,2,2-trifluoroethanone (1.3f) (0.847 g, 78%) was prepared according to the representative procedure from **1**-(2-Bromo-4-fluorophenyl)-2,2,2-trifluoroethanol **(1.2f)** to give a clear yellow oil. **^{1}H NMR** ($CDCl_3$, 400 MHz) δ ppm 7.19 (ddd, *J* = 8.80, 7.46, 2.57 Hz, 1 H) 7.50 (dd, *J* = 8.19, 2.57 Hz, 1 H) 7.78 (ddq, *J* = 8.76, 5.67, 1.30, 1.30, 1.30 Hz, 1 H) **^{13}C NMR** ($CDCl_3$, 101 MHz) δ ppm 111.6 – 120.3 (q, $J_{\mathbf{C\text{-}F}}$ = 292.0 Hz, CF_3) 115.2 (d, $J_{\mathbf{C\text{-}C\text{-}F}}$ = 21.3 Hz, CH) 123.4 (d, $J_{\mathbf{C\text{-}C\text{-}F}}$ = 24.2 Hz, CH) 124.3 (d, $J_{\mathbf{C\text{-}C\text{-}C\text{-}F}}$ = 9.5 Hz, C) 128.3 (d, $J_{\mathbf{C\text{-}C\text{-}C\text{-}C\text{-}F}}$ = 3.7 Hz, C) 132.7 (dq, $J_{\mathbf{C\text{-}C\text{-}C\text{-}F}}$ = 9.8, $J_{\mathbf{C\text{-}C\text{-}C\text{-}C\text{-}F}}$ = 3.2 Hz, CH) 164.9 (d, $J_{\mathbf{C\text{-}F}}$ = 263.4 Hz, C) 180.8 (q, $J_{\mathbf{C\text{-}C\text{-}F}}$ = 37.4 Hz, C) **^{19}F NMR** ($CDCl_3$, 377 MHz) δ ppm -105.06 (q, *J* = 7.00 Hz, 1 F) -76.13 (s, 3 F) **GC-MS** (EI) 272 ($[M]^+$, 8%), 270 ($[M]^+$, 8%), 203 (97%), 201 (100%), 175 (46%), 173 (46%), 94 (57%), 93 (11%), 74 (11%), 69 (9%). **HRMS** (ESI+) calcd for $C_8H_3BrF_4O$ $[M + H]^+$ 270.9382, found: 270.9379.

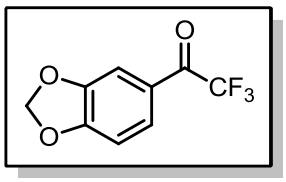

1-(Benzo[d][1,3]dioxol-5-yl)-2,2,2-trifluoroethanol (1.3g) (0.833 g, 97%) was prepared according to the representative procedure from 1-(benzo[d][1,3]dioxol-5-yl)-2,2,2-trifluoroethanol (**1.2g**) to give a clear yellow oil. **^{1}H NMR** ($CDCl_3$, 400 MHz) δ ppm 6.08 (d, *J* = 1.00 Hz, 2 H) 6.89 (d, *J* = 8.31 Hz, 1 H) 7.44 (d, *J* = 0.98 Hz, 1 H) 7.67 (d, *J*=8.31 Hz, 1 H) **^{13}C NMR** ($CDCl_3$, 101 MHz) δ ppm 102.7 (CH_2) 108.7 (CH) 109.4 (q, $J_{\mathbf{C\text{-}C\text{-}C\text{-}F}}$ = 2.2 Hz, CH) 112.7 – 121.4 (q, $J_{\mathbf{C\text{-}F}}$ = 291.2 Hz, CF_3) 124.6 (C) 127.8 (q, $J_{\mathbf{C\text{-}C\text{-}C\text{-}F}}$ = 2.9 Hz, CH) 148.9 (C) 154.3 (C) 178.8 (q, $J_{\mathbf{C\text{-}C\text{-}F}}$ = 34.5 Hz, C) **^{19}F NMR** ($CDCl_3$, 377 MHz) δ ppm -70.76 **GC-MS** (EI) 218 ($[M]^+$, 41%), 149 (100%), 121 (34%), 91 (10%), 69 (5%), 65 (24%), 63 (20%), 62 (10%) **HRMS** (ESI+), calcd for $C_9H_5F_3O_3$ $[M + H]^+$ 219.0269, found: 219.0257.

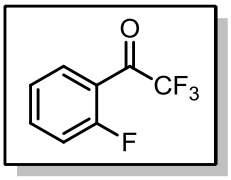

2,2,2-trifluoro-1-(2-fluorophenyl)ethanone (1.3h) (0.563 g, 73%) was prepared according to the representative procedure from 2,2,2-trifluoro-1-(2-fluorophenyl)ethanol **(1.2h)** to give a clear orange oil. **^{1}H NMR** ($CDCl_3$, 400 MHz) δ ppm 7.32 (t, *J* = 9.00 Hz, 1 H) 7.41 (t, *J* = 7.46 Hz, 1 H) 7.78 (d, *J* = 4.89 Hz, 1 H) 7.99 (t, *J* = 7.21 Hz, 1 H) **^{13}C NMR** ($CDCl_3$, 101 MHz) δ ppm 105.7 – 114.3 (q, $J_{\mathbf{C\text{-}F}}$ = 289.8 Hz, CF_3) 111.9 (d, $J_{\mathbf{C\text{-}C\text{-}F}}$ = 20.5 Hz, C) 113.6 (d, $J_{\mathbf{C\text{-}C\text{-}C\text{-}F}}$ = 10.3 Hz, CH) 119.2 (CH) 125.8 (CH) 131.7 (d, $J_{\mathbf{C\text{-}C\text{-}C\text{-}F}}$ = 8.8 Hz, CH) 156.1 (d, $J_{\mathbf{C\text{-}F}}$ = 262.6 Hz, C) 173.2 (q, $J_{\mathbf{C\text{-}C\text{-}F}}$ = 38.1 Hz, C) **^{19}F NMR** ($CDCl_3$, 376 MHz) δ ppm -107.72 - -107.48 (m, 1 F) -74.79 (d, *J* = 16.35 Hz, 3 F) **GC-MS** (EI) 192 ($[M]^+$, 7%), 123 (100%), 95 (54%), 75 (22%), 69 (9%) **HRMS** (ESI+) calcd for $C_8H_4F_4O$ $[M + H]^+$ 193.0277, found: 193.0310.

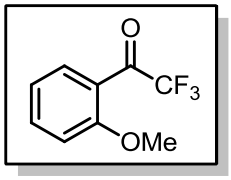

2,2,2-trifluoro-1-(2-methoxyphenyl)ethanone (1.3i) (0.814 g, 96%) was prepared according to the representative procedure from 2,2,2-trifluoro-1-(2-methoxyphenyl)ethanol **(1.2i)** to give a clear orange oil. **^{1}H NMR** ($CDCl_3$, 400 MHz) δ ppm 3.92 (s, 3 H) 7.01 - 7.10 (m, 2 H) 7.60 (ddd, *J* = 8.56, 7.34, 1.71 Hz, 1 H) 7.68 (d, *J* = 7.82 Hz, 1 H) **^{13}C NMR** ($CDCl_3$, 101 MHz) δ ppm 55.5 (CH_3) 111.5 – 120.2 (q, $J_{\mathbf{C\text{-}F}}$ = 290.5 Hz, CF_3) 111.8 (CH) 120.3 (CH) 121.3 (C) 130.9 (d, $J_{\mathbf{C\text{-}C\text{-}C\text{-}C\text{-}F}}$ = 1.5 Hz, CH) 135.5 (CH) 159.5 (C) 182.6 (q, $J_{\mathbf{C\text{-}C\text{-}F}}$ = 36.7 Hz, C) **^{19}F NMR** ($CDCl_3$,

377 MHz) δ ppm -74.17 **GC-MS** (EI) 204 ([M]$^+$, 21%), 136 (20%), 135 (100%), 92 (25%), 77 (35%), 69 (4%) **HRMS** (ESI+) calcd for $C_9H_7F_3O_2$ [M + H]$^+$ 205.0476, found: 205.0507.

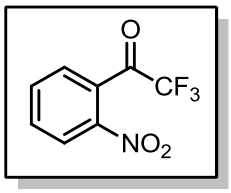

2,2,2-trifluoro-1-(2-nitrophenyl)ethanone (1.3j) (0.782 g, 89%) was prepared according to the representative procedure from 2,2,2-trifluoro-1-(2-nitrophenyl)ethanol **(1.2j)** to give a clear yellow oil. **^{1}H NMR** ($CDCl_3$, 400 MHz) δ ppm 7.55 (dd, *J* = 7.34, 1.22 Hz, 1 H) 7.82 (td, *J* = 8.10, 1.00 Hz, 1 H) 7.89 (td, *J* = 7.60, 1.22 Hz, 1 H) 8.31 (dd, *J* = 8.19, 0.86 Hz, 1 H) **^{13}C NMR** ($CDCl_3$, 101 MHz) δ ppm 110.4 – 119.0 (q, $J_{\mathbf{C\text{-}F}}$ = 290.5 Hz, CF_3) 123.8 (CH) 127.9 (CH) 129.2 (C) 132.3 (CH) 134.8 (CH) 145.3 (C) 183.4 (q, $J_{\mathbf{C\text{-}C\text{-}F}}$ = 38.9 Hz, C) **^{19}F NMR** ($CDCl_3$, 377 MHz) δ ppm -75.86 **GC-MS** (EI) 218 ([M]$^+$, 1%), 150 (100%), 123 (12%), 95 (15%), 76 (32%), 75 (12%), 74 (10%), 69 (9%), 51 (23%), 50 (18%) **HRMS** (ESI+) calcd for $C_8H_4F_3NO_3$ [M + H]$^+$ 220.0222, found: 220.0228.

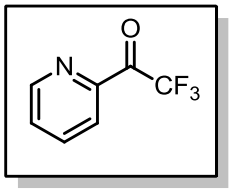

2,2,2-trifluoro-1-(pyridin-2-yl)ethanone (1.3k) (0.759 g, 96%) was prepared according to the representative procedure from 2,2,2-trifluoro-1-(pyridin-2-yl)ethanol **(1.3k)** (0.769 g, 0.00433mol) to give a powdery yellow solid (m.p. 81-83 ^{o}C, lit. 84-85 ^{o}C)[142]. **^{1}H NMR** (MeOD, 400 MHz) δ ppm 7.61 - 7.71 (m, 1 H) 7.94 - 8.03 (m, 1 H) 8.06 - 8.16 (m, 1 H) 8.74 - 8.84 (m, 1 H) **^{13}C NMR** (MeOD, 101 MHz) δ ppm 97.9 (q, $J_{\mathbf{C\text{-}C\text{-}F}}$ = 31.5 Hz, C) 120.7 – 129.2 (q, $J_{\mathbf{C\text{-}F}}$ = 286.8 Hz, CF_3) 125.4 (CH) 127.1 (CH) 139.9 (CH) 150.3 (CH) 154.7 (C) **^{19}F NMR** (MeOD, 377 MHz) δ ppm -81.66 **GC-MS** (EI) 175 ([M]$^+$, 7%), 106 (70%), 78 (100%), 69 (12%), 51 (24%), 50 (11%) **HRMS** (ESI+), calcd for $C_7H_4F_3NO$ [M + H]$^+$ 176.0323, found: 176.0300.

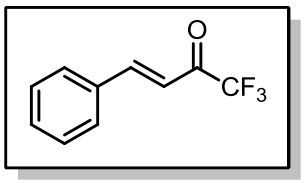

(E)-1,1,1-trifluoro-4-phenylbut-3-en-2-one (1.3o) (0.571 g, 72%) was prepared according to the representative procedure from (E)-1,1,1-trifluoro-4-phenylbut-3-en-2-ol (**1.2o**) to give a clear yellow oil. **^{1}H NMR** ($CDCl_3$, 400 MHz) δ ppm 7.02 (dd, *J* = 16.14, 0.98 Hz, 1 H) 7.40 - 7.54 (m, 3 H) 7.62 - 7.67 (m, 2 H) 7.97 (d, *J* = 16.14 Hz, 1 H) **^{13}C NMR** ($CDCl_3$, 101 MHz) δ ppm 112.3 – 121.0 (q, $J_{\mathbf{C\text{-}F}}$ = 291.2 Hz, CF_3) 116.9 (CH) 127.2 (CH) 127.4 (CH) 129.0 (CH) 129.5 (CH) 132.6 (CH) 133.6 (C) 150.4 (d, $J_{\mathbf{C\text{-}C\text{-}C\text{-}F}}$ = 1.5 Hz, CH) 180.3 (q, $J_{\mathbf{C\text{-}C\text{-}F}}$ = 35.2 Hz, C) **^{19}F NMR** ($CDCl_3$, 377 MHz) δ ppm -77.70 **GC-MS** (EI) 200 ([M]$^+$, 56%), 199 (12%), 132 (10%), 131 (100%), 103 (81%), 102 (13%), 77 (42%), 69 (6%), 51 (16%) **HRMS** (ESI+), calcd for $C_{10}H_7F_3O$ [M + H]$^+$ 201.0527, found: 201.0548.

[142] Ohno, A.; Nakai, J.; Nakamura, K. *Bull. Chem. Soc. Jpn*. **1981**, *54*, 3482.

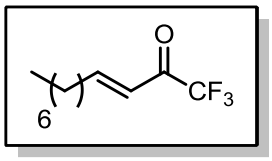

(E)-1,1,1- trifluoroundec -3-en-2-one (1.3p) (0.828 g, 93%) was prepared according to the representative procedure from 1,1,1-trifluoroundec-3-en-2-ol **(1.2p)** to give a clear yellow oil. **^{1}H NMR** ($CDCl_3$, 400 MHz) δ ppm 0.89 (t, *J* = 6.80 Hz, 3 H) 1.23 - 1.37 (m, 8 H) 1.51 - 1.56 (m, 2 H) 2.34 (qd, *J* = 7.60, 1.50 Hz, 2 H) 6.41 (dd, *J* = 15.65, 0.98 Hz, 1 H) 7.34 (dt, *J* = 15.89, 7.10 Hz, 1 H) **^{13}C NMR** ($CDCl_3$, 101 MHz) δ ppm 13.9 (CH_3) 22.5 (CH_2) 27.6 (CH_2) 28.9 (CH_2) 29.1 (CH_2) 31.6 (CH_2) 33.2 (CH_2) 111.9 – 120.6 (q, $J_{C\text{-}F}$ = 290.5 Hz, CF_3) 121.3 (CH) 156.9 (CH) 179.7 (q, $J_{C\text{-}C\text{-}F}$ = 35.2 Hz, C) **^{19}F NMR** ($CDCl_3$, 377 MHz) δ ppm -77.66 GC-MS (EI) 222 ($[M]^+$, 1%), 165 (13%), 153 (81%), 138 (37%), 110 (11%), 97 (23%), 95 (13%), 83 (19%), 81 (29%), 69 (63%), 68 (25%), 67 (18%), 57 (13%), 56 (15%), 55 (100%), 43 (53%), 41 (51%), 40 (22%), 39 (25%) **HRMS** (ESI+), calcd for $C_{11}H_{17}F_3O$ $[M + H]^+$ 223.1310, found: 223.1316.

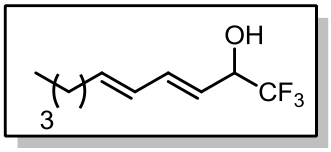

1,1,1-Trifluorodeca-3,5-dien-2-one (1.3q) (0.879 g, 99%) was prepared according to the representative procedure from 1,1,1-trifluorodeca-3,5-dien-2-ol **(1.2q)** to give a clear orange oil. **^{1}H NMR** ($CDCl_3$, 400 MHz) δ ppm 0.92 (t, *J* = 7.21 Hz, 3 H) 1.30 - 1.53 (m, 4 H) 2.26 (q, *J* = 7.17 Hz, 2 H) 6.24 - 6.50 (m, 3 H) 7.55 (dd, *J* = 15.28, 10.88 Hz, 1 H) **^{13}C NMR** ($CDCl_3$, 101 MHz) δ ppm 13.5 (CH_3) 22.0 (CH_2) 30.3 (CH_2) 32.9 (CH_2) 111.9 – 120.5 (q, $J_{C\text{-}F}$ = 290.5 Hz, CF_3) 118.1 (CH) 128.5 (CH) 150.4 (CH) 151.6 (CH) 180.0 (q, $J_{C\text{-}C\text{-}F}$ = 37.4 Hz, C) **^{19}F NMR** ($CDCl_3$, 377 MHz) δ ppm -77.54 **GC-MS** (EI) 206 ($[M]^+$, 8%), 149 (100%), 137 (16%), 95 (13%), 81 (32%), 79 (12%), 77 (10%), 69 (9%), 67 (14%), 66 (12%), 56 (11%), 53 (11%), 41 (17%), 39 (11%) **HRMS** (ESI+), calcd for $C_{10}H_{13}F_3O$ $[M + H]^+$ 207.0997, found: 207.0993.

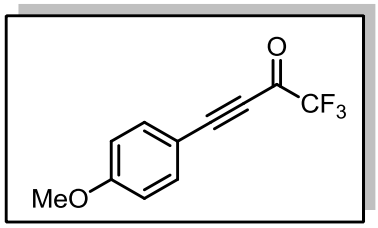

1,1,1-trifluoro-4-(4-methoxyphenyl)but-3-yn-2-one (1.3r) (0.773 g, 85%) was prepared according to the representative procedure from 1,1,1-trifluoro-4-(4-methoxyphenyl)but-3-yn-2-ol (**1.2r**) to give a clear orange oil. **^{1}H NMR** ($CDCl_3$, 400 MHz) δ ppm 3.92 (s, 3 H) 6.99 (d, *J* = 8.56 Hz, 2 H) 7.68 (d, *J* = 8.31 Hz, 2 H) **^{13}C NMR** ($CDCl_3$, 101 MHz) δ ppm 55.0 (CH_3) 83.5 (C) 101.8 (C) 109.1 (C) 110.0 – 118.6 (q, $J_{C\text{-}F}$ = 289.0 Hz, CF_3) 114.2 (CH) 135.7 (CH) 162.6 (C) 166.4 (q, $J_{C\text{-}C\text{-}F}$ = 42.5 Hz, C) **^{19}F NMR** ($CDCl_3$, 376 MHz) δ ppm -77.65 **GC-MS** (EI) 228 ($[M]^+$, 23%), 1620 (12%), 159 (100%), 144 (18%), 116 (15%), 88 (12%), 69 (3%) **HRMS** (ESI+), calcd for $C_{11}H_7F_3O_2$ $[M + H]^+$ 229.0476, found: 229.0474.

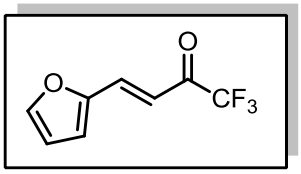

(E)-1,1,1-trifluoro-4-(furan-2-yl)but-3-en-2-one (1.3s) (0.518 g, 68%) was prepared according to the representative procedure from 1,1,1-trifluoro-4-(furan-2-yl)but-3-en-2-ol **(1.2s)** to give a clear yellow oil. **^{1}H NMR** ($CDCl_3$, 400 MHz) δ ppm 6.55 - 6.63 (m, 1 H) 6.87 - 6.92 (m, 2 H) 7.62 (s, 1 H) 7.69 (d, *J* = 15.41 Hz, 1 H) **^{13}C NMR** ($CDCl_3$, 101 MHz) δ ppm 108.8 – 117.4 (q, $J_{C\text{-}F}$ = 296.4 Hz, CF_3) 110.5 (2x CH) 117.1 (CH) 131.6 (CH) 144.4 (CH) 147.2 (C) 176.4 (q, $J_{C\text{-}C\text{-}F}$ = 35.2 Hz, C) **^{19}F NMR** ($CDCl_3$, 376 MHz) δ ppm -77.74

GC-MS (EI) 190 ([M]$^+$, 35%), 121 (100%), 69 (9%), 65 (49%), 63 (12%), 39 (15%) **HRMS** (ESI+), calcd for $C_8H_5F_3O_2$ [M + H]$^+$ 191.0320, found: 191.0328.

Procedure for Oxidation of Aliphatic α-CF$_3$ Alcohols

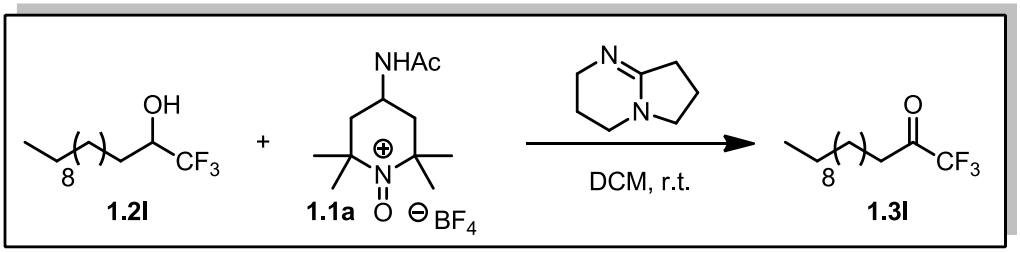

Preparation of 1,1,1-Trifluorododecanone (1.3l) To a one-neck 250 mL round bottom flask equipped with stirbar was added the α-CF_3 alcohol, **1.2l** (4.07 g, 16 mmol, 1 equiv.), 1,5-diazabicyclo[4.3.0]non-5-ene (5.48 g, 44 mmol, 2.75 equiv.) and dichloromethane (160 mL, 0.1M in the alcohol). After stirring at room temperature for about 10 min, the oxoammonium salt **1.1a** (14.41 g, 48 mmol, 3 equiv.) was added to the flask (***CAUTION***: mildly exothermic) and the reaction mixture immediately began to turn red. The flask was sealed with a rubber septum with a vent needle and stirred for 4 h at room temperature. The solvent was removed *in vacuo* to afford an orange solid. Anhydrous diethyl ether (≈ 30 mL) was added to the flask and allowed to stir for 10 min. ***Note:*** It is imperative that the sides of the flask be scraped to ensure all the nitroxide (**1.1b**) precipitates out releasing the product into solution. After stirring, the solution was filtered through a plug of silica (topped with a piece of filter paper to assist in recovery) and rinsed thoroughly (3-4 times) with anhydrous diethyl ether. The solvent was removed *in vacuo* by rotary evaporation in a room temperature water bath affording the crude TFMK. Further purification was accomplished by vacuum distillation through a 130 mm *Vigreux* column (b.p. 71-74 ^{o}C @ 0.10 mmHg) giving the pure **1.3l** (2.01 g, 50%) as a clear colorless oil.

^{1}H NMR ($CDCl_3$, 400 MHz) δ ppm 0.88 (t, *J* = 7.00 Hz, 3 H) 1.17 - 1.39 (m, 16 H) 1.67 (quin, *J* = 7.30 Hz, 2 H) 2.70 (td, *J* = 7.21, 0.73 Hz, 2 H) **^{13}C NMR** ($CDCl_3$, 101 MHz) δ ppm 14.4 (CH_3) 22.7 (CH_2) 23.0 (CH_2) 29.0 (CH_2) 29.5 (CH_2) 29.6 (CH_2) 29.6 (CH_2) 29.8 (CH_2) 29.9 (CH_2) 32.2 (CH_2) 36.7 (CH_2) 111.5-120.2 (q, $J_{C\text{-}F}$ = 292.7 Hz, CF_3) 191.9 (q, $J_{C\text{-}C\text{-}F}$ = 34.5 Hz, C) **^{19}F NMR** ($CDCl_3$, 377 MHz) δ ppm -82.66 GC-MS (EI) 252 (M$^+$, 0.1%), 223 (3%), 209 (5%), 191.05 (5%), 183 (85%), 163 (10%), 153 (21%), 150 (10%), 139 (28%) 135 (11%), 125 (12%) 111 (31%) 109 (13%), 97 (55%), 83 (52%), 69 (84%), 43 (100%), 41 (95%) **HRMS** (ESI+) calcd for $C_{13}H_{23}F_3O$ [M + H]$^+$ 253.1779, found: 253.1731.

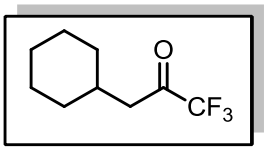

3-Cyclohexyl-1,1,1-trifluoropropan-2-one (1.3n) (1.98 g, 49%) was prepared according to the representative procedure from 3-cyclohexyl-1,1,1-trifluoropropan-2-ol (4.12g, 0.021 mol) (**1.2n**) *with the following modification*: An addition 0.5 equiv of **1.1a** (3.15 g, 0.0105 mol) and DBN (1.31 g 0.0105 mol) each was added after 4 hrs to achieve >90% conversion. Further Purification was accomplished by vacuum distillation (b.p. 71-74 ^{o}C @ 10

mmHg) to give a clear pale yellow oil. **^{1}H NMR** ($CDCl_3$, 500 MHz) δ ppm 0.93 - 1.04 (m, 2 H) 1.09 - 1.22 (m, 1 H) 1.22 - 1.36 (m, 2 H) 1.66 - 1.75 (m, 5 H) 1.93 (*apparent* dddt, *J* = 14.58, 10.96, 7.25, 3.47, 3.47 Hz, 1 H) 2.57 (d, *J* = 6.94 Hz, 2 H) **^{13}C NMR** ($CDCl_3$, 125 MHz) δ ppm 26.2 (CH_2) 26.3 (CH_2) 33.2 (CH_2) 33.2 (CH) 44.1 (CH_2) 115.8 (q, $J_{\mathbf{C\text{-}F}}$ = 292.3 Hz, CF_3) 191.3 (q, $J_{\mathbf{C\text{-}C\text{-}F}}$ = 33.9 Hz, C) **^{19}F NMR** ($CDCl_3$, 377 MHz) δ ppm -82.75 **GC-MS** (EI) 194 ($[M]^+$, .01%), 125 (100%), 97 (96%), 82 (72%), 69 (31%), 67 (48%), 55 (87%), 41 (33%), 39 (22%) **HRMS** (ESI+) calcd for $C_9H_{13}F_3O$ $[M + H]^+$ 195.0997, found: 195.1044.

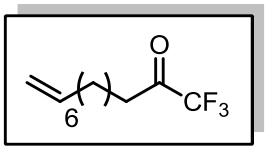

1,1,1-Trifluoroundec-10-en-2-one (1.3m) (2.937 g, 60%) was prepared according to the representative procedure from 1,1,1-trifluoroundec-10-en-2-ol (4.93 g, 0.022 mol) (**1.2m**) *with the following modification*: An addition 0.5 equiv of **1.1a** (3.15 g, 0.0105 mol) and DBN (1.31 g 0.0105 mol) each was added after 4 hrs to achieve >90% conversion. Further Purification was accomplished by vacuum distillation (b.p. 60-62 ^{o}C @ 1.5 mmHg) to give a clear colorless oil. **^{1}H NMR** ($CDCl_3$, 500 MHz) δ ppm 1.23 - 1.47 (m, 8 H) 1.61 - 1.74 (qint, *J* = 7.00 Hz, 2 H) 2.04 (q, *J* = 6.85 Hz, 2 H) 2.70 (t, *J* = 7.21 Hz, 2 H) 4.88 - 5.04 (m, 2 H) 5.80 (ddt, *J* = 16.96, 10.12, 6.76, 6.76 Hz, 1 H) **^{13}C NMR** ($CDCl_3$, 125 MHz) δ ppm 22.6 (CH_2) 29.0 (CH_2) 29.1 (CH_2) 29.1 (CH_2) 29.3 (CH_2) 34.0 (CH_2) 36.6 (CH_2) 115.9 (q, $J_{\mathbf{C\text{-}F}}$ = 290.0 Hz, CF_3) 114.5 (CH_2) 139.3 (CH) 191.9 (d, $J_{\mathbf{C\text{-}C\text{-}F}}$ = 35.0 Hz, C) **^{19}F NMR** ($CDCl_3$, 377 MHz) δ ppm -82.44 **GC-MS** (EI) 222 ($[M]^+$, 2%), 153 (14%), 138 (15%), 135 (29%), 110 (30%), 97 (11%), 95 (22%), 93 (11%), 83 (19%), 82 (24%), 81 (34%), 79 (11%), 70 (10%), 69 (87%), 68 (55%), 67 (38%), 56 (19%), 55 (100%), 54 (25%), 53 (15%), 43 (14%), 42 (25%), 41 (88%), 40 (14%), 39 (41%) **HRMS** (ESI+) calcd for $C_{11}H_{17}F_3O$ $[M + H]^+$ 223.1309, found: 223.1299.

Selective Oxidation of 2,2,2-Trifluoro-1-(4-(hydroxymethyl)phenyl)ethanol (1.2t)

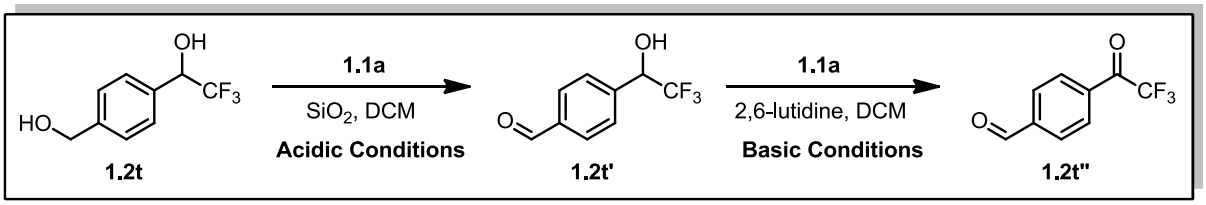

4-(2,2,2-Trifluoro-1-hydroxyethyl)benzaldehyde (1.2t′) (1.865 g, 91%) was prepared according to the standard oxidation procedure from 2,2,2-trifluoro-1-(4-(hydroxymethyl)phenyl)ethanol (**1.2t**) to give a powdery off-white solid (m.p. 67-69 ^{o}C).

^{1}H NMR ($CDCl_3$, 400 MHz) δ ppm 3.60 (br. s., 1 H) 5.15 (q, *J* = 6.36 Hz, 1 H) 7.67 (d, *J* = 8.07 Hz, 2 H) 7.90 (d, *J* = 8.31 Hz, 2 H) 9.99 (s, 1 H) **^{13}C NMR** ($CDCl_3$, 101 MHz) δ ppm 72.5 (q, $J_{\mathbf{C\text{-}C\text{-}F}}$ = 30.8 Hz, CH) 120.0 – 127.7 (q, $J_{\mathbf{C\text{-}F}}$ = 281.7 Hz, CF_3) 128.5 (d, $J_{\mathbf{C\text{-}C\text{-}C\text{-}C\text{-}F}}$ = 1.5 Hz, CH) 130.1 (CH) 137.1 (C) 140.8 (C) 192.6 (CH) **^{19}F NMR** (400 MHz, $CDCl_3$) δ ppm -79.11 (d, *J*=6.81 Hz) **GC-MS** (EI) 204 ($[M]^+$, 29%), 135 (100%), 133 (16%), 127 (11%), 105 (16%), 79 (56%), 77 (41%), 69 (6%), 51 (13%) **HRMS** (ESI+), calcd for $C_9H_7F_3O_2$ $[M + H]^+$ 205.0476, found: 205.0484.

4-(2,2,2-trifluoroacetyl)benzaldehyde (1.2t") (0.626 g, 78%) was prepared according to the general CF_3 carbinol oxidation procedure from 4-(2,2,2-Trifluoro-1-hydroxyethyl)benzaldehyde (**1.2t′**) to give a yellow solid (m.p. 86-88 ^{o}C).

^{1}H NMR (MeOD, 400 MHz) δ ppm 7.66 (d, *J* = 7.83 Hz, 2 H) 7.80 (d, *J* = 7.34 Hz, 2 H) 10.19 (br. s., 1 H) **^{13}C NMR** (MeOD, 101 MHz) δ ppm 98.5 (q, $J_{\mathbf{C\text{-}C\text{-}F}}$ = 32.3 Hz, C) 120.8 – 129.4 (q, $J_{\mathbf{C\text{-}F}}$ = 286.1 Hz, CF_3) 128.3 (CH) 129.9 (CH) 137.0 (C) 141.6 (C) **^{19}F NMR** (MeOD, 377 MHz) δ ppm -82.40 **GC-MS** (EI) 202 ($[M]^+$, 5%), 133 (100%), 105 (34%), 77 (26%), 76 (10%), 69 (5%), 51 (12%), 50 (10%) **HRMS** (ESI+), calcd for $C_9H_5F_3O_2$ $[M + H]^+$ 203.0320, found: 203.0341.

General Dehydrogenation Procedure of Perfluoroketones

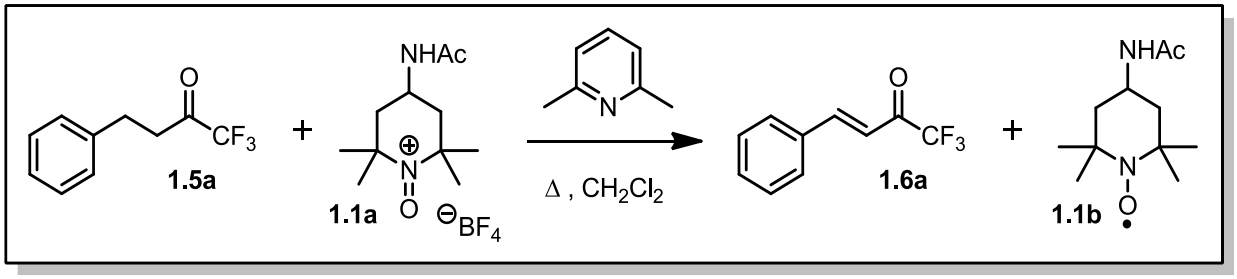

1,1,1-trifluoro-4-phenylbut-3-en-2-one (1.6a)

To a 250 mL round bottom flask equipped with stirbar was added **1.5a** (1.42 g, 7 mmol, 1 equiv.), 2,6-lutidine (1.65 g, 15.4 mmol, 2.2 equiv.) and DCM (70 mL, 0.1 M in **1.5a**). The reaction mixture was stirred vigorously for 10 minutes, then the oxoammonium salt **1.1a** (5.46 g, 18.2 mmol, 2.6 equiv.) was added to the flask. The flask was equipped with a reflux condenser and heated to reflux for 24-48 hrs[143]. The solvent was removed *in vacuo via* rotary evaporation affording a thick red residue. Anhydrous[144] Et_2O (≈ 50 mL) was added to the flask and allowed to stir for five minutes. This causes immediate precipitation of the nitroxide, **1.1b**. **Note**: *It is imperative that the sides of the flask be scraped to ensure complete precipitation of the **1.1b**, thereby releasing the product into solution*. After stirring for 10 minutes, the solution was filtered through a fritted funnel, washing thoroughly with anhydrous Et_2O (≈ 250 mL). **Note:** *Large chunks of nitroxide were crushed into fine particles, again to release any trapped product*. The resulting filtrate was concentrated *in vacuo* by rotary evaporation. The resulting red oil was then dry-packed on silica gel (using 1.5-2 weight equivalents relative to theortical yield of **1.9a**). The dry-packed material was carefully loaded on to a pad of silica gel (3.5 weight equivalents relative to the theoretical yield of **1.6a**) (*topped with a piece of filter paper to assist in recovery*) and the pad was eluted with ≈ 100-200 ml of 95:5 (Hex:EtOAc). The eluting solvent was removed *in vacuo* by rotary evaporation in a room temperature[145] water bath affording the pure α,β-unsaturated CF_3 ketone (**1.6a)** (0.9086 g, 65%) as a clear yellow oil.

^{1}H NMR ($CDCl_3$, 400 MHz) δ ppm 7.02 (dd, *J* = 15.89, 0.73 Hz, 1 H) 7.41 - 7.57 (m, 3 H) 7.60 - 7.70 (m, 2 H) 7.97 (d, *J* = 15.89 Hz, 1 H) **^{13}C NMR** ($CDCl_3$, 101 MHz) δ ppm 116.68 (q, $J_{C\text{-}F}$ = 291.20 Hz, CF_3) 116.90 (CH) 129.50 (C) 129.51 (CH) 132.59 (CH) 133.60 (CH) 150.41 (CH) 180.26 (q, $J_{C\text{-}C\text{-}F}$ = 35.90 Hz, C) **^{19}F NMR** ($CDCl_3$, 377 MHz) δ ppm -80.67 **GC-MS** (EI) 200

[143] Note that, especially in the case of the deactivated aryl systems, it is likely that these reaction are completed much sooner (<24 h) due to the appearance a deep red coloration at the time. This coloration indicates the presence of the nitroxide, **1.1b**, which likely means the reaction is complete. Unfortunately, monitoring by NMR is complicated by the presence of **1.1b**. Therefore it is recommended that the reaction is monitored by TLC or GC/MS to determine reaction progress.

[144] The authors found that the best yields were obtained when anhydrous Et_2O was used. We suspect this minimizes both hydrate formation and amount of nitroxide in the resulting solution.

[145] Note that it was necessary to keep the bath water at room temperature in most cases due to the volatility of TFMKs

([M]$^+$, 56%) 199 (12%) 132 (10%) 131 (100%) 103 (81%) 102 (13%) 77 (42%) 69 (6%) 51 (16%) **HRMS** (ESI+), calcd for $C_{10}H_7F_3O$ [M + H]$^+$ 201.0527, found: 201.0548

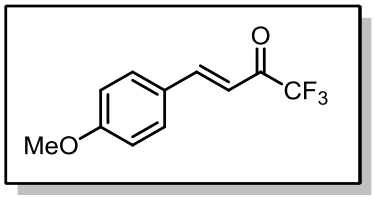

(E)-1,1,1-trifluoro-4-(4-methoxyphenyl)but-3-en-2-one (1.6b) (1.113 g, 69%) was prepared according to the representative procedure from 1,1,1-trifluoro-4-(4-methoxyphenyl)butan-2-one **(1.5b)** (1.625 g, 7 mmol) to give a yellow solid. **^{1}H NMR** ($CDCl_3$, 400 MHz) δ ppm 3.88 (s, 3 H) 6.89 (d, *J* = 15.65 Hz, 1 H) 6.95 (d, *J* = 8.80 Hz, 2 H) 7.61 (d, *J* = 8.56 Hz, 2 H) 7.94 (d, *J* = 15.65 Hz, 1 H) **^{13}C NMR** ($CDCl_3$, 101 MHz) δ ppm 55.63 (CH_3) 116.82 (q, J_{C-F} = 290.50 Hz, CF_3) 114.15 (CH) 114.95 (CH) 126.35 (C) 131.60 (CH) 150.16 (CH) 163.47 (C) 180.03 (q, J_{C-C-F} = 35.20 Hz, C) **^{19}F NMR** ($CDCl_3$, 377 MHz) δ ppm -80.44 **GC-MS** (EI) 230 ([M]$^+$, 39%) 161 (100%) 133 (35%) 118 (16%) 89 (16%) 69 (4%) 63 (10%)

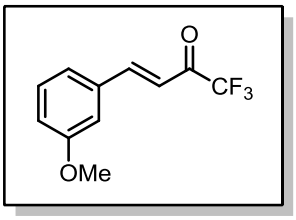

(E)-1,1,1-trifluoro-4-(3-methoxyphenyl)but-3-en-2-one (1.6c) (2.571 g, 74%) was prepared according to the representative procedure from 1,1,1-trifluoro-4-(3-methoxyphenyl)butan-2-one **(1.5c)** (3.484 g, 15 mmol) to give a clear yellow oil. **^{1}H NMR** ($CDCl_3$, 400 MHz) δ ppm 6.18 (d, *J* = 15.89 Hz, 1 H) 6.39 (dd, *J* = 8.31, 2.45 Hz, 1 H) 6.72 (s, 1 H) 7.12 (d, *J* = 7.82 Hz, 1 H) 7.65 (t, *J* = 8.10 Hz, 1 H) 9.89 (d, *J* = 15.89 Hz, 1 H) **^{13}C NMR** ($CDCl_3$, 101 MHz) δ ppm 55.63 (CH_3) 116.65 (q, J_{C-F} = 291.20 Hz, CF_3) 114.11 (CH) 117.14 (CH) 118.55 (CH) 122.23 (CH) 130.50 (CH) 134.90 (C) 150.36 (CH) 160.37 (C) 180.24 (q, J_{C-C-F} = 35.90 Hz, C) **^{19}F NMR** ($CDCl_3$, 377 MHz) δ ppm -80.64 **GC-MS** (EI) 230 ([M]$^+$, 57%) 199 (35%) 161 (100%) 133(26%) 118 (42%) 103 (11%) 90 (23%) 77 (13%) 63 (13%)

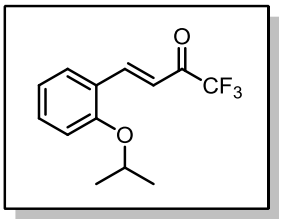

(E)-1,1,1-trifluoro-4-(2-isopropoxyphenyl)but-3-en-2-one (1.6d) (0.9975 g, 64%) was prepared according to the representative procedure from 1,1,1-trifluoro-4-(2-isopropoxyphenyl)butan-2-one **(1.5d)** (1.562 g, 6 mmol) to give a clear yellow oil. **^{1}H NMR** ($CDCl_3$, 400 MHz) δ ppm 1.42 (d, *J* = 5.87 Hz, 6 H) 4.68 (spt, *J* = 6.00 Hz, 1 H) 6.97 (t, *J* = 7.80 Hz, 2 H) 7.21 (d, *J* = 16.14 Hz, 1 H) 7.42 (td, *J* = 8.00, 1.00 Hz, 1 H) 7.58 (d, *J* = 7.58 Hz, 1 H) 8.27 (d, *J* = 16.14 Hz, 1 H) **^{13}C NMR** ($CDCl_3$, 101 MHz) δ ppm 22.25 (CH_3) 71.41 (CH) 116.87 (q, J_{C-F} = 291.20 Hz, CF_3) 113.96 (CH) 120.89 (CH) 123.46 (C) 131.00 (CH) 133.81 (CH) 146.54 (CH) 158.54 (C) 180.83 (q, J_{C-C-F} = 35.20 Hz, C) **^{19}F NMR** ($CDCl_3$, 377 MHz) δ ppm -80.78 **GC-MS** (EI) 258 ([M]$^+$, 12%) 147 (100%) 118 (11%) 103(22%) 91 (18) **HRMS** (ESI+), calcd for $C_{13}H_{13}F_3O_2$ [M + H]$^+$: 259.0946, found: 259.0945

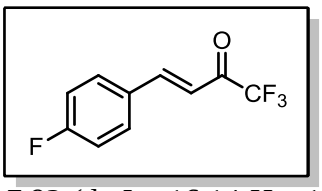

(E)-1,1,1-trifluoro-4-(4-fluorophenyl)but-3-en-2-one (1.6e) (1.750 g, 56%) was prepared according to the representative procedure from 1,1,1-trifluoro-4-(4-fluorophenyl)butan-2-one **(1.5e)** (3.170 g, 14.4 mmol) to give a yellow solid. **^{1}H NMR** ($CDCl_3$, 400 MHz) δ ppm 6.94 (d, *J* = 15.89 Hz, 1 H) 7.13 (t, *J* = 8.56 Hz, 2 H) 7.60 - 7.69 (m, 2 H) 7.92 (d, *J* = 16.14 Hz, 1 H) **^{13}C NMR** ($CDCl_3$, 101 MHz) δ ppm 116.61 (CH) 116.61 (q, J_{C-F} = 291.20 Hz, CF_3) 116.56 (d, $J_{C-C-C-C-F}$ = 2.20 Hz, C) 116.77 (d, J_{C-C-F} = 22.01 Hz, CH) 129.92 (d, $J_{C-C-C-C-C-F}$ = 3.67 Hz, CH) 131.63 (d, $J_{C-C-C-F}$ = 8.80 Hz, CH) 148.93 (CH) 165.35 (d, J_{C-F} =

255.29 Hz, C) 180.09 (q, $J_{C\text{-}C\text{-}F}$ = 35.90 Hz, C) **^{19}F NMR** ($CDCl_3$, 377 MHz) δ ppm -108.81 - -108.53 (m, 1 F) -80.66 (s, 3 F) **GC-MS** (EI) 218 ($[M]^+$, 27%) 200 (50%) 149 (91%) 131 (100%) 121 (48%) 103 (86%) 101 (51%) 77 (48%) 69 (17%) 51 (24%)

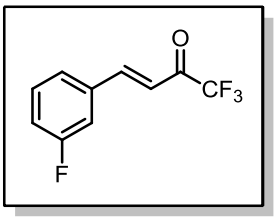

(E)-1,1,1-trifluoro-4-(3-fluorophenyl)but-3-en-2-one (1.6f) (0.922 g, 62%) was prepared according to the representative procedure from 1,1,1-trifluoro-4-(3-fluorophenyl)butan-2-one **(1.5f)** (1.500 g, 6.81 mmol) to give a clear yellow oil. **^{1}H NMR** ($CDCl_3$, 500 MHz) δ ppm 7.00 (dd, *J* = 15.92, 0.63 Hz, 1 H) 7.16 - 7.23 (m, 1 H) 7.33 (dt, *J* = 9.18, 1.64 Hz, 1 H) 7.40 - 7.47 (m, 2 H) 7.91 (d, *J* = 15.92 Hz, 1 H) **^{13}C NMR** ($CDCl_3$, 125 MHz) δ ppm 116.55 (q, $J_{C\text{-}F}$ = 289.80 Hz, CF_3) 115.48 (d, $J_{C\text{-}C\text{-}F}$ = 22.01 Hz, CH) 118.16 (s, CH) 119.47 (d, $J_{C\text{-}C\text{-}F}$ = 21.27 Hz, CH) 125.59 (d, $J_{C\text{-}C\text{-}C\text{-}C\text{-}F}$ = 3.67 Hz, CH) 131.14 (d, $J_{C\text{-}C\text{-}C\text{-}F}$ = 8.07 Hz, CH) 135.75 (d, $J_{C\text{-}C\text{-}C\text{-}F}$ = 8.07 Hz, C) 148.77 (d, $J_{C\text{-}C\text{-}C\text{-}C\text{-}C\text{-}F}$ = 1.47 Hz, CH) 163.32 (d, $J_{C\text{-}F}$ = 245.02 Hz, C) 180.13 (q, $J_{C\text{-}C\text{-}F}$ = 35.90 Hz, C) **^{19}F NMR** ($CDCl_3$, 377 MHz) δ ppm -114.82 - -114.52 (m, 1 F) -80.78 (s, 3 F) **GC-MS** (EI) 218 ($[M]^+$, 49%) 149 (100%) 121 (53%) 101 (64%) 95 (12%) 75 (22%) 69 (11%) **HRMS** (ESI+), calcd for $C_{10}H_6F_4O$ $[M + H]^+$: 219.0433, found: 219.0454

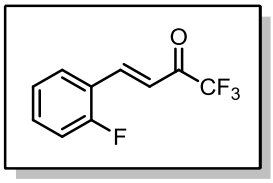

(E)-1,1,1-trifluoro-4-(2-fluorophenyl)but-3-en-2-one (1.6g) (1.050 g, 69%) was prepared according to the representative procedure from 1,1,1-trifluoro-4-(2-fluorophenyl)butan-2-one (**1.5g**) (1.541 g, 7 mmol) to give a clear yellow oil. **^{1}H NMR** ($CDCl_3$, 400 MHz) δ ppm 7.07 - 7.19 (m, 2 H) 7.23 (t, *J* = 7.58 Hz, 1 H) 7.42 - 7.53 (m, 1 H) 7.62 (td, *J* = 7.46, 1.47 Hz, 1 H) 8.07 (d, *J* = 16.14 Hz, 1 H) **^{13}C NMR** ($CDCl_3$, 101 MHz) δ ppm 116.60 (q, $J_{C\text{-}F}$ = 291.20 Hz, CF_3) 116.84 (d, $J_{C\text{-}C\text{-}F}$ = 22.01 Hz, C) 119.18 (d, $J_{C\text{-}C\text{-}C\text{-}F}$ = 7.34 Hz, CH) 121.89 (d, $J_{C\text{-}C\text{-}F}$ = 11.00 Hz, CH) 125.10 (d, $J_{C\text{-}C\text{-}C\text{-}C\text{-}F}$ = 3.67 Hz, CH) 130.35 (d, $J_{C\text{-}C\text{-}C\text{-}C\text{-}F}$ = 2.20 Hz, CH) 134.11 (d, $J_{C\text{-}C\text{-}C\text{-}F}$ = 8.80 Hz, CH) 142.93 (d, $J_{C\text{-}C\text{-}C\text{-}F}$ = 1.47 Hz, CH) 162.45 (d, $J_{C\text{-}F}$ = 256.76 Hz, C) 180.39 (q, $J_{C\text{-}C\text{-}F}$ = 35.20 Hz, 3 C) **^{19}F NMR** ($CDCl_3$, 377 MHz) δ ppm -115.16 - -114.96 (m, 1 F) -80.84 (s, 3 F) **GC-MS** (EI) 218 ($[M]^+$, 36%) 149 (100%) 212 (47%) 101 (68%) 75 (23%) 69 (10%) 51 (6%) **HRMS** (ESI+), calcd for $C_{10}H_6F_4O$ $[M + H]^+$: 219.0433, found: 219.0411

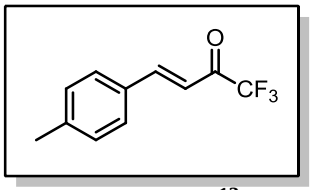

(E)-1,1,1-trifluoro-4-(p-tolyl)but-3-en-2-one (1.6h) (2.655 g, 83%) was prepared according to the representative procedure from 1,1,1-trifluoro-4-(p-tolyl)butan-2-one (**1.5h**) (3.243 g, 15 mmol) to give a yellow solid. **^{1}H NMR** ($CDCl_3$, 400 MHz) δ ppm 7.00 (d, *J* = 16.14 Hz, 1 H) 7.28 (d, *J* = 7.82 Hz, 2 H) 7.56 (d, *J* = 8.07 Hz, 2 H) 7.97 (d, *J* = 15.89 Hz, 1 H) **^{13}C NMR** ($CDCl_3$, 101 MHz) δ ppm 21.93 (CH_3) 116.76 (q, $J_{C\text{-}F}$ = 292.00 Hz, CF_3) 115.83 (CH) 129.61 (CH) 130.28 (CH) 130.97 (C) 143.66 (C) 150.51 (CH) 180.29 (q, $J_{C\text{-}C\text{-}F}$ = 35.20 Hz, C) **^{19}F NMR** ($CDCl_3$, 377 MHz) δ ppm -80.70 **GC-MS** (EI) 214 ($[M]^+$, 30%) 199 (56%) 145 (100%) 117 (45%) 115 (74%) 91 (32%) 69 (7%)

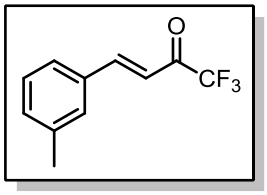

(E)-1,1,1-trifluoro-4-(m-tolyl)but-3-en-2-one (1.6i) (1.750 g, 56%) was prepared according to the representative procedure from 1,1,1-trifluoro-4-(m-tolyl)butan-2-one (**1.5i**) (1.513 g, 7 mmol) to give a clear yellow oil. **^{1}H NMR** ($CDCl_3$, 400 MHz) δ ppm 2.41 (s, 3 H) 7.01 (d, *J* = 16.14 Hz, 1 H) 7.29 - 7.39 (m, 2 H) 7.41 - 7.48 (m, 2 H) 7.95 (d, *J* = 15.89 Hz, 10 H)

^{13}C NMR ($CDCl_3$, 101 MHz) δ ppm 21.47 (CH_3) 116.70 (q, J_{C-F} =291.20 Hz, CF_3) 116.67 (s, CH) 126.80 (CH) 129.38 (CH) 130.05 (CH) 133.50 (CH) 133.58 (C) 139.30 (C) 150.66 (s, CH) 180.28 (q, J_{C-C-F} =35.20 Hz, C) **^{19}F NMR** ($CDCl_3$, 377 MHz) δ ppm -80.66 **GC-MS** (EI) 214 ($[M]^+$, 58%) 199 (58%) 145 (100%) 117 (44%) 115 (88%) 91 (37%) 69 (7%)

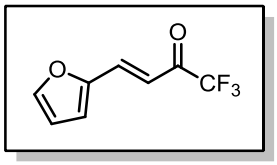

(E)-1,1,1-trifluoro-4-(furan-2-yl)but-3-en-2-one (1.6j) (0.398 g, 64%) was prepared according to the representative procedure from 1,1,1-trifluoro-4-(furan-2-yl)butan-2-one **(1.5j)** (0.606 g, 3.15 mmol) to give a clear yellow oil. **^{1}H NMR** ($CDCl_3$, 400 MHz) δ ppm 6.55 - 6.63 (m, 1 H) 6.87 - 6.92 (m, 2 H) 7.62 (s, 1 H) 7.69 (d, J = 15.41 Hz, 1 H) **^{13}C NMR** ($CDCl_3$, 101 MHz) δ ppm 108.75 – 117.41 (q, J_{C-F} = 296.40 Hz, CF_3) 110.48 (2 x CH) 117.12 (CH) 131.61 (CH) 144.36 (CH) 147.24 (C) 176.43 (q, J_{C-C-F} = 35.20 Hz, C) **^{19}F NMR** ($CDCl_3$, 377 MHz) δ ppm -77.74 **GC-MS** (EI) 190 ($[M]^+$, 35%) 121 (100%) 69 (9%) 65 (49%) 63 (12%) 39 (15%) **HRMS** (ESI+), calcd for $C_8H_5F_3O_2$ $[M + H]^+$ 191.0320, found: 191.0328

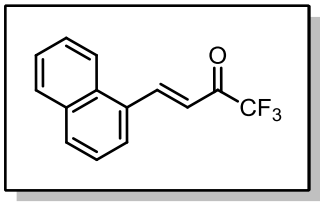

(E)-1,1,1-trifluoro-4-(naphthalen-1-yl)but-3-en-2-one (1.6k) (1.643 g, 98%) was prepared according to the representative procedure from 1,1,1-trifluoro-4-(naphthalen-1-yl)butan-2-one **(1.5k)** (1.690 g, 6.7 mmol) to give a clear yellow oil. **^{1}H NMR** ($CDCl_3$, 400 MHz) δ ppm 7.12 (d, J = 15.89 Hz, 1 H) 7.49 (t, J = 7.82 Hz, 1 H) 7.53 - 7.64 (m, 2 H) 7.81 - 7.92 (m, 2 H) 7.97 (d, J = 8.31 Hz, 1 H) 8.14 (d, J = 8.31 Hz, 1 H) 8.80 (d, J = 15.65 Hz, 1 H) **^{13}C NMR** ($CDCl_3$, 101 MHz) δ ppm 116.78 (q, J_{C-F} = 290.50 Hz, CF_3) 118.61 (CH) 122.95 (CH) 125.54 (CH) 126.22 (CH) 126.81 (CH) 127.83 (CH) 129.21 (CH) 130.44 (C) 131.96 (C) 132.98 (CH) 133.98 (C) 146.76 (CH) 180.05 (q, J_{C-C-F} = 35.20 Hz, C) **^{19}F NMR** ($CDCl_3$, 377 MHz) δ ppm -80.51 **GC-MS** (EI) 250 ($[M]^+$, 57%) 181 (100%) 153 (57%) 152 (92%) 76 (23%) 69 (4%).

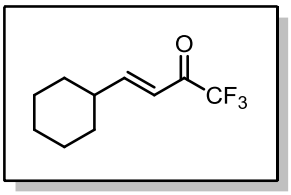

(E)-4-cyclohexyl-1,1,1-trifluorobut-3-en-2-one (1.6m) (0.532 g, 53%) was prepared according to the representative procedure from 4-cyclohexyl-1,1,1-trifluorobutan-2-one **(1.5m)** (1.015 g, 4.87 mmol) to give a clear yellow oil. **^{1}H NMR** ($CDCl_3$, 400 MHz) δ ppm 1.04 - 1.46 (m, 5 H) 1.55 - 1.97 (m, 5 H) 2.11 - 2.41 (m, 1 H) 6.26 - 6.45 (m, 1 H) 7.26 (dd, J = 15.90, 6.85 Hz, 1 H) **^{13}C NMR** ($CDCl_3$, 101 MHz) δ ppm 25.78 (CH_2) 26.01 (CH_2) 31.49 (CH_2) 41.68 (CH) 116.57 (q, J_{C-F} = 291.20 Hz, CF_3) 119.21 (CH) 161.55 (CH) 180.44 (q, J_{C-C-F} = 34.50 Hz, C) **^{19}F NMR** ($CDCl_3$, 376 MHz) δ ppm -80.64 **GC-MS** (EI) 206 ($[M]^+$, 3%) 137 (40%) 109 (7%) 95 (10%),94 (20%) 81 (100%) 79 (22%) 69 (17%) 67 (42%) 55 (46%) 53 (16%) 41 (25%) 37 (15%)

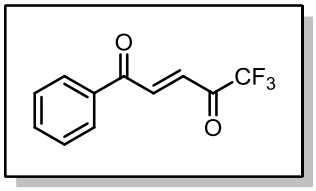

(E)-5,5,5-trifluoro-1-phenylpent-2-ene-1,4-dione (1.6n) (0.7721 g, 80%) was prepared according to the representative procedure from 5,5,5-trifluoro-1-phenylpentane-1,4-dioneone **(1.5n)** (0.9715 g, 4.22 mmol) to give a clear yellow oil. **^{1}H NMR** ($CDCl_3$, 400 MHz) δ ppm 7.46 (d, J = 15.41 Hz, 1 H) 7.62 (t, J = 6.85 Hz, 2 H) 7.69 - 7.81 (m, 1 H) 8.09 (d, J = 7.09 Hz, 2 H) 8.20 (d, J=15.41 Hz, 1 H) **^{13}C NMR** ($CDCl_3$, 101 MHz) δ ppm 114.07 (q, J_{C-F} = 290.50 Hz, CF_3) 127.30 (CH) 127.44 (CH) 127.48 (CH) 132.88 (C) 134.34

(CH) 138.11 (s, CH) 178.62 (q, $J_{C\text{-}C\text{-}F}$ = 37.40 Hz, C) 186.37 (C) **^{19}F NMR** ($CDCl_3$, 377 MHz) δ ppm -80.95 **GC-MS** (EI) 228 ($[M]^+$, 12%) 159 36(%) 131 (15%) 105 (100%) 77 (68%) 69 (8%) 51 (23%) **HRMS** (ESI+), calcd for $C_{11}H_7F_3O_2$ $[M + H]^+$: 229.0476, found: 229.0469

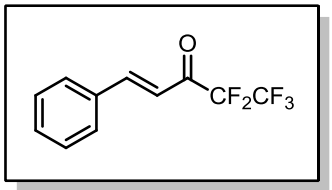

(E)-4,4,5,5,5-pentafluoro-1-phenylpent-1-en-3-one (1.6q) (1.150 g, 77%) was prepared according to the representative procedure from 1,1,1,2,2-pentafluoro-5-phenylpentan-3-one **(1.5q)** (1.513 g, 6 mmol) to give a clear yellow oil. **^{1}H NMR** ($CDCl_3$, 400 MHz) δ ppm 7.14 (d, *J* = 15.89 Hz, 1 H) 7.40 - 7.56 (m, 3 H) 7.61 - 7.70 (m, 2 H) 7.99 (d, *J* = 15.65 Hz, 1 H) **^{13}C NMR** ($CDCl_3$, 101 MHz) δ ppm 107.98 (tq, $J_{C\text{-}F}$ = 265.60, $J_{C\text{-}C\text{-}F}$ = 38.10 Hz, CF_2) 118.32 (qt, $J_{C\text{-}F}$ = 286.80, $J_{C\text{-}C\text{-}F}$ = 34.50 Hz, CF_3) 116.88 (t, $J_{C\text{-}C\text{-}C\text{-}F}$ = 1.50 Hz, CH) 129.46 (CH) 129.60 (CH) 132.66 (CH) 133.55 (CH) 150.32 (CH) 182.48 (t, $J_{C\text{-}C\text{-}F}$ =25.70 Hz, C) **^{19}F NMR** ($CDCl_3$, 377 MHz) δ ppm -126.63 (s, 2 F) -84.98 (s, 3 F) **GC-MS** (EI) 250 ($[M]^+$, 43%) 131 (100%) 103 (77%) 77 (42%) 69 (6%) 51 (18%)

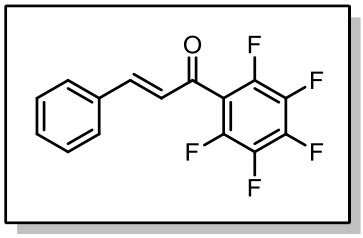

(E)-1-(perfluorophenyl)-3-phenylprop-2-en-1-one (1.6r) (0.543 g, 26%) was prepared according to the representative procedure from 1-(perfluorophenyl)-3-phenylpropan-1-one **(1.5r)** (2.101 g, 7 mmol) to give a yellow solid.**^{1}H NMR** ($CDCl_3$, 400 MHz) δ ppm 7.03 (d, *J* = 16.14 Hz, 1 H) 7.38 - 7.49 (m, 3 H) 7.53 (d, *J* = 15.89 Hz, 1 H) 7.56 - 7.64 (m, 2 H) **^{13}C NMR** ($CDCl_3$, 101 MHz) δ ppm 114.50 - 115.19 (m, C) 126.33 (CH) 129.13 (CH) 129.38 (CH) 131.94 (CH) 133.85 (C) 137.90 (dm, $J_{C\text{-}F}$ = 256.76 Hz, CF) 142.75 (dm, $J_{C\text{-}F}$ = 257.49 Hz, CF) 144.32 (dm, $J_{C\text{-}F}$ = 252.36 Hz, CF) 148.48 (CH) 183.97 (C) **^{19}F NMR** ($CDCl_3$, 376 MHz) δ ppm -163.44 - -162.81 (m, 2 F) -153.77 - -153.26 (m, 1 F) -143.97 - -143.42 (m, 2 F) **GC-MS** (EI) 298 ($[M]^+$, 59%) 297 (100%) 195 (8%) 167 (11%) 131 (22%) 103 (37%) 77 (29%) 51 (11%)

General Procedure for the Grignard Reaction of Perfluoroalkyl Ketones and Trimethylsilyl-methylmagnesium Chloride

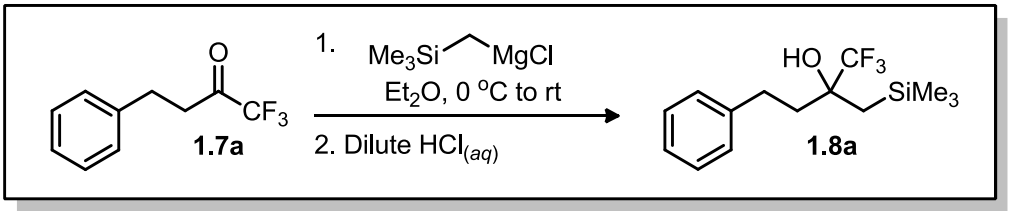

1,1,1-trifluoro-4-phenyl-2-((trimethylsilyl)methyl)butan-2-ol (1.8a) The following is a modification of the procedure outlined by O'Doherty.[146] To a 100 mL round bottom flask was added crushed magnesium turnings (0.6807 g, 28 mmol, 1.4 equiv) and a stirbar. The flask was sealed with a rubber septum, the atmosphere was evacuated from the flask *via* an inlet needle, and the flask flamed dried under vacuum.[147] The flask was flushed with nitrogen and placed in a room temperature oil bath. Chloromethyltrimethylsilane (2.9125 g, 24 mmol, 1.2 equiv) dissolved in anhydrous Et_2O (14 mL) was added to the flask dropwise[148] *via* an addition funnel atop a reflux condenser. The reaction mixture was heated to reflux for 1.5 h while under a N_2 atmosphere. The reaction mixture gradually became cloudy then dark grey. After this time the flask was cooled to 0 ^oC in an ice bath for ten minutes. Subsequently the 1,1,1-trifluoro-4-phenylbutan-2-one, **1.7a** (4.00 g, 20 mmol, 1 equiv) dissolved in anhydrous Et_2O was added to the flask dropwise. Ten minutes after completion of this addition, the ice bath was removed and the solution was stirred at rt for 12 h. After this time, the solution was was quenched with 0.5 M aqueous HCl (20 mL) and transferred to a separatory funnel. The phases were separated and the aqueous layer was extracted with Et_2O (3 x 100 mL). The combined organic layers were washed with sat. $NaHCO_3$ (≈150 mL), brine (≈150 mL), and dried with Na_2SO_4. The solvent was removed *in vacuo* by rotary evaporation to give the pure carbinol **1.8a** (3.552 g, 61 %) as a clear, colorless liquid.

^{1}H NMR ($CDCl_3$, 400 MHz) δ ppm 0.16 (s, 9 H) 1.16 (d, J = 15.16 Hz, 1 H) 1.27 (d, J = 15.16 Hz, 1 H) 1.90 (s, 1 H) 1.99 - 2.08 (m, 2 H) 2.72 - 2.81 (m, 2 H) 7.19 - 7.26 (m, 3 H) 7.28 - 7.36 (m, 2 H); **^{13}C NMR** ($CDCl_3$, 100 MHz) δ ppm 0.5 (CH_3) 23.6 (CH_2) 29.9 (CH_2) 38.8 (CH_2) 76.4 (q, $J_{C\text{-}C\text{-}F}$ = 27.90 Hz, C) 126.5 (CH) 127.0 (q, $J_{C\text{-}F}$ = 286.1 Hz, CF_3) 128.6 (CH) 128.9 (CH) 141.5 (C); **^{19}F NMR** ($CDCl_3$, 377 MHz) δ ppm -84.13; **GC-MS** (EI) 290 ($[M]^+$, 2%) 200 (10%) 161 (39%) 146 (6%) 129 (7%) 91 (100%) 77 (15%) 73 (27%); **HRMS** (DART), calcd for $C_{14}H_{21}F_3OSi$ $[M + NH_4]^+$: 308.1658, found 308.1665.

[146] Haukaas, M. H.; O'Doherty, G. A. *Org. Lett.*, **2001**, *3*, 401.
[147] The flask and addition funnel were flame dried a total of 3 times with cooling in between *via* N_2.
[148] Care should be taken during this addition. If added too fast the reaction will exotherm quite vigorously.

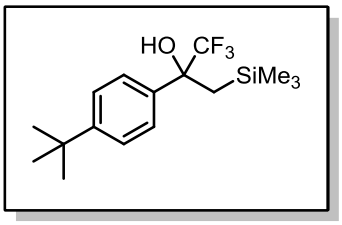

4-(4-(tert-butyl)phenyl)-1,1,1-trifluoro-2-((trimethylsilyl)methyl)butan-2-ol (1.8b) (1.491 g, 76%) was prepared according to the representative procedure for the synthesis of **1.8a** from 1-(4-(tert-butyl)phenyl)-2,2,2-trifluoroethanone, **1.7b** (1.42 g, 6.17 mmol) affording the pure α-perfluoroalkyl-β-trimethylsilyl- carbinol as a clear, orange oil. **^{1}H NMR** ($CDCl_3$, 500 MHz) δ ppm -0.17 (s, 9 H) 1.34 (s, 9 H) 1.47 (d, J = 14.82 Hz, 1 H) 1.65 (d, J = 14.98 Hz, 1 H) 2.33 (s, 1 H) 7.40 (d, J = 8.20 Hz, 2 H) 7.48 (d, J = 8.20 Hz, 2 H); **^{13}C NMR** ($CDCl_3$, 125 MHz) δ ppm 0.01 (CH_3) 25.3 (CH_2) 31.6 (CH_3) 34.77 (C) 77.6 (q, $J_{C\text{-}C\text{-}F}$ = 28.8 Hz, C) 125.3 (CH) 126.1 (CH) 126.3 (q, $J_{C\text{-}F}$ = 285.7 Hz, CF_3) 135.4 (C) 151.6 (C); **^{19}F NMR** ($CDCl_3$, 377 MHz) δ ppm -85.06; **GC-MS** (EI) 228 ($[M]^+$, 20%) 213 (100%) 185 (45%) 164 (4%) 151 (4%) 129 (5%) 128 (8%) 115 (11%) 69 (2%) 41 (6%); **HRMS** (DART), calcd for $C_{16}H_{25}F_3OSi$ $[M + NH_4]^+$: 336.1970, found: 336.1955.

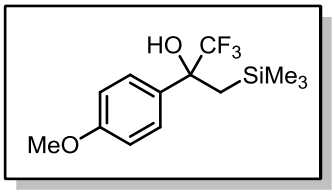

1,1,1-trifluoro-2-(4-methoxyphenyl)-3-(trimethylsilyl)propan-2-ol (1.8c) (3.683 g, 85%) was prepared according to the representative procedure for the synthesis of **1.8a** from 2,2,2-trifluoro-1-(4-methoxyphenyl)ethanone, **1.7c** (3.023 g, 14.8 mmol) affording the pure carbinol as a pale yellow solid (m.p. 63-65 ^{o}C). **^{1}H NMR** ($CDCl_3$, 300 MHz) δ ppm -0.16 (s, 9 H) 1.38 - 1.48 (m, 1 H) 1.63 (d, J = 15.17 Hz, 1 H) 2.26 (s, 1 H) 3.82 (s, 3 H) 6.86 - 6.94 (m, 2 H) 7.46 (d, J = 9.22 Hz, 2 H); **^{13}C NMR** ($CDCl_3$, 125 MHz) δ ppm 0.1 (CH_3) 25.1 (CH_2) 55.5 (CH_3) 77.4 (q, $J_{C\text{-}C\text{-}F}$ = 28.8 Hz, C) 113.7 (CH) 126.2 (q, $J_{C\text{-}F}$ = 284.8 Hz, CF_3) 127.8 (CH) 130.4 (C) 159.8 (C); **^{19}F NMR** ($CDCl_3$, 377 MHz) δ ppm -85.47; **GC-MS** (EI) 202 ($[M]^+$, 98%) 186 (5%) 159 (7%) 133 (100%) 118 (13%) 109 (30%) 103 (11%) 89 (16%) 69 (5%) 63 (13%); **HRMS** (DART), calcd for $C_{13}H_{19}F_3O_2Si$ $[M - OH]^+$: 275.1079, found: 275.1080.

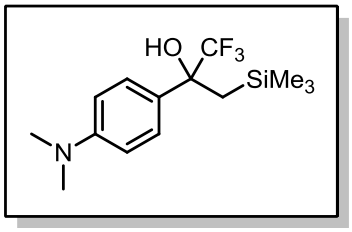

2-(4-(dimethylamino)phenyl)-1,1,1-trifluoro-3-(trimethylsilyl)propan-2-ol (1.8d) (4.463 g, 91%) was prepared according to the representative procedure for the synthesis of **1.8a** from 1-(4-(dimethylamino)phenyl)-2,2,2-trifluoroethanone, **1.7d** (3.475 g, 16 mmol) affording the pure carbinol as clear, orange oil. **^{1}H NMR** ($CDCl_3$, 400 MHz) δ ppm -0.16 (s, 9 H) 1.47 (d, J = 14.92 Hz, 1 H) 1.67 (d, J = 15.16 Hz, 1 H) 2.41 (s, 1 H) 2.94 - 3.04 (m, 6 H) 6.75 (d, J = 9.05 Hz, 2 H 7.41 (d, J = 8.80 Hz, 2 H); **^{13}C NMR** ($CDCl_3$, 100 MHz) δ ppm 0.2 (CH_3) 24.8 (CH_2) 40.6 (CH_3) 77.3 (q, $J_{C\text{-}C\text{-}F}$ = 28.6 Hz, C) 112.1 (CH) 126.4 (q, $J_{C\text{-}F}$ = 286.1 Hz, CF_3) 125.8 (CH) 127.3 (C) 150.6 (C); **^{19}F NMR** ($CDCl_3$, 377 MHz) δ ppm -85.24; **GC-MS** (EI) 305 ($[M]^+$, 18%) 287 (4%) 236 (40%) 220 (20%) 214 (22%) 196 (12%) 178 (9%) 146 (100%) 75 (12%) 73 (10%); **HRMS** (ESI+), calcd for $C_{14}H_{22}F_3NOSi$ $[M + H]^+$: 306.1501, found: 306.1479.

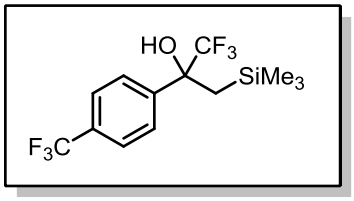

1,1,1-trifluoro-2-(4-(trifluoromethyl)phenyl)-3-(trimethylsilyl)propan-2-ol (1.8e) (1.978 g, 91%) was prepared according to the representative procedure for the synthesis of **1.8a** from 2,2,2-trifluoro-1-(4-(trifluoromethyl)phenyl)ethanone, **1.7e** (1.600 g, 6.6 mmol) affording the pure carbinol as a clear, pale yellow oil. **^{1}H NMR** ($CDCl_3$, 400 MHz) δ ppm -0.17 (s, 9 H) 1.46 - 1.53 (m, 1 H) 1.63 - 1.71 (m, 1 H) 2.40 (s, 1 H) 7.66 (d, J = 8.80 Hz, 2 H) 7.72 (d, J = 8.31 Hz, 2 H); **^{13}C NMR** ($CDCl_3$, 100 MHz) δ ppm 0.01 (CH_3) 25.3 (CH_2) 77.6 (q, $J_{C\text{-}C\text{-}F}$ = 29.3 Hz, C) 124.3 (q, $J_{C\text{-}F}$ = 272.2 Hz, CF_3) 125.8 (q, $J_{C\text{-}F}$ = 286.8 Hz, CF_3) 125.4 (q, $J_{C\text{-}C\text{-}F}$ =3.7 Hz, CH) 127.2 (d, $J_{C\text{-}C\text{-}C\text{-}C\text{-}F}$ = 1.5 Hz, CH) 131.0 (q, $J_{C\text{-}C\text{-}F}$ = 33.0 Hz, C) 142.3 (C); **^{19}F NMR** ($CDCl_3$, 377 MHz) δ ppm -84.90 (s, 3 F) -65.72 (s, 3 F); **GC-MS** (EI) 240 ($[M]^+$, 86%) 221 (40%) 201 (4%) 171 (100%) 169 (14 %) 151 (95%) 145 (12%) 102 (15%) 75 (12%) 69 (12%) 50 (5%); **HRMS** (DART), calcd for $C_{13}H_{16}F_6OSi$ $[M + HF]^+$: 350.0937, found: 350.0978 FTIR (cm^{-1}, neat, ATR) = 3622, 2958, 2362, 1622, 1327, 1168, 1129, 841.

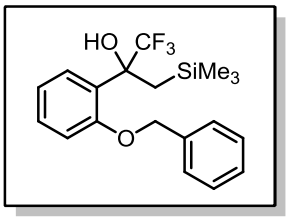

2-(2-(benzyloxy)phenyl)-1,1,1-trifluoro-3-(trimethylsilyl)propan-2-ol (1.8f) (3.250 g, 79%) was prepared according to the representative procedure for the synthesis of **1.8a** from 1-(2-(benzyloxy)phenyl)-2,2,2-trifluoroethanone, **1.7f** (3.097 g, 11.13 mmol) affording the pure carbinol as a cloudy, pale yellow oil. **^{1}H NMR** ($CDCl_3$, 500 MHz) δ ppm -0.07 (s, 9 H) 1.52 (d, J = 14.98 Hz, 1 H) 1.68 (dd, J = 14.82, 2.84 Hz, 1 H) 5.18 (d, J = 2.36 Hz, 2 H) 6.23 - 6.40 (m, 1 H) 7.02 - 7.11 (m, 2 H) 7.32 - 7.41 (m, 3 H) 7.41 - 7.49 (m, 4 H); **^{13}C NMR** ($CDCl_3$, 125 MHz) δ ppm 0.5 (CH_3) 23.2 (CH_2) 72.2 (CH_2) 79.6 (q, $J_{C\text{-}C\text{-}F}$ = 29.7 Hz, C) 114.3 (CH) 121.8 (CH) 126.5 (q, $J_{C\text{-}F}$ = 287.4 Hz, CF_3) 126.1 (CH) 128.0 (CH) 128.9 (CH) 129.2 (CH) 130.4 (CH) 130.8 (C) 135.8 (C) 157.9 (C); **^{19}F NMR** ($CDCl_3$, 377 MHz) δ ppm -85.44; **GC-MS** (EI) 368 ($[M]^+$, 10%) 260 (16%) 175 (12%) 149 (23%) 91 (100%) 75 (10%) 65 (9%); **HRMS** (DART), calcd for $C_{19}H_{23}F_3O_2Si$ $[M - OH]^+$: 351.1392, found: 351.1438.

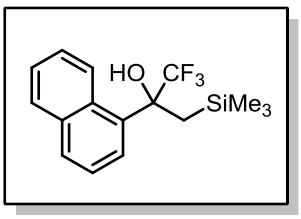

1,1,1-trifluoro-2-(naphthalen-1-yl)-3-(trimethylsilyl)propan-2-ol (1.8g) (2.618 g, 79%) was prepared according to the representative procedure for the synthesis of **1.8a** from 2,2,2-trifluoro-1-(naphthalen-1-yl)ethanone, **1.7g** (2.386 g, 10.64 mmol) affording the pure carbinol as a cloudy, pale yellow oil. **^{1}H NMR** ($CDCl_3$, 400 MHz) δ ppm -0.16 (s, 9 H) 1.69 (d, J = 15.41 Hz, 1 H) 2.23 (d, J = 15.41 Hz, 1 H) 2.60 (s, 1 H) 7.43 - 7.58 (m, 3 H) 7.74 - 7.84 (m, 1 H) 7.89 (d, J = 7.82 Hz, 2 H) 8.73 - 8.95 (m, 1 H); **^{13}C NMR** ($CDCl_3$, 100 MHz) δ ppm 0.2 (CH_3) 26.7 (CH_2) 80.5 (q, $J_{C\text{-}C\text{-}F}$ = 29.3 Hz, C) 126.6 (q, $J_{C\text{-}F}$ = 286.8 Hz, CF_3) 124.6 (CH) 125.6 (CH) 126.1 (CH) 127.0 (q, $J_{C\text{-}C\text{-}C\text{-}F}$ = 1.5 Hz, C) 127.4 (br. s., CH) 129.4 (CH) 130.7 (CH) 131.9 (C) 133.9 (C) 135.2 (C); **^{19}F NMR** ($CDCl_3$, 377 MHz) δ ppm -82.01; **GC-MS** (EI) 312 ($[M]^+$, 13%) 243 (26%) 227 (12%) 201 (8%) 183 (30%) 153 (100%) 127 (10%) 115 (5%) 73 (13%); **HRMS** (DART), calcd for $C_{16}H_{19}F_3OSi$ $[M]^+$: 312.1157, found: 312.1183.

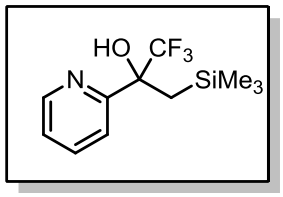

1,1,1-trifluoro-2-(pyridin-2-yl)-3-(trimethylsilyl)propan-2-ol (1.8h) (1.266 g, 23%) was prepared according to the representative procedure for the synthesis of **1.8a** from 2,2,2-trifluoro-1-(pyridin-2-yl)ethanone, **1.7h** (3.600 g, 21 mmol)[149] affording the pure carbinol as a clear, brown oil. **^{1}H NMR** ($CDCl_3$, 400 MHz) δ ppm -0.23 (s, 9 H) 1.43 (d, J = 14.92 Hz, 1 H) 1.71 (d, J = 14.67 Hz, 1 H) 6.39 (s, 1 H) 7.31 - 7.37 (m, 1 H) 7.53 (dd, J = 8.07, 0.98 Hz, 1 H) 7.78 (td, J = 7.70, 1.59 Hz, 1 H) 8.57 (dq, J = 4.89, 0.82 Hz, 1 H); **^{13}C NMR** ($CDCl_3$, 100 MHz) δ ppm -0.1 (CH_3) 23.1 (CH_2) 76.3 (q, $J_{C\text{-}C\text{-}F}$ = 28.6 Hz, C) 125.9 (q, $J_{C\text{-}F}$ = 286.1 Hz, CF_3) 122.1 (q, $J_{C\text{-}C\text{-}C\text{-}C\text{-}F}$ = 2.2 Hz, CH) 124.0 (CH) 137.6 (CH) 147.4 (CH) 155.9 (C); **^{19}F NMR** ($CDCl_3$, 377 MHz) δ ppm -84.71; **GC-MS** (EI) 263 ($[M]^+$, 15%) 248 (24%) 242 (17%) 194 (26%) 190 (12%) 178 (35%) 154 (100%) 150 (13%) 134 (42%) 104 (62%) 78 (30%) 73 (30%) 45 (11%); **HRMS** (ESI+), calcd for $C_{11}H_{16}F_3NOSi$ $[M + H]^+$: 264.1032, found: 264.1056.

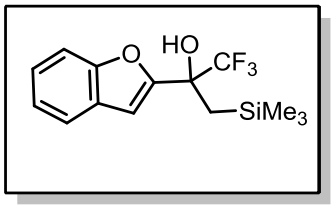

2-(benzofuran-2-yl)-1,1,1-trifluoro-3-(trimethylsilyl)propan-2-ol (1.8i) (1.9367 g, 94%) was prepared according to the representative procedure for the synthesis of **1.8a** from 1-(benzofuran-2-yl)-2,2,2-trifluoroethanone, **1.7i** (1.450 g, 6.8 mmol) affording the pure carbinol as a clear, pale yellow oil. **^{1}H NMR** ($CDCl_3$, 500 MHz) δ ppm -0.09 (s, 9 H) 1.48 - 1.57 (m, 1 H) 1.63 (s, 1 H) 2.89 (s, 1 H) 6.82 (d, J = 0.73 Hz, 1 H) 7.23 - 7.36 (m, 2 H) 7.48 - 7.53 (m, 1 H) 7.57 - 7.61 (m, 1 H); **^{13}C NMR** ($CDCl_3$, 125 MHz) δ ppm -0.2 (CH_3) 22.5 (CH) 75.5 (q, $J_{C\text{-}C\text{-}F}$ = 30.8 Hz, C) 105.6 (CH) 111.7 (CH) 125.2 (q, $J_{C\text{-}F}$ = 286.1 Hz, CF_3) 121.7 (CH) 123.5 (CH) 125.2 (CH) 128.1 (C) 153.9 (C) 155.0 (C); **^{19}F NMR** ($CDCl_3$, 377 MHz) δ ppm -85.44; GC-MS (EI) 302 ($[M]^+$, 16%) 233 (36%) 212 (28%) 193 (41%) 165 (4%) 143 (100%) 131 (7%) 115 (25%) 73 (19%); **HRMS** (DART), calcd for $C_{14}H_{17}F_3O_2Si$ $[M - CF_3]^+$: 233.0993, found: 233.1025.

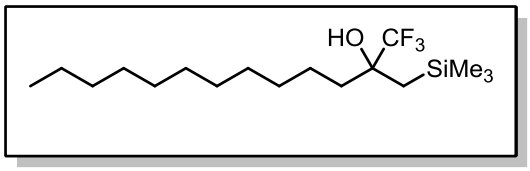

1,1,1-trifluoro-2-((trimethylsilyl)methyl)tridecan-2-ol (1.8j) (3.416 g, 90%) was prepared according to the representative procedure for the synthesis of **1.8a** from 1,1,1-trifluorotridecan-2-one, **1.7j** (2.800 g, 11.1 mmol) affording the pure carbinol as clear, pale yellow oil. **^{1}H NMR** ($CDCl_3$, 500 MHz) δ ppm 0.06 (s, 9 H) 0.85 - 0.91 (m, 3 H) 1.06 (d, J = 15.13 Hz, 1 H) 1.15 (d, J = 15.13 Hz, 1 H) 1.23 - 1.34 (m, 16 H) 1.35 - 1.45 (m, 2 H) 1.60 - 1.74 (m, 2 H) 1.76 - 2.01 (m, 1 H); **^{13}C NMR** ($CDCl_3$, 125 MHz) δ ppm 0.4 (CH_3) 14.4 (CH_3) 23.0 (CH_2) 23.3 (CH_2) 23.5 (CH_2) 29.6 (CH_2) 29.8 (CH_2) 29.9 (2 x CH_2) 29.9 (CH_2) 30.3 (CH_2) 32.2 (CH_2) 37.0 (CH_2) 76.5 (q, $J_{C\text{-}C\text{-}F}$ = 28.0 Hz, C) 127.1 (q, $J_{C\text{-}F}$ = 285.7 Hz, CF_3); **^{19}F NMR** ($CDCl_3$, 377 MHz) δ ppm -84.31; **GC-MS** (EI) 340 ($[M]^+$, 2%) 222 (3%) 193 (5%) 180 (5%) 165 (7%) 151 (7%) 140 (5%) 131 (7%) 125 (6%) 111 (30%) 103 (10%) 97 (49%) 89 (12%) 83 (48%) 70 (65%) 57 (91%) 43 (100%); **HRMS** (DART), calcd for $C_{17}H_{35}F_3OSi$ $[M + NH_4]^+$: 358.2753, found: 358.2759.

[149] Note that this ketone required rigorous drying before use. We found that azeotropic removal of water using benzene and a Dean-Stark apparatus followed by rapid solvent removal and immediate use proved optimal.

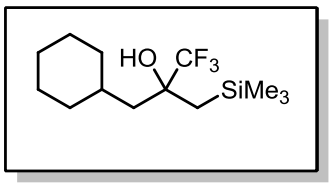

3-cyclohexyl-1,1,1-trifluoro-2-((trimethylsilyl)methyl)propan-2-ol (1.8k) (2.728 g, 89%) was prepared according to the representative procedure for the synthesis of **1.8a** from 3-cyclohexyl-1,1,1-trifluoropropan-2-one, **1.7k** (2.100 g, 10.8 mmol) affording the pure carbinol as a clear, pale yellow oil. **^{1}H NMR** ($CDCl_3$, 400 MHz) δ ppm 0.10 (s, 9 H) 0.91 - 1.36 (m, 8 H) 1.52 - 1.60 (m, 2 H) 1.60 - 1.74 (m, 4 H) 1.76 (s, 1 H) 1.83 - 1.93 (m, 1 H); **^{13}C NMR** ($CDCl_3$, 100 MHz) δ ppm 0.4 (CH_3) 24.4 (CH_2) 26.4 (CH_2) 26.6 (CH_2) 26.7 (CH_2) 33.3 (CH) 35.2 (CH_2) 35.6 (CH_2) 43.7 (CH_2) 77.0 (q, $J_{C\text{-}C\text{-}F}$ = 27.9 Hz, C) 127.0 (q, $J_{C\text{-}F}$ = 286.1 Hz, CF_3); **^{19}F NMR** ($CDCl_3$, 377 MHz) δ ppm -84.53; **GC-MS** (EI) 282 ($[M]^+$, 2%) 213 (3%) 153 (10%) 133 (26%) 131 (11%) 125 (8%) 111 (13%) 83 (100%) 73 (77%); **HRMS** (DART), calcd for $C_{13}H_{25}F_3OSi$ $[M + H]^+$: 283.1705, found: 283.1701.

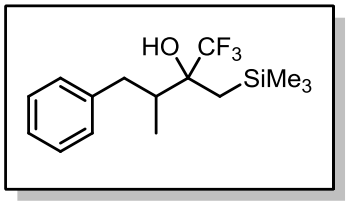

1,1,1-trifluoro-3-methyl-4-phenyl-2-((trimethylsilyl)methyl)butan-2-ol (1.8l) (1.9725 g, 88%) was prepared according to the representative procedure for the synthesis of **1.8a** from 1,1,1-trifluoro-3-methyl-4-phenylbutan-2-one, **1.7l** (1.600 g, 7.9 mmol) affording the pure carbinol as a clear, colorless oil. **^{1}H NMR** ($CDCl_3$, 400 MHz) δ ppm 0.20 (apparent doublet, J = 5.38 Hz, 9 H) 0.94 (t, J = 7.58 Hz, 3 H) 1.09 - 1.27 (m, 2 H) 2.05 (br. s., 1 H) 2.10 - 2.34 (m, 2 H) 3.23 (t, J = 11.70 Hz, 1 H) 7.18 - 7.28 (m, 3 H) 7.30 - 7.37 (m, 2 H); **^{13}C NMR** ($CDCl_3$, 100 MHz) δ ppm 0.5 (CH_3) 0.5 (CH_3) 13.9 (q, $J_{C\text{-}C\text{-}C\text{-}C\text{-}F}$ = 2.2 Hz, CH_3) 14.0 (d, $J_{C\text{-}C\text{-}C\text{-}C\text{-}F}$ = 1.5 Hz, CH_3) 20.1 (CH_2) 21.8 (CH_2) 37.4 (d, $J_{C\text{-}C\text{-}C\text{-}F}$ = 1.5 Hz, CH) 37.6 (d, $J_{C\text{-}C\text{-}C\text{-}F}$ = 2.2 Hz, CH) 42.7 (CH_2) 43.1 (CH_2) 78.7 (q, $J_{C\text{-}C\text{-}F}$ = 26.4 Hz, C) 79.0 (q, $J_{C\text{-}C\text{-}F}$ = 26.4 Hz, C) 127.3 (q, $J_{C\text{-}F}$ = 287.6 Hz, CF_3) 127.4 (q, $J_{C\text{-}F}$ = 287.6 Hz, CF_3) 141.0 (C) 141.3 (C); **^{19}F NMR** ($CDCl_3$, 377 MHz) δ ppm -79.49 (s, 3 F) -78.92 (s, 3 F); **GC-MS** (EI) 304 ($[M]^+$, 4%) 214 (4%) 194 (6%) 175 (16%) 147 (4%) 117 (6%) 91 (100%) 73 (24%); **HRMS** (DART), calcd for $C_{15}H_{23}F_3OSi$ $[M + NH_4]^+$: 322.1814, found: 322.1849.

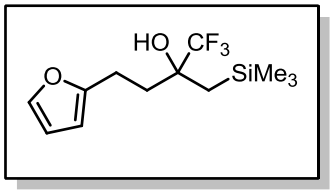

1,1,1-trifluoro-4-(furan-2-yl)-2-((trimethylsilyl)methyl)butan-2-ol (1.8m) (5.280 g, 73%) was prepared according to the representative procedure for the synthesis of **1.8a** from 1,1,1-trifluoro-4-(furan-2-yl)butan-2-one, **1.7m** (4.9956 g, 26 mmol) affording the pure carbinol as a clear, brown oil. **^{1}H NMR** ($CDCl_3$, 400 MHz) δ ppm 0.12 (s, 9 H) 1.06 - 1.15 (m, 1 H) 1.16 - 1.24 (m, 1 H) 1.92 (s, 1 H) 2.02 - 2.12 (m, 2 H) 2.79 (dd, J = 10.39, 6.48 Hz, 2 H) 6.02 (d, J = 3.18 Hz, 1 H) 6.29 (dd, J = 3.18, 1.96 Hz, 1 H) 7.32 (d, J = 1.22 Hz, 1 H); **^{13}C NMR** ($CDCl_3$, 100 MHz) δ ppm 0.3 (CH_3) 22.4 (CH_2) 23.5 (CH_2) 34.9 (CH_2) 76.1 (q, J = 28.6 Hz, C) 105.4 (CH) 110.5 (CH) 126.9 (q, J = 286.1 Hz, CF_3) 141.5 (CH) 155.1 (C); **^{19}F NMR** ($CDCl_3$, 377 MHz) δ ppm -84.07; **GC-MS** (EI) 280 ($[M]^+$, 5%) 262 (8%) 170 (21%) 151 (9%) 141 (4%) 123 (11%) 103 (9%) 94 (14%) 81 (100%) 73 (44%) 53 (17%) 45 (10%); **HRMS** (DART), calcd for $C_{12}H_{19}F_3O_2Si$ $[M + H]^+$: 281.1185, found: 281.1179.

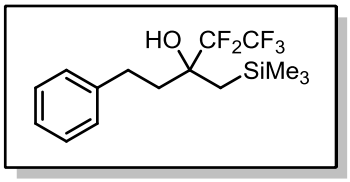

1,1,1,2,2-pentafluoro-5-phenyl-3-((trimethylsilyl)methyl)pentan-3-ol (1.8n) (1.508 g, 93%) was prepared according to the representative procedure for the synthesis of **1.8a** from 1,1,1,2,2-pentafluoro-5-phenylpentan-3-one, **1.7n** (1.200 g, 4.76 mmol) affording the pure carbinol as a clear, yellow oil. **^{1}H NMR** ($CDCl_3$, 400 MHz) δ ppm 0.19 (s, 8 H) 1.19 - 1.27 (m, 1 H) 1.33 - 1.41 (m, 1 H) 2.03 (s, 1 H) 2.10 (dd, *J* = 11.25, 6.11 Hz, 2 H) 2.72 - 2.83 (m, 2 H) 7.19 - 7.25 (m, 3 H) 7.30 - 7.37 (m, 2 H); **^{13}C NMR** ($CDCl_3$, 100 MHz) δ ppm 0.7 (CH_3) 23.5 (CH_2) 30.0 (br. s, CH_2) 39.2 (CH_2) 77.3 (t, $J_{C\text{-}C\text{-}F}$ = 22.70 Hz, C) 115.9 (tq, $J_{C\text{-}F}$ = 261.2, 34.5 Hz, CF_2) 119.9 (qt, $J_{C\text{-}F}$ = 288.3, 37.4 Hz, CF_3) 126.5 (CH) 128.6 (CH) 128.9 (CH) 141.4 (C); **^{19}F NMR** ($CDCl_3$, 377 MHz) δ ppm -125.31 - -123.20 (m, 2 F) -80.98 (s, 3 F); **GC-MS** (EI) 340 ($[M]^+$, 4%) 250 (11%) 231 (9%) 211 (8%) 191 (5%) 161 (9%) 129 (7%) 119 (3%) 105 (8%) 91 (100%) 73 (28%); **HRMS** (DART), calcd for $C_{15}H_{21}F_5OSi$ $[M + NH_4]^+$: 358.1626, found: 358.1640.

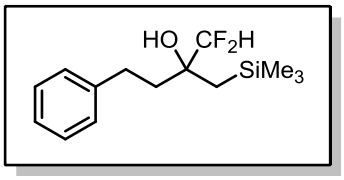

1,1-difluoro-4-phenyl-2-((trimethylsilyl)methyl)butan-2-ol (1.8o) (4.7627 g, 92%) was prepared according to the representative procedure for the synthesis of **1.8a** from 1,1-difluoro-4-phenylbutan-2-one, **1.7o** (3.500 g, 19 mmol) affording the pure carbinol as a clear, orange oil. **^{1}H NMR** ($CDCl_3$, 400 MHz) δ ppm 0.14 (s, 9 H) 1.09 (d, *J* = 11.74 Hz, 2 H) 1.75 (s, 1 H) 1.89 - 1.98 (m, 2 H) 2.69 - 2.80 (m, 2 H) 5.62 (t, *J* = 57.00 Hz, 1 H) 7.17 - 7.24 (m, 3 H) 7.27 - 7.34 (m, 2 H); **^{13}C NMR** ($CDCl_3$, 100 MHz) δ ppm 0.7 (CH_3) 23.3 (CH_2) 29.6 (CH_2) 38.7 (t, $J_{C\text{-}C\text{-}C\text{-}F}$ = 1.8 Hz, CH_2) 75.5 (t, $J_{C\text{-}C\text{-}F}$ = 21.3 Hz, C) 117.9 (t, $J_{C\text{-}F}$ = 248.7 Hz, CF_2H) 126.3 (CH) 128.6 (CH) 128.8 (CH) 142.0 (C); **^{19}F NMR** ($CDCl_3$, 377 MHz) δ ppm -134.72 (dd, *J* = 276.56, 55.86 Hz, 1 F) -133.29 (dd, *J* = 276.57, 57.22 Hz, 1 F); **GC-MS** (EI) 272 ($[M]^+$, 3%) 254 (2%) 221 (6%) 182 (8%) 162 (10%) 143 (45%) 128 (16%) 104 (11%) 91 (100%) 73 (31%) 65 (8%) 47 (7%); **HRMS** (DART), calcd for $C_{14}H_{22}F_2OSi$ $[M + NH_4]^+$: 290.1752, found: 290.1770.

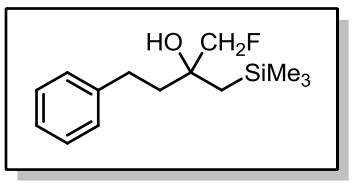

1-fluoro-4-phenyl-2-((trimethylsilyl)methyl)butan-2-ol (1.8p) (1.98 g, 52%) was prepared according to the representative procedure for the synthesis of **1.8a** from 1-fluoro-4-phenylbutan-2-one, **1.7p** (2.49 g, 15 mmol) *with the following modification*: Further purification was accomplished by FCC (gradient Hex to 95:5 Hex: EtOAc to 9:1 Hex:EtOAc). The pure carbinol was obtained as an off white semi-solid. **^{1}H NMR** ($CDCl_3$, 400 MHz) δ ppm 0.20 (s, 9 H) 1.07 (*apparent quartet of doublets*, *J* = 12.00, 2.00 Hz, 2 H) 1.95 (dd, *J* = 11.25, 6.11 Hz, 2 H) 2.04 (s, 1 H) 2.77 (*apparent doublet of doublets*, *J* = 10.88, 5.80 Hz, 2 H) 4.33 (dq, *J* = 47.80, 8.60 Hz, 2 H) 7.27 (m, 3 H) 7.36 (*apparent triplet*, *J* = 7.20 Hz, 2 H); **^{13}C NMR** ($CDCl_3$, 100 MHz) δ ppm 0.7 (CH_3) 25.3 (d, $J_{C\text{-}C\text{-}C\text{-}F}$ = 3.1 Hz, CH_2) 30.5 (CH_2) 40.9 (d, $J_{C\text{-}C\text{-}C\text{-}F}$ = 3.3 Hz, CH_2) 74.7 (d, $J_{C\text{-}C\text{-}F}$ = 17.6 Hz, C) 89.3 (d, $J_{C\text{-}F}$ = 174.1 Hz, CFH_2) 126.2 (CH) 128.5 (CH) 128.7 (CH) 142.2 (C); **^{19}F NMR** ($CDCl_3$, 377 MHz) δ ppm -227.55 (t, *J* = 47.70 Hz); **GC-MS** (EI) 254 ($[M]^+$, 1%) 236 (2%) 221 (8%) 164 (4%) 149 (10%) 145 (18%) 129 (29%) 117 (19%) 104 (12%) 91 (100%) 75 (29%) 65 (11%) 57 (15%) 45 (9%); **HRMS** (DART), calcd for $C_{14}H_{23}F_1OSi$ $[M + NH_4]^+$: 272.1846, found: 272.1842.

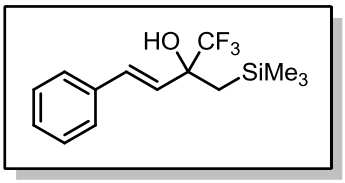

(E)-1,1,1-trifluoro-4-phenyl-2-((trimethylsilyl)methyl)but-3-en-2-ol (1.8q) (3.514 g, 81%) was prepared according to the representative procedure for the synthesis of **1.8a** from (E)-1,1,1-trifluoro-4-phenylbut-3-en-2-one, **1.7q** (2.900 g, 15 mmol) *with the following modification*: A gradient was used (pentane to 95:5 pentane:EtOAc) when eluting the off the silica gel plug.[150] The pure carbinol was obtained as a pale yellow oil. **^{1}H NMR** ($CDCl_3$, 400 MHz) δ ppm 0.04 (s, 9 H) 1.23 - 1.41 (m, 2 H) 2.16 (s, 1 H) 6.21 (d, *J* = 16.14 Hz, 1 H) 6.85 (d, *J* = 16.14 Hz, 1 H) 7.26 - 7.48 (m, 5 H); **^{13}C NMR** ($CDCl_3$, 100 MHz) δ ppm 0.5 (CH_3) 24.1 (CH_2) 76.8 (q, $J_{C\text{-}C\text{-}F}$ = 29.3 Hz, C) 125.9 (q, $J_{C\text{-}F}$ = 286.1 Hz, CF_3) 127.0 (CH) 128.5 (CH) 129.0 (CH) 131.8 (CH 136.1 (C); **^{19}F NMR** ($CDCl_3$, 377 MHz) δ ppm -86.05; **GC-MS** (EI) 288 ($[M]^+$, 3%) 219 (53%) 203 (10%) 177 (12%) 159 (45%) 129 (100%) 115 (9%) 73 (22%) 69 (1%); **HRMS** (DART), calcd for $C_{14}H_{19}F_3OSi$ [M - CF_3]$^+$: 219.1205, found: 219.1198.

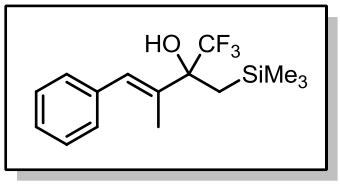

(E)-1,1,1-trifluoro-3-methyl-4-phenyl-2-((trimethylsilyl)methyl)but-3-en-2-ol (1.8r) (3.150 g, 87%) was prepared according to the representative procedure for the synthesis of **1.8a** from (E)-1,1,1-trifluoro-3-methyl-4-phenylbut-3-en-2-one, **1.7r** (2.570 g, 12 mmol) affording the pure carbinol as a clear, pale yellow oil. **^{1}H NMR** ($CDCl_3$, 500 MHz) δ ppm 0.15 (s, 9 H) 1.33 (d, *J* = 14.98 Hz, 1 H) 1.53 (d, *J* = 15.13 Hz, 1 H) 1.95 (s, 3 H) 2.21 (s, 1 H) 6.93 (s, 1 H) 7.30 (d, *J* = 7.09 Hz, 3 H) 7.37 - 7.44 (m, 2 H); **^{13}C NMR** ($CDCl_3$, 125 MHz) δ ppm 0.3 (CH_3) 15.2 (CH_3) 22.6 (CH_2) 79.0 (q, $J_{C\text{-}C\text{-}F}$ = 28.0 Hz, C) 126.3 (q, $J_{C\text{-}F}$ = 287.4 Hz, CF_3) 127.1 (CH) 128.5 (CH) 128.8 (CH) 129.3 (CH) 135.2 (C) 137.6 (C); **^{19}F NMR** ($CDCl_3$, 377 MHz) δ ppm -83.65; **GC-MS** (EI) 302 ($[M]^+$, 9%) 233 (99%) 217 (11%) 197 (14%) 177 (19%) 173 (35%) 143 (100%) 128 (78%) 115 (39%) 91 (16%) 73 (40%) 69 (2%); **HRMS** (DART), calcd for $C_{15}H_{21}F_3OSi$ [M - OH]$^+$: 285.1286, found: 285.1277.

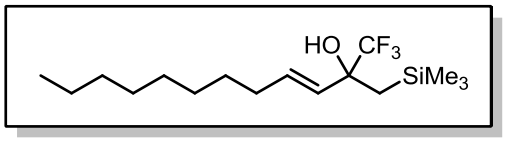

(E)-1,1,1-trifluoro-2-((trimethylsilyl)methyl)dodec-3-en-2-ol (1.8s) (2.339 g, 92%) was prepared according to the representative procedure for the synthesis of **1.8a** from (E)-1,1,1-trifluorododec-3-en-2-one**, 1.7s** (1.820 g, 8.19 mmol) affording the pure carbinol as a clear, colorless oil. **^{1}H NMR** ($CDCl_3$, 400 MHz) δ ppm 0.07 - 0.11 (m, 9 H) 0.87 - 0.96 (m, 3 H) 1.13 (d, *J* = 14.92 Hz, 1 H) 1.26 (d, *J* = 14.92 Hz, 1 H) 1.32 (s, 8 H) 1.39 - 1.51 (m, 2 H) 2.05 - 2.09 (m, 1 H) 2.12 (d, *J* = 7.09 Hz, 2 H) 5.51 (d, *J* = 15.65 Hz, 1 H) 5.92 (d, *J* = 15.65 Hz, 1 H); **^{13}C NMR** ($CDCl_3$, 100 MHz) δ ppm 0.5 (CH_3) 14.3 (CH_3) 22.9 (CH_2) 23.7 (CH_2) 29.1 (CH_2) 29.4 (CH_2) 29.5 (CH_2) 32.1 (CH_2) 32.4 (CH_2) 76.3 (q, $J_{C\text{-}C\text{-}F}$ = 28.6 Hz, C) 126.0 (q, $J_{C\text{-}F}$ = 285.4 Hz, CF_3) 128.0 (CH) 133.3 (CH); **^{19}F NMR** ($CDCl_3$, 377 MHz) δ ppm -86.47; **GC-MS** (EI) 324 ($[M]^+$, 2%) 251 (8%) 224 (3%) 177 (4%) 139 (11%) 115 (11%) 97 (16%) 84 (32%) 73 (15%) 69 (71%) 56 (81%) 43 (100%); **HRMS** (DART), calcd for $C_{16}H_{31}F_3OSi$ [M - H]$^+$: 323.2018, found: 323.2014.

[150] We observed both 1,2- addition and 1,4-addition. These two species were determined to be separable by TLC and therefore FCC was performed.

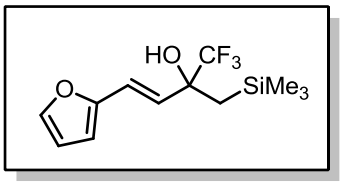

(E)-1,1,1-trifluoro-4-(furan-2-yl)-2-((trimethylsilyl)methyl)but-3-en-2-ol (1.8t) (1.627 g, 61%) was prepared according to the representative procedure for the synthesis of **1.8a** from (E)-1,1,1-trifluoro-4-(furan-2-yl)but-3-en-2-one, **1.7t** (1.82 g, 9.47 mmol), *with the following modification*: A gradient was used (pentane to 95:5 pentane:EtOAc) when eluting the off the silica gel plug.**Error! Bookmark not defined.** The pure carbinol was obtained as a clear, brown oil. **^{1}H NMR** ($CDCl_3$, 400 MHz) δ ppm 0.04 - 0.12 (m, 9 H) 1.25 (d, *J* = 14.92 Hz, 1 H) 1.32 (d, *J* = 14.67 Hz, 1 H) 2.18 (br. s., 1 H) 6.16 (d, *J* = 15.89 Hz, 1 H) 6.33 (d, *J* = 3.18 Hz, 1 H) 6.40 (dd, *J* = 3.30, 1.83 Hz, 1 H) 6.66 (d, *J* = 15.89 Hz, 1 H) 7.38 (d, *J* = 1.47 Hz, 1 H); **^{13}C NMR** ($CDCl_3$, 100 MHz) δ ppm 0.4 (CH_3) 24.3 (CH_2) 76.6 (q, $J_{C\text{-}C\text{-}F}$ = 29.3 Hz, C) 109.7 (CH) 111.7 (CH) 120.3 (CH) 125.9 (q, $J_{C\text{-}F}$ = 285.4 Hz, CF_3) 125.5 (CH) 143.0 (CH) 152.0 (C); **^{19}F NMR** ($CDCl_3$, 377 MHz) δ ppm -85.93; **GC-MS** (EI) 278 ([M]$^+$, 29%) 209 (83%) 193 (19%) 188 (10%) 170 (12%) 159 (11%) 149 (14%) 141 (7%) 119 (100%) 109 (10%) 91 (69%) 81 (10%) 77 (26%) 73 (68%) 65 (15%) 55 (21%); **HRMS** (DART), calcd for $C_{12}H_{17}F_3O_2Si$ [M + H]$^+$: 279.1028, found: 279.1032.

General Procedure for Alkene Synthesis

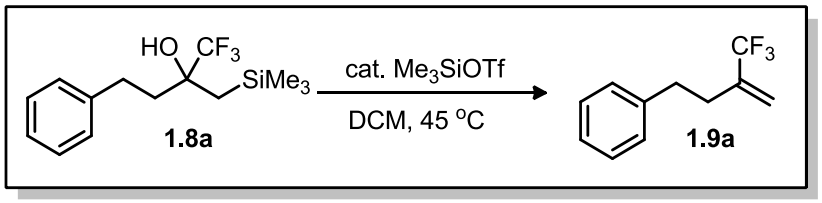

(3-(trifluoromethyl)but-3-en-1-yl)benzene (1.9a) To a 100 mL one neck round bottom was equipped with stirbar was added the carbinol, **1.8a** (1.45 g, 5 mmol, 1 equiv) and DCM (25 mL, 0.2 M in the alcohol).[151] The solution was cooled to 0 °C *via* an ice-water bath and stirred for ten minutes at this temperature. After this time, TMSOTf (0.167 g, 0.14 mL, 0.15 equiv) was added to the flask dropwise over one minute. The flask was then equipped with a reflux condenser and heated to reflux for 4 h.[152] After this time, the flask was cooled to room temperature and quenched with 50 mL of aqueous saturated $NaHCO_3$. The reaction mixture was transferred to a separatory funnel and diluted with pentane (≈150 mL). The layers were separated and the aqueous layer was extracted with pentane (3 x 75 mL). The combined organic layers were washed with brine (≈150 mL) and dried with Na_2SO_4. The solvent was removed *in vacuo* by rotary evaporation. The crude product was gently added atop a silica gel plug and eluted with pentane[153] (2-3 column volumes). The solvent was removed *in vacuo* by rotary evaporation affording the pure alkene **1.9a** (0.745 g, 74%) as a clear, colorless oil.

[151] Hexanes can also be used in place of DCM.
[152] It is recommended that, when attempting dehydrative desilylation using this protocol on substrates not outlined here, the reaction is monitored by TLC, NMR, or GC/MS to determine reaction progress. The rate and success of dehydrative desilylation of these CF_3 alcohols is dependent on the stability of the theoretical α-CF_3 cation. Hence α-aryl or α-alkenyl carbinols typically do not require heating and be conducted at room temperature over very short periods of time. However, α-alkyl or electron deficient α-aryl substitution demands heating. In some cases alternative solvents (i.e. DCE) are needed to access high temperature ranges.
[153] Hexanes can also be used.

^{1}H NMR ($CDCl_3$, 400 MHz) δ ppm 2.53 (t, *J* = 8.07 Hz, 2 H) 2.81 - 2.89 (m, 2 H) 5.30 (d, *J* = 1.22 Hz, 1 H) 5.69 (s, 1 H) 7.18 - 7.25 (m, 3 H) 7.28 - 7.35 (m, 2 H); **^{13}C NMR** ($CDCl_3$, 100 MHz) δ ppm 31.5 (CH_2) 34.1 (CH_2) 118.5 (q, $J_{C\text{-}C\text{-}C\text{-}F}$ = 5.9 Hz, CH_2) 124.1 (q, $J_{C\text{-}F}$ = 273.6 Hz, CF_3) 126.5 (CH) 128.7 (CH) 128.8 (CH) 138.1 (q, $J_{C\text{-}C\text{-}F}$ = 29.3 Hz, C) 140.9 (C); **^{19}F NMR** ($CDCl_3$, 377 MHz) δ ppm -71.49; **GC-MS** (EI) 200 ($[M]^+$, 24%) 161 (6%) 128 (4%) 115 (4%) 91 (100%) 69 (4%) 51 (5%).

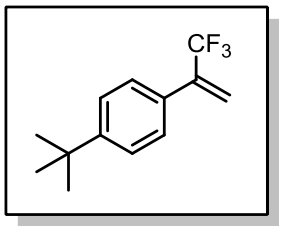

1-(tert-butyl)-4-(3,3,3-trifluoroprop-1-en-2-yl)benzene (1.9b) (0.868 g, 86%) was prepared according to the representative procedure for the synthesis of **1.9a** from 2-(4-(tert-butyl)phenyl)-1,1,1-trifluoro-3-(trimethylsilyl)propan-2-ol, **1.8b** (1.40 g, 4.4 mmol), *with the following modification*: Reaction was stirred for 15 min at room temperature. The pure CF_3 alkene was obtained as a clear, colorless oil. **^{1}H NMR** ($CDCl_3$, 400 MHz) δ ppm 1.38 - 1.40 (m, 9 H) 5.80 (q, *J* = 1.70 Hz, 1 H) 5.96 (q, *J* = 1.40 Hz, 1 H) 7.46 (s, 4 H); **^{13}C NMR** ($CDCl_3$, 100 MHz) δ ppm 31.5 (CH_3) 34.9 (C) 119.85 (q, $J_{C\text{-}C\text{-}C\text{-}F}$ = 5.9 Hz, CH_2) 123.8 (q, $J_{C\text{-}F}$ = 273.8 Hz, CF_3) 125.8 (CH) 127.3 (CH) 131.0 (C) 139.1 (q, $J_{C\text{-}C\text{-}F}$ = 30.5 Hz, C) 152.5 (C); **^{19}F NMR** ($CDCl_3$, 377 MHz) δ ppm -67.87; **GC-MS** (EI) 228 ($[M]^+$, 20%) 213 (100%) 185 (45%) 128 (8%) 115 (11%) 77 (4%) 69 (2%).

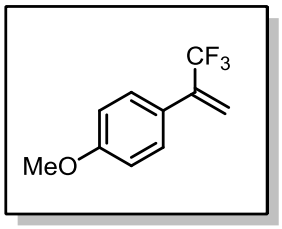

1-methoxy-4-(3,3,3-trifluoroprop-1-en-2-yl)benzene (1.9c) (0.811 g, 80%) was prepared according to the representative procedure for the synthesis of **1.9a** from 1,1,1-trifluoro-2-(4-methoxyphenyl)-3-(trimethylsilyl)propan-2-ol, **1.8c** (1.46 g, 5 mmol, *with the following modification*: Reaction was stirred for 15 min at room temperature. The pure CF_3 alkene was obtained as a clear, pale yellow oil. **^{1}H NMR** ($CDCl_3$, 400 MHz) δ ppm 3.82 - 3.85 (m, 3 H) 5.71 (q, *J* = 1.71 Hz, 1 H) 5.86 - 5.90 (m, 1 H) 6.89 - 6.95 (m, 2 H) 7.42 (d, *J* = 8.31 Hz, 2 H); **^{13}C NMR** ($CDCl_3$, 100 MHz) δ ppm 55.5 (CH_3) 114.2 (CH) 119.1 (q, $J_{C\text{-}C\text{-}C\text{-}F}$ = 5.6 Hz, CH_2) 123.8 (q, $J_{C\text{-}F}$ = 273.2 Hz, CF_3) 126.3 (CH) 128.91 (C) 138.7 (q, $J_{C\text{-}C\text{-}F}$ = 30.1 Hz, C) 160.5 (C); **^{19}F NMR** ($CDCl_3$, 377 MHz) δ ppm -67.91; **GC-MS** (EI) 202 ($[M]^+$, 98%) 183 (5%) 159 (7%) 133 (100%) 118 (13%) 109 (30%) 103 (11%) 89 (16%) 69 (5%) 63 (13%).

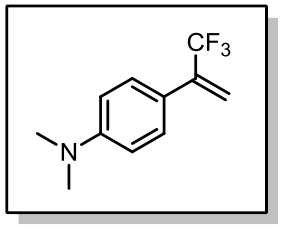

N,N-dimethyl-4-(3,3,3-trifluoroprop-1-en-2-yl)aniline (1.9d) (1.33 g, 95%) was prepared according to the representative procedure for the synthesis of **1.9a** from 2-(4-(dimethylamino)phenyl)-1,1,1-trifluoro-3-(trimethylsilyl)propan-2-ol, **1.8d** (1.99 g, 6.5 mmol, *with the following modification*: Reaction was heated at reflux in DCE for 4.5 h. (b) 0.3 equiv of TMSOTf was used. (c) A silica gel plug was not required. The pure CF_3 alkene was obtained as an orange, crystalline solid (m.p. 49-50 ^{o}C). **^{1}H NMR** ($CDCl_3$, 400 MHz) δ ppm 3.01 (s, 6 H) 5.69 (d, *J* = 1.71 Hz, 1 H) 5.80 (d, *J* = 0.98 Hz, 1 H) 6.73 (d, *J* = 9.05 Hz, 2 H) 7.40 (d, *J* = 8.56 Hz, 2 H); **^{13}C NMR** ($CDCl_3$, 100 MHz) δ ppm 40.5 (CH_3) 112.2 (CH) 116.8 (q, $J_{C\text{-}C\text{-}C\text{-}F}$ = 5.9 Hz, CH_2) 124.1 (q, $J_{C\text{-}F}$ = 274.4 Hz, CF_3) 121.4 (C) 128.3 (CH) 138.7 (q, $J_{C\text{-}C\text{-}F}$ = 29.3 Hz, C) 151.00 (C); **^{19}F NMR** ($CDCl_3$, 377 MHz) δ

ppm -67.52; **GC-MS** (EI) 215 ([M]$^+$, 100%) 199 (19%) 151 (7%) 146 (23%) 130 (11%) 102 (8%) 69 (4%); **HRMS** (ESI+), calcd for $C_{11}H_{12}F_3N$ [M + H]$^+$: 216.1000, found: 216.0984.

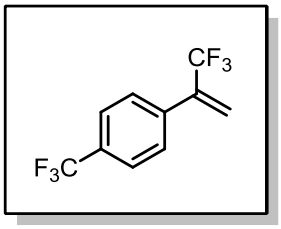

1-(trifluoromethyl)-4-(3,3,3-trifluoroprop-1-en-2-yl)benzene (1.9e) (0.759 g, 63%) was prepared according to the representative procedure for the synthesis of **1.9a** from 1,1,1-trifluoro-2-(4-(trifluoromethyl)phenyl)-3-(trimethylsilyl)propan-2-ol, **1.8e** (1.65 g, 5 mmol) affording the pure CF_3 alkene as a clear, colorless oil. **^{1}H NMR** ($CDCl_3$, 400 MHz) δ ppm 5.85 (q, *J* = 1.47 Hz, 1 H) 6.04 - 6.10 (m, 1 H) 7.55 - 7.61 (m, 2 H) 7.63 - 7.69 (m, 2 H); **^{13}C NMR** ($CDCl_3$, 100 MHz) δ ppm 122.4 (q, $J_{C\text{-}C\text{-}C\text{-}F}$ = 5.9 Hz, CH_2) 123.3 (q, $J_{C\text{-}F}$ = 272.9 Hz, CF_3) 124.2 (q, $J_{C\text{-}F}$ = 272.2 Hz, CF_3) 125.9 (q, $J_{C\text{-}C\text{-}C\text{-}F}$ = 3.7 Hz, CH) 128.2 (d, $J_{C\text{-}C\text{-}C\text{-}C\text{-}F}$ = 1.5 Hz, CH) 131.4 (q, $J_{C\text{-}C\text{-}F}$ = 32.3 Hz, C) 137.4 (C) 138.4 (q, $J_{C\text{-}C\text{-}F}$ = 30.8 Hz, C); **^{19}F NMR** ($CDCl_3$, 377 MHz) δ ppm -68.01 (s, 3 F) -66.03 (s, 3 F); **GC-MS** (EI) 240 ([M]$^+$, 86%) 221 (40%) 201 (4%) 171 (100%) 169 (14%) 151 (95%) 145 (12%) 102 (15%) 75 (12%) 69 (12%).

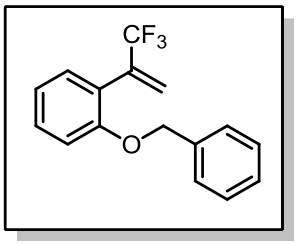

1-(benzyloxy)-2-(3,3,3-trifluoroprop-1-en-2-yl)benzene (1.9f) (1.18g, 85%) was prepared according to the representative procedure for the synthesis of **1.9a** from 2-(2-(benzyloxy)phenyl)-1,1,1-trifluoro-3-(trimethylsilyl)propan-2-ol, **1.8f** (1.84 g, 5 mmol), *with the following modification*: Reaction was stirred for 15 min at room temperature. The pure CF_3 alkene was obtained as a clear, pale yellow oil. **^{1}H NMR** ($CDCl_3$, 400 MHz) δ ppm 5.07 (s, 2 H) 5.64 (d, *J* = 1.19 Hz, 1 H) 6.07 (d, *J* = 1.19 Hz, 1 H) 6.90 - 6.98 (m, 2 H) 7.19 - 7.39 (m, 7 H); **^{13}C NMR** ($CDCl_3$, 100 MHz) δ ppm 70.6 (CH_2) 113.0 (CH) 120.9 (C) 123.5 (q, $J_{C\text{-}F}$ = 273.6 Hz, CF_3) 123.7 (q, $J_{C\text{-}C\text{-}C\text{-}F}$ = 5.1 Hz, CH_2) 124.0 (CH) 127.3 (CH) 128.1 (CH) 128.8 (CH) 130.5 (CH) 131.1 (CH) 136.3 (q, $J_{C\text{-}C\text{-}F}$ = 31.5 Hz, C) 137.2 (CH) 156.8 (C); **^{19}F NMR** ($CDCl_3$, 377 MHz) δ ppm -68.49; **GC-MS** (EI) 279 ([M]$^+$, 7%) 258 (4%) 209 (2%) 186 (5%) 118 (3%) 109 (7%) 91 (100%) 69 (12%); **HRMS** (DART), calcd for $C_{16}H_{13}F_3O$ [M + NH_4]$^+$: 296.1262, found: 296.1279.

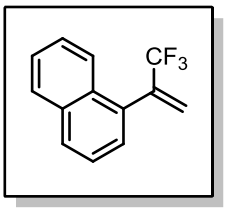

1-(3,3,3-trifluoroprop-1-en-2-yl)naphthalene (1.9g) (1.01 g, 91%) was prepared according to the representative procedure for the synthesis of **1.9a** from 1,1,1-trifluoro-2-(naphthalen-1-yl)-3-(trimethylsilyl)propan-2-ol, **1.8g** (1.56 g, 5 mmol), *with the following modification*: Reaction was stirred for 15 min at room temperature. The pure CF_3 alkene was obtained as a clear, colorless oil. **^{1}H NMR** ($CDCl_3$, 400 MHz) δ ppm 5.72 (d, *J* = 0.98 Hz, 1 H) 6.39 (d, *J* = 1.47 Hz, 1 H) 7.47 - 7.62 (m, 4 H) 7.87 - 7.97 (m, 2 H) 7.98 - 8.06 (m, 1 H); **^{13}C NMR** ($CDCl_3$, 100 MHz) δ ppm 123.5 (q, $J_{C\text{-}F}$ = 273.6 Hz, CF_3) 124.4 (q, $J_{C\text{-}C\text{-}C\text{-}F}$ = 5.9 Hz, CH_2) 125.2 (CH) 125.6 (CH) 126.4 (CH) 126.9 (CH) 127.7 (CH) 128.6 (CH) 129.6 (CH) 131.8 (C) 132.4 (C) 134.0 (C) 137.6 (q, $J_{C\text{-}C\text{-}F}$ = 31.2 Hz, C); **^{19}F NMR** ($CDCl_3$, 377 MHz) δ ppm -69.79; **GC-MS** (EI) 222 ([M]$^+$, 39%) 201 (22%) 183 (7%) 153 (100%) 151 (20%) 126 (6%) 69 (5%).

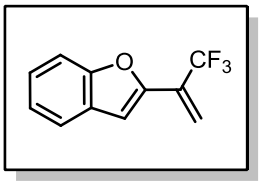

2-(3,3,3-trifluoroprop-1-en-2-yl)benzofuran (1.9i) (0.967 g, 86%) was prepared according to the representative procedure for the synthesis of **1.9a** from 2-(benzofuran-2-yl)-1,1,1-trifluoro-3-(trimethylsilyl)propan-2-ol, **1.8i** (1.60 g, 5.3 mmol), *with the following modification*: Reaction was stirred for 15 min at room temperature. The pure CF_3 alkene was obtained as a clear, colorless oil. **^{1}H NMR** ($CDCl_3$, 500 MHz) δ ppm 6.06 (s, 1 H) 6.36 (s, 1 H) 6.97 (s, 1 H) 7.32 (t, *J* = 7.60 Hz, 1 H) 7.41 (t, *J* = 7.40 Hz, 1 H) 7.55 (d, *J* = 8.20 Hz, 1 H) 7.65 (d, *J* = 7.72 Hz, 1 H); **^{13}C NMR** ($CDCl_3$, 125 MHz) δ ppm 106.5 (q, $J_{C\text{-}C\text{-}C\text{-}C\text{-}F}$ = 1.7 Hz, CH) 111.4 (CH) 118.3 (q, $J_{C\text{-}C\text{-}C\text{-}F}$ = 5.1 Hz, CH_2) 122.8 (q, $J_{C\text{-}F}$ = 272.1 Hz, CF_3) 122.0 (CH) 123.6 (CH) 126.0 (CH) 128.7 (C) 129.7 (q, $J_{C\text{-}C\text{-}F}$ = 32.2 Hz, C) 148.7 (C) 155.0 (C) **^{19}F NMR** ($CDCl_3$, 377 MHz) δ ppm -68.70; **GC-MS** (EI) 212 ($[M]^+$, 100%) 183 (3%) 143 (54%) 133 (7%) 115 (49%) 89 (9%) 69 (6%); **HRMS** (DART), calcd for $C_{11}H_7F_3O$ $[M]^+$: 212.0449, found: 212.0443.

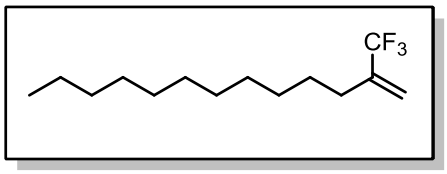

2-(trifluoromethyl)tridec-1-ene (1.9j) (1.10 g, 88%) was prepared according to the representative procedure for the synthesis of **1.9a** from 1,1,1-trifluoro-2-((trimethylsilyl)methyl)tridecan-2-ol, **1.8j** (1.70 g, 5 mmol) affording the pure CF_3 alkene as a clear, colorless oil. **^{1}H NMR** ($CDCl_3$, 500 MHz) δ ppm 0.89 (t, *J* = 7.10 Hz, 3 H) 1.21 - 1.38 (m, 16 H) 1.47 - 1.56 (m, 2 H) 2.19 (t, *J* = 7.80 Hz, 2 H) 5.29 (q, *J* = 1.40 Hz, 1 H) 5.65 (d, *J* = 1.42 Hz, 1 H); **^{13}C NMR** ($CDCl_3$, 125 MHz) δ ppm 14.4 (CH_3) 23.0 (CH_2) 27.7 (CH_2) 29.4 (CH_2) 29.7 (CH_2) 29.7 (CH_2) 29.7 (CH_2) 29.9 (CH_2) 29.9 (CH_2) 30.0 (CH_2) 32.2 (CH_2) 117.5 (q, $J_{C\text{-}C\text{-}C\text{-}F}$ = 5.9 Hz, CH_2) 124.2 (q, $J_{C\text{-}F}$ = 273.8 Hz, CF_3) 139.1 (q, $J_{C\text{-}C\text{-}F}$ = 28.8 Hz, C); **^{19}F NMR** ($CDCl_3$, 377 MHz) δ ppm -71.75; **GC-MS** (EI) 250 ($[M]^+$, 2%) 194 (4%) 165 (7%) 131 (7%) 111 (30%) 97 (49%) 83 (48%) 70 (65%) 57 (91%) 43 (100%); **HRMS** (DART), calcd for $C_{14}H_{25}F_3$ $[M - C_4H_9]^+$: 193.1199, found: 193.1233; FTIR (cm^{-1}, neat, ATR) = 2926, 2855, 1467, 1168, 1125, 937, 792, 637.

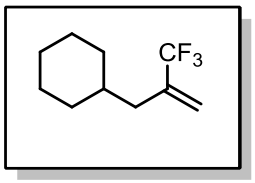

(2-(trifluoromethyl)allyl)cyclohexane (1.9k) (0.622 g, 65%) was prepared according to the representative procedure for the synthesis of **1.9a** from 3-cyclohexyl-1,1,1-trifluoro-2-((trimethylsilyl)methyl)propan-2-ol, **1.8k** (1.42 g, 5 mmol) affording the pure CF_3 alkene as a clear, colorless oil. **^{1}H NMR** ($CDCl_3$, 400 MHz) δ ppm 0.82 - 0.93 (m, 2 H) 1.10 - 1.31 (m, 3 H) 1.46 - 1.57 (m, 1 H) 1.63 - 1.79 (m, 5 H) 2.08 (d, *J* = 7.25 Hz, 2 H) 5.27 (s, 1 H) 5.69 (s, 1 H); **^{13}C NMR** ($CDCl_3$, 100 MHz) δ ppm 26.4 (CH_2) 26.7 (CH_2) 33.3 (CH_2) 35.9 (CH) 38.1 (CH_2) 119.1 (q, $J_{C\text{-}C\text{-}C\text{-}F}$ = 5.9 Hz, CH_2) 124.2 (q, $J_{C\text{-}F}$ = 273.8 Hz, CF_3) 137.2 (q, $J_{C\text{-}C\text{-}F}$ = 28.8 Hz, C); **^{19}F NMR** ($CDCl_3$, 377 MHz) δ ppm -71.39; **GC-MS** (EI) 192 ($[M]^+$, 3%) 153 (3%) 133 (6%) 127 (2%) 115 (3%) 109 (6%) 83 (100%) 69 (4%) 55 (70%) 41 (22%); **HRMS** (DART), calcd for $C_{10}H_{15}F_3$ $[M - C_3H_4 + H]^+$: 153.0891, found: 153.0917; FTIR (cm^{-1}, neat, ATR) = 2926, 2854, 1450, 1167, 1123, 936, 842.

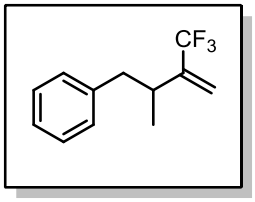

(2-methyl-3-(trifluoromethyl)but-3-en-1-yl)benzene (1.9l) (0.900 g, 84%) was prepared according to the representative procedure for the synthesis of **1.9a** from 1,1,1-trifluoro-3-methyl-4-phenyl-2-((trimethylsilyl)methyl)butan-2-ol, **1.8l** (1.52 g, 5 mmol) affording the pure CF_3 alkene as a clear, colorless oil. **^{1}H NMR** ($CDCl_3$, 400 MHz) δ ppm 1.17 (d, *J* = 6.85 Hz, 3 H) 2.64 (dd, *J* = 13.33, 8.93 Hz, 1 H) 2.74 - 2.84 (m, 1 H) 3.03 (dd, *J* = 13.45, 5.38 Hz, 1 H) 5.39 - 5.44 (m, 1 H) 5.81 (q, *J* = 1.47 Hz, 1 H) 7.21 - 7.26 (m, 2 H) 7.26 - 7.31 (m, 1 H) 7.33 - 7.39 (m, 2 H); **^{13}C NMR** ($CDCl_3$, 100 MHz) δ ppm 19.8 (CH_3) 35.7 (CH) 42.9 (CH_2) 117.7 (q, $J_{C\text{-}F}$ = 5.9 Hz, CH_2) 124.5 (q, $J_{C\text{-}F}$ = 274.4 Hz, CF_3) 126.5 (CH) 128.6 (CH) 129.5 (CH) 140.0 (C) 143.7 (q, $J_{C\text{-}C\text{-}F}$ = 27.9 Hz, C); **^{19}F NMR** ($CDCl_3$, 377 MHz) δ ppm -70.44; **GC-MS** (EI) 214 ($[M]^+$, 11%) 175 (5%) 128 (6%) 91 (100%) 69 (7%); **HRMS** (DART), calcd for $C_{12}H_{13}F_3$ $[M + H]^+$: 215.1048, found: 215.1032.

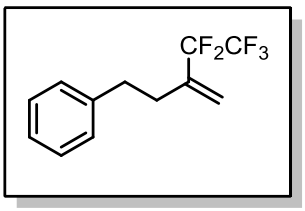

(4,4,5,5,5-pentafluoro-3-methylenepentyl)benzene (1.9n) (0.772 g, 75%) was prepared according to the representative procedure for the synthesis of **1.9a** from 1,1,1,2,2-pentafluoro-5-phenyl-3-((trimethylsilyl)methyl)pentan-3-ol, **1.8n** (1.40 g, 4.11 mmol), *with the following modification*: Reaction was heated for 4 h at reflux in DCE. The pure CF_3 alkene was obtained as a clear, colorless oil. **^{1}H NMR** ($CDCl_3$, 400 MHz) δ ppm 2.58 (t, *J* = 8.07 Hz, 2 H) 2.90 (t, *J* = 7.80 Hz, 2 H) 5.54 (s, 1 H) 5.78 (s, 1 H) 7.23 - 7.31 (m, 3 H) 7.33 - 7.40 (m, 2 H); **^{13}C NMR** ($CDCl_3$, 100 MHz) δ ppm 31.7 (CH_2) 34.5 (CH_2) 113.7 (tq, $J_{C\text{-}F}$ = 253.1, $J_{C\text{-}C\text{-}F}$ = 37.4 Hz, CF_2) 119.5 (qt, $J_{C\text{-}F}$ = 286.8, $J_{C\text{-}C\text{-}F}$ = 38.9 Hz, CF_3) 121.3 (t, $J_{C\text{-}C\text{-}C\text{-}F}$ = 8.8 Hz, CH_2) 126.6 (CH) 128.7 (CH) 128.8 (CH) 137.6 (t, $J_{C\text{-}C\text{-}F}$ = 21.3 Hz, C) 140.8 (C); **^{19}F NMR** ($CDCl_3$, 377 MHz) δ ppm -119.29 (s, 2 F) -86.87 (s, 3 F); **GC-MS** (EI) 250 ($[M]^+$, 25%) 211 (5%) 191 (3%) 91 (100%) 69 (3%) 65 (13%); **HRMS** (DART), calcd for $C_{12}H_{11}F_5$ $[M - C_5H_6F_5 - H]^+$: 91.0548, found: 91.0579; FTIR (cm^{-1}, neat, ATR) = 3066, 3030, 2931, 2362, 1605, 1453, 1332, 1202, 1122, 1023, 940, 698.

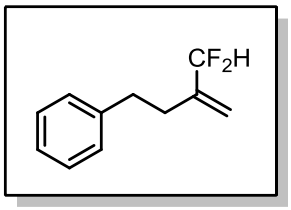

(3-(difluoromethyl)but-3-en-1-yl)benzene (1.9o) (0.838 g, 92%) was prepared according to the representative procedure for the synthesis of **1.9a** from 1,1-difluoro-4-phenyl-2-((trimethylsilyl)methyl)butan-2-ol, **1.8o** (1.36 g, 5 mmol), *with the following modification*: Reaction was stirred for 15 min at room temperature. The pure CF_3 alkene was obtained as a clear, colorless oil. **^{1}H NMR** ($CDCl_3$, 400 MHz) δ ppm 2.58 (t, *J* = 8.07 Hz, 2 H) 2.92 (t, *J* = 8.30 Hz, 2 H) 5.26 - 5.31 (m, 1 H) 5.44 (s, 1 H) 6.09 (t, *J* = 56.00 Hz, 1 H) 7.26 - 7.33 (m, 3 H) 7.34 - 7.42 (m, 2 H); **^{13}C NMR** ($CDCl_3$, 100 MHz) δ ppm 30.5 (t, $J_{C\text{-}C\text{-}C\text{-}F}$ = 1.5 Hz, CH_2) 34.2 (CH_2) 117.8 (q, $J_{C\text{-}F}$ = 237.7 Hz, CF_2H) 117.9 (t, *J* = 10.00 Hz, CH_2) 126.4 (CH) 128.7 (CH) 128.7 (CH) 141.4 (C) 142.3 (t, *J* = 20.5 Hz, C); **^{19}F NMR** ($CDCl_3$, 377 MHz) δ ppm -118.44 (d, *J* = 55.86 Hz); **GC-MS** (EI) 182 ($[M]^+$, 20%) 128 (3%) 115 (3%) 104 (2%) 91 (100%) 77 (4%) 65 (16%) 51 (8%).

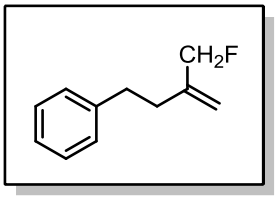

(3-(fluoromethyl)but-3-en-1-yl)benzene (1.9p) (0.709 g, 72%) was prepared according to the representative procedure for the synthesis of **1.9a** from 1,1-difluoro-4-phenyl-2-((trimethylsilyl)methyl)butan-2-ol, **1.8p** (1.53 g, 6 mmol), with the following modifications: (a) Reaction

was stirred for 15 min at room temperature. (b) Further purification was accomplished by FCC utilizing hexanes as an elutant. The pure CF_3 alkene was obtained as a clear, colorless oil. **^{1}H NMR** ($CDCl_3$, 400 MHz) δ ppm 2.45 (t, *J* = 7.90 Hz, 2 H) 2.83 (t, *J* = 8.50 Hz, 2 H) 4.83 (dq, *J* = 47.54, 0.60 Hz, 2 H) 5.04 (ddt, *J* = 2.03, 1.35, 0.69, Hz, 1 H) 5.15 (qspt, *J* = 2.00, 1.30 Hz, 1 H) 7.19 - 7.25 (m, 3 H) 7.28 - 7.35 (m, 2 H); **^{13}C NMR** ($CDCl_3$, 100 MHz) δ ppm 34.2 (d, $J_{C\text{-}C\text{-}C\text{-}F}$ = 1.9 Hz, CH_2) 34.3 (CH_2) 85.7 (d, $J_{C\text{-}F}$ = 167.8 Hz, CH_2F) 113.4 (d, $J_{C\text{-}C\text{-}C\text{-}F}$ = 10.4 Hz, CH_2) 126.2 (CH) 128.6 (CH) 128.6 (CH) 141.8 (C) 144.4 (d, $J_{C\text{-}C\text{-}F}$ = 14.5 Hz, CH); **^{19}F NMR** ($CDCl_3$, 377 MHz) δ ppm -218.52 (td, *J* = 47.70); **GC-MS** (EI) 164 ([M]$^+$, 100%) 144 (6%) 131 (22%) 129 (19%) 115 (14%) 104 (17%) 77 (13%) 59 (3%); **HRMS** (DART), calcd for $C_{11}H_{13}F$ [M - F]$^+$: 145.1017, found: 145.1023.

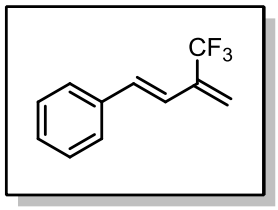

(E)-(3-(trifluoromethyl)buta-1,3-dien-1-yl)benzene (1.9q) (4.09 g, 85%) was prepared according to the representative procedure for the synthesis of **1.9a** from (E)-1,1,1-trifluoro-4-phenyl-2-((trimethylsilyl)methyl)but-3-en-2-ol, **1.8q** (7.00 g, 24.3 mmol), *with the following modification*: Reaction was stirred for 15 min at room temperature. The pure CF_3 alkene was obtained as a clear, colorless liquid. ^{1}H NMR ($CDCl_3$, 400 MHz) δ ppm 5.70 (d, *J* = 30.64 Hz, 1 H) 6.66 (d, *J* = 16.36 Hz, 1 H) 6.89 (d, *J* = 16.66 Hz, 1 H) 7.23 - 7.47 (m, 6 H); ^{13}C NMR ($CDCl_3$, 100 MHz) δ ppm 119.4 (q, $J_{C\text{-}C\text{-}C\text{-}F}$ = 5.9 Hz, CH2) 121.8 (CH) 123.4 (q, $J_{C\text{-}F}$ = 274.4 Hz, CF_3) 127.1 (CH) 128.8 (CH) 129.0 (CH) 133.2 (CH) 136.8 (q, $J_{C\text{-}C\text{-}F}$ = 30.1 Hz, C) 136.5 (C); ^{19}F NMR ($CDCl_3$, 377 MHz) δ ppm -68.91; GC-MS (EI) 198 ([M]$^+$, 33%) 177 (24%) 159 (5%) 129 (100%) 127 (22%) 102 (7%) 77 (8%) 69 (7%) 51 (9%).

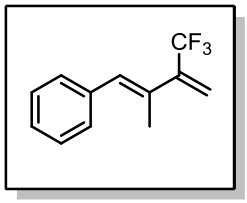

(E)-(2-methyl-3-(trifluoromethyl)buta-1,3-dien-1-yl)benzene (1.9r) (0.914 g, 86%) was prepared according to the representative procedure for the synthesis of **1.9a** from (E)-1,1,1-trifluoro-3-methyl-4-phenyl-2-((trimethylsilyl)methyl)but-3-en-2-ol, **1.8r** (1.51 g, 5 mmol), *with the following modification*: Reaction was stirred for 15 min at room temperature. The pure CF_3 alkene was obtained as a clear, colorless oil. **^{1}H NMR** ($CDCl_3$, 500 MHz) δ ppm 2.08 (s, 3 H) 5.68 (d, *J* = 1.58 Hz, 1 H) 5.87 (s, 1 H) 6.86 (s, 1 H) 7.28 - 7.35 (m, 3 H) 7.38 - 7.43 (m, 2 H); **^{13}C NMR** ($CDCl_3$, 125 MHz) δ ppm 16.5 (CH_3) 119.0 (q, $J_{C\text{-}C\text{-}C\text{-}F}$ = 5.9 Hz, CH_2) 123.7 (q, $J_{C\text{-}F}$ = 275.5 Hz, CF_3) 127.4 (CH) 128.5 (CH) 129.6 (CH) 130.8 (CH) 131.4 (C) 137.4 (C) 141.4 (q, $J_{C\text{-}C\text{-}F}$ = 28.8 Hz, C); **^{19}F NMR** ($CDCl_3$, 377 MHz) δ ppm -66.26; **GC-MS** (EI) 212 ([M]$^+$, 23%) 197 (31%) 191 (12%) 177 (59%) 143 (100%) 128 (92%) 115 (31%) 91 (9%) 69 (7%); **HRMS** (DART), calcd for $C_{12}H_{11}F_3$ [M + H]$^+$: 213.0891, found: 213.0900.

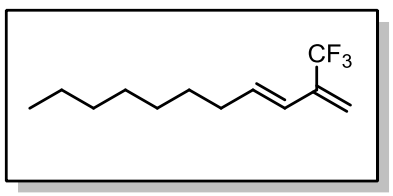

(E)-2-(trifluoromethyl)dodeca-1,3-diene (1.9s) (0.936 g, 85%) was prepared according to the representative procedure for the synthesis of **1.9a** from (E)-1,1,1-trifluoro-2-((trimethylsilyl)methyl)dodec-3-en-2-ol, **1.8s** (1.55 g, 5 mmol), *with the following modification*: Reaction was stirred for 1 h at room temperature. The pure CF_3 alkene was obtained as clear, colorless oil. **^{1}H NMR** ($CDCl_3$, 400 MHz) δ ppm 0.85 - 0.94 (m, 3 H) 1.30 (s, 8 H) 1.38 - 1.50

(m, 2 H) 2.14 (q, J = 6.85 Hz, 2 H) 5.43 (s, 1 H) 5.59 (s, 1 H) 5.93 - 6.12 (m, 2 H); **^{13}C NMR** ($CDCl_3$, 100 MHz) δ ppm 14.3 (CH_3) 23.0 (CH_2) 29.2 (CH_2) 29.5 (CH_2) 32.1 (CH_2) 33.6 (CH_2) 117.4 (q, $J_{C\text{-}C\text{-}C\text{-}F}$ = 5.4 Hz, CH_2) 123.5 (q, $J_{C\text{-}F}$ = 274.4 Hz, CF_3) 123.3 (CH) 136.4 (CH) 136.9 (q, $J_{C\text{-}C\text{-}F}$ = 29.7 Hz, C); **^{19}F NMR** ($CDCl_3$, 377 MHz) δ ppm -69.48; **GC-MS** (EI) 234 ($[M]^+$, 2%) 220 (24%) 191 (13%) 178 (15%) 164 (46%) 149 (40%) 136 (35%) 127 (21%) 122 (23%) 115 (85%) 109 (33%) 95 (100%) 81 (35%) 69 (82%) 56 (86%) 41 (94%); **HRMS** (DART), calcd for $C_{13}H_{21}F_3$ $[M - C_4H_9]^+$: 163.0729, found: 163.0745; FTIR (cm^{-1}, neat, ATR) = 2957, 2927, 2855, 1467, 1305, 1207, 1165, 967.

Application Reactions Utilizing α-CF_3 Alkenes

Cyclopropanation

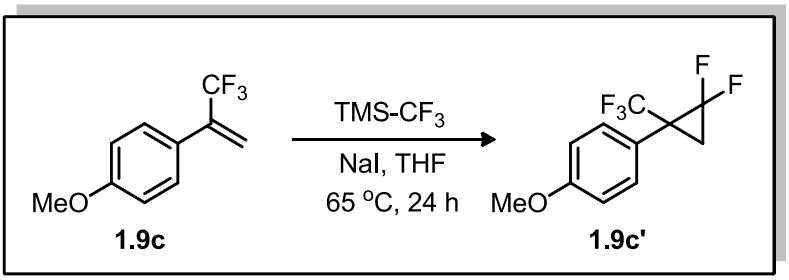

1-(2,2-difluoro-1-(trifluoromethyl)cyclopropyl)-4-methoxybenzene (1.9c′) This protocol is a modification of the procedure outlined by Prakash.[51] To a 25 mL screw top vial equipped with stirbar was added **1.9c** (1.01 g, 5 mmol, 1 equiv), NaI (0.150, 1 mmol, 0.2 equiv), and anhydrous THF (7.2 mL, 0.7 M in the alkene). The contents of the vial were stirred for five minutes and after this time $TMSCF_3$ (1.78 g, 12.5 mmol, 2.5 equiv) was added all at once to the vial. The vial was sealed and heated to 65 °C. Progress of the reaction was monitored by GC/MS. After 12 h the reaction appeared to stall and the vial was (after cooling) charged with more NaI (0.075 g, 0.5 mmol, 0.1 equiv) and $TMSCF_3$ (0.355 g, 2.5 mmol. 0.5 equiv). The solution was heated to 65 °C and after 6 hours was judged to be complete. The solution was cooled to room temperature and the solvent was removed *in vacuo* by rotary evaporation[154] to give an off-yellow semi-solid. The solid material was taken up in Et_2O (≈100 mL) and deionized water (≈ 100 mL) and transferred to a separatory funnel. The phases were separated and the aqueous layer was extracted with Et_2O (2 x 50 mL). The combine organic layers were washed with saturated aqueous sodium thiosulfate (≈ 100 mL), saturated aqueous $NaHCO_3$ (≈ 100 mL), deionized water (≈ 100 mL), and finally with brine (≈ 150 mL). The organic layer was dried with Na_2SO_4 and the solvent was removed *in vacuo* by rotary evaporation. The crude product was adhered to silica gel using ≈ 1.5 weight equivalents silica gel (relative to the theoretical yield). The dry-packed material was gently added atop a silica gel plug. The plug was eluted with a 95:5 by volume mixture of Hex:EtOAc (2-3 column volumes). The solvent was removed *in vacuo* by rotary evaporation affording the pure cyclopropane **1.9c′** (1.12 g, 89%) as a clear, yellow oil.

[154] Note that due to the volatility of highly fluorinated species, it is ***imperative*** that higher pressures (40 mmHg or greater) and low water bath temperature (less than 32 °C) be used during rotary evaporation to ensure good yields.

^{1}H NMR ($CDCl_3$, 400 MHz) δ ppm 1.85 - 1.94 (m, 1 H) 2.29 (s, 1 H) 3.82 (s, 3 H) 6.90 - 6.96 (m, 2 H) 7.35 (d, *J* = 8.80 Hz, 2 H); **^{13}C NMR** ($CDCl_3$, 100 MHz) δ ppm 20.1 (ddt, $J_{C\text{-}C\text{-}F}$ = 10.8, 7.2, 3.1, Hz, CH_2) 36.4 (qdd, *J* = 33.9, 12.7, 9.9 Hz, C) 55.3 (CH_3) 109.9 (ddq, *J* = 292.0, 285.3, 3.1, Hz, CF_2) 114.5 (CH) 121.2 (C) 124.0 (qd, $J_{C\text{-}F}$ = 275.1, 2.9 Hz, CF_3) 132.4 (d, $J_{C\text{-}C\text{-}C\text{-}C\text{-}F}$ = 2.2 Hz, CH) 160.8 (C); **^{19}F NMR** ($CDCl_3$, 377 MHz) δ ppm -141.23 (dquind, *J* = 160.76, 13.60, 4.08 Hz, 1 F) -132.06 (dqd, *J* = 160.77, 7.50, 4.10 Hz, 1 F) -69.82 (dd, *J* = 13.63, 2.72 Hz, 3 F); **GC-MS** (EI) 252 ($[M]^+$, 29%) 231 (4%) 202 (7%) 183 (100%) 169 (11%) 163 (26%) 151 (9%) 145 (9%) 133 (30%) 109 (8%) 69 (4%); **HRMS** (ESI+), calcd for $C_{11}H_9F_5O$ $[M + H]^+$: 253.0652, found: 253.0662.

Bromination Elimination

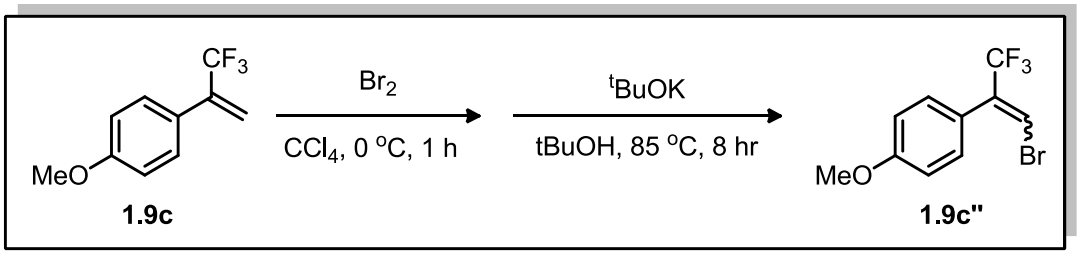

1-(1-bromo-3,3,3-trifluoroprop-1-en-2-yl)-4-methoxybenzene (1.9c″) This protocol is a modification of the procedure outlined by Zuilhof.[52] To a 50 mL one neck round bottom flask equipped with stirbar was added **1.9c** (1.21 g, 6 mmol, 1 equiv) and CCl_4 (6 mL, 1 M in the alkene). The flask was sealed with a rubber septum and placed under an N_2 atmosphere via an inlet needle. The flask was cooled to 0 °C in an ice bath and, after 5 minutes, Br_2 (1.055 g, 0.34 mL, 6.6 mmol, 1.1 equiv) was added to the flask dropwise via a syringe. Five minutes after complete addition, the flask was allowed to warm to room temperature over ten minutes. After this time, the solvent was removed *in vacuo* by rotary evaporation. The crude semi-solid material was taken up in ^{t}BuOH (21 mL) and stirred for five minutes. After this time, KO^{t}Bu (0.741 g, 6.6 mmol, 1.1 equiv) was added to the flask and was refluxed for 1 hour. After this time the reaction appeared to have stalled[155] and an additional loading of KO^{t}Bu (0.741 g, 6.6 mmol, 1.1 equiv) was added. The reaction was refluxed for an additional six hours and complete conversion was achieved. The solution was then cooled to room temperature and deionized water (≈ 20 mL) was added to the reaction mixture. The solution was transferred to a separatory funnel and extracted with Et_2O (3 x 100 mL). The combine organic layers were washed with deionized water (2 x 100 mL) and brine (≈ 150 mL). The organic layer was dried with Na_2SO_4 and the solvent was removed *in vacuo*, giving the pure bromide **1.9c″** (1.32 g, 78%) as a light brown oil.

^{1}H NMR ($CDCl_3$, 400 MHz) (*E* isomer) δ ppm 3.85 (s, 3 H) 6.94 - 6.99 (m, 2 H) 7.25 - 7.29 (m, 2 H) 7.30 (q, *J* = 1.71 Hz, 1 H); **^{13}C NMR** ($CDCl_3$, 100 MHz) (*E* isomer) δ ppm 55.4 (CH_3) 114.3 (C) 116.6 (q, $J_{C\text{-}C\text{-}C\text{-}F}$ = 7.1 Hz, CH) 122.7 (q, $J_{C\text{-}F}$ = 275.8 Hz, CF_3) 123.9 (CH) 130.8 (C) 136.3 (q, $J_{C\text{-}C\text{-}F}$ = 30.1 Hz, C) 160.6 (C); **^{19}F NMR** ($CDCl_3$, 377 MHz) (*E* isomer) δ ppm -68.15; **GC-MS** (EI) (*E* isomer) 281($[M]^+$, 100%) 279 (99%) 211 (24%) 201 (10%) 186 (15%) 181 (20%) 169 (10%) 158 (39%) 151 (12%) 138 (13%) 117 (24%) 89 (35%) 75 (10%) 69 (13%) 63

[155] Reaction progress determined by ^{1}H NMR.

(21%); **^{1}H NMR** ($CDCl_3$, 400 MHz) (*Z* isomer) δ ppm 3.83 (s, 3 H) 6.77 (s, 1 H) 6.90 (d, *J* = 8.80 Hz, 2 H) 7.20 - 7.24 (m, 2 H); **^{13}C NMR** ($CDCl_3$, 100 MHz) (*Z* isomer) ppm 55.5 (CH_3) 113.0 (q, $J_{C\text{-}C\text{-}C\text{-}F}$ = 3.7 Hz, CH) 114.2 (CH) 122.9 (q, $J_{C\text{-}F}$ = 275.8 Hz, CF_3) 123.9 (CH) 129.9 (C) 137.2 (q, $J_{C\text{-}C\text{-}F}$ = 31.5 Hz, C) 160.6 (C); **^{19}F NMR** ($CDCl_3$, 377 MHz) (*Z* isomer) δ ppm -62.87; **GC-MS** (EI) (*Z* isomer) 281 ($[M]^+$, 99%) 279 (100%) 213 (18%) 211 (13%) 201 (7%) 186 (11%) 181 (15%) 169 (7%) 158 (29%) 151 (9%) 138 (9%) 117 (17%) 89 (26%) 75 (8%) 69 (9%) 63 (16%); **HRMS** (ESI+), calcd for $C_{10}H_8BrF_3O$ $[M + H]^+$: 280.9789, found: 280.9802.

gem-Difluoroalkene Synthesis

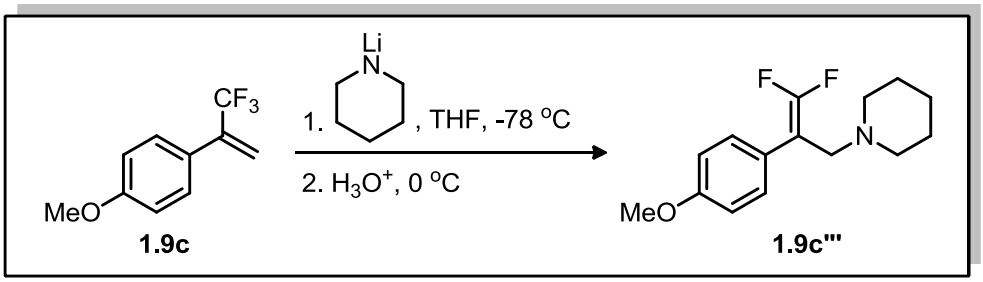

1-(3,3-difluoro-2-(4-methoxyphenyl)allyl)piperidine (1.9c′′′) This protocol is a modification of the procedure outlined by Bonnet-Delpon.[53] To a flamed dried flask equipped with stirbar, rubber septum, and N_2 inlet needle, was added piperidine (0.685 g, 0.795 mL, 8.05 mmol, 1.15 equiv) and anhydrous THF (47 mL, 0.15 M in the olefin). The flask was cooled to -78 °C *via* a dry ice/acetone bath and, after cooling for ten minutes, a 2.5 M solution of *n*-BuLi (3.2 mL, 8.05 mmol, 1.15 equiv) in hexanes was added dropwise to the flask over five minutes. The solution was allowed to stir at -78 °C for 1 h and gradually became cloudy and white. After this time, **1.9c** (1.42 g, 7 mmol, 1 equiv) was added to the flask dropwise over five minutes. The solution was allowed to stir at -78 °C for 1 h and, after this time was warmed to 0 °C in an ice-water bath. The solution was stirred at 0 °C for 1 h and then was poured into a separatory funnel containing saturated aqueous NH_4Cl (≈ 100 mL). The biphasic mixture was diluted with Et_2O (≈ 100 mL) and the layers were separated. The aqueous layer was extracted with Et_2O (3 x 50 mL) and the combine organic layers were washed with deionized water (≈ 100 mL), followed by brine (≈ 150 mL). The combine organic layers were dried with Na_2SO_4. The solvent was removed *in vacuo* to give the crude difluoroalkene as an orange-tinged oil. Further purification was accomplished by FCC (gradient Hex to 7:3 Hex:EtOAc) to give the pure difluoroalkene (1.17 g, 63%) as a light yellow-orange oil.

^{1}H NMR ($CDCl_3$, 400 MHz) δ ppm 1.41 (br. sxt, *J* = 4.90 Hz, 2 H) 1.53 (quin, *J* = 5.56 Hz, 4 H) 2.38 (br. t, *J* = 4.70 Hz, 4 H) 3.22 (dd, *J* = 3.07, 1.75 Hz, 2 H) 3.81 (s, 3 H) 6.88 (dt, *J* = 8.81, 2.90 Hz, 2 H) 7.43 (dd, *J* = 8.86, 1.07 Hz, 2 H); **^{13}C NMR** ($CDCl_3$, 100 MHz) δ ppm 24.6 (CH_2) 26.2 (CH_2) 54.2 (CH_2) 55.3 (CH_2) 56.5 (d, $J_{C\text{-}C\text{-}C\text{-}F}$ = 3.9 Hz, CH_2) 89.4 (dd, $J_{C\text{-}C\text{-}F}$ 18.7, 11.8 Hz, C) 113.9 (CH) 126.6 (t, $J_{C\text{-}C\text{-}C\text{-}F}$ = 3.5 Hz, C) 129.7 (t, $J_{C\text{-}C\text{-}C\text{-}C\text{-}F}$ = 3.4 Hz, CH) 155.3 (dd, $J_{C\text{-}F}$ = 292.1, 288.0 Hz, CF_2) 158.9 (C); **^{19}F NMR** ($CDCl_3$, 377 MHz) δ ppm -93.19 (d, *J* = 39.51 Hz, 1 F) -92.88 (d, *J* = 39.51 Hz, 1 F); **GC-MS** (EI) 267 ($[M]^+$, 4%) 224 (1%) 184 (62%) 169 (4%) 151 (4%) 140 (5%) 133 (21%) 118 (5%) 98 (100%) 70 (5%); **HRMS** (ESI+), calcd for $C_{15}H_{19}F_2NO$ $[M + H]^+$: 268.1513, found: 268.1536.

Dihydroxylation

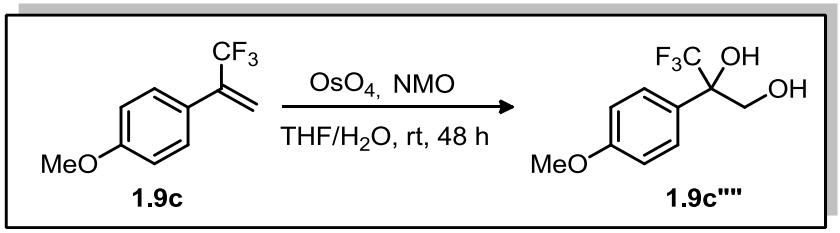

3,3,3-trifluoro-2-(4-methoxyphenyl)propane-1,2-diol (1.9c′′′′) To a 50 mL one neck round bottom flask was added **1.9c** (1.21 g, 6 mmol, 1 equiv), THF (4.5 mL), and deionized water (1.5 mL). The flask was cooled to 0 ^{o}C in an ice bath. After cooling for ten minutes, 50 % w/w NMO in H_2O (2.76 g, 12 mmol, 2 equiv) was added to flask followed by 4% w/w OsO_4 in H_2O (3.814 g, 3.37 mL, 0.6 mmol, 0.1 equiv). Five minutes after this addition, the ice bath was removed and the solution was allowed to stir at room temperature overnight. After 24 h, the reaction appeared to have stalled[155] and an additional loading of NMO (2.76 g, 12 mmol, 2 equiv) and OsO_4 (3.814 g, 3.37 mL, 0.6 mmol, 0.1 equiv) was added. The reaction was stirred for an additional 24 h and after this time was judged to be complete. The solution was transferred to a separatory funnel and diluted with deionized water (≈ 100 mL) and Et_2O (≈ 100 mL). The phases were separated and the aqueous layer was extracted with Et_2O (3 x 100 mL). The combine organic layers were washed with brine (≈ 150 mL) and dried with Na_2SO_4. The solvent was removed *in vacuo* to give the crude diol as a thick, dark brown oil. The crude product was adhered to silica gel using ≈ 1.5 weight equivalents silica gel (relative to the theoretical yield). The dry-packed material was gently added atop a SiO_2 plug. The plug was eluted with EtOAc. The solvent was removed *in vacuo* by rotary evaporation affording the pure diol **1.9c′′′′** (1.20 g, 85%) as a clear, brown oil.

^{1}H NMR ($CDCl_3$, 400 MHz) δ ppm 3.82 (s, 3 H) 3.88 (dd, *J* = 11.98, 1.47 Hz, 1 H) 4.25 (d, *J* = 11.98 Hz, 1 H) 6.89 - 6.97 (m, 2 H) 7.48 (d, *J* = 8.56 Hz, 2 H); **^{13}C NMR** ($CDCl_3$, 100 MHz) δ ppm 55.5 (CH_3) 65.0 (q, $J_{C\text{-}C\text{-}C\text{-}F}$ = 1.5 Hz, CH_2) 76.3 (q, $J_{C\text{-}C\text{-}F}$ = 27.9 Hz, C) 114.2 (CH) 125.4 (q, $J_{C\text{-}F}$ = 286.1 Hz, CF_3) 127.5 (CH) 127.7 (q, $J_{C\text{-}C\text{-}C\text{-}F}$ = 1.5 Hz, C) 160.2 (C); **^{19}F NMR** ($CDCl_3$, 377 MHz) δ ppm -80.64; **GC-MS** (EI) 236 ($[M]^+$, 16%) 205 (100%) 135 (89%) 121 (13%) 108 (21%) 92 (10%) 77 (15%) 69 (3%); **HRMS** (ESI+), calcd for $C_{10}H_{11}F_3O_3$ $[M + NH_4]^+$: 254.1004, found: 254.1022.

Appendix III: *Quantum Chemical Calculation Details*

GENERAL CALCULATION DETAILS FOR CF_3 CYCLOPROPANE SECTION

Quantum chemical calculations were performed using Gaussian 09.[58] All optimized geometries were calculated using B3LYP[77], a hybrid density functional, with the 6-31+G(d) basis set[78]. For γ-stannyl systems, geometry optimizations were carried out using B3LYP and a mixed basis set of LANL2DZ[79] for Sn and 6-31+G(d) for all other atoms. This modified calculation was employed to more accurately describe the electronic nature of the γ-stannyl group. The addition of diffuse functions to the double split-valence basis set ensured an adequate description of the charged systems and the effect of the $-CF_3$ group. Stationary points were characterized by frequency calculations at 298 K, with structures at energy minima showing no negative frequencies and transition-states showing one negative frequency. Intrinsic reaction coordinate (IRC) calculations followed by optimization and frequency calculation were performed on transition state structures to connect the two respective ground states. Thermal energies, enthalpies and Gibbs free energies were corrected using the appropriate thermodynamic correction factor. Solvation energies were evaluated using a self-consistent field (SCRF) using the polarization continuum model (PCM)[81] model. All energetic values shown are in kcal mol^{-1}; bond lengths are reported in Ångstroms (Å), bond and pyramidalization angles in degrees (˚). Figures were generated using CYLView.[82]

Details of Kinetic Isotope Studies

Table 22: Energies of methyl system stationary points used in the theoretically derived KIE

System	E^a	ΔE
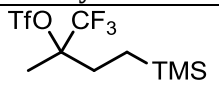	-1170160.858	-
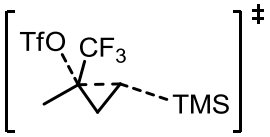	-1170141.649	19.20869
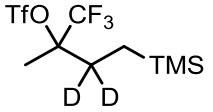	-1170165.159	-
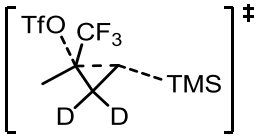	-1170145.962	19.19677

[a]Sum of electronic and zero point energies (E, in kcal mol^{-1}, solvent = CF_3CH_2OH) using B3LYP/6-31+G(d).

Table 23: Energies of phenyl system stationary points used in the theoretically derived KIE

System	E^a	ΔE
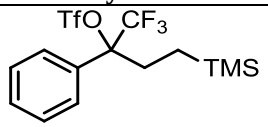	-1290442.213	-
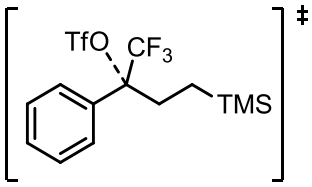	-1290434.513	7.700169
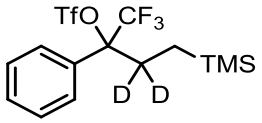	-1290446.536	-
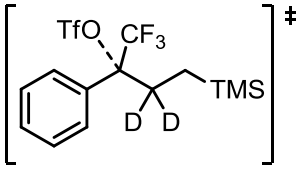	-1290438.86	7.675696

[a]Sum of electronic and zero point energies (E, in kcal mol^{-1}, solvent = CF_3CH_2OH) using B3LYP/6-31+G(d).

Derived from the Arrhenius equation:

$$\frac{k(\mathrm{H})}{k(\mathrm{D})} = \mathbf{e}^{\left(\frac{\Delta E(\mathrm{D}) - \Delta E(\mathrm{H})}{\mathrm{RT}}\right)}$$

For methyl system (Data provided in Table 22):

$$\frac{k(\mathrm{H})}{k(\mathrm{D})} = \mathbf{e}^{\left(\frac{\mathbf{19.19677 - 19.20869}}{\mathbf{0.0019872041 * 298.15}}\right)}$$

$$\frac{k(\mathrm{H})}{k(\mathrm{D})} = \mathbf{0.980}$$

EXPERIMENTAL VALUE = 1.00

For phenyl system (Data provided in Table 23):

$$\frac{k(\mathrm{H})}{k(\mathrm{D})} = \mathbf{e}^{\left(\frac{\mathbf{7.675696 - 7.700169}}{\mathbf{0.0019872041 * 298.15}}\right)}$$

$$\frac{k(\mathrm{H})}{k(\mathrm{D})} = \mathbf{0.960}$$

EXPERIMENTAL VALUE = 0.980

Transition-State Geometries

Figure 64: Optimized transition-state geometries, **TS-2.5a-e**, for the ionization step leading to the discrete carbenium ion intermediate. These structures are presented in Figure 22.

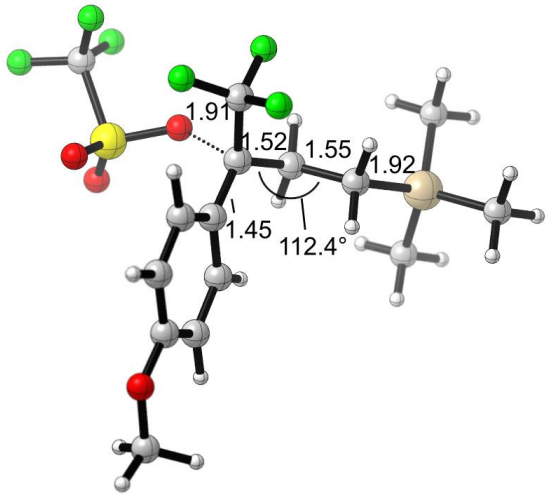

TS-2.5a

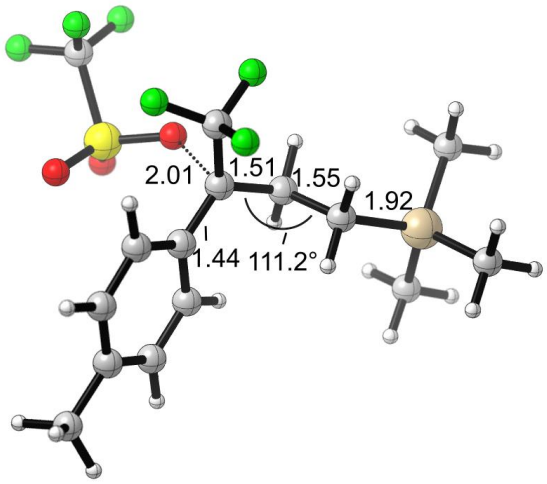

TS-2.5b

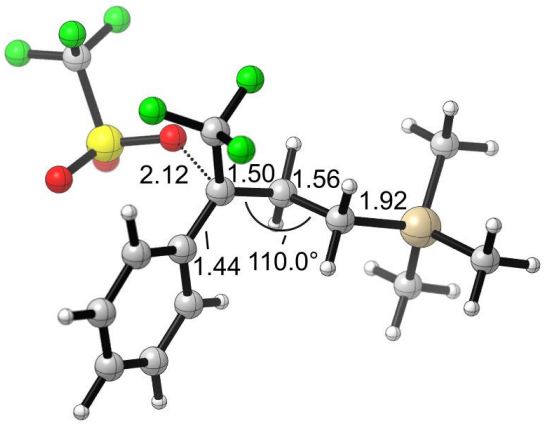

TS-2.5c

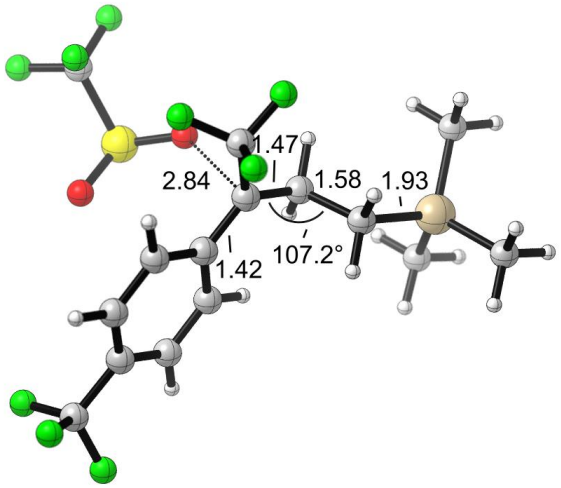

TS-2.5d

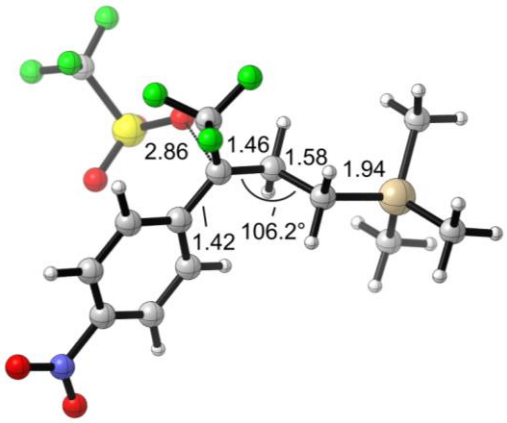

TS2.5e

Figure 65: Optimized transition-state geometries, **TS-2.7a-e**, for 1,3-γ-silyl-elimination leading to trifluoromethyl cyclopropanes. These structures are presented in Figure 22.

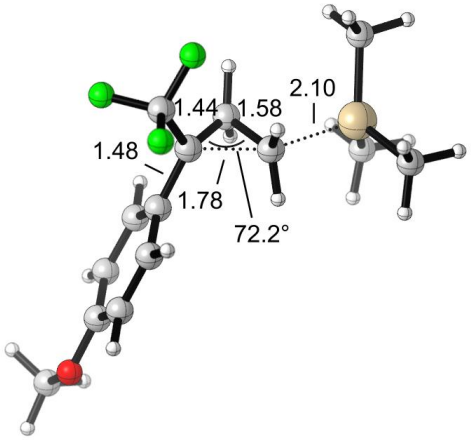

TS-2.7a

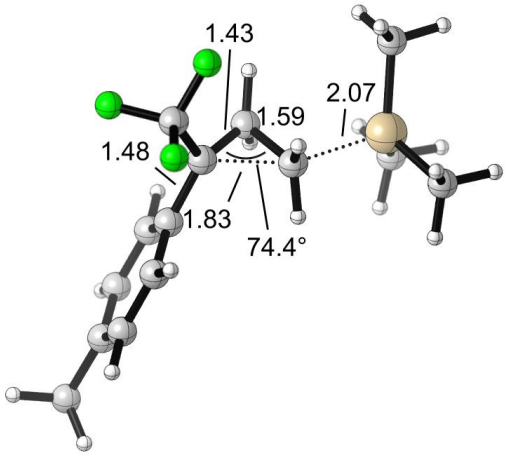

TS-2.7b

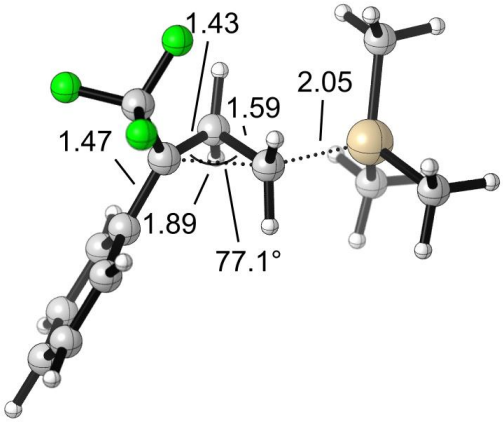

TS-2.7c

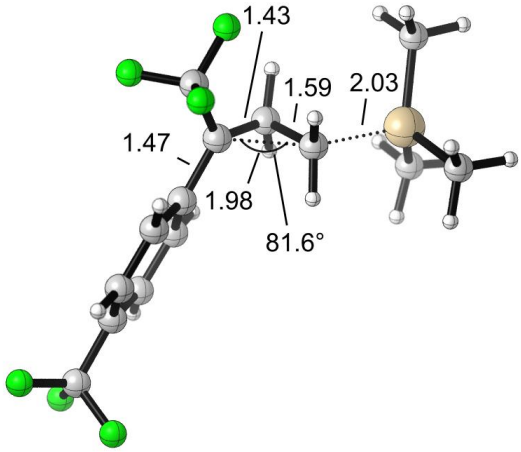

TS-2.7d

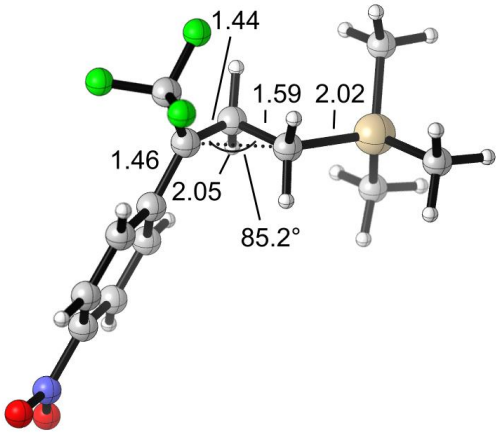

TS-2.7e

Figure 66: Optimized transition-state geometries, **TS-2.10a,b**, for the E1-like elimination leading to trifluoromethyl alkenes. These structures are presented in Figure 23.

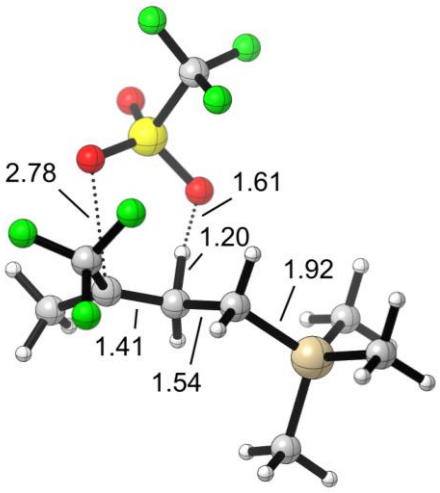

TS-2.10a

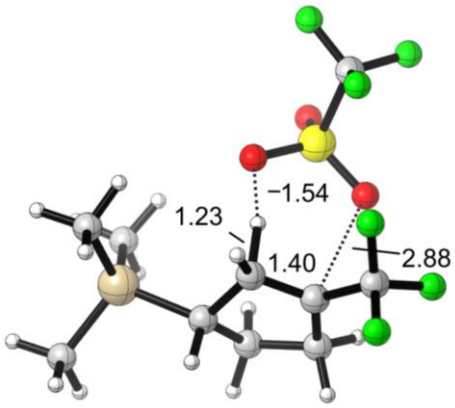

TS-2.10b

Figure 67: Optimized transition-state geometries, **TS-2.12a,c-e,** for the 1,3-γ-silyl-elimination leading to trifluoromethyl cyclopropanes These structures are presented in Figure 23.

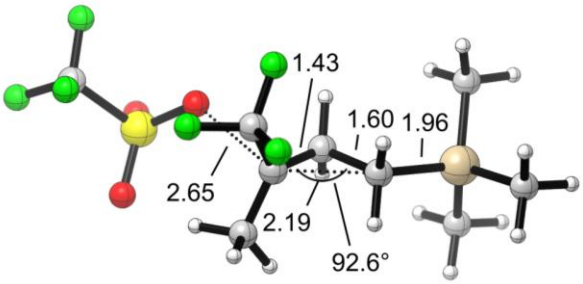

TS-2.12

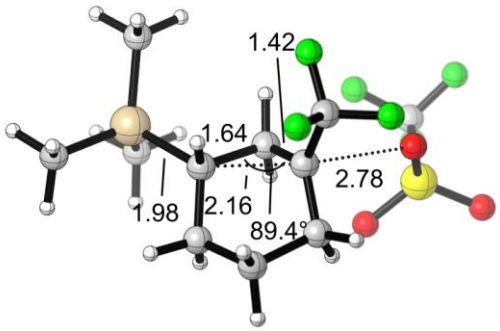

TS-2.12c

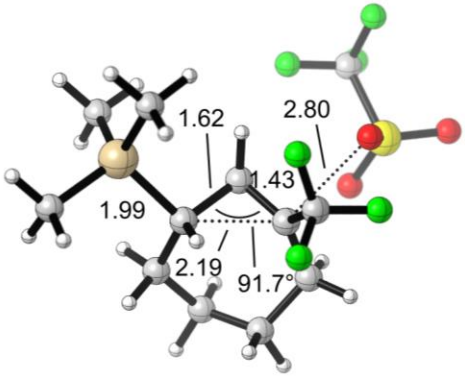

TS-2.12d

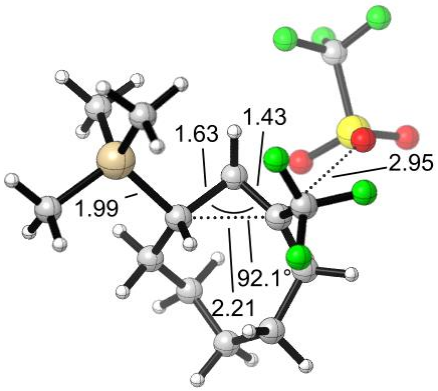

TS-2.12e

Figure 68: Optimized transition-state geometries for the stepwise cyclopropanation, **TS-2.15,** leading to the ionized cyclobutyl intermediate, then to the trifluoromethyl bicyclobutane, **TS-2.17**. These structures are presented in Figure 24.

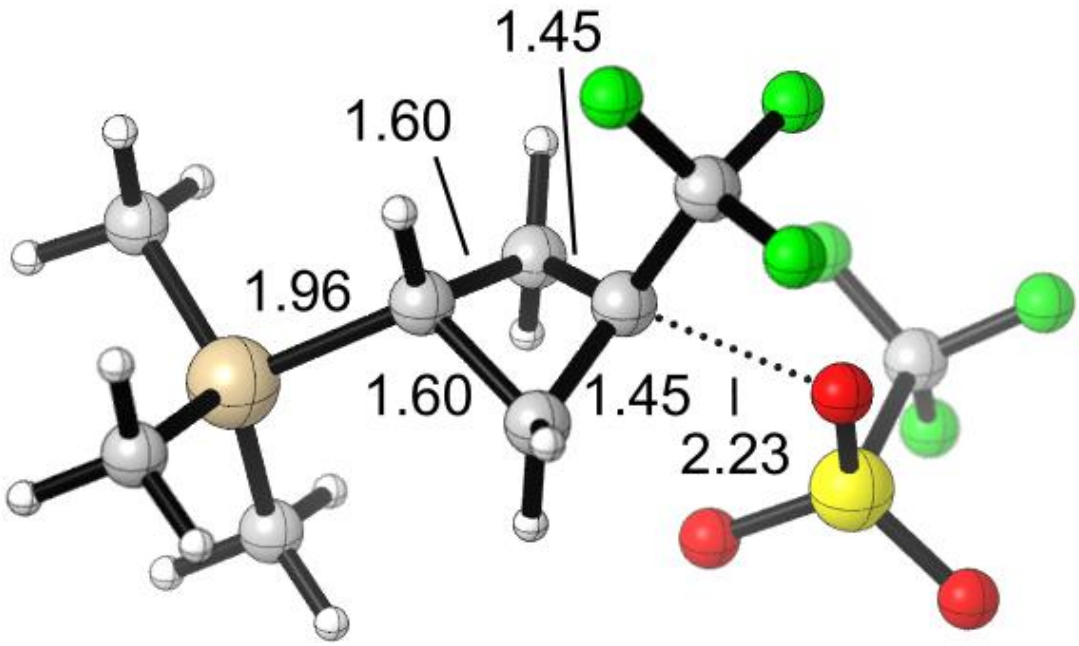

TS-2.15

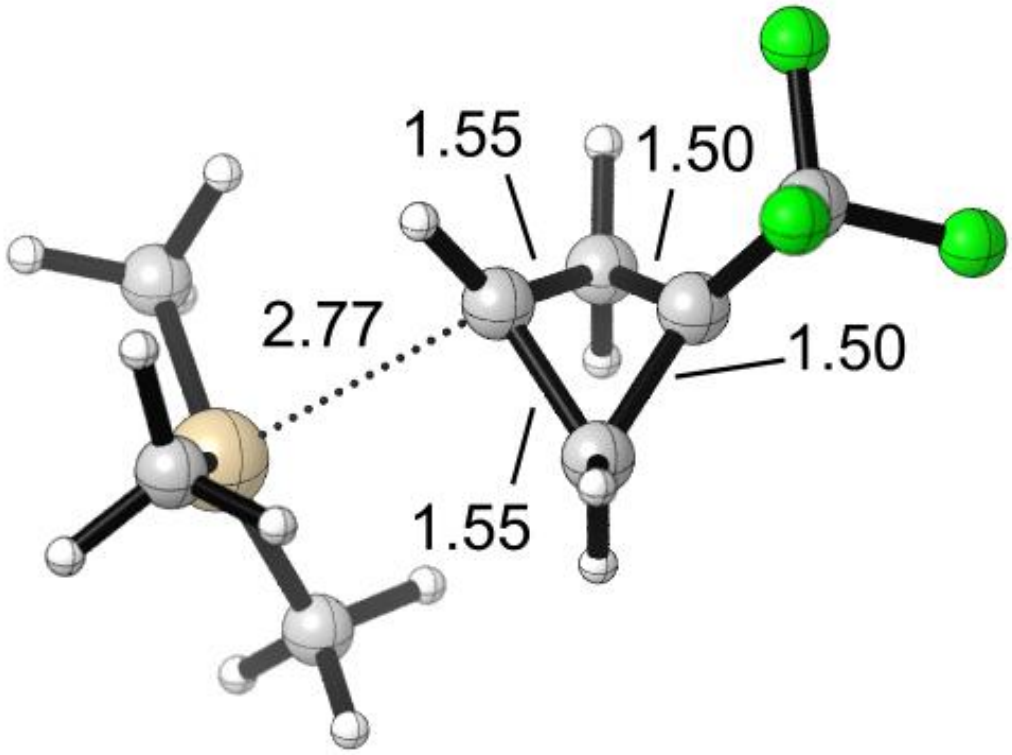

TS-2.17

Stationary Point Energies

Table 24: Various energy values for the stationary points included in the 1,3-γ-silyl mediated cyclopropanation section.

Structure	$E^{a,b}$	$H^{a,b}$	$G^{a,b}$
Ia	-1210.149244	-1210.125917	-1210.2022
Ib	-1134.944301	-1134.921756	-1134.996507
Ic	-1095.653142	-1095.632461	-1095.702679
Id	-1432.710285	-1432.685876	-1432.766023
Ie	-1300.166399	-1300.143089	-1300.220471
If	-797.882379	-797.863771	-797.929035
Ig	-511.719268	-511.699161	-511.769909
IIa	-957.903577	-957.882881	-957.952736
IIb	-882.687859	-882.667958	-882.735984
IIc	-843.389056	-843.371009	-843.434457
IId	-1180.433702	-1180.411874	-1180.485704
IIe	-1047.883321	-1047.862506	-1047.934933
IIf	-545.654296	-545.638034	-545.698027
IIIa	-1209.337124	-1209.313894	-1209.389922
IIIb	-1134.121806	-1134.099424	-1134.173601
IIIc	-1094.823544	-1094.803024	-1094.872517
IIId	-1431.869336	-1431.845056	-1431.924899
IIIe	-1299.319812	-1299.296594	-1299.374072
IIIf	-797.087729	-797.069162	-797.133663
IIIg	-510.926419	-510.906374	-510.976535
IVa	-958.71636	-958.695505	-958.765799
IVb	-883.511564	-883.491377	-883.561371
IVc	-844.220278	-844.202038	-844.266453
IVd	-1181.277328	-1181.25536	-1181.329807
IVe	-1048.733351	-1048.712481	-1048.784162
IVf	-546.44966	-546.433494	-546.492849
2.4a	-2170.947979	-2170.916289	-2171.012676
2.4b	-2095.74253	-2095.711533	-2095.807745
2.4c	-2056.450481	-2056.421462	-2056.511639
2.4d	-2393.505412	-2393.472661	-2393.572564
2.4e	-2260.960059	-2260.928366	-2261.025848
TS-2.5a	-2170.942146	-2170.910529	-2171.008537
TS-2.5b	-2095.733296	-2095.702367	-2095.799427
TS-2.5c	-2056.43821	-2056.409249	-2056.500721
TS-2.5d	-2393.48531	-2393.452915	-2393.556112
TS-2.5e	-2260.935951	-2260.904517	-2261.00724
2.6a	-1209.33719	-1209.313924	-1209.390225
2.6b	-1134.121906	-1134.099482	-1134.173749
2.6c	-1094.82369	-1094.803124	-1094.872992
2.6d	-1431.86922	-1431.84498	-1431.924647
2.6e	-1299.319839	-1299.29664	-1299.373937
TS-2.7a	-1209.315261	-1209.292726	-1209.365927
TS-2.7b	-1134.108726	-1134.086925	-1134.15906
TS-2.7c	-1094.815881	-1094.795915	-1094.863778

Structure	E[a,b]	H[a,b]	G[a,b]
TS-2.7d	-1431.867362	-1431.843768	-1431.920988
TS2.7e	-1299.319763	-1299.297259	-1299.372278
2.8a	-800.352507	-800.338213	-800.39292
2.8b	-725.148057	-725.134524	-725.188005
2.8c	-685.861889	-685.850047	-685.899504
2.8d	-1022.914197	-1022.898873	-1022.957385
2.8e	-890.370626	-890.356427	-890.411631
2.9a	-1864.769948	-1864.74421	-1864.82668
2.9b	-1902.864399	-1902.839781	-1902.919705
2.9c	-1942.152266	-1942.125928	-1942.20959
2.9d	-1981.422772	-1981.395249	-1981.481082
2.9e	-2020.697708	-2020.669032	-2020.756922
TS-2.10a	-1864.734469	-1864.708489	-1864.792357
TS-2.10b	-1902.832532	-1902.806986	-1902.889592
2.11a	-902.761395	-902.744264	-902.805789
2.11b	-940.858156	-940.841157	-940.902448
TS-2.12a	-1864.739337	-1864.713288	-1864.797226
TS-2.12c	-1942.123702	-1942.096925	-1942.183393
TS-2.12d	-1981.399763	-1981.371819	-1981.460291
TS-2.12e	-2020.673753	-2020.64453	-2020.736641
2.13a	-494.172561	-494.163793	-494.204833
2.13c	-571.553088	-571.543394	-571.58724
2.13d	-610.843457	-610.832875	-610.87847
2.13e	-650.120556	-650.10885	-650.156761
2.14	-1863.554247	-1863.529792	-1863.609789
TS-2.15	-1863.529698	-1863.504987	-1863.586241
2.16	-901.918478	-901.902411	-901.960548
TS-2.17	-901.887367	-901.872325	-901.928072
2.18	-492.932161	-492.924202	-492.964057
2.19a	-902.748289	-902.732076	-902.791739
2.20a	-650.464621	-650.451389	-650.502628
2.21a	-901.918478	-901.902411	-901.960548
2.22a	-651.31932	-651.305566	-651.358494
2.19b	-942.039661	-942.021157	-942.086386
2.20b	-689.767559	-689.751813	-689.809439
2.21b	-941.203975	-941.185666	-941.249645
2.22b	-690.606839	-690.59089	-690.649451
2.23a	-942.039661	-942.021157	-942.086386
2.23b	-689.767559	-689.751813	-689.809439
2.23c	-941.203975	-941.185666	-941.249645
2.23d	-690.606839	-690.59089	-690.649451
OTf^-	-961.609638	-961.601423	-961.642198
HOTf	-962.005744	-961.996921	-962.039088
TMS^+	-408.960647	-408.951919	-408.993126

[a] Computed at the B3LYP/6-31+G(d) level. [b]Energy values displayed in Hartrees

GENERAL CALCULATION DETAILS FOR OXIDATION OF METHANOL BY AN OXOAMMONIUM CATION

This computational study serves to elucidate the kinetics and thermodynamics governing base mediated oxidations. Quantum chemical calculations were performed using Gaussian 09.[58] All optimized geometries were calculated using B3LYP[77], a hybrid density functional, with the 6-31+g(d) basis set[78]. Single point calculations were computed on the respective optimized structures using B3LYP/6-311++g(d,p). The addition of diffuse functions to the double split-valence basis set ensured an adequate description of the key hydride transfer and prerequisite hydrogen bonding. Stationary points were characterized by frequency calculations at 298 K, with structures at energy minima showing no negative frequencies and transition-states showing one negative frequency. Intrinsic reaction coordinate (IRC) calculations followed by optimization and frequency calculation were performed to unambiguously connect transition-state structures with associated reactants and products along the reaction coordinate. Thermal energies, enthalpies and Gibbs free energies were corrected using the appropriate thermodynamic correction factor. Solvation energies were evaluated using a self consistent field (SCRF) using the polarization continuum model (PCM)[81] model. All energetic values shown are in kcal mol^{-1}; bond lengths are reported in Ångstroms (Å), bond and dihedral angles in degrees (˚).

Transition-State Geometries

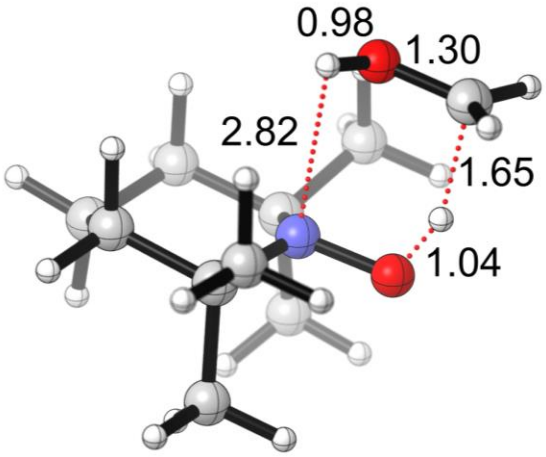

2.25a

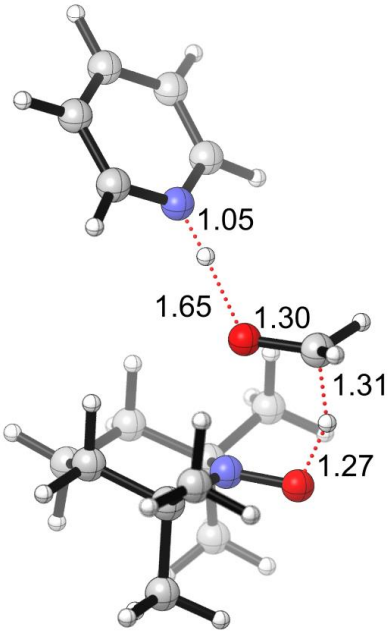

2.25b

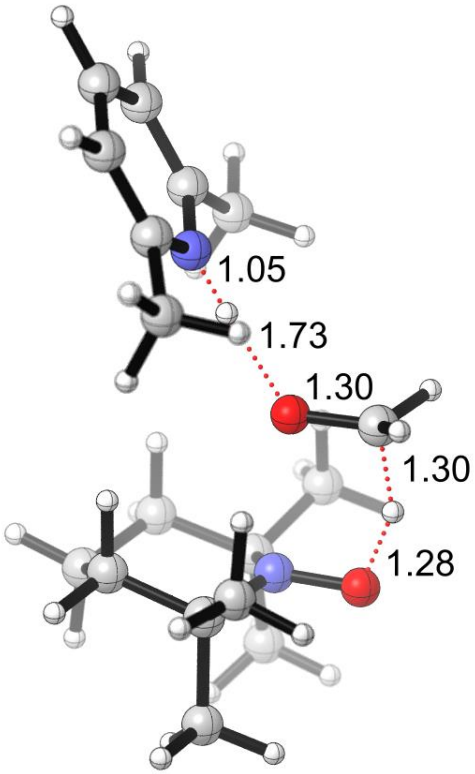

2.25c

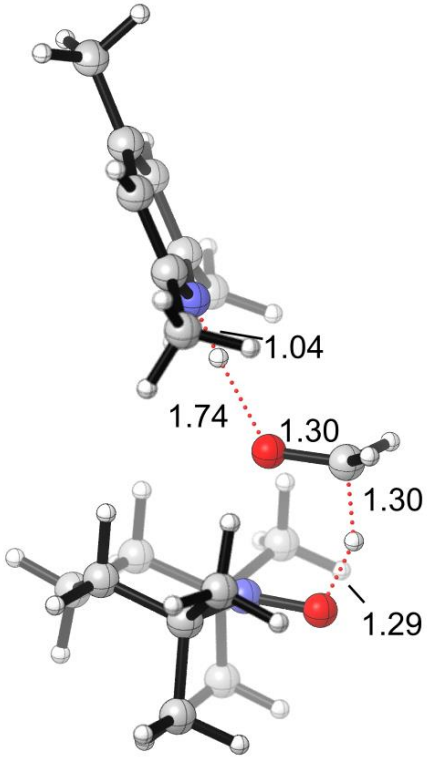

2.25d

Stationary Point Energies

	6-311++G(d,p)	
	H **(kcal mol^{-1})**	***G*** **(kcal mol^{-1})**
methanol	-72612.08	-72628.82519
2,2,6,6-tetramethyl-1-oxopiperidin-1-ium	-303330.50	-303359.6873
pyridine	-155787.00	-155806.966
2,6-lutidine	-205111.69	-205136.924
2,4,6-collidine	-229773.01	-229801.369
pyridine H-bond complex	-228403.57	-228432.5942
2,6-lutidine H-bond complex	-277727.96	-277760.7517
2,4,6-collidine H-bond complex	-302389.49	-302425.08
TS (no base) (2.25a)	-375911.70	-375950.6753
pyridine TS (2.25b)	-531721.63	-531767.9851
2,6-lutidine TS (2.25c)	-581046.91	-581098.6003
2,4,6-collidine TS (2.25d)	-605709.84	-605764.4896
1-hydroxy-2,2,6,6-tetramethylpiperidin-1-ium	-304092.39	-304121.4828
pyridin-1-ium	-156053.48	-304121.4828
2,6-dimethylpyridin-1-ium	-205382.11	-205406.7652
2,4,6-trimethylpyridin-1-ium	-230045.45	-230072.0202
formaldehyde	-71860.00	-71875.74277
2,2,6,6-tetramethylpiperidin-1-ol	-303830.16	-303859.6276

	6-311++G(d,p)	
	ΔH_{rxn} (kcal mol^{-1})	**ΔG_{rxn} (kcal mol^{-1})**
pyridine + methanol → H bond complex	-4.5	3.2
2,6-lutidine + methanol → H bond complex	-4.2	5.0
2,4,6-collidine + methanol → H bond complex	-4.4	5.1
Methanol → TS	30.9	37.8
pyridine H-bond complex → TS	12.4	24.3
2,6-lutidine H-bond complex → TS	11.5	21.8
2,4,6-collidine H-bond complex → TS	10.1	20.3
TS → products	-40.7	-46.5
TS → products	-22.0	-41.1
TS → products	-25.3	-43.5
TS → products	-25.8	-42.9

GENERAL CALCULATION DETAILS FOR OXIDATION OF METHANOL BY AN OXOAMMONIUM CATION

The analysis is broken down into three subject areas based on the substitution pattern of the substrate C-H bond being oxidized: oxidations that occur α to a C-O bond, α to a C-N bond, and those lacking any heteroatom substitution. Both experimental evidence and computationally-derived data are reported in these sections. Quantum chemical calculations were performed using Gaussian 09.[58] The method used for the calculations of non-metal containing system reported in our paper follows: (i) geometry optimization and vibrational frequency calculations in implicit dichloromethane or acetonitrile using CPCM[156] at the B3LYP[77]/6-31+G(d)[78] level of theory, (ii) single-point solvation free energy calculation in dichloromethane or acetonitrile using CPCM with B3LYP/6-311++G(d,p). The method used for the calculations of iron containing systems reported in our paper follows: (i) geometry optimization and vibrational frequency calculations in implicit dichloromethane or acetonitrile using CPCM at the B3LYP/LANL2DZ[79] level of theory for iron and B3LYP/6-31+G(d) level of theory for the rest of the atoms in the system, (ii) single-point solvation free energy calculation in dichloromethane or acetonitrile using CPCM with B3LYP/SDD[157] for iron and B3LYP/6-311++G(d,p) for the rest of the atoms in the system. Gibbs free energies in solution are obtained by adding the thermal correction to the Gibbs free energy from (i) to the solvation electronic energy calculated in (ii). Stationary points were characterized by frequency calculations at 298 K, with structures at energy minima showing no negative frequencies and transition-states showing one negative frequency. Intrinsic reaction coordinate (IRC) calculations[80] followed by optimization and frequency calculations were performed to unambiguously connect transition-state structures with associated reactants and products along the reaction coordinate. All energetic values shown are in kcal mol^{-1}; bond lengths are reported in Ångstroms (Å), bond angles in degrees (˚). Figures were generated using CYLView.[82]

[156] (a) Baron, V.; Cossi, M. *J. Phys, Chem. A.* **1998**, *19*, 404; (b) Cossi, M.; Rega, N.; Scalmani, G.; Barone, V. *J. Comp. Chem.* **2003**, 255, 327.
[157] Cao, X. Y.; Dolg, M. *J. Mol. Struct. (Theochem),* **2002**, *581*, 139.

Entropic Penalty for Pre-oxidation Complexation

Table 25: Thermodynamics of complexation

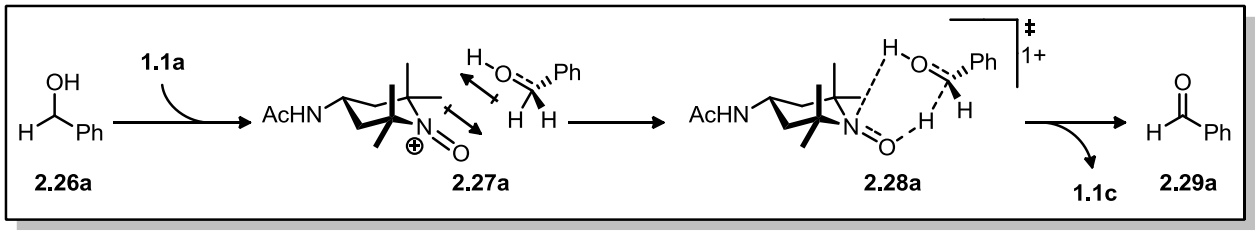

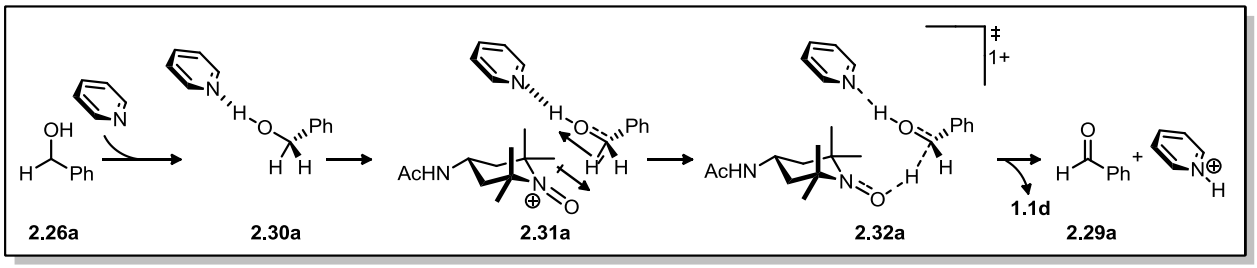

System	$\Delta H^{\ddagger}$ (kcal mol^{-1})	$\Delta G^{\ddagger}$ (kcal mol^{-1})	$\Delta S^{\ddagger}$ (kcal mol^{-1})
2.26a → 2.27a	-1.06	7.80	-0.0297
2.26a → 2.30a	-4.57	3.56	-0.0276
2.30a → 2.31a	-2.03	9.02	-0.0371

Representative Transition-State Geometries

Figure 69: Transition-state geometries for non-base assisted (left) pathway from Figure 34 and base assisted pathway (right) from Figure 35

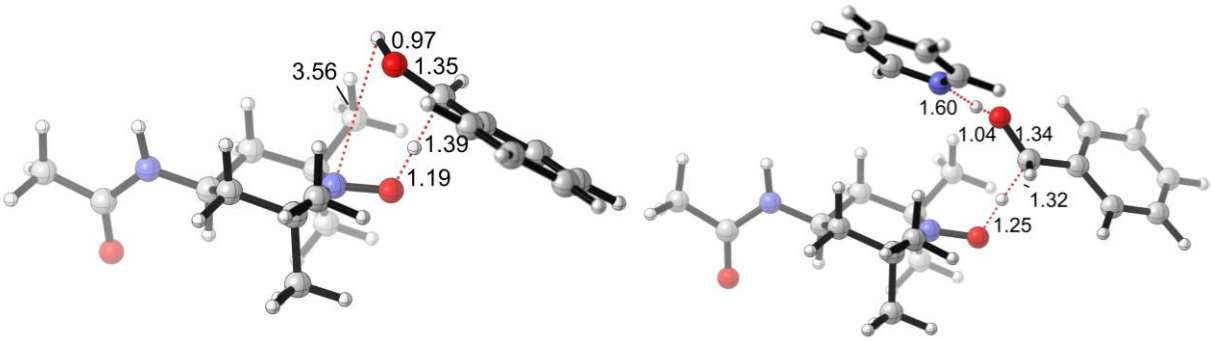

2.28a **2.32a**

Figure 70: Transition-state geometries of ionic hydride abstraction (top, left), radical hydride abstraction (top, right), and nucleophic addition (bottom) from Figure 42

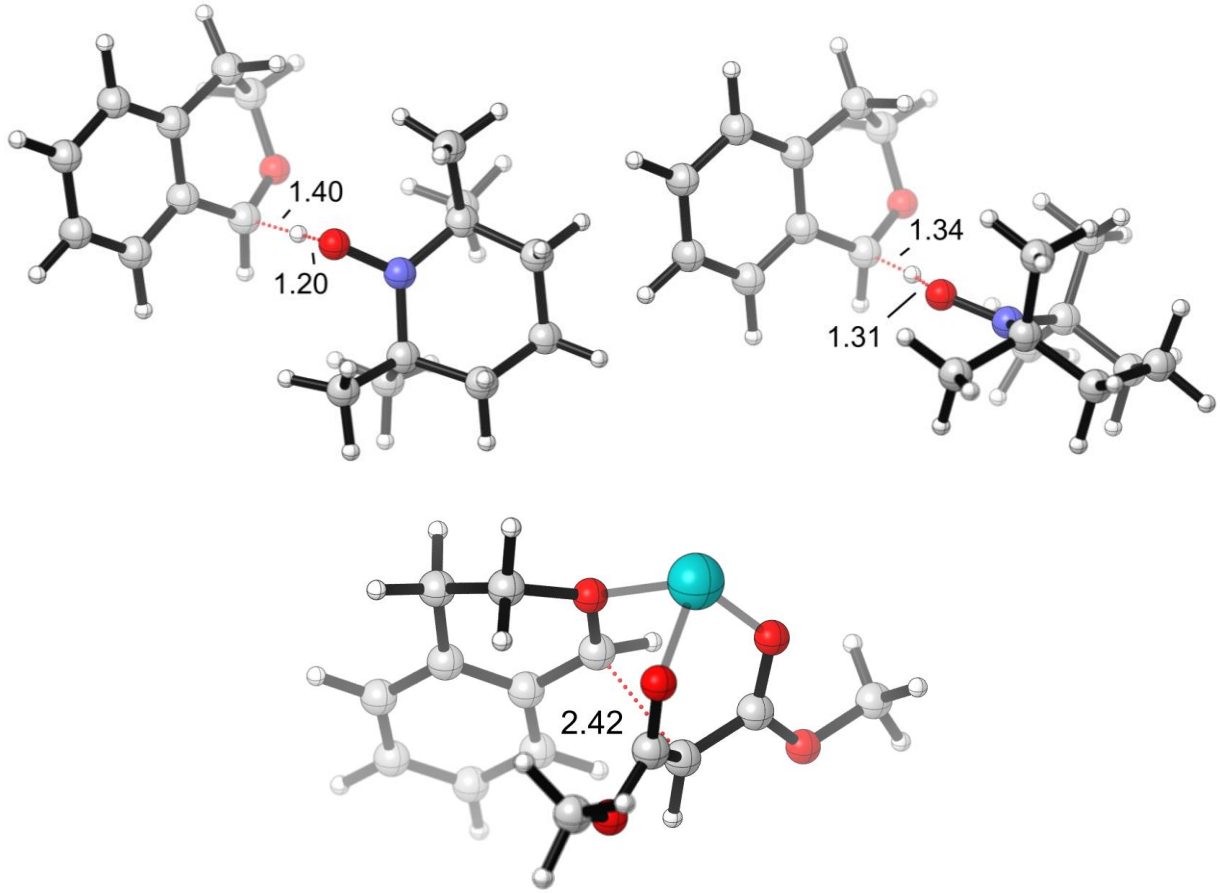

Figure 71: Transition-state geometry for the hydride transfer of the silylated intermediate in Figure 44

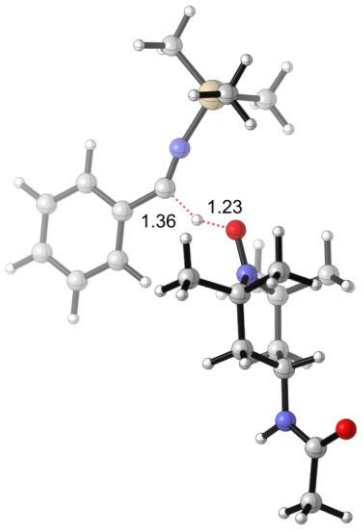

Figure 72: Transition-state geometries for the hydride transfer in the ene system (top, left), nucleophilic addition into the ene system (top, right), and 6-membered transition-state (bottom) in Figure 47

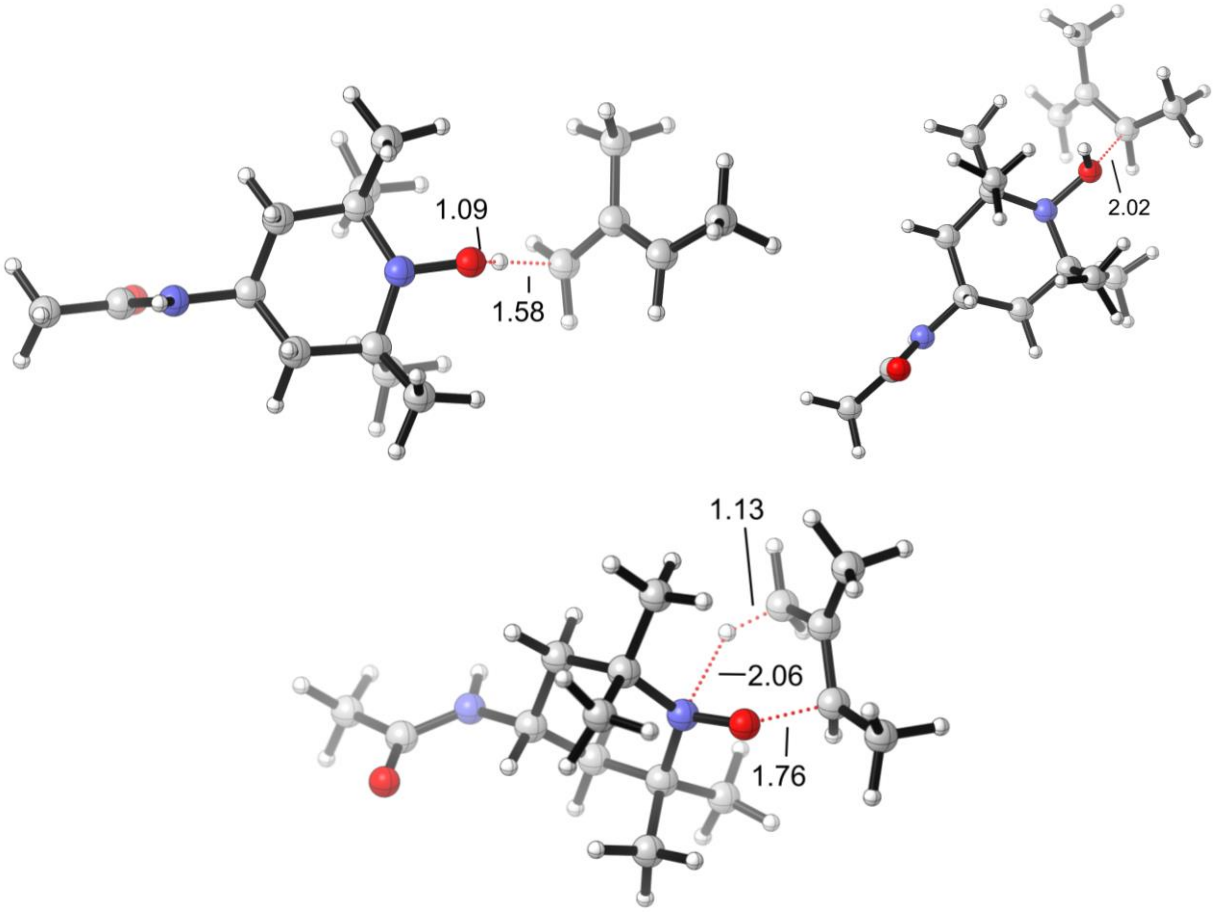

Stationary Point Energies

identifier	system	solvent	correction to Gibbs free energy	SCF energy
1.1a	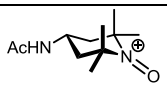	DCM	0.275101	-691.7448201
1.1d	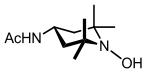	DCM	0.284965	-692.5540214
1.1c	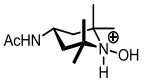	DCM	0.299435	-692.9900916
1.1a	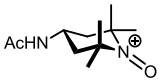	MeCN	0.27534	-691.7519528
1.1d		MeCN	0.284965	-692.5553871
1.1c	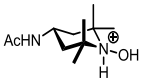	MeCN	0.29911	-692.9978183
-		DCM	0.227877	-483.662676
-	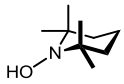	DCM	0.237396	-484.4689012
-	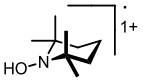	DCM	0.255612315	-484.2710507
2.26a	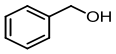	DCM	0.100926	-346.8814631
2.26b	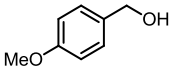	DCM	0.130108	-461.4398615
2.26c	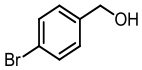	DCM	0.088288	-2920.424317
2.26d	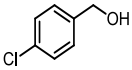	DCM	0.089044	-806.5046467
2.26e	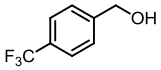	DCM	0.098735	-684.032319
2.26f	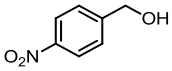	DCM	0.098942	-551.4500136
2.26g	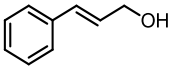	DCM	0.13084	-424.3042794
2.26h	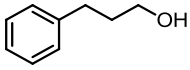	DCM	0.153806	-425.5326442
2.26i	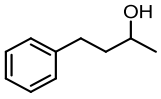	DCM	0.179912	-464.8618887
2.26j		DCM	0.133178	-273.0732287
2.26k	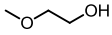	DCM	0.083046	-269.6499073

2.26l	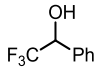	DCM	0.052568	-684.0327084
2.26m		DCM	0.100596	-492.252843
2.27a	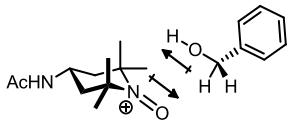	DCM	0.392613	-1038.630275
2.27b	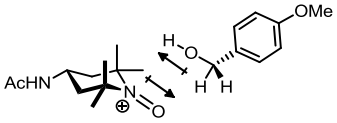	DCM	0.421879	-1153.18881139
2.27c	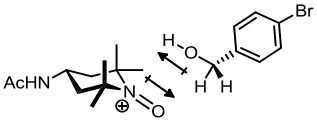	DCM	0.379793	-3612.172524
2.27d	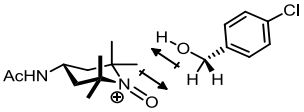	DCM	0.38107	-1498.252834
2.27e	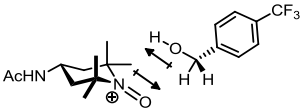	DCM	0.391399	-1375.779905
2.27f	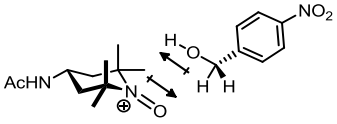	DCM	0.38938	-1243.196413
2.27g	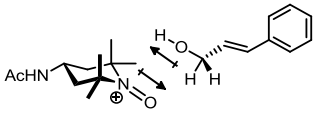	DCM	0.421511	-1116.052476
2.27h	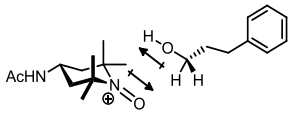	DCM	0.44711	-1117.280569
2.27i	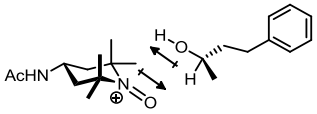	DCM	0.471656	-1156.607455
2.27j	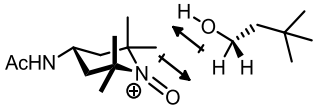	DCM	0.425919	-964.8215711
2.27k	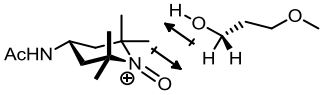	DCM	0.374069	-961.4017983
2.27l	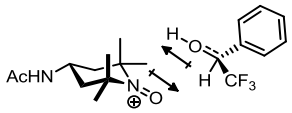	DCM	0.38872	-1375.778215
2.27m	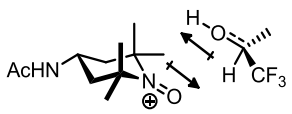	DCM	0.341948	-1184.00099950

2.28a	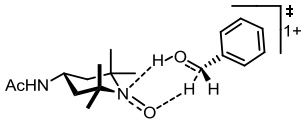	DCM	0.393942	-1038.602674
2.28b	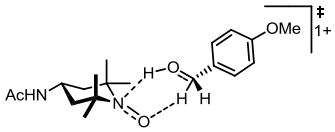	DCM	0.420075	-1153.166385
2.28c	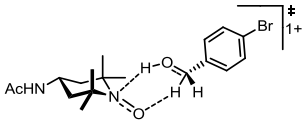	DCM	0.382539	-3612.143926
2.28d	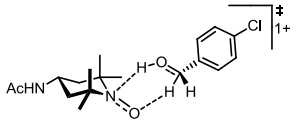	DCM	0.380264	-1498.224368
2.28e	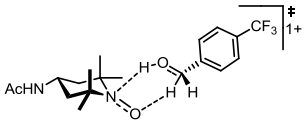	DCM	0.390277	-1375.748238
2.28f	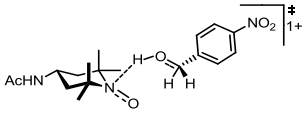	DCM	0.389995	-1243.162912
2.28g	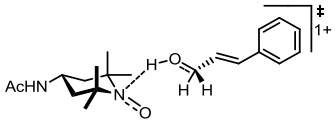	DCM	0.421287	-1116.031445
2.28h	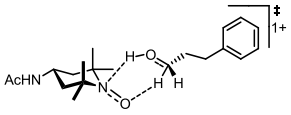	DCM	0.445133	-1117.245805
2.28i	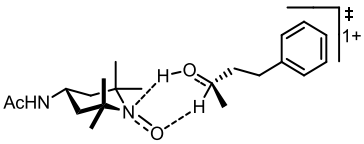	DCM	0.471003	-1156.577998
2.28j	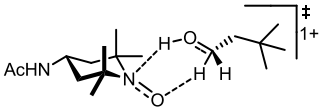	DCM	0.424959	-964.7835125
2.28k	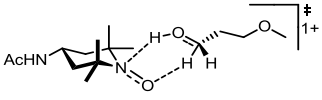	DCM	0.374474	-961.3551158
2.28l	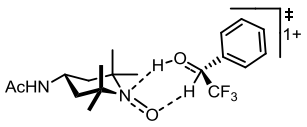	DCM	0.392976	-1375.731578
2.28m	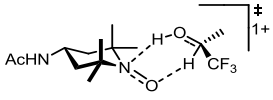	DCM	0.344718	-1183.941076
2.29a	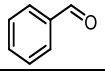	DCM	0.079319	-345.67554

2.29b	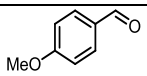	DCM	0.108618	-460.2367186
2.29c	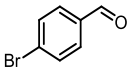	DCM	0.067146	-2919.150277
2.29d	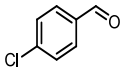	DCM	0.067396	-805.2979274
2.29e	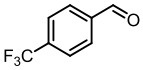	DCM	0.076789	-682.8233504
2.29f	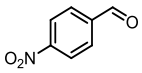	DCM	0.076953	-550.238763
2.29g	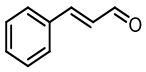	DCM	0.10908	-423.1016274
2.29h	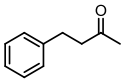	DCM	0.155728	-424.3194346
2.29i		DCM	0.109956	-271.8619972
2.29j	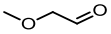	DCM	0.059218	-268.4343417
2.29k		DCM	0.027675	-682.8159781
2.29l		DCM	0.078241	-491.0332497
2.29m		DCM	0.061535	-248.355926959
2.30a	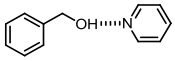	DCM	0.177743	-595.2468595
2.30b	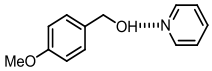	DCM	0.207396	-709.804445
2.30c	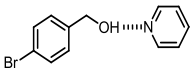	DCM	0.166455	-3168.790391
2.30d	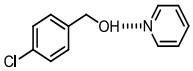	DCM	0.166789	-1054.870622
2.30e	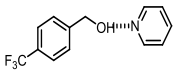	DCM	0.17674	-932.2222375
2.30f	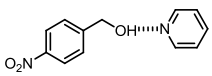	DCM	0.1762	-799.8171197
2.30g	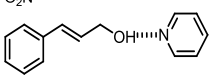	DCM	0.208382	-672.4614422
2.30h	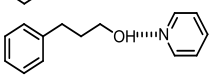	DCM	0.232204	-673.8972113
2.30i	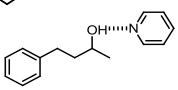	DCM	0.257834	-712.9655277
2.30j	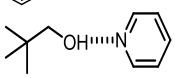	DCM	0.210774	-521.4382761
2.30k	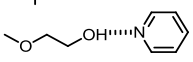	DCM	0.162122	-518.0176093
2.30l	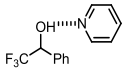	DCM	0.130657	-740.6213736
2.30m	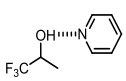	DCM	0.1784	-932.4014303

2.31a	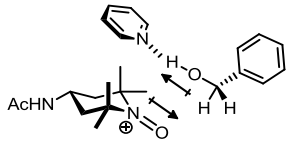	DCM	0.472631	-1286.997094
2.31b	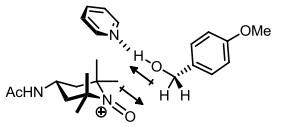	DCM	0.501457	-1401.554794
2.31c	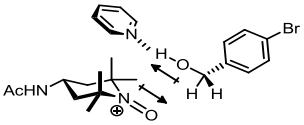	DCM	0.459823	-3860.539658
2.31d	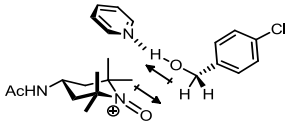	DCM	0.459675	-1746.620145
2.31e	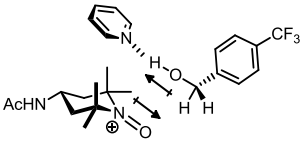	DCM	0.470968	-1624.148144
2.31f	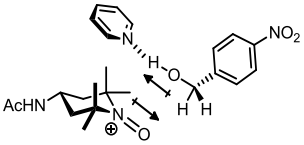	DCM	0.471422	-1491.565387
2.31g	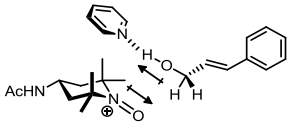	DCM	0.501286	-1364.420655
2.31h	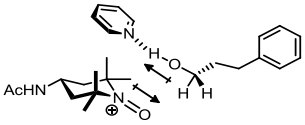	DCM	0.52414	-1365.64757
2.31i	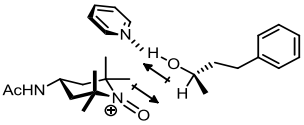	DCM	0.551453	-1365.64757
2.31j	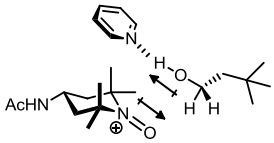	DCM	0.506652	-1213.187671
2.31k	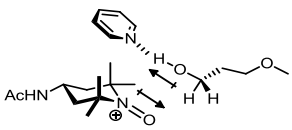	DCM	0.455501	-1209.767166

2.31l	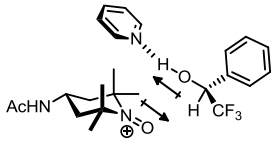	DCM	0.472783	-1624.14742
2.31m	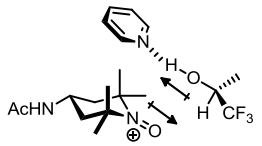	DCM	0.423637	-1432.370192
2.32a	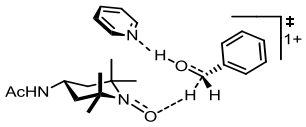	DCM	0.470647	-1286.979337
2.32b	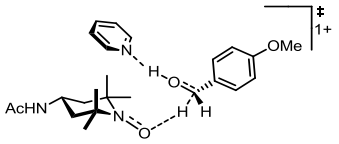	DCM	0.499905	-1401.541258
2.32c	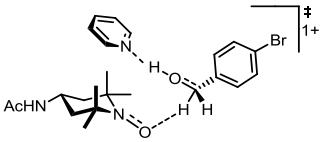	DCM	0.463966	-3860.523729
2.32d	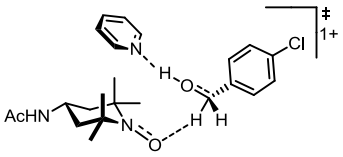	DCM	0.463276	-1746.604
2.32e	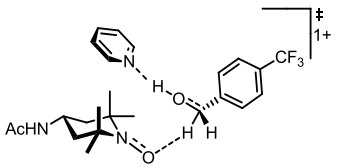	DCM	0.474132	-1624.131291
2.32f	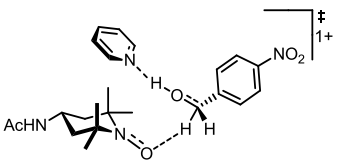	DCM	0.47377	-1491.548298
2.32g	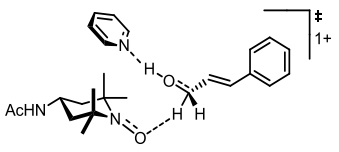	DCM	0.499895	-1364.405851
2.32h	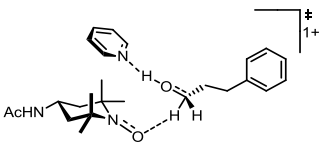	DCM	0.526619	-1365.628641
2.32i	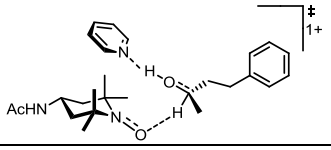	DCM	0.554119	-1404.95324

2.32j	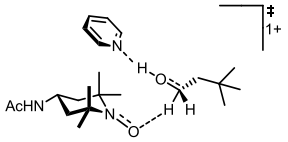	DCM	0.424959	-1213.165012
2.32k	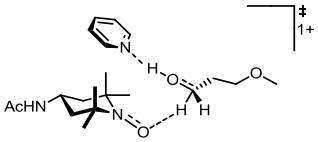	DCM	0.457424	-1209.747149
2.32l	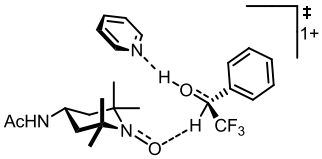	DCM	0.473307	-1624.124222
2.32m	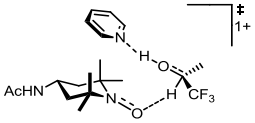	DCM	0.424863	-1432.342129
2.33	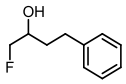	DCM	0.171583	-564.1285801
-	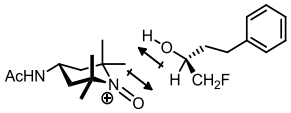	DCM	0.461479	-1255.875471
-	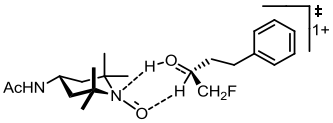	DCM	0.463225	-1255.830588
-	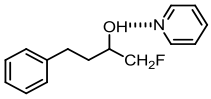	DCM	0.249779	-812.4904851
-	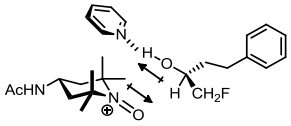	DCM	0.542851	-1504.23892656
-	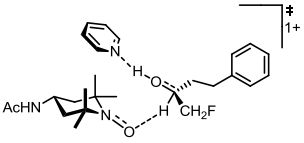	DCM	0.546841	-1504.219029
-	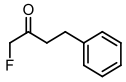	DCM	0.147897	-562.9163126
2.34	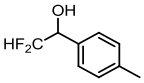	DCM	0.13405	-624.0816833
-	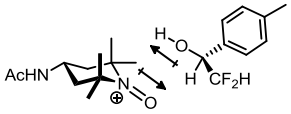	DCM	0.423931	-1315.82653
-	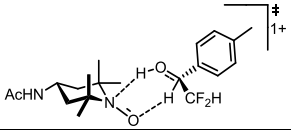	DCM	0.426154	-1315.786119

-	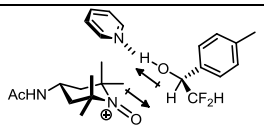	DCM	0.506056	-1564.195275
-	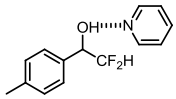	DCM	0.213395	-872.4457079
-	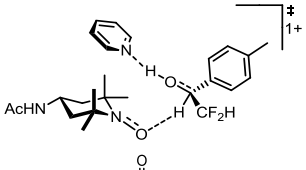	DCM	0.507658	-1564.172774
-	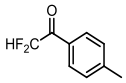	DCM	0.111942	-622.8676013
-	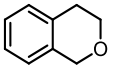	DCM	0.136731	-424.3085326
-	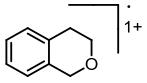	DCM	0.134081	-424.0642685
-	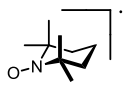	DCM	0.225601	-483.8553965
-	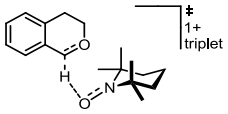	DCM	0.377091	-907.9355347
-	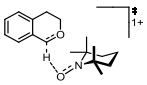	DCM	0.381069	-907.9529564
-	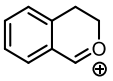	DCM	0.127884	-423.5144416
-	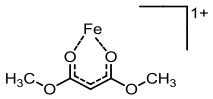	DCM	0.087264	-619.5367162
-	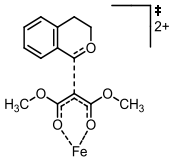	DCM	0.238305	-1043.038213
-	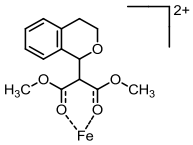	DCM	0.242184	-1043.075833
-	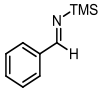	DCM	0.181641	-734.5468486
-	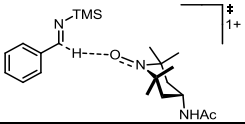	DCM	0.469418	-1426.270441

-	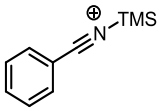	DCM	0.170589	-733.767648
-		DCM	-0.014006	-424.7630849
-	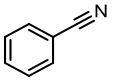	DCM	0.06897	-324.584913
-		DCM	-0.014211	-324.6664399
-		DCM	0.081542	-509.2819144
-		MeCN	0.106221	-196.602
-	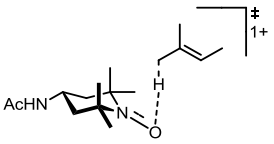	MeCN	0.39553	-888.321
-	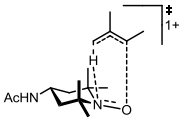	MeCN	0.404728	-888.332
-		MeCN	0.095225	-195.772
-	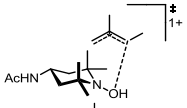	MeCN	0.404148	-888.333
-	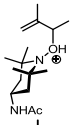	MeCN	0.404939	-888.335
-	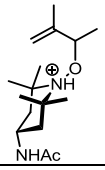	MeCN	0.407835	-888.378

Appendix IV: *Experimental Procedures for Continuous Flow Processing*

Raman Spectroscopy As a Tool For Monitoring Mesoscale Continuous-Flow Organic Synthesis

Specifics of Raman spectrometer / flow chemistry interface

The Raman system used was an Enwave Optronics Spectrometer, Model EZRaman-L (www.enwaveopt.com). The continuous-flow unit used was a Vapourtec E-series. A Starna 583.65.65-Q-5/Z20 flow-cell (width: 6.5 mm, height: 20 mm, path length: 5 mm) was placed in-line after the back-pressure regulator using 1mm i.d. PFA tubing. The flow cell was secured in place in a custom-made box and the fiber-optic probe from the spectrometer inserted so it touched the wall of the flow cell.

EXCITATION SOURCE: NIR, frequency stabilized, narrow line width diode laser at 785 nm. Laser power at sample ~200 mW. Line width < 2 cm^{-1}. Fiber-coupled laser output (100 µm, 0.22 NA).

FIBER-OPTIC PROBE: Permanently-aligned two single fiber combination 100 µm excitation fiber, 200 µm collection fiber (0.22 NA). Working distance: 8 mm (standard). Rayleigh rejection: O.D. > 7 at laser wavelength.

CCD DETECTOR: High sensitivity linear CCD array. Temperature regulated (at 13 °C) operation for long integration time and stable dark reference subtraction. Pixel Size: 14 µm x 200 µm (2048 pixels); 16 bit digitization.

SPECTROGRAPH: Symmetrical crossed Czerny-Turner design. Resolution: ~10 cm^{-1} at 785 nm. Excitation spectral coverage: 200 cm^{-1} to 2400 cm^{-1}. Built-in software calibration.

SYSTEM SOFTWARE: EZ Raman 3.5.4MAS. Data files exported into Microsoft Excel.

The flow system used in the study was a Vapourtec E-series (www.vapourtec.co.uk) equipped with a 10 mL PFA reactor coil.

The flow cell used for spectroscopic studies was a Starna 583.65.65-Q-5/Z20 cell (width: 6.5 mm, height: 20 mm, path length: 5 mm) (www.starnacells.com).

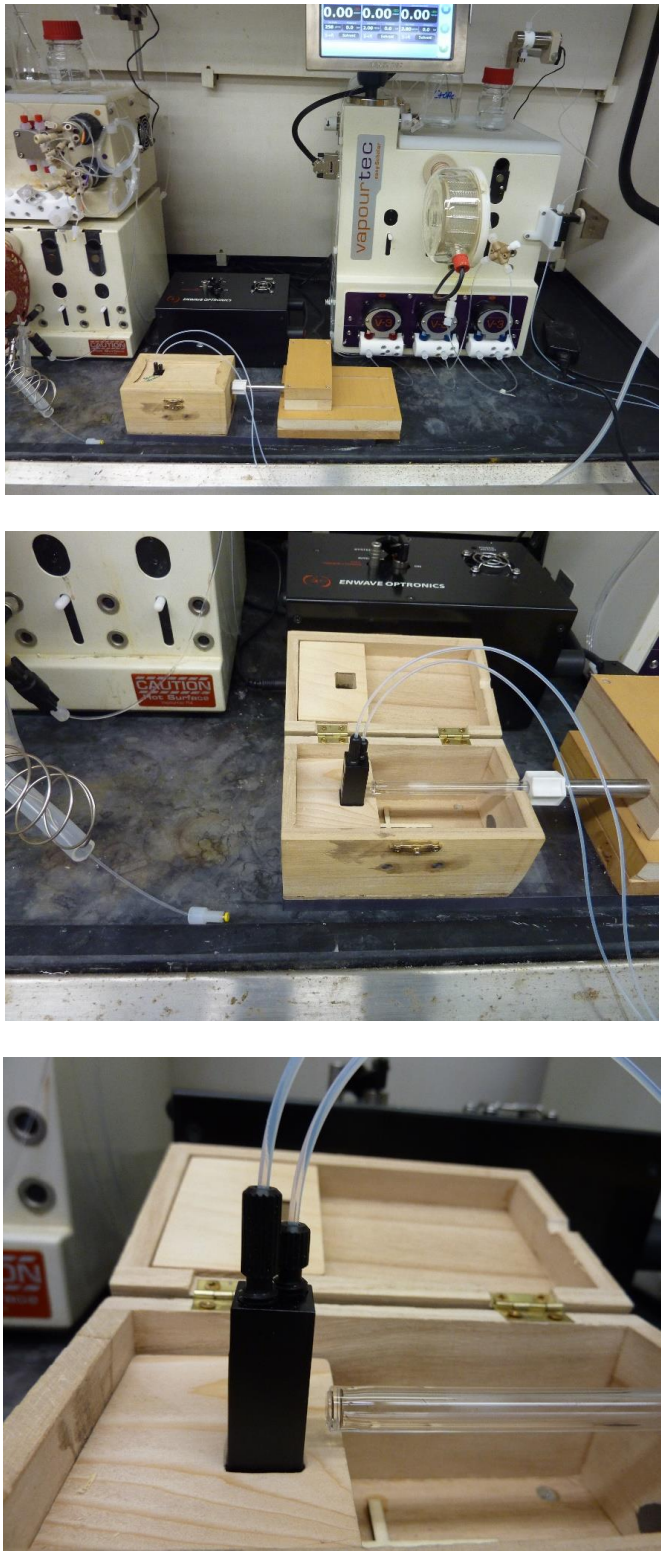

Figure 73: Photographs of the entire setup (top), Enwave Raman spectrometer and box (middle), and close up of quatrz tube focused on the flow cell (bottom)

Experimental Details for the Various Reactions

Preparation of Coumarins

3-Acetylcoumarin (3.1a):

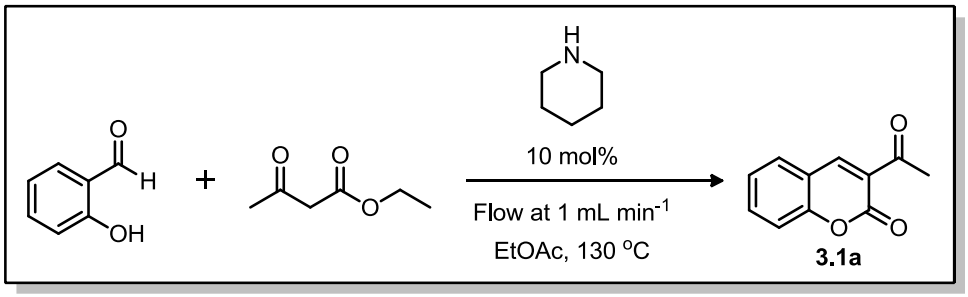

Into a 50 mL volumetric flask was added salicylaldehyde (6.106 g, 50 mmol, 1 equiv.) and ethyl acetoacetate (6.507 g, 50 mmol, 1 equiv.). Ethyl acetate was added to bring the total volume to 50 mL (1 M) and the reagents were thoroughly mixed. An aliquot of this solution (10 mL) was transferred to a 20 mL vial equipped with a Teflon-coated stir bar. The flow reactor was readied using the equipment manufacturer's suggested start-up sequence. Ethyl acetate was pumped at 1 mL min^{-1} to fill the reactor coil. The back-pressure regulator was adjusted to 7 bar and the reactor coil heated to 65 °C. After the heating coil, the product stream was intercepted with a stream of acetone (1 mL min^{-1}) by means of a T-piece to ensure complete solubility of the product. The Raman probe was inserted into the box containing the flow cell and was properly focused. A background scan of the ethyl acetate / acetone solvent system was taken. This background was then automatically subtracted from all subsequent scans, thereby removing any signals from the solvent. The Raman spectrometer was set to acquire a spectrum every 15 s throughout the run, with 10 s integration time, boxcar = 3, and average = 1. When the flow unit was ready, piperidine (0.099 mL, 0.1 mmol, 0.1 equiv.) was injected all at once into the vial containing the reagents and, after mixing for 15 s, the reaction mixture was loaded into the reactor at a flow rate of 1 mL min^{-1}. After the reaction mixture had been completely loaded into the reactor, ethyl acetate was again pumped through the coil at 1 mL min^{-1}. After the product had been fully discharged from the flow cell, the scans were halted. After the product had been fully discharged from the flow cell, the scans were halted and the resulting clear yellow solution was then concentrated *in vacuo* by rotary evaporation. The crude was transferred to a filter funnel and washed with cold hexanes. The product was recrystallized from ethanol to afford 3-acetylcoumarin **3.1a** (1.56 g, 85%) as a pale yellow solid.

^{1}H NMR ($CDCl_3$, 500 MHz) δ ppm 2.73 (s, 3 H), 7.31 - 7.40 (m, 2 H), 7.65 (ddd, *J* = 7.53, 4.37, 2.60 Hz, 2 H), 8.51 (s, 1 H). **^{13}C NMR** ($CDCl_3$, 125 MHz) δ ppm 30.84 (CH_3), 117.00 (CH), 118.56 (C), 124.86 (CH), 125.27 (CH), 130.51 (CH), 134.68 (C), 147.74 (CH), 155.64 (C), 159.52 (C), 195.77 (C).

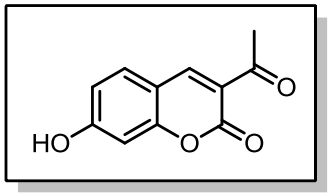

3-Acetyl-7-hydroxy-2H-chromen-2-one (3.1a')

(70% NMR conversion) was prepared according to the representative procedure for the synthesis of **3.1a** from 2,4-dihydroxybenzaldehyde (1.3812 g, 10 mmol).

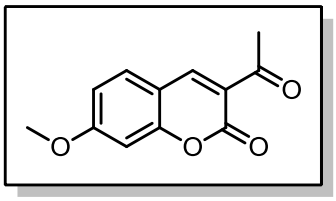

3-Acetyl-7-methoxy-2H-chromen-2-one (3.1a")

(73% NMR conversion) was prepared according to the representative procedure for the synthesis of **3.1a** from 2-hydroxy-4-methoxy benzaldehyde (1.5215 g, 10 mmol). One modification was made: intercept with acetone flowing at 3 mL min^{-1}.

Knoevenagel Reaction

(*Z*)-Ethyl 2-benzylidene-3-oxobutanoate (3.1b):

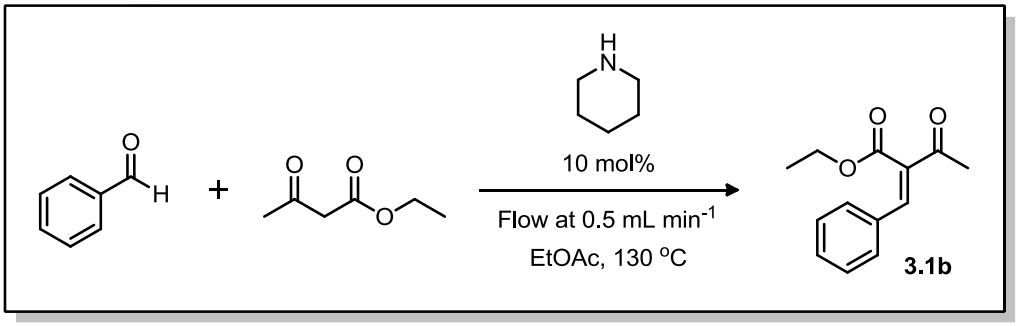

Into a 50 mL volumetric flask was added benzaldehyde (5.306 g, 50 mmol, 1 equiv.) and ethyl acetoacetate (6.507 g, 50 mmol, 1 equiv.). EtOAc was added to bring the total volume to 50 mL (1 M) and the reagents were thoroughly mixed. An aliquot of this solution (10 mL) was transferred to a 20 mL vial equipped with a Teflon-coated stir bar. The flow reactor was readied using the equipment manufacturer's suggested start-up sequence. Ethyl acetate was pumped at 1 mL min^{-1} to prime the system as the coil was heated to 130 °C. The back-pressure regulator was adjusted to 7 bar to prevent the solvent from boiling in the coil. The Raman probe was inserted into the box containing the flow cell and was properly focused. The background scan of the solvent system was taken that would be subtracted from all subsequent scans. Piperidine (0.099 mL, 0.1 mmol, 0.1 equiv.) was injected all at once and, after mixing for 15 s, the reaction mixture was loaded into the reactor at a flow rate of 1 mL min^{-1}. Product collection was commenced immediately after this switch. After the reaction mixture had been completely loaded into the reactor, the reactor pump was set back to pumping ethyl acetate. The resulting clear yellow solution was poured over aqueous 2 M HCl and extracted with ethyl acetate. The combined organic layers washed with brine, dried over Na_2SO_4, and the solvent was removed *in vacuo* by rotary evaporation affording the crude product. The crude product was loaded on a 15-cm silica gel column (55 g silica gel) and a gradient eluting system (99:1, 95:5, 90:10; Hex:EtOAc) was used to obtain (*Z*)-ethyl 2-benzylidene-3-oxobutanoate, **3.1b** (1.3095 g, 60%) as a clear yellow oil.

^{1}H NMR ($CDCl_3$, 400 MHz) δ ppm 1.26 (t, *J* = 7.21 Hz, 3 H), 2.41 (s, 3 H), 4.32 (q, *J* = 7.09 Hz, 2 H), 7.33 - 7.41 (m, 3 H), 7.42 - 7.47 (m, 2 H), 7.56 (s, 1 H). **^{13}C NMR** ($CDCl_3$, 100 MHz) δ ppm 14.08 (CH_3), 26.74 (CH_3), 61.92 (CH_2), 129.06 (CH), 129.74 (CH), 130.93 (CH), 133.17 (C), 134.88 (C), 141.48 (CH), 168.00 (C), 194.87 (C).

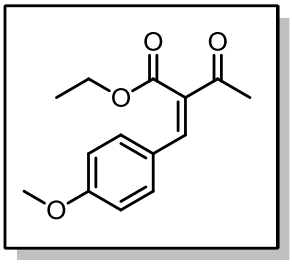

(*Z*)-Ethyl 2-(4-methoxybenzylidene)-3-oxobutanoate (3.1c)
(53% GC conversion) was prepared according to the representative procedure for the synthesis of **3.1b** from 4-methoxybenzaldehyde (1.3615 g, 10 mmol).

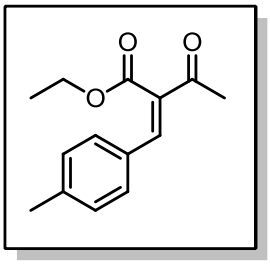

(*Z*)-Ethyl 2-(4-methylbenzylidene)-3-oxobutanoate (3.1d)
(66% GC conversion) was prepared according to the representative procedure for the synthesis of **3.1b** from 4-methylbenzaldehyde (1.2015 g, 10 mmol).

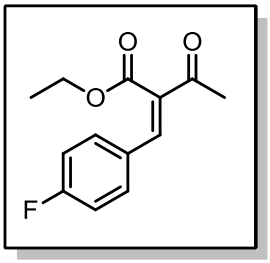

(*Z*)-Ethyl 2-(4-fluorobenzylidene)-3-oxobutanoate (3.1e)

(63% GC conversion) was prepared according to the representative procedure for the synthesis of **3.1b** from 4-fluorobenzaldehyde (1.2411 g, 10 mmol).

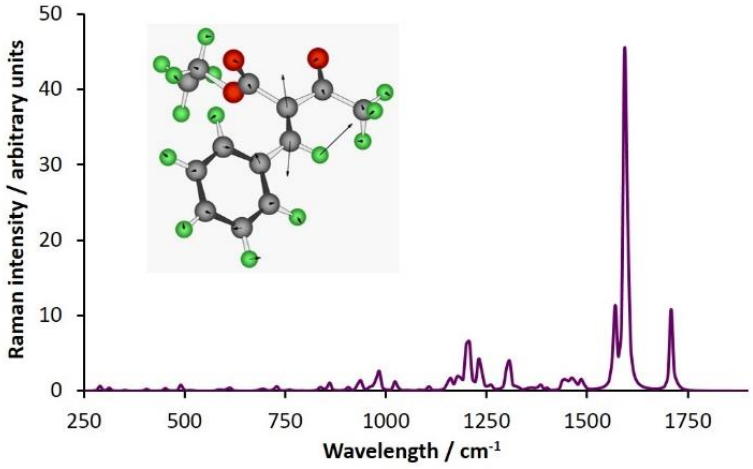

Figure 74: The Raman spectrum of 3.1b generated using Gaussian 09 at the B3LYP/6-31G(d) level of theory. The inset molecule illustrates the complex stretching mode responsible for the signal calculated at 1600 cm^{-1} (actual: 1598 cm^{-1}).

Claisen-Schmidt Reaction

(*E*)-3-(4-Fluorophenyl)-3-phenylprop-2-en-1-one (3.1f):

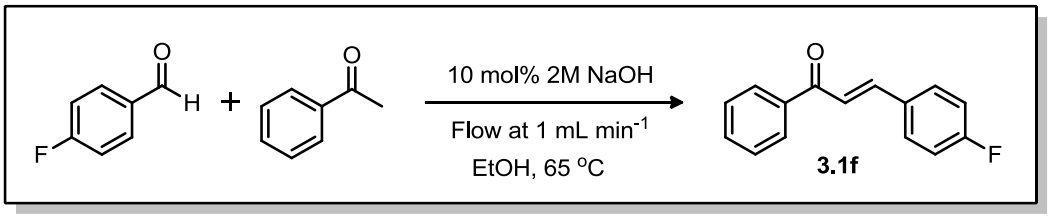

Into a 50 mL volumetric flask was added 4-fluorobenzaldehyde (1.551 g, 12.5 mmol, 1 equiv.) and ethyl acetoacetate (1.637 g, 12.5 mmol, 1 equiv.). Ethanol was added to bring the total volume to 50 mL (0.25 M) and the reagents were thoroughly mixed. An aliquot of this solution (10 mL) was transferred to a 20 mL vial equipped with a Teflon-coated stir bar. The flow reactor was readied using the equipment manufacturer's suggested start-up sequence. Ethanol was pumped at 0.5 mL min^{-1} to prime the system as the coil was heated to 65 °C. The back-pressure regulator was adjusted to 7 bar to prevent the solvent from boiling in the coil. After the heating coil, the product stream was intercepted by pumping acetone at 0.5 mL min^{-1} by means of a T-piece to ensure complete solubility of the product. The Raman probe was inserted into the box containing the flow cell and was properly focused. The background scan of the solvent system was taken that would be subtracted from all subsequent scans. 2 M NaOH (0.125 mL, 0.25 mmol) was injected all at once and after mixing for 15 s the reaction mixture was loaded into the reactor coil at a flow rate of 0.5 mL min^{-1}. Product collection was commenced immediately after this switch. After the reaction mixture had been completely loaded into the reactor, the reactor pump was set back to pumping ethanol. The Raman spectrometer was programmed to take continuous scans using the same parameters as the coumarin synthesis, above. After the product had been fully discharged from the flow cell, the scans were halted. The yellow solution was poured into a beaker containing ice (100 g) causing an immediate precipitation of the product. To ensure complete precipitation, the solution was stirred at 0 °C. The solid product was collected via vacuum filtration and washed with cold ethanol. The material was dried on top of the oven for 6 hours to yield (E)-3-(4-fluorophenyl)-3-phenylprop-2-en-1-one, **3.1f** (0.5421 g, 91%) as a pale yellow solid.

^{1}H NMR ($CDCl_3$, 400 MHz) δ ppm 7.11 (t, J = 8.68 Hz, 2 H), 7.46 (d, J = 15.89 Hz, 1 H), 7.49 - 7.55 (m, 2 H), 7.56 - 7.69 (m, 3 H), 7.78 (d, J = 15.65 Hz, 1 H), 8.02 (d, J = 7.34 Hz, 2 H). **^{13}C NMR** ($CDCl_3$, 100 MHz) δ ppm 116.42 (d, $J_{C\text{-}C\text{-}F}$ = 22.01 Hz, CH), 122.09 (d, $J_{C\text{-}C\text{-}C\text{-}C\text{-}F}$ = 2.20 Hz, C), 128.76 (s, 10 C), 128.94 (s, 9 C), 130.62 (d, $J_{C\text{-}C\text{-}C\text{-}F}$ = 8.80 Hz, CH), 131.45 (d, $J_{C\text{-}C\text{-}C\text{-}C\text{-}C\text{-}F}$ = 3.67 Hz, CH), 133.12 (C), 138.43 (C), 143.78 (CH), 164.35 (d, $J_{C\text{-}F}$ = 250.89 Hz, C), 190.59 (C). **^{19}F NMR** ($CDCl_3$, 377 MHz) δ ppm -113.59 - -111.32 (m, 1 F).

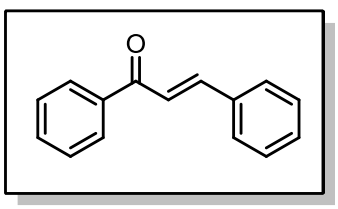

Chalcone (3.1g)

(90% GC conversion) was prepared according to the representative procedure for the synthesis of **3.1f** from benzaldehyde (0.2653 g, 2.5 mmol).

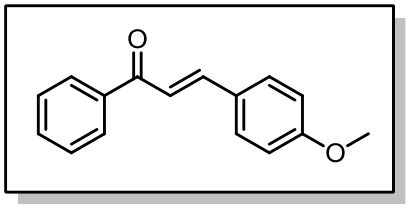

(E)-3-(4-methoxyphenyl)-1-phenylprop-2-en-1-one (3.1h)

(66% GC conversion) was prepared according to the representative procedure for the synthesis of **3.1f** from 4-methoxybenzaldehyde (0.3404 g, 2.5 mmol).

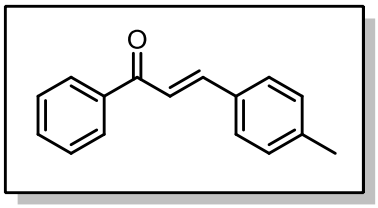

(E)-1-phenyl-3-(p-tolyl)prop-2-en-1-one (3.1i)

(84% GC conversion) was prepared according to the representative procedure for the synthesis of **3.1f** from 4-methylbenzaldehyde (0.3004 g, 2.5 mmol).

Biginelli Reaction

Ethyl-6-methyl-2-oxo-4-phenyl-1,2,3,4-tetrahydropyrimidine-5-carboxylate (3.1j):

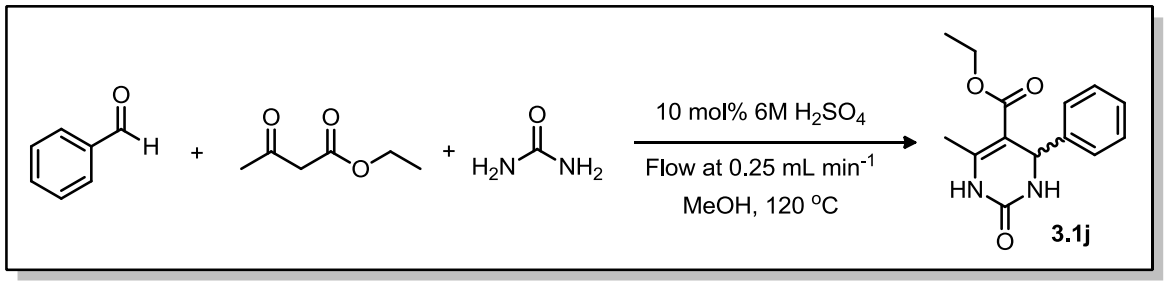

In a 50 mL volumetric flask was dissolved urea (3.003 g, 50 mmol, 1 equiv.) in methanol (~30 mL). Into the flask was then added benzaldehyde (1.306 g, 50 mmol, 1 equiv.), ethyl acetoacetate (6.507 g, 50 mmol, 1 equiv.). Methanol was added to bring the total volume to 50 mL (1 M) and the reagents were thoroughly mixed. An aliquot of this solution (10 mL) was transferred to a 20 mL vial equipped with a Teflon-coated stir bar. The flow reactor was readied using the equipment manufacturer's suggested start-up sequence. Methanol was pumped at 0.25 mL min^{-1} to prime the system as the coil was heated to 130 °C. The back-pressure regulator was adjusted to 7 bar to prevent the solvent from boiling in the coil. After the heating coil, the product stream was intercepted by pumping DMF (0.25 mL min^{-1}) by means of a T-piece to ensure complete solubility of the product. The Raman spectrometer was set to acquire a spectrum every 25 s, with 20 s integration time, boxcar = 3, and average = 1. When the flow unit was ready, 6 M H_2SO_4 (0.2 mL, 0.1 equiv.) was injected all at once and after mixing for 15 s the reaction mixture was loaded into the reactor coil at a flow rate of 0.25 mL min^{-1}. After the reaction mixture had been completely loaded into the reactor, methanol was again pumped through the coil at 0.25 mL min^{-1}. Product collection was commenced immediately after this switch. After the reaction mixture had been completely loaded into the reactor, the reactor pump was set back to pumping methanol. After the product had been fully discharged from the flow cell, the scans were halted. The reaction mixture was transferred to a separatory funnel, diluted with diethyl ether and sat. $NaHCO_3$ (100 mL) and water (100 mL) added. The layers were

separated and the aqueous layer extracted with ether (3 × 100 mL). The combined organics were washed with brine (2 × 100 mL) and dried over Na_2SO_4. The solvent was removed *in vacuo* by rotary evaporation affording the crude product. The resulting solid was transferred to a filter funnel, washed with cold methanol and air dried to afford **3.1j** (2.03 g, 78%) as a fluffy white solid.

^{1}H NMR (d_6-DMSO, 500 MHz) δ ppm 1.18 (s., 3 H), 2.34 (s., 3 H), 3.67 - 4.60 (m, 2 H), 5.24 (s., 1 H), 7.34 (s., 5 H), 7.80 (s., 1 H), 7.74 (s, 1 H), 9.26 (s., 1 H). **^{13}C NMR** (d_6-DMSO, 125 MHz) δ ppm 14.5 (CH_3), 18.2 (CH_3), 54.4 (CH), 59.6 (CH_2), 99.7 (C), 126.7 (CH), 127.7 (CH), 128.8 (CH), 145.3 (C), 148.8 (C), 152.6 (C), 165.8 (C).

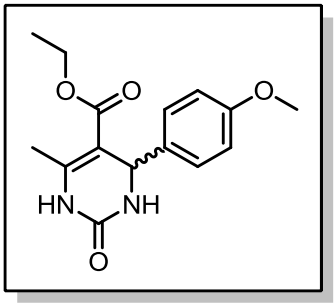

Ethyl-4-(4-methoxyphenyl)-6-methyl-2-oxo-1,2,3,4-tetrahydropyrimidine-5-carboxylate (3.1k)
(85% GC conversion) was prepared according to the representative procedure for the synthesis of **3.1j** from 4-methoxybenzaldehyde (1.3615 g, 10 mmol).

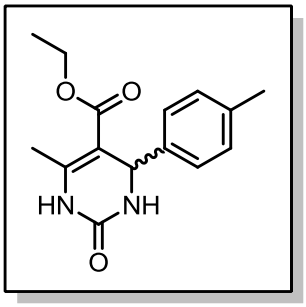

Ethyl-6-methyl-2-oxo-4-(p-tolyl)-1,2,3,4-tetrahydropyrimidine-5-carboxylate (3.1l)
(87% GC conversion) was prepared according to the representative procedure for the synthesis of **3.1j** from 4-methylbenzaldehyde (1.2015 g, 10 mmol).

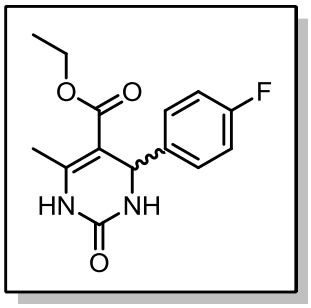

Ethyl-4-(4-fluorophenyl)-6-methyl-2-oxo-1,2,3,4-tetrahydropyrimidine-5-carboxylate (3.1m)
(91% GC conversion) was prepared according to the representative procedure for the synthesis of **3.1j** from 4-fluorobenzaldehyde (1.2411 g, 10 mmol).

Experimental Design

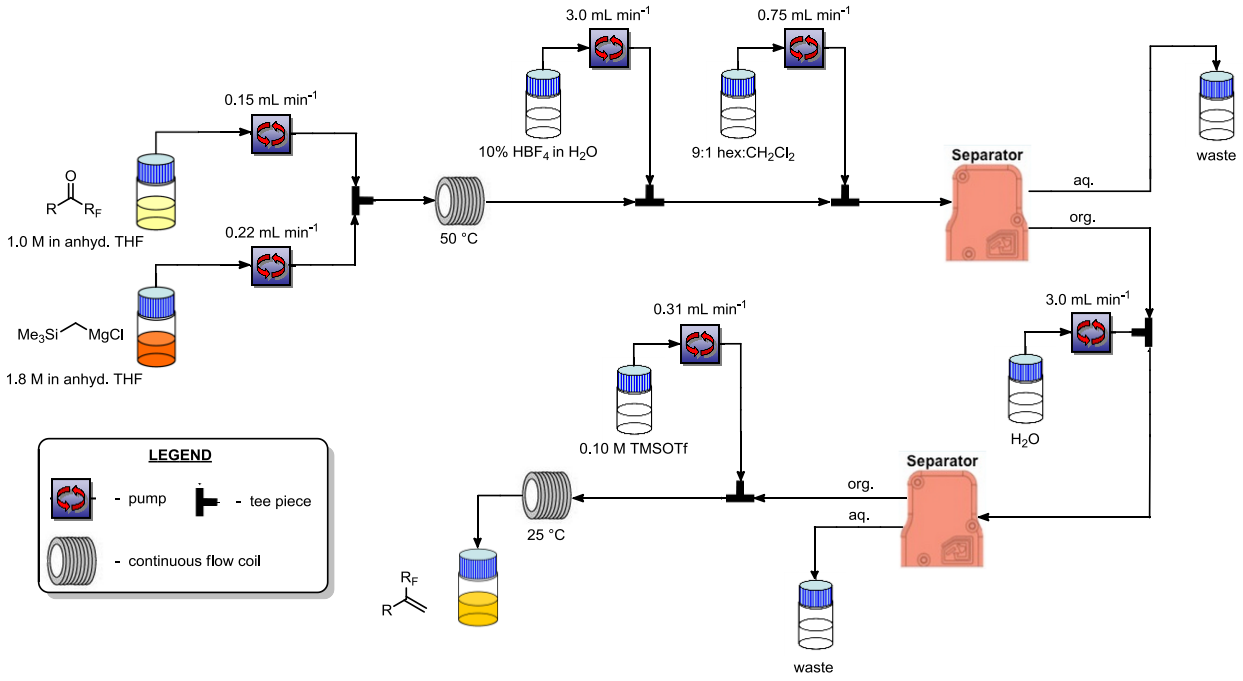

Flow configuration: Reactions were performed using a Vapourtec E series, (Pumps P1, P2, P6), Uniqsis FlowSyn (Pumps P3, P5), and an Agilent 1100 Series HPLC pump G1312A paired with a degasser G1379A (P4). Standard PTFE tubing (i.d. 1.0 mm, o.d. 1.8 mm) was utilized. The two reactor coils used were made of PFA, had an internal volume of 10 mL and are available from Vapourtec Ltd. PEEK Tee-mixers (Tee-connector, 0.02" thru-hole) were purchased from Upchurch Scientific (part # P-712) and modified to have 0.04" thru-hole. The liquid-liquid separators, equipped with 1 μm porosity membranes, are available from Zaiput Flow Technologies. The configuration shown on page S2 was assembled using the aforementioned equipment. The anhyd. THF was freshly distilled over sodium metal and benzophenone prior to use. Prior to running an experiment, the system was primed and flushed with the respective solvents (THF through P1 and P2, aq. deionized water through P3 and P5, 9:1 hexane/dichloromethane through P4, and hexane through P6. Prior to commencing the run, the Grignard reagent solution was set to flow at a rate of 0.5 mL min-1 so as to purge any residual water in the system. After an initial slug of 1 mL, the system was returned to solvent for all pumps. With the reaction coils and separators completely filled with their respective solutions, the first and second coils were heated to 50 °C and 25 °C, respectively. No back pressure regulators were needed because the solvents were not heated above their respective boiling points. The product exit stream was collected in a flask containing excess sat. sodium bicarbonate to quench the elimination reaction.

General Protocol for the Preparation of Perfluoroalkyl Alkenes using Continuous Flow Processing

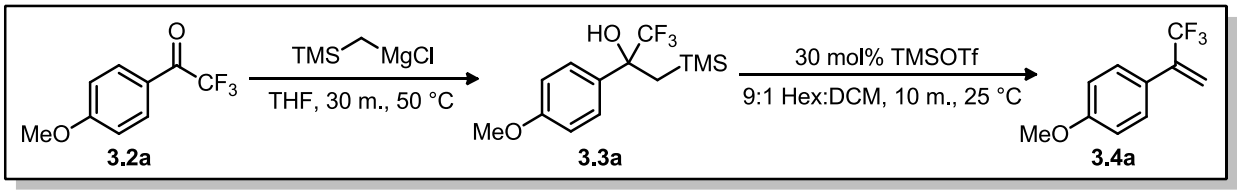

Representative Procedure for Alkene Synthesis:

1-methoxy-4-(3,3,3-trifluoroprop-1-en-2-yl)benzene (3.4a)

To a 15 mL conical flask was added **3.2a** (0.500 g, 2.4 mmol, 1 equiv) and anhyd. THF (2.4 mL, 1 M in the TFMK). This solution was kept under an N_2 atmosphere *via* an inlet needle. Another 15 mL conical flask was charged with a previously prepared ≈ 1.8 M solution of ((trimethylsilyl)methyl)magnesium chloride in anhyd. THF (~5 mL) and kept under an N_2 atmosphere *via* an inlet needle.[158] To prepare a stock solution of TMSOTf, TMSOTf (0.733 g, mmol) and hexane (30 mL, 0.1 M in the TMSOTf) were charged to a conical flask. The system was readied as outlined above. Then the TFMK was loaded into the reactor coil at a flow rate of 0.15 mL min^{-1} and the Grignard solution was set to flow at a rate of 0.22 mL min^{-1}. At this same time the TMSOTf was set to flow at a rate of 0.31 mL min^{-1}. Once the material was completely loaded (≈ 30 min), the system was set to flow anhyd. THF for the TFMK and Grignard streams. When the reaction mixture was judged to have completely exited the system, the reactor was shut down. The resulting reaction mixture was transferred from the collection flask to a separatory funnel. The layers were separated and the aqueous layer was extracted with hexane (3 x 75 mL). The combine organic layers were washed with brine (≈150 mL) and dried with Na_2SO_4. The solvent was removed *in vacuo* by rotary evaporation. The crude product was gently added atop a silica gel plug and eluted with hexane (2-3 column volumes). The solvent was removed *in vacuo* by rotary evaporation affording the pure alkene (0.4160 g, 84%) as a clear, pale yellow oil.

^{1}H NMR ($CDCl_3$, 400 MHz) δ ppm 3.83 (s, 3 H) 5.70 (q, *J* = 1.71 Hz, 1 H) 5.87 (q, *J* = 1.22 Hz, 1 H) 6.88 - 6.93 (m, 2 H) 7.40 (d, *J* = 8.31 Hz, 2 H)**^{13}C NMR** ($CDCl_3$, 125 MHz) δ ppm 55.51 (CH_3) 114.24 (CH) 119.08 (q, $J_{C\text{-}C\text{-}C\text{-}F}$ = 5.62 Hz, CH_2) 123.79 (q, $J_{C\text{-}F}$ = 273.60 Hz, CF_3) 126.3 (CH) 128.91 (C) 138.66 (q, $J_{C\text{-}C\text{-}F}$ = 30.10 Hz, C) 160.47 (C) **^{19}F NMR** ($CDCl_3$, 377 MHz) δ ppm -67.85 **GC-MS** (EI) 202 ($[M]^+$, 100%) 187 (5%) 183 (4%) 159 (7%) 151 (5%) 133 (90%) 118 (11%) 109 (27%) 103 (9%) 89 (14%) 77 (7%) 63 (13%)

[158] This solution can be conveniently prepared from (chloromethyl)trimethylsilane using the protocol outlined in: Hamlin, T. A.; Kelly, C. B.; Cywar, R. M. Leadbeater, N. E. *J. Org. Chem.* **2014**, *79*, 1145.

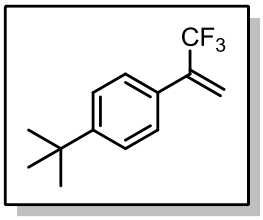

1-(*tert*-butyl)-4-(3,3,3-trifluoroprop-1-en-2-yl)benzene (3.4b) (0.4461 g, 90%) was prepared according to the representative procedure for the synthesis of **3.4a** from **3.2b** (0.5000 g, 2.2 mmol). The pure CF_3 alkene was obtained as a clear, colorless oil. **^{1}H NMR** ($CDCl_3$, 400 MHz) δ ppm 1.42 (s, 9 H) 5.81 - 5.85 (m, 1 H) 5.97 - 6.01 (m, 1 H) 7.51 (d, *J*=2.20 Hz, 4 H) **^{13}C NMR** ($CDCl_3$, 125 MHz) δ ppm 31.46 (CH_3) 34.89 (C) 123.82 (q, $J_{C\text{-}F}$ = 272.90 Hz, CF_3) 119.78 (q, $J_{C\text{-}C\text{-}C\text{-}F}$ = 5.87 Hz, CH_2) 125.81 (CH) 127.32 (CH) 130.99 (C) 139.12 (q, $J_{C\text{-}C\text{-}F}$ = 29.30 Hz, C) 152.44 (C) **^{19}F NMR** ($CDCl_3$, 377 MHz) δ ppm -67.66 **GC-MS** (EI) 228 ([M]$^+$, 18%) 213 (100%) 185 (44%) 153 (4%) 128 (7%) 115 (9%) 77 (4%)

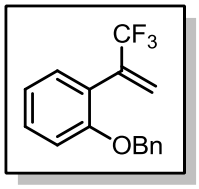

1-(benzyloxy)-2-(3,3,3-trifluoroprop-1-en-2-yl)benzene (3.4c) (0.4419 g, 89%) was prepared according to the representative procedure for the synthesis of **3.4a** from **3.2c** (0.5000 g, 1.8 mmol). The pure CF_3 alkene was obtained as a clear, pale yellow oil. **^{1}H NMR** ($CDCl_3$, 400 MHz) δ ppm 5.18 (s, 2 H) 5.73 - 5.80 (m, 1 H) 6.16 - 6.23 (m, 1 H) 7.02 - 7.10 (m, 2 H) 7.33 - 7.44 (m, 3 H) 7.44 - 7.54 (m, 4 H) **^{13}C NMR** ($CDCl_3$, 125 MHz) δ ppm 70.56 (CH_2) 112.96 (CH) 120.90 (C) 123.49 (q, $J_{C\text{-}F}$ = 274.40 Hz, CF_3) 123.72 (q, $J_{C\text{-}C\text{-}C\text{-}F}$ = 5.13 Hz, CH_2) 123.96 (CH) 127.28 (CH) 128.07 (CH) 128.77 (CH) 130.47 (CH) 131.12 (CH) 136.27 (q, $J_{C\text{-}C\text{-}F}$ = 31.50 Hz, C) 137.16 (C) 156.76 (C) **^{19}F NMR** ($CDCl_3$, 377 MHz) δ ppm -68.38 **GC-MS** (EI) 278 ([M]$^+$, 7%) 258 (5%) 187 (5%) 167 (2%) 159 (2%) 118 (4%) 109 (9%) 91 (100%) 65 (10%) 51 (4%)

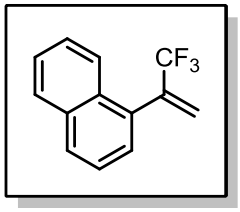

1-(3,3,3-trifluoroprop-1-en-2-yl)naphthalene (3.4d) (0.4559 g, 92%) was prepared according to the representative procedure for the synthesis of **3.4a** from **3.2d** (0.5000 g, 2.2 mmol). The pure CF_3 alkene was obtained as a clear, colorless oil. **^{1}H NMR** ($CDCl_3$, 400 MHz) δ ppm 5.76 (d, *J* = 1.22 Hz, 1 H) 6.46 (d, *J* = 1.47 Hz, 1 H) 7.57 - 7.60 (m, 2 H) 7.62 - 7.66 (m, 2 H) 7.96 - 8.02 (m, 2 H) 8.09 - 8.14 (m, 1 H) **^{13}C NMR** ($CDCl_3$, 125 MHz) δ ppm 123.53 (q, $J_{C\text{-}F}$ = 273.60 Hz, CF_3) 124.41 (q, $J_{C\text{-}C\text{-}C\text{-}F}$ = 5.10 Hz, CH_2) 125.18 (CH) 125.57 (CH) 126.37 (CH) 126.89 (CH) 127.69 (CH) 128.63 (CH) 129.56 (CH) 131.79 (C) 132.45 (C) 133.99 (C) 137.63 (q, $J_{C\text{-}C\text{-}F}$ = 31.50 Hz, C) **^{19}F NMR** ($CDCl_3$, 377 MHz) δ ppm -69.60 **GC-MS** (EI) 222 ([M]$^+$, 41%) 201 (20%) 183 (6%) 170 (3%) 153 (100%) 126 (6%) 75 (6%)

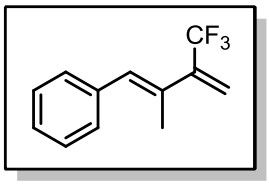

(*E*)-(2-methyl-3-(trifluoromethyl)buta-1,3-dien-1-yl)benzene (3.4e) (0.4549 g, 92%) was prepared according to the representative procedure for the synthesis of **3.4a** from **3.2e** (0.5000 g, 2.3 mmol). The pure CF_3 alkene was obtained as a clear, colorless oil. **^{1}H NMR** ($CDCl_3$, 400 MHz) δ ppm 2.15 (s, 3 H) 5.74 (q, *J* = 2.04 Hz, 1 H) 5.94 (d, *J* = 0.49 Hz, 1 H) 7.33 - 7.43 (m, 3 H) 7.43 - 7.51 (m, 2 H) **^{13}C NMR** ($CDCl_3$, 125 MHz) δ ppm 16.48 (CH_3) 118.90 (q, $J_{C\text{-}C\text{-}C\text{-}F}$ = 5.87 Hz, CH_2) 123.78 (q, $J_{C\text{-}F}$ = 275.10 Hz, CF_3) 127.44 (CH) 128.48 (CH) 129.57 (CH) 130.79 (C) 131.41 (q, $J_{C\text{-}C\text{-}C\text{-}C\text{-}F}$ = 1.50 Hz, CH) 137.44 (C) 141.46 (q, $J_{C\text{-}C\text{-}F}$ = 28.60 Hz, C) **^{19}F NMR** ($CDCl_3$, 377 MHz) δ ppm -66.18 **GC-MS** (EI)

213 ([M]$^+$, 23%) 197 (32%) 191 (12%) 177 (58%) 143 (100%) 128 (94%) 115 (33%) 91 (10%) 69 (8%)

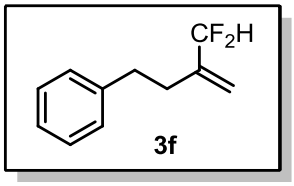

3-(difluoromethyl)but-3-en-1-yl)benzene (3.4f) (0.4650 g, 94%) was prepared according to the representative procedure for the synthesis of **3.4a** from **3.2f** (0.5000 g, 2.7 mmol). The pure CF_3 alkene was obtained as a clear, colorless oil. **^{1}H NMR** ($CDCl_3$, 400 MHz) δ ppm 2.58 (t, *J* = 7.80 Hz, 2 H) 2.92 (t, *J* = 8.60 Hz, 2 H) 5.28 (t, *J* = 1.71 Hz, 1 H) 5.44 (t, *J*=2.20 Hz, 1 H) 6.09 (t, *J* = 55.80 Hz, 1 H) 7.26 - 7.32 (m, 3 H) 7.34 - 7.42 (m, 2 H) **^{13}C NMR** ($CDCl_3$, 125 MHz) δ ppm 30.54 (t, $J_{C\text{-}C\text{-}C\text{-}F}$ = 1.50 Hz, CH_2) 34.20 (CH_2) 116.74 (t, $J_{C\text{-}F}$ = 238.40 Hz, CF_3) 117.85 (t, $J_{C\text{-}F}$ = 9.90 Hz, CF_2H) 126.36 (CH) 128.65 (CH) 128.69 (CH) 141.43 (C) 142.34 (t, $J_{C\text{-}C\text{-}F}$ = 20.50 Hz, C) **^{19}F NMR** ($CDCl_3$, 377 MHz) δ ppm -118.44 (d, *J* = 55.86 Hz) **GC-MS** (EI) 182 ([M]$^+$, 23%) 143 (3%) 128 (4%) 115 (5%) 91 (100%) 77 (5%) 65 (16%) 51 (11%)

Appendix IV: *Permissions*

Copyright Clearance Center RightsLink®

Home | Create Account | Help | Live Chat

ACS Publications Most Trusted. Most Cited. Most Read.

Title: Oxidation of α-Trifluoromethyl Alcohols Using a Recyclable Oxoammonium Salt
Author: Christopher B. Kelly, Michael A. Mercadante, Trevor A. Hamlin, et al
Publication: The Journal of Organic Chemistry
Publisher: American Chemical Society
Date: Sep 1, 2012
Copyright © 2012, American Chemical Society

LOGIN
If you're a copyright.com user, you can login to RightsLink using your copyright.com credentials. Already a RightsLink user or want to learn more?

PERMISSION/LICENSE IS GRANTED FOR YOUR ORDER AT NO CHARGE

This type of permission/license, instead of the standard Terms & Conditions, is sent to you because no fee is being charged for your order. Please note the following:

- Permission is granted for your request in both print and electronic formats, and translations.
- If figures and/or tables were requested, they may be adapted or used in part.
- Please print this page for your records and send a copy of it to your publisher/graduate school.
- Appropriate credit for the requested material should be given as follows: "Reprinted (adapted) with permission from (COMPLETE REFERENCE CITATION). Copyright (YEAR) American Chemical Society." Insert appropriate information in place of the capitalized words.
- One-time permission is granted only for the use specified in your request. No additional uses are granted (such as derivative works or other editions). For any other uses, please submit a new request.

BACK | CLOSE WINDOW

Copyright Clearance Center RightsLink®

Home | Create Account | Help | Live Chat

ACS Publications Most Trusted. Most Cited. Most Read.

Title: Methylenation of Perfluoroalkyl Ketones using a Peterson Olefination Approach
Author: Trevor A. Hamlin, Christopher B. Kelly, Robin M. Cywar, et al
Publication: The Journal of Organic Chemistry
Publisher: American Chemical Society
Date: Feb 1, 2014
Copyright © 2014, American Chemical Society

LOGIN
If you're a copyright.com user, you can login to RightsLink using your copyright.com credentials. Already a RightsLink user or want to learn more?

PERMISSION/LICENSE IS GRANTED FOR YOUR ORDER AT NO CHARGE

This type of permission/license, instead of the standard Terms & Conditions, is sent to you because no fee is being charged for your order. Please note the following:

- Permission is granted for your request in both print and electronic formats, and translations.
- If figures and/or tables were requested, they may be adapted or used in part.
- Please print this page for your records and send a copy of it to your publisher/graduate school.
- Appropriate credit for the requested material should be given as follows: "Reprinted (adapted) with permission from (COMPLETE REFERENCE CITATION). Copyright (YEAR) American Chemical Society." Insert appropriate information in place of the capitalized words.
- One-time permission is granted only for the use specified in your request. No additional uses are granted (such as derivative works or other editions). For any other uses, please submit a new request.

BACK | CLOSE WINDOW

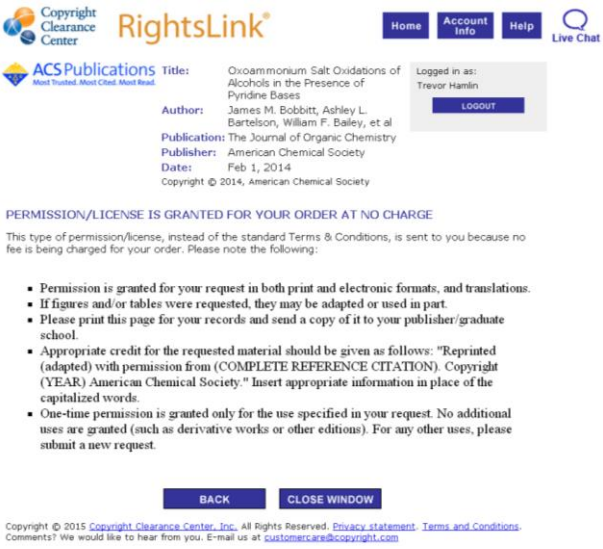

Copyright Clearance Center RightsLink®

Home | Account Info | Help | Live Chat

ACS Publications Most Trusted. Most Cited. Most Read.

Title: Oxoammonium Salt Oxidations of Alcohols in the Presence of Pyridine Bases
Author: James M. Bobbitt, Ashley L. Bartelson, William F. Bailey, et al
Publication: The Journal of Organic Chemistry
Publisher: American Chemical Society
Date: Feb 1, 2014
Copyright © 2014, American Chemical Society

Logged in as: Trevor Hamlin
LOGOUT

PERMISSION/LICENSE IS GRANTED FOR YOUR ORDER AT NO CHARGE

This type of permission/license, instead of the standard Terms & Conditions, is sent to you because no fee is being charged for your order. Please note the following:

- Permission is granted for your request in both print and electronic formats, and translations.
- If figures and/or tables were requested, they may be adapted or used in part.
- Please print this page for your records and send a copy of it to your publisher/graduate school.
- Appropriate credit for the requested material should be given as follows: "Reprinted (adapted) with permission from (COMPLETE REFERENCE CITATION). Copyright (YEAR) American Chemical Society." Insert appropriate information in place of the capitalized words.
- One-time permission is granted only for the use specified in your request. No additional uses are granted (such as derivative works or other editions). For any other uses, please submit a new request.

BACK | CLOSE WINDOW

Copyright Clearance Center RightsLink®

Home | Account Info | Help | Live Chat

ACS Publications Most Trusted. Most Cited. Most Read.

Title: A Continuous-Flow Approach to 3,3,3-Trifluoromethylpropenes: Bringing Together Grignard Addition, Peterson Elimination, Inline Extraction, and Solvent Switching
Author: Trevor A. Hamlin, Gillian M. L. Lazarus, Christopher B. Kelly, et al
Publication: Organic Process Research & Development
Publisher: American Chemical Society
Date: Oct 1, 2014
Copyright © 2014, American Chemical Society

Logged in as: Trevor Hamlin
LOGOUT

PERMISSION/LICENSE IS GRANTED FOR YOUR ORDER AT NO CHARGE

This type of permission/license, instead of the standard Terms & Conditions, is sent to you because no fee is being charged for your order. Please note the following:

- Permission is granted for your request in both print and electronic formats, and translations.
- If figures and/or tables were requested, they may be adapted or used in part.
- Please print this page for your records and send a copy of it to your publisher/graduate school.
- Appropriate credit for the requested material should be given as follows: "Reprinted (adapted) with permission from (COMPLETE REFERENCE CITATION). Copyright (YEAR) American Chemical Society." Insert appropriate information in place of the capitalized words.
- One-time permission is granted only for the use specified in your request. No additional uses are granted (such as derivative works or other editions). For any other uses, please submit a new request.

BACK | CLOSE WINDOW

Title: Dehydrogenation of Perfluoroalkyl Ketones by Using a Recyclable Oxoammonium Salt
Author: Trevor A. Hamlin,Christopher B. Kelly,Nicholas E. Leadbeater
Publication: European Journal of Organic Chemistry
Publisher: John Wiley and Sons
Date: May 7, 2013

Order Completed

Thank you for your order.

This Agreement between Trevor A Hamlin ("You") and John Wiley and Sons ("John Wiley and Sons") consists of your license details and the terms and conditions provided by John Wiley and Sons and Copyright Clearance Center.

Your confirmation email will contain your order number for future reference.

Get the printable license.

License Number	3618320601158
License date	Apr 29, 2015
Licensed Content Publisher	John Wiley and Sons
Licensed Content Publication	European Journal of Organic Chemistry
Licensed Content Title	Dehydrogenation of Perfluoroalkyl Ketones by Using a Recyclable Oxoammonium Salt
Licensed Content Author	Trevor A. Hamlin,Christopher B. Kelly,Nicholas E. Leadbeater
Licensed Content Date	May 7, 2013
Licensed Content Pages	4
Type of use	Dissertation/Thesis
Requestor type	Author of this Wiley article
Format	Print and electronic
Portion	Full article
Will you be translating?	No
Title of your thesis / dissertation	Development of New Synthetic Methods, Mechanistic Elucidation of Novel Organic Reactions Using Quantum Calculations, and Harnessing the Power of Continuous Flow Technologies
Expected completion date	May 2015
Expected size (number of pages)	200
Requestor Location	Trevor A Hamlin 1 Lakeshore Blvd STAFFORD SPRINGS, CT 06076 United States Attn: Trevor A Hamlin
Billing Type	Invoice
Billing address	Trevor A Hamlin 1 Lakeshore Blvd STAFFORD SPRINGS, CT 06076 United States Attn: Trevor A Hamlin
Total	0.00 USD

ORDER MORE | CLOSE WINDOW